

1973

# The prediction of drying shrinkage of reinforced concrete members.

Omar A. El-Zein  
*University of Windsor*

Follow this and additional works at: <http://scholar.uwindsor.ca/etd>

---

## Recommended Citation

El-Zein, Omar A., "The prediction of drying shrinkage of reinforced concrete members." (1973). *Electronic Theses and Dissertations*. Paper 4171.

This online database contains the full-text of PhD dissertations and Masters' theses of University of Windsor students from 1954 forward. These documents are made available for personal study and research purposes only, in accordance with the Canadian Copyright Act and the Creative Commons license—CC BY-NC-ND (Attribution, Non-Commercial, No Derivative Works). Under this license, works must always be attributed to the copyright holder (original author), cannot be used for any commercial purposes, and may not be altered. Any other use would require the permission of the copyright holder. Students may inquire about withdrawing their dissertation and/or thesis from this database. For additional inquiries, please contact the repository administrator via email ([scholarship@uwindsor.ca](mailto:scholarship@uwindsor.ca)) or by telephone at 519-253-3000ext. 3208.



THE PREDICTION OF DRYING SHRINKAGE  
OF REINFORCED CONCRETE MEMBERS

A Thesis

Submitted to the Faculty of Graduate Studies through the  
Department of Civil Engineering in Partial Fulfilment  
of the Requirements for the Degree of  
Doctor of Philosophy of Applied Science  
at the University of Windsor.

by

Omar A. El-Zein

Windsor, Ontario, Canada

1973

© Omar A. El-Zein 1973

487705

## ABSTRACT

The available methods of predicting the drying shrinkage of reinforced concrete do not provide a practical solution to the problem. Most of the methods suggested for the prediction of shrinkage force and deformation require an experimental evaluation of several constants which vary for different concretes, percentages of reinforcement, sizes of member, and the ambient conditions. No experimental work was done by some researchers, and very limited experimental work was done by others.

A review of the available literature, reveals that the drying shrinkage of plain concrete can be adequately described by linear diffusion theory. However, this method still requires the experimental evaluation of the ultimate shrinkage of concrete.

To the knowledge of the writer, no previous attempt has been made to apply diffusion theory to the prediction of the drying shrinkage of reinforced concrete members. The first investigation in this research programme was, therefore, designed to apply diffusion theory to the prediction of drying shrinkage of reinforced concrete.

The second investigation was to establish a quick method to evaluate the ultimate shrinkage of plain and reinforced concrete, and to provide formulae to predict shrinkage forces and deformation in reinforced concrete members.

The third investigation was designed to study the development and distribution of shrinkage stresses in reinforced concrete members, in an attempt to take into account the effect of member length.

A wide range of slabs, rectangular beams, and columns (over 500 specimens) were cast and prepared throughout this research programme.

The experimental results indicate that diffusion analogy seems to provide an adequate means of predicting the drying shrinkage of reinforced concrete members, taking into account the effect of reinforcement, bar diameter, size of member, type of cement, and the ambient condition. The shrinkage diffusion coefficient of plain and reinforced concrete appear to be a function of the Fourier number  $t/b^2$ .

The ultimate shrinkage of plain concrete dried under normal conditions, can be evaluated as a function of the ultimate shrinkage of similar oven dried specimens and the ambient relative humidity.

The theoretical formulae developed in this thesis to predict the ultimate shrinkage strain in steel show good agreement with the experimental results of symmetrically and eccentrically reinforced members.

It appears that shrinkage stresses along the reinforcing bar increases gradually from the ends of the member towards the

centre over a distance which is short compared with the usual length of the member. A uniform stress is developed in the central portion.

In general, a practical and more accurate method of predicting shrinkage strain, force, and deformation in reinforced concrete members is presented.

## ACKNOWLEDGEMENTS

The author wishes to express his sincere gratitude to his mentor Dr. Cameron MacInnis for his guidance and constructive suggestions throughout the preparation of this work. His encouragement and support will be always appreciated.

The author is also grateful to Dr. Norbert Becker for his valuable comments and helpful discussions.

The technical assistance, of Mr. M. Horan, V. Hebert, G. Michalczuk, J. Eising, and V. Fazio, was a valuable asset in conducting the experimental work.

Thank is due to fellow graduate comrades Dr. J. Beaudoin, O. Marzouk, Dr. H. Ali, and M. Sid-Ahmed for their valuable discussions.

Thank is due to the author's wife Mrs. Faizah El-Zein for her encouragement, patience, and for typing the manuscript.

The financial assistance of the National Research Council is greatly appreciated.



## LIST OF SYMBOLS

$A_c$	=	area of concrete section
$A_g$	=	gross area of concrete section
$A_s$	=	area of steel in tension fibers
$A_s'$	=	area of steel in compression fibers
$A_w$	=	deflection coefficient of uniform member
$2b$	=	width of member drying from one or two sides
$C$	=	the amount of diffusing substance
$C_o$	=	ultimate moisture loss
$e$	=	eccentricity of reinforcing bars
$E_c$	=	Young's modulus of elasticity of concrete
$E_e' E_c'$	=	$E_c/(1+m)$ effective modulus of elasticity
$E_s'$	=	Young's modulus of elasticity of steel
$f$	=	surface factor
$I_c$	=	moment of inertia of concrete section
$K$	=	diffusion coefficient
$K_o$	=	diffusion parameter
$L$	=	length of concrete member
$m$	=	creep strain to elastic strain
$M$	=	shrinkage moment = $P \cdot e$
$n$	=	$E_s/E_c'$
$\phi$	=	shrinkage curvature

$P_s$	=	percentage of reinforcement
$P$	=	shrinkage force
$P_c$	=	shrinkage forces in concrete
$P_s$	=	shrinkage forces in steel
$R$	=	relative humidity condition
$S$	=	shrinkage strain
$S_{av}$	=	average shrinkage of plain or reinforced concrete
$S_{cn}$	=	shrinkage strain in concrete
$S_f$	=	free drying shrinkage of plain concrete
$S_s$	=	shrinkage strain in steel
$S_u$	=	ultimate shrinkage
$S_{uc}$	=	ultimate shrinkage strain of plain concrete
$S_{us}$	=	ultimate shrinkage strain in steel
$S_{uov}$	=	ultimate shrinkage of oven dried concrete
$t$	=	time of drying
$t/b^2$	=	Fourier number to an arbitrary scale
$U$	=	the moisture concentration = $C/C_0$
$\bar{U}$	=	the average moisture concentration
$1-\bar{U}$	=	the average moisture concentration loss
$V/S$	=	volume to surface ratio
$x, y, z$	=	rectangular coordinates
$\delta$	=	shrinkage deflection

## TABLE OF CONTENTS

	Page
ABSTRACT .....	iii
ACKNOWLEDGEMENTS .....	vi
LIST OF SYMBOLS .....	vii
TABLE OF CONTENTS .....	ix
I <u>INTRODUCTION</u> .....	1
II <u>THE PREDICTION OF DRYING SHRINKAGE OF PLAIN CONCRETE</u> .....	3
<u>EMPIRICAL APPROACH</u> .....	3
<u>DIFFUSION THEORY APPROACH</u> .....	8
<u>SUMMARY</u> .....	10
III <u>THE PREDICTION OF DRYING SHRINKAGE OF REINFORCED CONCRETE</u> .....	12
<u>SHRINKAGE STRESSES</u> .....	12
<u>SHRINKAGE DEFORMATIONS</u> .....	16
<u>SUMMARY</u> .....	20
IV <u>RESEARCH AIMS</u> .....	22
<u>APPLICATION OF DIFFUSION ANALOGIES</u> .....	22
<u>EVALUATION OF THE ULTIMATE SHRINKAGE</u> .....	23
Theoretical Analysis .....	24
<u>SHRINKAGE STRESS DEVELOPMENT</u> .....	24
V <u>THEORETICAL CONSIDERATION</u> .....	25
<u>DIFFUSION THEORY</u> .....	25
Initial and Boundary Conditions .....	27

	Page
Rectangular Members Drying from 1, 2, or 4 Sides .....	28
Slabs or Beams Drying from 1, or 2 Sides .....	28
Beams or Columns Drying from 4 Sides .....	29
Shrinkage Diffusion Analogies .....	30
<u>THEORETICAL ANALYSIS</u> .....	31
Assumptions .....	31
Equilibrium of Forces .....	32
Compatibility of Strains .....	32
Eccentrically Single-Reinforced Member .....	32
Symmetrically Reinforced Member .....	33
Shrinkage Deformation .....	34
VI <u>EXPERIMENTAL PROGRAMME AND PROCEDURES</u> .....	37
<u>EXPERIMENTAL INVESTIGATIONS</u> .....	37
Drying Shrinkage of Reinforced Concrete Members .....	37
Ultimate Shrinkage Development Under Accelerated Drying Condition .....	38
Shrinkage Stress Development .....	39
<u>MATERIALS</u> .....	40
Cement .....	40
Sand .....	41
Coarse Aggregate .....	41
Reinforcing Bars .....	41
Screw Inserts .....	42
Strain Gages .....	42

	Page
<u>EXPERIMENTAL PROCEDURES</u> .....	43
Mix Proportions .....	43
Mixing Procedure .....	43
Form Preparation .....	44
Moulding and Compaction .....	44
Curing .....	45
Sealing .....	46
Storage .....	46
Reading and Measuring Techniques .....	48
Readings .....	48
Measuring Techniques .....	49
VII <u>DISCUSSION OF RESULTS</u> .....	51
<u>MOISTURE LOSS VERSUS SHRINKAGE OF REINFORCED CONCRETE</u> ....	52
<u>APPLICATION OF DIFFUSION ANALOGIES TO THE SHRINKAGE OF</u> <u>REINFORCED CONCRETE</u> .....	54
Diffusion Analogies of Constant Diffusion Coefficients.	54
Diffusion Analogies of Variable Diffusion Coefficients.	55
Band of Theoretical Diffusion Curves .....	57
Equations of Best Fit .....	60
<u>SHRINKAGE STRESS DEVELOPMENT</u> .....	61
<u>PREDICTION OF THE ULTIMATE SHRINKAGE</u> .....	62
Quick Method of Evaluating the Ultimate Shrinkage !....	63
Evaluation of the Ultimate Shrinkage Strain in Steel ..	65
<u>EXPERIMENTAL ERRORS</u> .....	69

	Page
Preparation of Specimens .....	69
Sealing and Storage Process .....	70
Measuring Process .....	70
Carbonation and Creep .....	72
<u>ADDITIONAL FINDINGS</u> .....	72
VIII <u>CONCLUSIONS</u> .....	74
<u>OBSERVATION AND CONCLUSIONS</u> .....	74
Drying Versus Shrinkage of Reinforced Concrete .....	74
Diffusion analogy and the Shrinkage of Reinforced Concrete .....	75
Shrinkage Stress Development .....	76
Ultimate Shrinkage of Plain and Reinforced Concrete ..	76
<u>RECOMMENDED METHOD OF PREDICTING DRYING SHRINKAGE</u> .....	78
<u>RECOMMENDED FUTURE RESEARCH</u> .....	79
APPENDIX A: SHRINKAGE OF CONCRETE .....	80
APPENDIX B: FIGURES .....	99
APPENDIX C: EXPERIMENTAL MATERIALS .....	197
APPENDIX D: MOISTURE LOSS AND SHRINKAGE DATA.....	205
REFERENCES .....	243
VITA AUCTORIS .....	249

## CHAPTER I

### INTRODUCTION

Concrete, like many other materials, tends to shrink or swell with each change in moisture content. Drying shrinkage is believed to be one major cause of cracking in concrete members. Such cracking occurs when the concrete member is not allowed to shrink freely in its principal direction.

The presence of steel in concrete members reduces the amount of drying shrinkage. As a result, appreciable shrinkage stresses and deformations are developed. These stresses and deformations, when combined with those due to live and dead loads could become critical and may lead to failure of concrete structures.

Elstner and Hognestad (48), investigated the failure of (AMC Warehouse, Wilkins Air Force Department, Ohio, August 1955) a rigid frame concrete structure. They stated that the collapse took place by a combination of diagonal tension due to dead loads and axial tension due to shrinkage and temperature changes. Abeles (48), in a discussion of Elstner's and Hognestad's investigation confirmed that shrinkage stresses, in addition to principal stresses due to shear, had played an important part in the failure.

Although some investigators have suggested different

formulae for predicting shrinkage stresses and deformations, their methods require an experimental evaluation of several constants which vary for different concretes, percentages of reinforcements and ambient conditions...etc. The purpose of the writers research programme was therefore, to provide a practical and reliable means of predicting the drying shrinkage of reinforced concrete members.

A summary of the literature dealing with the structure of concrete, the various volume changes which take place in concrete and the main factors affecting the drying shrinkage of concrete are presented in Appendix A.



## CHAPTER II

### THE PREDICTION OF DRYING SHRINKAGE OF PLAIN CONCRETE

Over the past 40 years, many investigators have carried out studies on the drying shrinkage of cement paste, mortar, and plain concrete, and have attempted to develop equations for predicting this phenomenon. Most of the equations suggested for the prediction of concrete shrinkage were obtained empirically and were of limited use. In recent years, some investigators have applied diffusion theory to describe the shrinkage of plain concrete.

The various methods which have been used to predict the shrinkage of plain concrete will be reviewed here.

#### EMPIRICAL APPROACH:

Ross (28), in 1943, 1944, presented a rheological model, to describe the shrinkage of concrete, of the form:

$$S_f = \sigma \cdot \alpha (1 - e^{-(\phi t/\alpha)}) \dots \dots \dots (1)$$

where,

$S_f$  = free drying shrinkage at time  $t$ ,

$\sigma$  = force in the model causing shrinkage,

- $\alpha$  = spring compliance in the rheological model,
- $\phi$  = fluidity of the viscous element in the model.

The coefficients needed to apply this equation were empirically determined from the measured data. He found that the shrinkage development varies enormously with the size and shape of a concrete member. He suggested that the rate of shrinkage is a function of the volume to surface ratio of the member.

Pickett (22), and Dutron (25), in 1956-1957, proposed numerical formulae, to predict the shrinkage of concrete as a function of the free drying shrinkage of cement paste, and the volume concentration of aggregate, cement, and air (voids). Dutron's formula, included coefficients which vary with the maximum size of aggregate and the relative humidity.

Lyse (33), in 1960, proposed a formula, to predict drying shrinkage, of the form:

$$S_f = S_{uo} (1 - e^{-nt}) P_c \dots\dots\dots(2)$$

where,

- $S_{uo}$  = ultimate shrinkage of concrete per 1 percent of cement paste (by weight),
- $n$  = an exponent varies with the relative humidity,
- $P_c$  = percent of cement paste in the concrete.

From his results, he concluded that the shrinkage of concrete is approximately proportional to the amount of cement paste. His formula necessitates finding the ultimate shrinkage of concrete per one percent of cement paste.

Hansen and Mattock (29), in 1966, studied the influence of size and shape of concrete members on shrinkage. Their results, for I-beams and cylindrical specimens which cover a range of values of volume to surface ratio from about 1 in. to 6 in., showed that this parameter does not reflect adequately the variations of both size and shape.

Dutron (25), derived the following equation relating the shrinkage at 50% relative humidity, and the shrinkage at any other relative humidity condition:

$$S_f = S_{50} \left( 0.96 \log \frac{105 - R}{5} \right) \dots \dots \dots (2)$$

where,

$S_{50}$  = free drying shrinkage in 50% R.H. at time  $t$ ,

$R$  = ambient relative humidity in percent.

Wallo et al., (34), in 1968, presented the following equation for predicting the drying shrinkage of concrete at any time:

$$S_f = S_u \left( 1 - e^{-0.1 \left( \frac{s}{\sqrt{v}} \right) t^{0.65}} \right) \dots \dots \dots (4)$$

where,

$$S_u = (2400 - 2100V_{hc}) (1 - V_s) (0.96 \log \frac{105 - R}{5}) 10^{-6} \quad (5)$$

= ultimate free drying shrinkage at  $t = \infty$ ,

$s/v$  = surface to volume ratio,

$V_{hc}$  = volume concentration of hydrated cement,

$V_s$  = volume concentration of solids.

The constants were empirically obtained by fitting the shrinkage results of three different size specimens, and two different mixes. They used the same equation suggested by Lyse assuming "n" is a function of the surface to volume ratio ( $s/v$ ).

The equation for ultimate shrinkage combines both the equations of Pickett and Dutron. It assumes the ultimate shrinkage to be functions of the volume concentrations of hydrated cement and solids, as well as, the ambient relative humidity. Wallo's equation fails to take into account such factors as the type, composition, and fineness of cement, the type and gradation of aggregate...etc. An example of their results is presented in figure 10. The proposed analytical expressions seem to over estimate the drying shrinkage of the small size specimens, and their results do not agree with the method recommended by the Comité Européen du Béton (C.E.B.).

Fintel and Khan <sup>(35)</sup>, in Dec. 1969, presented a procedure for predicting creep and shrinkage strain based on the present

state of the art. They suggested one single curve, figure 11, for the fractional shrinkage or creep as a function of time. This implies that the rate of shrinkage and creep is constant, for different sized specimens. They also proposed correction factors to account for the relative humidity, volume to surface ratio, and percentage of reinforcement.

ACI Technical Committee 209 (36), in 1970, prepared a report in which a method for predicting shrinkage is presented. This method suggested the application of a "shrinkage factor" in the design of structural concrete elements. The following hyperbolic equation was recommended for predicting the shrinkage of concrete at any time t:

$$S_f = \frac{t^e}{f+t^e} S_u \dots\dots\dots(6)$$

where, "e" and "f" must be obtained experimentally. The following ranges for the constants, gathered from the data reported by many investigators, are:

- e = 0.90 to 1.10
- f = 20 to 130
- S<sub>u</sub> = 415 x 10<sup>-6</sup> to 1070 x 10<sup>-6</sup> .....(7)

The following "standard conditions" were established to which adjustments must be made to fit a particular set of actual

conditions:

Relative humidity = 40%

Thickness = 6 inch

$S_u = 800 \times 10^{-6}$  for 20-year period....(8)

$S_f = \frac{t}{35 + t} S_u$  .....(9)

For different relative humidity conditions, and thicknesses, correction factors to adjust the ultimate shrinkage ( $S_u$ ), were proposed.

It can be seen that the method proposed by the ACI Committee 209, is rather limited in its use due to the number of empirical constants required. Also, it fails to include all the factors affecting shrinkage.

DIFFUSION THEORY APPROACH:

The application of diffusion analogies, to describe the drying shrinkage of concrete was first suggested by Carlson (37), in 1937. From his limited results based on the shrinkage of large concrete members, he concluded that the linear diffusion theory could not be used to predict accurately the shrinkage of plain concrete.

Pickett (27), in 1946, used the linear diffusion theory suggested by Carlson and presented solutions for the drying

shrinkage of concrete and the warping caused by unsymmetric drying of beams. His results for the small slab specimens of cement paste fitted the theoretical curves well. However, for larger specimens a notable discrepancy was observed. He concluded that the shrinkage diffusion coefficient is not constant but rather some function of the shrinkage or of time.

Rostasy (21), in 1958, using linear diffusion theory, presented a more complete analysis of shrinkage stresses in concrete. He used Jacobi's Theta and D-functions to solve the diffusion equation. An example of his results is presented in figure 12. His specimens ( 40 x 40 x 20 cm ), prepared of mortar mixes ( 1:4 by weight ) and dried in 65% relative humidity condition, have shown a good agreement between the experimental and theoretical results, specially at later ages.

Becker (15), in 1970, assumed that the shrinkage diffusion coefficients are constant and obtained solutions for the fractional average shrinkage ( $S_{av}/S_u$ ) as a function of the Fourier number to an arbitrary scale ( $t/b^2$ ). After fitting a large variety of data, he concluded that the shrinkage diffusion coefficient is not significantly influenced by the specimen size, the length of moist curing, or by the relative humidity to which the specimens were subjected during drying. In addition he found that the suggested theoretical method is not significantly affected

by the cement and water content; by the cement composition or fineness; by the type and gradation of aggregate; by the size and shape of specimen; or by the ambient relative humidity. He showed that the shrinkage diffusion coefficient is relatively constant and that all the data which was fitted could be enveloped by theoretical curves, figure 13, obtained by assuming  $K = 0.016 \text{ in}^2/\text{day}$ , and  $K = 0.006 \text{ in}^2/\text{day}$ .

The band of theoretical curves obtained over this range of  $K$  values, is very narrow and can be approximated by a single theoretical curve assuming  $K = 0.01$ . The data which was fitted within this band cover a wide variety of cement pastes, mortars, and concretes, different sizes and shapes of members, different relative humidity, different types of aggregate and cement, etc. The experimental data he considered included many specimens he fabricated himself as well, as data reported by many investigators from different countries of the world using native materials.

#### SUMMARY:

From the foregoing discussion it can be seen that, most of the equations suggested to predict the shrinkage of concrete were obtained empirically, and can only be accurately applied to fit the particular results of these researchers.

It appears that diffusion analogies may be used to predict



accurately the shrinkage of plain concrete; however, this method still requires an experimental evaluation of the ultimate shrinkage of the particular concrete being studied.

## CHAPTER III

### THE PREDICTION OF DRYING SHRINKAGE OF REINFORCED CONCRETE

It has been reported by many investigators that the presence of steel in concrete reduces the drying shrinkage of concrete. The restraining effect of steel depends largely on the percentage and location of reinforcement in the concrete member. The restraining action causes compressive stresses in the steel and tensile stresses in the concrete. These stresses are believed to be transferred from the concrete to the reinforcing bars by bond between the two materials.

Only a few investigators have tried to develop methods of predicting the shrinkage of reinforced concrete members. Most of the methods suggested for the prediction of shrinkage stresses and deformations of reinforced concrete members required an experimental evaluation of several constants, and were limited in their use.

While some investigators have suggested equations for predicting this phenomenon without experimental verification, others have provided a very limited amount of experimental work.

#### SHRINKAGE STRESSES:

Glanville (31), in 1930, studied the shrinkage of

symmetrically reinforced concrete members (6x6x36"), He suggested the following formula for calculating the shrinkage strain in steel:

$$S_B = \frac{S_f}{\frac{E_s A_s}{E_c' A_c} + 1} \dots\dots\dots(10)$$

where,

$$E_c' = \frac{E_c}{1 + m}$$

$S_f$  = drying shrinkage of plain concrete,

$A_s$  = area of steel,

$A_c$  = area of concrete,

$E_s$  = modulus of elasticity of steel,

$E_c$  = modulus of elasticity of concrete,

$m$  = ratio of creep to elastic strain.

He stated that the value of  $E_s/E_c'$  is generally about 15 and will not usually vary beyond the limiting values of 10 and 20. His experimental results did not agree with the above equation, which he attributed to break down of the concrete in tension.

Shank (38), in 1935, developed the following equation for the prediction of shrinkage stresses in reinforced concrete members (on a similar basis to that for columns):

$$\text{The shrinkage force } P = \frac{E_s S_f}{1/pbd+n/bd+ne/I_t} \dots\dots\dots(11)$$

where,

$P$  = percentage of reinforcement,

$n$  =  $E_s/E_c$ ,

$b$  = width of the beam,

$e$  = eccentricity,

$I_t$  = moment of inertia of the transformed section.

He considered perfect bond between concrete and the reinforcing bars. His analysis implies that the whole transformed section of the member resists the restraining force. He did not experimentally verify the accuracy of the above equation.

Odman (39), studied theoretically the drying shrinkage of a general I-beam with an arbitrary number of layers of reinforcement. He presented the final formulae without describing the mathematical approach used to derive these formulae, or the significance of the constants. These formulae were presented for the calculation of:

- a. shortening and deflection of the beam,
- b. distribution of the bond stresses at the contact phase between concrete and reinforcing bars, and
- c. the corresponding distribution of the normal stresses of both materials acting at an arbitrary cross-sectional area of the beam.

Odman did not report on the success of any attempt to fit

experimental data to these formulae.

Elvery and Shaffi (40), in 1970, using the same approach as Glanville, presented similar formulae for the prediction of shrinkage stresses and deformations of eccentrically reinforced concrete beams. Their results of shrinkage force and tensile strain in the concrete at the level of the steel were respectively, lower and higher than the corresponding calculated values. They explained that such discrepancies could be due to some error in the creep data used. Their experimental work was limited to two rectangular beams 4 in wide, 5 in deep, and 5 ft. long cast from a single concrete mix. An example of their results is presented on figure 14.

Keeton (41), in Nov. 1970, performed shrinkage tests on reinforced concrete specimens of 5 in. width, 12 in. long, and thicknesses of 1, 2, and 4 inches. The specimens were reinforced with steel mesh of no. 12 (0.10 in. diameter) or no. 14 (0.08 in. diameter). The specimens were allowed to dry from the 5x12 inch faces, thus simulating a continuous slab with the thickness being the only variable. His study concentrated on attempts to predict the overall shrinkage of reinforced concrete slab specimens rather than the induced stresses. He suggested that the shrinkage of reinforced concrete could be predicted on the basis of the ratio of the exposed surface area to volume. He presented an empirical equation and correction factors for different relative

humidities and thicknesses to predict the overall shrinkage of reinforced concrete slabs. His method was similar to that proposed by ACI Committee 209. He explained that the constants he derived for the ACI formulae are applicable only to the concrete mixes he used in his experiments.

#### SHRINKAGE DEFORMATIONS:

A number of researchers studied the effect of drying shrinkage on the warping or deflection of eccentrically reinforced concrete members.

Miller <sup>(42)</sup>, in 1958, studied the effect of shrinkage on the warping of unsymmetrically reinforced beams. He assumed that, "steel reinforcement restricts but does not prevent shrinkage in its effective direction. It prevents free shrinkage of the concrete immediately adjacent to the steel to which it bonds, thereby inducing tension in the concrete and compression in the steel. The amount of concrete that participates in this interaction determines the compressive effect on the steel". This implies that plane sections before the shrinkage effect has taken place, may not necessarily remain plane afterwards. This does not agree with the assumption of linear strain distribution across the section on which he based the following relationship of strain-curvature in his analysis:

$$\text{Shrinkage curvature } \phi = \frac{S_f - S_g}{d} \dots\dots\dots(12)$$

$$= \frac{S_f}{d} \frac{(1 - S_s)}{S_f} \dots \dots \dots (13)$$

and the deflection " $\delta_{max}$ "

$$\delta_{max} = \frac{S_f}{8d} L^2 \left[ 1 - \frac{S_s}{S_f} \right] \dots \dots \dots (14)$$

where,

$S_s$  = shrinkage strain in the steel,

$S_f$  = free drying shrinkage of concrete,

$d$  = effective depth of member above steel level,

$L$  = the length of the member.

He stated that  $S_s/S_f$  is constant and dependent on the cover of the steel rather than the percentage of steel. The above equation can be only used when  $d \geq 2/3$  the total depth of the member.

Corely and Sozen (43), in 1966, suggested the use of the following expression to estimate the ultimate shrinkage curvature  $\phi_u$ :

$$\phi_u = \frac{0.035}{d} (P - P') \dots \dots \dots (15)$$

where,

$P'$ ,  $P$  = Compression and tension reinforcement ratios respectively,

$d$  = Effective depth of member above steel level.

Equation 15, was limited to concrete having an ultimate drying shrinkage, of 500  $\mu$  in./in.. To account for the shrinkage curvature at any time, they suggested the following factor  $G$  :

$$G = 0.13 \ln (t + 1) \dots\dots\dots(16)$$

$$\phi_t = G \cdot \phi_u \dots\dots\dots(17)$$

$$= \frac{.00455}{d} (P - P') \ln (t + 1) \dots\dots\dots(18)$$

Elvery and Shaffi (40), in 1970, considered the curvature  $\phi$  due to shrinkage according to the assumption for Working Stress Design as:

$$\phi = \frac{M}{EI} = \frac{\text{bending moment}}{\text{flexural rigidity}} \dots\dots\dots(19)$$

from which the following equation for the deflection was obtained:

$$\delta_{\text{max}} = \frac{p \cdot e \cdot L^2}{8 E_e I_c} \dots\dots\dots(20)$$

- where
- p = shrinkage force,
  - L = length of member,
  - e = eccentricity.

The effect of creep was taken into account by using an effective value of static elastic modulus of the concrete,



$$E_e = \frac{E_c}{(1+m)} \dots\dots\dots(21)$$

where,

$E_c$  = Young's modulus of concrete,

$m$  = ratio of creep to elastic strain.

ACI Committee 209 (36), suggested the following equation for predicting shrinkage deflection of eccentrically reinforced concrete members:

$$\delta_{\max} = A_w \phi L^2 \dots\dots\dots(20a)$$

where,

$A_w$  = deflection coefficient,

= 1/2 for cantilever members,

= 1/8 for simply supported members,

$\phi$  = shrinkage curvature,

$$= \frac{P_e e}{E_e I}$$

$E_e$  =  $E_c/(1+m)$

$P$  =  $(A_s - A_s') S_f E_s$

$m$  = creep strain to elastic strain,

Based on the available experimental data on creep, they suggested the use of an average value for  $\mu$  equal to 1.0. Their expression for the shrinkage force assumes the shrinkage strain in steel equal to the free drying shrinkage of plain concrete.


Washa (46)(47), presented experimental results of shrinkage and creep deformations of reinforced concrete slabs and beams. The specimens were dried in air where the temperature varied from 70 to 86°F and the ambient relative humidity varied from 20 to 80 percent. He admits that the estimated shrinkage deformations of the tested specimens are not completely valid, but they provide a rough estimation. He concluded that the presence of compression reinforcing in concrete members results in lower creep and shrinkage deformation than in members with tension reinforcing only.

#### SUMMARY:

From the foregoing it can be seen that, most of the methods suggested for the prediction of shrinkage stresses and deformations require an experimental evaluation of several constants which vary for different concretes, percentages of reinforcement and ambient conditions...etc.

Figure 14a shows typical shrinkage results of reinforced slabs fitted with the most current empirical Equations suggested

by Fintel and Khan (35) and ACI Committee 209 (36) (Based on the present state of the art, 1970). This figure clearly shows the deficiency of current empirical methods for the prediction of drying shrinkage of reinforced concrete.



## CHAPTER IV

### RESEARCH AIMS

It has been shown that the shrinkage of plain concrete can be described by linear diffusion theory. However, this method still requires an experimental evaluation of the ultimate shrinkage of the concrete.

Only a limited amount of experimental data has been published on the shrinkage of reinforced concrete. Based on the limited results which have been published, the methods which have been suggested for predicting the shrinkage of reinforced concrete do not appear to provide a practical solution to the problem. The effect of such factors as the percentage of reinforcement, bar diameter, and specimen size of reinforced concrete members have not yet been adequately established.

In general, therefore, the writer's research aim was to develop a practical method for predicting the shrinkage of reinforced concrete members. In detail this involved the following:

#### APPLICATION OF DIFFUSION ANALOGIES:

Since diffusion theory seems to take into account all the main variables affecting the shrinkage of plain concrete, the

author attempted to apply this method to the prediction of the drying shrinkage of reinforced concrete. In general terms, this entailed developing a diffusion analogy which would adequately take into account the effects of specimen size, different bar diameters, different percentages of reinforcement, and different ambient relative humidities. It was also necessary to determine how the shrinkage diffusion coefficients of plain and reinforced concrete vary as a function of the different variables mentioned above.

#### EVALUATION OF THE ULTIMATE SHRINKAGE:

Since diffusion theory requires the experimental evaluation of the ultimate shrinkage, it would be advantageous to establish a quick method to evaluate the ultimate shrinkage of plain and reinforced concrete.

The second part of this research programme was, therefore, to study the shrinkage of plain and reinforced concrete dried under accelerated conditions. In specific terms this investigation was designed to establish a quick method to evaluate the ultimate shrinkage of plain and reinforced concrete for different ambient relative humidities and to determine how the moisture loss and the shrinkage development of plain and reinforced concrete are related under accelerated conditions of drying.

### Theoretical Analysis:

The purpose of the theoretical analysis was to establish a relationship between the ultimate shrinkage of reinforced concrete members and the ultimate shrinkage of similar plain concrete members, taking into account the effect of different percentages of reinforcement located symmetrically and eccentrically with respect to the concrete section.

### SHRINKAGE STRESS DEVELOPMENT:

The third part of this research programme was designed to study the development and distribution of shrinkage stresses in reinforced concrete members, in an attempt to take into account the effect of member length.

CHAPTER V

THEORETICAL CONSIDERATIONS

From the foregoing, it can be seen that the problem of predicting the drying shrinkage of reinforced concrete members is a difficult one. It has been shown that diffusion theory can be applied to predict the drying shrinkage of plain concrete. The analytical methods which have been suggested for predicting the shrinkage of reinforced concrete need more experimental verifications and do not appear to provide a practical solution to the problem.

The writer believes that to achieve a more practical method of predicting the shrinkage of reinforced concrete, diffusion theory combined with a theoretical analysis to establish the relationship between the shrinkage of reinforced concrete and the shrinkage of similar plain concrete represents the most promising approach.

DIFFUSION THEORY:

Diffusion is the process by which matter is transported from one part of a system to another as a result of random molecular motions. The transfer of molecules usually takes place from the region of higher to that of lower concentration (44).

Transfer of heat by conduction is also due to random molecular motions. The mathematical theory of diffusion was first introduced by Fick, based on the mathematical equation of heat conduction derived some years earlier by Fourier. The drying of porous solids can be described by the theory of heat diffusion, which is based on the hypothesis that the rate of transfer of diffusing substance through unit area of a section is proportional to the concentration gradient measured normal to the section, i.e.,

$$\frac{\partial C}{\partial t} = K \frac{\partial C}{\partial x} \dots\dots\dots(22)$$

In general, the differential equation of diffusion takes the form:

$$\frac{\partial C}{\partial t} = \text{div. } (K \text{ grad. } (C)) \dots\dots\dots(23)$$

where,

- C = The amount of diffusing substance
- t = time
- K = diffusion coefficient
- (x,y,z.) = rectangular coordinates.

When the diffusion coefficient K is constant equation 23,



becomes,

$$\frac{\partial C}{\partial t} = K \left[ \frac{\partial^2 C}{\partial x^2} + \frac{\partial^2 C}{\partial y^2} + \frac{\partial^2 C}{\partial z^2} \right] \dots \dots \dots (24)$$

Initial and Boundary Conditions:

The initial moisture content ( $C_0$ ) is considered constant throughout the body, i.e.,

$$C = C_0 \quad \text{at} \quad t = 0 \dots \dots \dots (25)$$

The boundary conditions are expressed by formulae analogous to Newton's Law of cooling at the boundaries, i.e.,

$$\frac{\partial C}{\partial N} = \frac{\partial C}{\partial x} = \frac{\partial C}{\partial y} = \frac{\partial C}{\partial z} = \frac{f}{K} (C_0 - C) \quad \text{at exposed boundaries.} (26)$$

$$\frac{\partial C}{\partial N} = \frac{\partial C}{\partial x} = \frac{\partial C}{\partial y} = \frac{\partial C}{\partial z} = 0 \quad \text{at sealed boundaries,} \dots (27)$$

where,

f = surface factor,

N = normal to the surface.

For slow drying material such as clay, brick, and concrete, the parameter,  $fb/k$ , may be considered equal to infinity. The error introduced by this assumption is negligible, when the value of the parameter,  $fb/k$ , exceeds 100. This assumption was made by Terzaghi and Frohlich (27), Carlson (37), and many other investigators. Accordingly, the initial and boundary conditions become:

$$C = C_0 \quad \text{at } t = 0 \text{ in the interior} \dots\dots(25)$$

and  $C = 0 \quad \text{at } t = 0 \text{ at exposed surface} \dots\dots(28)$

Solution of the diffusion equation was obtained using the above simplified boundary conditions, and can be found in References 27, and 44.

#### Rectangular Members Drying from 1, 2, or 4 Sides:

Only the exact solution of the diffusion equation by Fourier series will be presented. A discussion of the different methods used to solve the diffusion equation can be found in References 15 and 44.

Slabs or Beams Drying from one or two Sides (2b): In this case, the general linear diffusion equation 24, reduces to:

$$\frac{\partial C}{\partial t} = K \frac{\partial^2 C}{\partial y^2} \dots \dots \dots (29)$$

The solution of equation 29 is therefore,

$$C = \frac{4C_0}{\pi} \sum_{n=1}^{\infty} \frac{(-1)^{n-1}}{(2n-1)} \exp \frac{1-(2n-1)^2 \pi^2 Kt}{4b^2} \cos \frac{(2n-1)\pi y}{2b} \quad (30)$$

The above equation can be modified to obtain the fractional moisture loss (1-U) such as,

$$(1-U) = \frac{C_0 - C}{C_0} = 1 - \frac{4}{\pi} \sum_{n=1}^{\infty} \frac{(-1)^{n-1}}{(2n-1)} \exp \frac{1-(2n-1)^2 \pi^2 Kt}{4b^2} \cos \frac{(2n-1)\pi y}{2b} \dots \dots \dots (31)$$

where,

$$U = \frac{C}{C_0}$$

The average fractional moisture loss (1-Ū) can be obtained by integrating the above equation with respect to y and dividing the integral by the depth b, i.e.,

$$(1-\bar{U}) = \frac{1}{b} \int_0^b (1-U) dy \dots \dots \dots (32)$$

$$= 1 - \frac{8}{\pi^2} \sum_{n=1}^{\infty} \frac{1}{(2n-1)^2} \exp \frac{-(2n-1)^2 \pi^2 Kt}{4b^2} \dots (33)$$

Beams or Columns Drying from Four Sides: The solutions for

rectangular members drying from four sides can be obtained by superposition from the slab solution.

Rewriting equation 33, in the form

$$(1-\bar{U})_S = (1 - \text{series (B)}) \dots \dots \dots (34)$$

Solution for the average fractional moisture loss of rectangular members (2b x 2a) can be obtained such as,

$$(1-\bar{U})_R = 1 - (\text{series (B)}) \cdot (\text{series (A)}) \dots \dots (35)$$

#### Shrinkage Diffusion Analogies:

The application of diffusion theory to describe the drying shrinkage of plain concrete was made on the assumption of a linear relationship between moisture loss and shrinkage (15)(27). Accordingly the following mathematical assumptions can be made:

$$(1-\bar{U}) = f (S_{av}/S_u)_f = (S_{av}/S_u)_S \dots \dots \dots (36)$$

where,

- $(1-\bar{U})$  = the average fractional moisture loss
- $(S_{av}/S_u)_f$  = the average fractional free drying shrinkage of concrete.
- $(S_{av}/S_u)_S$  = the average fractional shrinkage strain in steel.

Solutions of the diffusion equation for rectangular members drying from 1, 2, or 4 sides are presented, for the average fractional shrinkage ( $S_{av}/S_u$ ) versus the Fourier number to an arbitrary scale, in figures 15 to 19.

#### THEORETICAL ANALYSIS:

From the foregoing, it can be seen that diffusion theory can be used to develop equations for the average shrinkage of plain and reinforced concrete as a function of the ultimate shrinkage. The evaluation of the ultimate shrinkage is still to be determined. The following analysis is therefore, intended to establish a relationship between the ultimate shrinkage of reinforced concrete members, and the ultimate shrinkage of similar plain concrete members, taking into account the effect of different percentages of reinforcement located symmetrically and eccentrically with respect to the concrete section.

#### Preliminary Assumption:

It is obvious that for unrestrained members, the shrinkage force acting on the steel and concrete portions must be equal, and act in opposite directions. Also neglecting slip, the strain in the steel will be equal to the resultant strain in concrete ( $S_f - S_{cn}$ ), figure 20. In more specific terms the assumptions for the equilibrium conditions are,

Equilibrium of Forces: In each member the sum of forces in the concrete is equal to the sum of forces in the steel, act in the opposite direction, and lie on the same line since the sum of moments of both forces is equal to zero, i.e.,

$$P_c = P_s = P \dots\dots\dots(37)$$

Compatibility of Strains: Assuming no bond slip away from the ends of the member, the sum of strain of both materials at steel level is equal to the free shrinkage of a similar plain concrete member, i.e.,

$$S_s + S_{cn} = S_f \dots\dots\dots(38)$$

where,

- $S_s$  = the shrinkage strain in steel,
- $S_{cn}$  = the shrinkage strain in concrete,
- $S_f$  = the free drying shrinkage of a similar plain concrete member.

Using the above assumptions, the shrinkage force (P), and hence, the shrinkage strain in steel ( $S_s$ ) were derived for the following cases:

Eccentrically Single-Reinforced Member:

The shrinkage force is therefore,

$$P = \frac{A_s A_c E_s I_c}{I_c (nA_s + A_c) + nA_s A_c e^2} S_{fc} \dots\dots\dots (39)$$

and the shrinkage strain in steel is,

$$S_s = \frac{A_c I_c}{I_c (nA_s + A_c) + nA_s A_c e^2} S_{fc} \dots\dots\dots (40)$$

where,

$A_c$  = area of concrete,

$A_s$  = area of steel,

$I_c$  = moment of inertia of the concrete section,

$n = E_s / E_c \cdot (1+m)$

$m$  = creep to elastic strain ratio,

$e$  = the eccentricity.

Symmetrically Reinforced Member:

The shrinkage force, and the shrinkage strain in steel can be easily obtained by substituting the eccentricity  $e$  in equations 39 and 40, to be equal to zero. Thus,

$$P = \frac{A_s A_c E_s}{(nA_s + A_c)} S_{fc} \dots\dots\dots (41)$$

$$S_s = \frac{A_c}{(nA_s + A_c)} S_{fc} \dots\dots\dots(42)$$

Considering the gross area  $A_G = A_s + A_c$  and the percentage of reinforcement  $P_s = A_s/A_G$  equation 42, can be written in the form:

$$S_s = \frac{1 - P_s}{1 + (n-1)P_s} S_{fc} \dots\dots\dots(43)$$

The previous equation can be applied to obtain the shrinkage force P, and the shrinkage strain in steel  $S_s$ , for long members.

For short members, the average strain over the length of the reinforcing bars  $S_{sa}$  will be less than the strain in the central portion  $S_s$  due to the bond slip at the ends.

Shrinkage Deformation:

In eccentrically reinforced members, the shrinkage force P tends to cause bending moments acting on the concrete section which cause the member to warp or deflect depending on the location of steel with respect to the concrete section. Neglecting the end portions, and for long members such moments will be constant along the member, i.e.,

$$M = P.e \dots\dots\dots(44)$$



and the shrinkage curvature is,

$$\phi = \frac{M}{E_c' I_c} \dots\dots\dots(19a)$$

Thus, the maximum shrinkage deflection  $\delta_{max}$ , for uniform member, is therefore,

$$\delta_{max} = A_w \phi L^2 \dots\dots\dots(20a)$$

where,

- $A_w$  = deflection coefficient
- = 1/2 for cantilever member
- = 1/8 for simply supported member...etc.,

- $E_c'$  = effective modulus of elasticity
- =  $\frac{E_c}{(1+m)}$

$m$  = creep strain to elastic strain

$I_c$  = moment of inertia of the concrete section

$L$  = the span of the member.

The maximum shrinkage deflection can be written in the form,

$$\delta_{max} = \frac{A_w \cdot P \cdot e \cdot L^2}{E_c' I_c} \dots\dots\dots(45)$$

The maximum value of  $m$  ranges from 1.5 to 2.0 . Based on the

available creep data reported by many investigators, ACI Committee 209 (36), suggested that a value of  $m$  equal to 1.0 can be used with reasonable accuracy in predicting the shrinkage deflection.

For concrete members with tension and compression reinforcements, the principle of superposition can be used for evaluating the shrinkage force and deflection. Thus,

$$P = P_t + P_c$$

and

$$\delta = \delta_t - \delta_c$$

where,

$P_t, P_c$  = shrinkage force of concrete member due to tension and compression reinforcement respectively

$\delta_t, \delta_c$  = shrinkage deflection of concrete member due to tension and compression reinforcement respectively.

## CHAPTER VI

### EXPERIMENTAL PROGRAMME AND PROCEDURES

#### EXPERIMENTAL INVESTIGATIONS:

The purpose of this experimental programme was; to provide a wide range of experimental data to test the theoretical methods developed by the author to predict the shrinkage of reinforced concrete members; to establish a quick method of evaluating the ultimate shrinkage of plain and reinforced concrete; and to study the development of shrinkage stresses in reinforced concrete.

The experimental programme can be considered to include the following three separate investigations:

#### Drying Shrinkage of Reinforced Concrete Members:

This investigation was designed to cover a wide range of slabs, rectangular beams, and columns to establish whether diffusion theory can take into account the effects of specimen size, percentage of reinforcement, bar diameter, and the ambient relative humidity. Since this involves long term experimentation, this investigation was initiated as soon as possible in the author's programme. The variables which were included in this investigation are the following:

1. Cement: .....Type I and Type III.

2. Plain and Reinforced Concrete Specimens:..slabs drying from two sides having widths of 3,6,9, and 12 inches. Beams drying from four sides having a height of 3 inches and widths of 3,6,9, and 12 inches. Square columns drying from four sides having dimensions of 4x4, 6x6, and 8x8 inches.
3. Reinforcement:.....symmetrical reinforcement, slabs and beams having percentages of reinforcement of 2.22%, 3.45%, and 4.9% using #4, #5, and #6 steel bars respectively. Columns having percentages of reinforcement of 1.25, 2.5%, 3.75% and 5% using #4 bars with the 4x4 inch specimens #6 bars with the 6x6 inch specimens, and #8 bars with the 8x8 inch specimens, figures 21, and 22.
4. Relative humidities:.....7%, 32%, 54%, and 76% under constant temperature of 70<sup>+</sup>2<sup>o</sup>F.

Ultimate Shrinkage Development Under Accelerated Drying Condition:

The purpose of this investigation was to establish a quick test for the determination of the ultimate shrinkage of plain and reinforced concrete members. This investigation also considered the relationship between moisture loss and shrinkage of plain and reinforced concrete under the accelerated conditions of drying. The mixes were made using Type I cement. The variables which were included in this investigation are the following:

1. Length of moist Curing:..... 1,3, and 7 days.
2. Plain and Reinforced Specimens:...slabs drying from two sides having widths of 3,6, and 9 inches.
3. Reinforcement:...symmetrical reinforcement using #5 bars with a percentage of reinforcement of 3.45% for all specimens.
4. Drying Condition:....by the application of 15 psig vacuum at a temperature of 100 °F, and by the application of heat at a temperature of 220 °F.

#### Shrinkage Stress Development:

The purpose of this investigation was to study the bond stress developed between the concrete and the reinforcing bars due to shrinkage, and the distribution of shrinkage stresses along the reinforcing bars in an attempt to take into account the effect of member length. The mixes were made using Type I cement. The specimens were dried in a relative humidity of 7% at a constant temperature of  $70 \pm 2^{\circ}\text{F}$ . The variables which were included in this investigation are the following:

1. Plain and Reinforced Specimens:...square columns drying from four sides having dimensions of 4x4, 6x6, and 8x8 inches.
2. Reinforcement:.....symmetrical reinforcement  $P_s = 1.25\%, 2.75\%$   
6 specimens with unsymmetrical reinforcement  $P_s = 1.25\%, e=t/4$

3. Specially Reinforced Specimens:..square columns drying from four sides having dimensions of 4x4 and 6x6 inches, symmetrically reinforced using #6 and #8 modified steel bars with effective percentages of reinforcement of 2.2% and 1.86% respectively.
4. Type of specimens:...Group I specimens, include all the reinforced specimens, applying strain gages at 4 or 5 locations along the 12" long reinforcing bars. Group II specimens, include all the reinforced and plain concrete specimens, using screw inserts attached to the reinforcing bars or embeded in the concrete at both ends respectively; the screw inserts will be discussed later in this chapter.

#### MATERIALS:

##### Cement:

Both Type I ordinary and Type III high early cements were used in the first investigation. Only Type I cement was used in the subsequent investigations. These cements were Lake Ontario ordinary and Canada High Early Cement. Each type of cement was thoroughly blended, according to ASTM specification before it was used. The compound composition and physical tests of both cements are presented in Appendix C.

Sand:

The sand used in this experimental programme was a well-graded natural sand obtained from the west pit at Paris, Ontario, which meets ASTM specification C33. The sand was oven-dried for 24 hours at a temperature of 220°F, and then stored in sealed metal drums to cool to room temperature before being used. The properties of the sand are presented in Appendix C.

Coarse Aggregate:

The coarse aggregate used in this programme was a locally obtained crushed limestone, conforming to ASTM specifications for concrete aggregates C33. The maximum size of aggregate was 3/4 inch, and the sieve analysis results are presented in Appendix C. The coarse aggregate was used in a saturated surface dried condition. This was accomplished by soaking the aggregate for 24 hours and then drying the surface before being used.

Reinforcing Bars:

The reinforcing bars used in this programme were intermediate grade deformed bars conforming to ACI specifications, supplied by a local company, and were cut to a length of 12 inches. Each bar was drilled at both ends with an 8/29 drill to a depth of

$3/4$ " , and was tapped with an 8-32NC tap. Screws of  $1\frac{1}{2}$ " long were then inserted into the bars. After the screws were tightened, the heads were then cut and filed. A  $3/8$ " hexagonal brass stud of  $3/4$ " length and with  $1/2$ " tapped hole was tightened to each screw when the reinforced specimens were stored into the drying chambers.

#### Screw Inserts:

For the plain concrete specimens, 8-32NC screws, of  $1\frac{1}{2}$ " long were embeded at both ends for a distance of  $3/4$ " , and were tightened to the forms by nuts and washers. The brass studs were tightened to these screw inserts later in the storage process which will be discussed later in this chapter.

#### Strain Gages:

The strain gages used in the third investigation were supplied by W.T, Bean Inc., Detroit, Michigan. The gages had a gage factor of  $2.02 \pm 0.2$  Ohms, and a gage length of  $1/8$  inch. A smooth clean surface was achieved at all gage locations. The gages were fixed using Type 910 cement and then coated with special moisture preventing coats. The gages were placed outside, except for the modified bars where the gages were placed on the inside after the bar was cut into two halves. The two halves were then fixed together by a special steel cement . The gages were located as shown in figure 23.



EXPERIMENTAL PROCEDURES:

Mix Proportions:

The mix proportions were obtained using the ACI standard method for the design of concrete mixes. The mix was then modified experimentally to give a slump of 2 to 3 inches and a 28 day strength of about 5000 psi. The mix proportions may be found in Appendix C.

Mixing Procedure:

The mixes for the first and second investigations were prepared using a drum mixer manufactured by Soiltest Inc., of 1 1/2 cubic foot capacity and powered by a 1/3 H.P. electric motor. The coarse aggregate and water were first placed in the mixer. The cement and sand were then gradually added as mixing commenced. The materials were then mixed for a period of 2 minutes, followed by a 1 minute rest, and 2 minutes of further mixing. This method was found experimentally to give more homogeneous mixing.

The workability of the batches was established using the slump test, which was conducted according to ASTM specification C143.

The mixes for the third investigation were prepared using a Counter-Current Rapid Mixer, manufactured by Eirich Inc. of West Germany, of 5 cubic foot capacity and powered by a 7.5.H.P. Tamper

A.C.Motor. The concrete was mixed according to ASTM specification C192.

Forms Preparation:

The column specimens were prepared using steel forms designed and machined by the writer. 1/8" diameter holes were drilled through the base of the forms at different locations according to the type of specimen. These holes were used later to hold the screw inserts for the plain concrete specimens as well as the prepared reinforcing bars for the reinforced specimens. At the top, 1/4" thick steel strips with holes were used to hold the bars and the screw inserts. The forms were covered with a very thin coat of clear form oil before being used.

The slab and beam specimens were prepared using wooden forms. Similar holes were drilled through both ends at the required location according to the size of specimen to hold the bars and the screw inserts. Polyethylene sheets (6MIL), were placed inside the forms to prevent any moisture loss through the forms. The sheets were held by masking tape and tacks at each corner.

Moulding and Compaction:

For all column specimens steel forms were used. However, due to the large number and different sizes of slab and beam specimens, wooden forms were used to accelerate the manufacturing of these specimens. The batches were kept within 1 to 1.3 cubic

feet to avoid spill of concrete during mixing.

The forms were placed on the vibrating table (VIBCO Table Vibrator, model U.S. 450, 115 Volts, 2.8 amp., and 10,000 V.P.M.) and were not removed at any time during the filling and tamping operations. The concrete was placed in three layers in the forms. After each layer was placed the concrete was tamped with 3/4" diameter steel rod about 25 times. The filling and vibrating operation took about 8 to 10 minutes. This casting operation was found to give well compacted concrete in the corners and around the steel bars.

Due to the large number of batches required to manufacture all specimens, the specimens were divided into groups according to the Type of cement and the ambient relative humidity condition. Each group of specimens was prepared in one day by mixing 4 or 5 batches daily.

#### Curing:

Immediately after moulding, the specimens were placed in a moist curing chamber, which was maintained at  $70 \pm 2^{\circ}\text{F}$  and about 100 percent relative humidity. The specimens were placed on wooden shelves built inside the chamber, and were covered with 6 mil polyethylene sheets to avoid dripping of water on the surface of the fresh specimens. The next day the forms were stripped and the concrete specimens were returned to the moist chamber for a

further six days after which they were sealed and stored in the preconditioned drying chambers.

#### Sealing:

After 7 days of moist curing the specimens were removed from the moist chamber to another temperature-controlled lab. The column and beam specimens were sealed at both ends, while the slabs were sealed on both ends and on top and bottom to allow drying horizontally. The sealing was done using a commercial asphalt, and 4 mil and 6 mil polyethylene vapour-tight sheets.

The specimens were surface dried using paper towels. The asphalt was applied using a paint brush. Immediately after the first asphalt coat was applied a precut strip of 4 mil polyethylene was placed on the wet coat. This strip was then covered with another asphalt coat and a 6 mil polyethylene strip was finally placed on the sealed area. To avoid sliding of the polyethylene strips, they were held by elastic bands. Additional masking tape was fixed at the two edges of the polyethylene strips for the slab specimens only.

#### Storage:

The sealed specimens were placed in preconditioned relative humidity chambers or vacuum drums according to the condition of drying.

The humidity chambers were built of 3/4" ply wood. Each chamber had a top, a bottom, and two ends. The two open sides were either 8 or 10 ft long and between 12 to 20 inches high depending on the number of shelves required to store the specimens in one or three rows. The width of these chambers was 12", which was the same length of the specimens. The chambers were covered with 6 mil polyethylene sheets all around. The screw inserts of each specimen were then punctured through the polyethylene sheets and the hexagonal brass studs were tightened with washers to these screws to insure proper seating for the extensometer which was used later to take the shrinkage readings.

The relative humidity was accomplished by using special saturated salt solutions. The salt solutions were stored in pyrex glass pans at the bottom of each chamber. To insure the exact relative humidity through every chamber, special vacuum-pressure air pumps were used to draw the air through these salt solutions and back to the pump through 3 holes at the top of the chamber. The salts used in this programme to provide the required relative humidities were:

Sodium Hydroxide.....7% R.H.,  
 Calcium chloride.....32% R.H.,  
 Magnesium nitrate.....54% R.H., and  
 Sodium chloride.....76% R.H..

Figure 24, shows a typical humidity chamber.

The vacuum drums were of 45 gallon capacity. Movable wooden shelves were built inside each drum to provide proper storage of the specimens. Sodium chloride crystals were placed in the bottom of the drums to absorb any available moisture. To insure against leakage through the drums, a clamped cover with a rubber liner was used to seal the top. A 15 psig vacuum pressure was applied to these drums, and the temperature was maintained at  $100 \pm 2^{\circ}\text{F}$  by means of an electric heater and fan built inside the storage room previously used as a moist-chamber in this experimental programme.

The oven-dried specimens were placed in the oven immediately after sealing and the zero readings were then recorded. The temperature in the oven was  $105^{\circ}\text{C}$  throughout the drying process. Before taking the subsequent readings the specimens were allowed to cool for 12 hours to room temperature.

#### Readings and Measuring Technique:

Readings: After the specimens were placed inside the humidity chambers, the polyethylene cover was sealed with masking tape. The zero shrinkage readings were then recorded for every specimen; the readings were measured using a specially designed extensometer, figure 25.

For the specimens stored in the vacuum drums, the zero shrinkage readings and original weight were recorded before placing

the specimens inside the drum. Additional readings were taken after removing the specimens from the drums when necessary. The vacuum had to be removed for an hour to enable recording of the readings. This was not done for the specimens stored in the humidity chambers as the shrinkage readings were taken from the outside without disturbing the specimens.

Measuring Technique: The water loss was measured using a Fairbanks Morse Scale of 36 lbs capacity, and 0.01 lbs accuracy. The only exception, was for the 4x4 oven-dried specimens, where the water loss was measured using a Berkel Scale of 10 kg capacity and  $\frac{1}{2}$  gm accuracy.

The two extensometers used to measure the length changes were specially built of  $1\frac{1}{2}$  x  $1\frac{1}{2}$  x  $\frac{1}{4}$  steel T-Section as shown in figure 25. The extensometer was seated freely on the hexagonal brass studs. It had a micro head at one end and 1" travel dial gage at the other end, with an accuracy of  $1 \times 10^{-4}$  inches. This was found to give a minimum seating error of  $1 \times 10^{-4}$  in. A small water level was used to insure consistency in the position of the extensometer. To avoid any temperature effect, the extensometer was calibrated and checked frequently during the reading process with a standard 12" long invar bar with brass studs fitted on its ends. The extensometer was kept at the same temperature as the stored specimens.

Budd switch and balance units and a Budd strain recorder were used to measure the strain readings in the third investigation. The system had an accuracy of  $5 \times 10^{-6}$   $\mu$  in/in.



## CHAPTER VII

### DISCUSSION OF RESULTS

After the shrinkage readings were taken at the selected gage points as described in chapter VI, the average shrinkage strain in steel ( $S_{av}$ ) of the reinforced specimens, as well as, the average free drying shrinkage ( $S_{av}$ ) of the corresponding plain concrete specimens were then calculated. The ultimate shrinkage values ( $S_u$ ) for each group of specimens dried under normal condition were reached after approximately 250 days of drying of the 3 x 3 in. slab and the 4 x 4 in. column specimens. The average fractional shrinkage readings ( $S_{av}/S_u$ ) were then calculated and tabulated in Appendix D.

The ultimate shrinkage and the ultimate moisture loss of the specimens dried by the application of 15 psig vacuum and 100°F were reached after 120 days of drying of the 3 x 3 in. slab specimens. Similarly the average fractional shrinkage ( $S_{av}/S_u$ ) and the average fractional moisture loss ( $1 - \bar{U}$ ) were calculated and then tabulated in Appendix D.

Each group of specimens was classified by a code system located at the upper left hand corner of every table and graph. For example, Series III -S-32%,  $P_g=3.45\%$ . represents the slab specimens made of Type III cement, reinforced with 3.45 per cent

steel, and dried in an ambient relative humidity condition of 32%.

MOISTURE LOSS VERSUS SHRINKAGE OF REINFORCED CONCRETE:

The application of diffusion analogies for the prediction of reinforced concrete shrinkage was based on assuming a linear relationship between moisture loss and drying shrinkage. To verify this assumption, 54 reinforced concrete specimens were tested. The specimens were subjected to 15 psig vacuum, at a temperature of 100°F. The results of the average fractional shrinkage ( $S_{av}/S_u$ ) were plotted against the corresponding average fractional moisture loss ( $1 - \bar{U}$ ) and are presented in figures 26 to 28. Each graph is identified by a code system on the upper left hand corner. For example, I-S-3D-VAC.,  $P_s = 3.45\%$ , represents the slab specimens made of Type I cement, moist cured for 3 days, reinforced with 3.45% steel, and subjected to the vacuum drying condition mentioned above.

An examination of these graphs shows that, at early ages a comparatively small amount of shrinkage occurs as compared with the relatively large amount of moisture loss. This is probably due to an excess of moisture at the surface before the specimens were subjected to drying. Also the shrinkage readings represent the average shrinkage values along the width of the slab at a minimum distance of  $1\frac{1}{2}$  inches from the drying surface as the bars and the

brass inserts could not be located at the surface, where a large amount of shrinkage probably occurs at the early ages of drying.

At later ages, plots of the results show a relatively linear relationship that may be approximated by a straight line. The 7-day moist cured specimens show less scatter than the 1 and 3-day moist cured ones. This could be due to a change in the initial drying temperature ( $100^{\circ}\text{F}$ ) that was encountered with the 1 and 3-day moist cured specimens. The slope of the lines appear to be independent of the reinforcement, size of specimen and the length of moist curing.

The results of the average fractional moisture loss ( $1-\bar{U}$ ) and the average fractional shrinkage ( $S_{av}/S_u$ ) were then plotted against the Fourier number ( $t/b^2$ ) and are presented in figures 29 to 34. The theoretical curves which fit the results best were then plotted and the corresponding diffusion coefficients  $K$  were located on the inside left hand corner of each graph.

An examination of these graphs shows that there is less scatter in the moisture loss plots than the shrinkage ones. Also more scatter was observed in the shrinkage plots of the 1 and 3-day moist cured specimens than with the 7-day moist cured ones. The length of moist curing seems to have little effect on the moisture diffusion coefficient  $K$ .

The moisture diffusion coefficient  $K$  of the reinforced specimens was slightly higher than that of the plain concrete ones. This is due to the fact that, the steel bars replace some of the concrete, and the ultimate moisture losses of the reinforced specimens were less than those of the plain concrete specimens.

APPLICATION OF DIFFUSION ANALOGIES TO THE SHRINKAGE OF  
REINFORCED CONCRETE:

The shrinkage results of the reinforced concrete specimens, over 500, which cover a wide range of columns, and slabs, are tabulated in Appendix D. The results of the average fractional shrinkage strain in steel ( $S_{av}/S_u$ ), as well as, the average free drying shrinkage of a similar plain concrete ( $S_{av}/S_u$ ) were plotted versus the Fourier number ( $t/b^2$ ), and are presented in figures 35 to 68.

Diffusion Analogies of Constant Diffusion Coefficients K:

Solutions of the diffusion equation of constant diffusion coefficients K, for rectangular members drying from 1, 2, or 4 sides were obtained for the average fractional shrinkage ( $S_{av}/S_u$ ) versus the Fourier number ( $t/b^2$ ), to an arbitrary scale and are presented in figures 15 to 19. The theoretical curves which fit the results best were then plotted (solid curve) and the corresponding diffusion coefficients K were located on the inside left hand corner of each graph.

An examination of these graphs shows that the shrinkage results of reinforced concrete tend to fall on a single theoretical curve regardless of specimen size. The shrinkage diffusion

coefficients  $K$  of the theoretical curves used to fit the data seem to be relatively unaffected by the percentage of reinforcement, bar diameter, type of cement, and the ambient relative humidity condition. It should be noted that the shrinkage data tends to fall above the theoretical curves at early ages (lower  $t/b^2$ ) and below the curves at later ages (higher  $t/b^2$ ). This means that the diffusion curves tend slightly to underestimate the average fractional shrinkage ( $S_{av}/S_u$ ) at lower values of  $t/b^2$  and to overestimate ( $S_{av}/S_u$ ) at higher values of  $t/b^2$ . The random scatter in some of the shrinkage data may be attributed to some errors during the preparation of the specimens and the measuring process. These errors will be discussed in detail later in this chapter. The effects of autogenous shrinkage, carbonation shrinkage, and creep are also included in the shrinkage readings and may have contributed to the scatter.

#### Diffusion Analogies of Variable Diffusion Coefficients:

To improve the fit of shrinkage results, an empirical assumption for the diffusion coefficients  $K$  was introduced. This assumption considered the diffusion coefficient  $K$  to be a function of the Fourier number ( $t/b^2$ ) and takes the form:

$$K = K_0 (A + B \ln (t/b^2)) \dots\dots\dots(46)$$

Introducing such an assumption in the solutions of the diffusion equation for rectangular members causes the theoretical curves to rotate depending on the values of the constants, A and B.

Several values of the constants A and B were assumed in order to arrive at the following expression for the diffusion coefficient K :

$$K = K_0 (1.0 - 0.1 \ln (t/b^2)) \dots\dots\dots(47)$$

This expression for the diffusion coefficient K causes the diffusion coefficient to decrease with time and the theoretical curves to give higher values of  $(S_{av}/S_u)$  for values of  $(t/b^2)$  less than 1.0 and lower values of  $(S_{av}/S_u)$  for values of  $(t/b^2)$  larger than 1.0. Solutions of the diffusion equation for rectangular members drying from 1, 2, and 4 sides using such an expression for the diffusion coefficient K were obtained for the average fractional shrinkage  $(S_{av}/S_u)$  versus the Fourier number  $(t/b^2)$  to an arbitrary scale, and are presented in figure 69.

The theoretical curves which fit the shrinkage results best were then plotted (dashed curve), and the corresponding  $K_0$  values were located on the inside left hand corner of each graph, figures 35 to 68.

An examination of these graphs shows that a better fit of the shrinkage results of reinforced and plain concrete specimens was obtained. Also the diffusion parameter  $K_0$  of the theoretical curves, used to fit the data, seem to be relatively independent of the percentage of reinforcement, bar diameter, type of cement and the ambient relative humidity condition.

Band of Theoretical Diffusion Curves:

The shrinkage diffusion coefficients  $K$  and the shrinkage diffusion parameters  $K_0$  of the theoretical curves which best fit the shrinkage results are presented in tables 1 and 2.

An examination of the  $K$  and  $K_0$  values, as affected by the different variables considered in this study, shows that the diffusion coefficients are not significantly affected by the percentage of reinforcement even when different bar diameters were used to give the same percentage of reinforcement. This means that only the percentages of reinforcement affect the ultimate shrinkage of reinforced concrete. Also the types of cement and the ambient relative humidity conditions seem to have no significant influence on the  $K$  and  $K_0$  values.

By plotting all the theoretical curves used to fit the data as shown in figures 70 and 71, it appears that most of these curves tend to fall within a very narrow band that can be

## SHRINKAGE DIFFUSION COEFFICIENTS

(K) and ( $K_0$ )

## Series I - C

R.H.		76%	54%	32%	7%
$P_s$					
0%-P.C.	K	.009	.013	.012	.010
	$K_0$	.008	.014	.012	.011
1.25%	K	.008	.010	.009	.010
	$K_0$	.009	.011	.010	.010
2.50%	K	.012	.010	.009	.010
	$K_0$	.012	.012	.008	.010
3.75%	K	.012	.010	.009	.010
	$K_0$	.012	.012	.010	.011
5.00%	K	.009	.010	.009	.008
	$K_0$	.010	.011	.009	.009

## Series III - C

R.H.		76%	54%	32% *	7%
$P_s$					
0%-P.C.	K	.012	.016	.020	.015
	$K_0$	.014	.016	.020	.014
1.25%	K	.008	.009	.012	.010
	$K_0$	.010	.010	.013	.011
2.50%	K	.010	.009	.014	.011
	$K_0$	.012	.010	.014	.013
3.75%	K	.011	.009	.010	.010
	$K_0$	.012	.010	.011	.011
5.00%	K	.010	.009	.009	.010
	$K_0$	.012	.011	.011	.011

Table I



SHRINKAGE DIFFUSION COEFFICIENTS  
(K) and ( $K_0$ )

Series I - S

$P_s$	R.H.	76%	54%	32%	7%
	0%-P.C.	K	.024	.023	.020
$K_0$		.030	.028	.021	.023
2.22%	K	.033	.020	.020	.020
	$K_0$	.038	.020	.023	.020
3.45%	K	.039	.023	.019	.020
	$K_0$	.041	.023	.023	.022
4.90%	K	.022	.030	.021	.020
	$K_0$	.028	.030	.024	.020

Series III - S

$P_s$	R.H.	54%	32%	7%
	0%-P.C.	K	.030	.020
$K_0$		.033	.023	.026
2.22%	K	.030	.020	.023
	$K_0$	.032	.023	.030
3.45%	K	.030	.020	.024
	$K_0$	.034	.024	.027
4.90%	K	.022	.023	.020
	$K_0$	.025	.030	.027

Table 2

approximated, without introducing any significant error, by a single theoretical curve. This means that the average shrinkage strain in steel ( $S_{av}$ ) can be predicted as a percentage of the ultimate shrinkage strain ( $S_u$ ), for any size member, percentage of reinforcement, type of cement, and dried under any ambient relative humidity condition.

Equation of Best Fit:

Three different empirical equations were also used to fit some selected shrinkage data. The least squares method was used to obtain the constants. These equations are

$$S_{av}/S_u = \exp(A + B(t/b^2)) \dots\dots\dots(48)$$

$$S_{av}/S_u = \exp(A + B \ln(t/b^2)) \dots\dots\dots(49)$$

$$S_{av}/S_u = A + B \ln(t/b^2) \dots\dots\dots(50)$$

The best correlation factor ( $R = 0.96$ ) was obtained using equation 50. The results were then plotted and are presented in figures 72 and 73. The  $X^2$  values were obtained and then compared with the  $X^2$  values obtained using the theoretical diffusion curve. It was found that the diffusion curves fitted the results better than the proposed empirical equation.

SHRINKAGE STRESSES DEVELOPMENT OF REINFORCED CONCRETE:

Shrinkage stresses developed due to non-uniform shrinkage of plain concrete members and the internal stresses caused by the restraining action of aggregates have been studied by Pickett (27), and are not considered in this study.

The main purpose of this investigation was to study the shrinkage stresses developed due to the restraining action of reinforcing bars introduced in the concrete member and to provide the pattern of stress distribution along the reinforcing bars. A number of reinforced concrete specimens (23) were then cast and prepared to study this phenomenon. The shrinkage strain readings along the reinforcing bars were recorded and plotted against the distance from the end of the member and are presented in figures 74 to 77. The dotted line represents the average shrinkage strain along the reinforcing bar.

The central strain results were also plotted against drying time along with the calculated values (solid curve) obtained from the theoretical equations and are presented in figures 78 to 86.

It is seen that these results support those of Glanville (31) that the shrinkage strain along the reinforcing bar increases towards the centre over a distance of about 3 in. from the end of the member. A constant strain value is observed over the central portion of the bar.

The central shrinkage strain in the steel was found to be about 20% more than the recorded average shrinkage strain of the 12" long members.

Also a reasonably good agreement was found between the experimental and the calculated values of the shrinkage strain in steel, for both symmetrically and eccentrically reinforced members. The location of the strain gages whether on the outside surface of the bars or on the inside of the modified bars, had no significant effect on the shrinkage strain in the steel.

The shrinkage stresses in steel and concrete were plotted versus time for a selected group of specimens, figures 87 and 88. Shrinkage stresses above 8000 psi compression in steel, and 300 psi tension in the concrete were observed in this investigation.

It appears that the higher the percentage of steel the lower the compressive stresses in steel, but the higher the tensile stresses in concrete. This can be attributed to the high shrinkage force developed due to the restraining action introduced by the large amount of reinforcing in the concrete member.

#### PREDICTION OF THE ULTIMATE SHRINKAGE:

From the foregoing discussion, it is apparent that for predicting the average shrinkage strain  $S_{av}$  of symmetrically and eccentrically reinforced members, we still have to be able to evaluate the ultimate shrinkage  $S_u$ .

The ultimate shrinkage can be obtained experimentally by drying a small specimen, subjected to any desired ambient humidity condition. This requires long time experimentation. It would be advantageous to establish a quick method to evaluate the ultimate shrinkage of plain and reinforced concrete.

It was found that the ultimate shrinkage of plain and reinforced concrete members, dried by the application of 15 psig vacuum and  $100^{\circ}\text{F}$ , was reached after 120 days, while the ultimate shrinkage under normal condition of drying was reached after about 250 days. This indicates that the vacuum temperature drying condition was not sufficiently effective to reduce the ultimate drying time enough to be of practical value.

The results obtained by drying at  $220^{\circ}\text{F}$  showed that the ultimate shrinkage of plain concrete was reached within 7 days, figure 89. However, the ultimate shrinkage of reinforced concrete could not be determined using this method due to the bond slippage that occurred during heating.

#### Quick Method of Evaluating the Ultimate Shrinkage:

The ultimate shrinkage of plain concrete members dried at any relative humidity condition ( $S_{UR}$ ) may be considered as a function of the ultimate shrinkage of similar oven-dried specimens ( $S_{UOV}$ ) and the relative humidity condition (R), such as:

$$S_{uR} = A S_{uov} f(R) \dots\dots\dots(51)$$

where,

A = a parameter independent of  $S_u$  and R,

f(R) = an expression dependent on the relative humidity (R).

The equation derived by Dutron (25), relating the shrinkage at any relative humidity condition ( $S_R$ ) to the shrinkage at 50% relative humidity ( $S_{50}$ ) is of the form:

$$S_R = S_{50} (0.96 \log \frac{105 - R}{5}) \dots\dots\dots(3)$$

Considering f(R) equal to  $\log(\frac{105-R}{5})$ , thus equation 51 can be written in the form:

$$S_{uR} = A \cdot S_{uov} \cdot \log \frac{(105 - R)}{5} \dots\dots\dots(52)$$

Based on the shrinkage results, tables 3 and 4, A was determined, and the ultimate shrinkage of plain concrete members at a relative humidity condition ( $R \leq 55\%$ ) can be evaluated as follows:

$$S_{uR} = 1.27 \cdot S_{uov} \cdot \log \frac{(105 - R)}{5} \dots\dots\dots(53)$$

For a wider range of relative humidity condition ( $R \leq 80\%$ )

the following equation that best fit the shrinkage results can also be used to evaluate ( $S_{UR}$ ):

$$S_{UR} = 1.54 S_{uov} - .84R \dots \dots \dots (54)$$

Evaluation of the Ultimate Shrinkage Strain in Steel ( $S_{us}$ ):

The results of the ultimate shrinkage strain in steel ( $S_{us}$ ) of the 12" long members dried under normal condition, are presented in tables 3 and 4. These results represent the average shrinkage strain along the reinforcing bars.

The central shrinkage strain in steel ( $S_{us}$ ) away from the ends of the member, was about 20% more than the average value. The ratios ( $S_{us}/S_{uc}$ ) were then plotted against the percentage of reinforcement and are presented in figures 90 and 91. The theoretical values of ( $S_{us}/S_{uc}$ ) were then calculated by substituting the properties of both materials ( $E_s$ ,  $E_c$ , and  $m=1$ ) in the theoretical equation, and were plotted against the percentage of reinforcement as presented by the solid curve, figures 90 and 91.

An examination of these results shows that while there are some differences between the experimental and theoretical values of ( $S_{us}/S_{uc}$ ) at some percentages of reinforcement, there are little or no difference at the other percentages of

ULTIMATE SHRINKAGE DATA

$(S_u)$  u in/in

Series I - C

R.H. \ $P_s$	0%-P.C.	1.25%	2.50%	3.75%	5.00%
76%	347	290	250	236	216
54%	367	300	270	253	223
32%	388	315	300	286	268
7%	405	320	305	293	250

Series III - C

R.H. \ $P_s$	0%-P.C.	1.25%	2.50%	3.75%	5.00%
76%	334	310	290	250	233
54%	359	305	280	260	243
32%	384	320	300	300	270
7%	405	330	312.5	293	275

Table 3



ULTIMATE SHRINKAGE DATA(S<sub>u</sub>) u in/inSeries I - S - B

R.H. \ P <sub>s</sub>	0%-P.C.	2.22%	3.45%	4.90%
76%	334	285	275	220
54%	367	290	270	220
32%	384	320	290	245
7%	396	325	300	240

Series III - S - B

R.H. \ P <sub>s</sub>	0%-P.C.	2.22%	3.45%	4.90%
76%	330	250	237.5	225
54%	348	285	250	232.5
32%	371	285	272.5	242.5
7%	405	320	300	275

Table 4

reinforcement. The variations appear independent of the percentage of reinforcement, type of cement, or the ambient relative humidity condition.

It appears that the ultimate shrinkage strain in steel ( $S_{us}$ ), may be obtained as a percentage of the ultimate free drying shrinkage of plain concrete ( $S_{uc}$ ) using the theoretical equations derived in chapter VI, without introducing a significant error.

### EXPERIMENTAL ERRORS:

From the foregoing, it can be seen that some scatter in the experimental results was observed. This scatter may be attributed to some factors which are usually encountered in this type of experimental work. The writer has made every reasonable effort to minimize the errors that are contributed by such factors.

### Preparation of Specimens:

Over 500 specimens were prepared to provide a wide range of shrinkage data for reinforced concrete members. The preparation of such specimens took a period of three months. Each group of specimens was cast and prepared out of 4 or 5 batches daily. It is therefore, reasonable to assume that some variations in the properties of the materials, and batches may have occurred. Also the lab, in which the specimens were prepared, was neither temperature nor humidity controlled. However, the preparation process of one batch of specimens took approximately 15 minutes, after which the specimens were stored in the controlled moist-curing chamber.

The column specimens were prepared using steel forms, while the slab and beam specimens were prepared using wooden forms.

Therefore some small variations may have occurred in the size of slab and beam specimens.

#### Sealing and storage Process:

After the specimens were removed from the moist-curing chamber, the specimens were then surface-dried and sealed as prescribed in chapter VII. The specimens were then stored in the preconditioned humidity chambers. This process took about one to two hours. To ensure the required relative humidity throughout the storage chambers air pumps were used to circulate the air through the saturated salt solutions and back to the pumps through 3 holes at the top of each chamber. It still took several hours before the equilibrium relative humidities were reached. The lab temperature was maintained at  $70 \pm 2^{\circ}\text{F}$ . This minimized the effect of fluctuation of temperature in the chambers ( $\pm 4^{\circ}\text{F}$ ). However, some errors may have occurred due to such small variations in temperature and relative humidity.

#### Measuring Process:

Due to the larger number of specimens prepared for this study, some errors may have occurred during the measuring process. Drying shrinkage represented the majority of recorded data.

Measurements were also taken for the weight loss studies (the second investigation), and for the shrinkage strain along the steel bars (the third investigation).

The two extensometers used to measure the length changes have a seating error of 1 to  $2 \times 10^{-4}$  (approximately 8 to 17 u in/in shrinkage strain for the 12" long specimens). Since the shrinkage readings at early ages were between 8 and 50 u in/in, this seating error may have affected the early readings. However, at later ages such error was much smaller (less than 5 to 10%). The writer believes that, these extensometers were probably the most practical devices to measure the length changes for such large number of specimens, since they eliminated any built-up errors as they were calibrated to a standard 12" long invar bar before and after the readings.

The weight loss measurements were very accurate as the amount of moisture loss was much higher than the accuracy of the scales used even at early ages.

The electrical strain recorder used to measure the strain readings in the third investigation had an accuracy of  $\pm 5 \times 10^{-6} \mu$  in/in. This system provided a very accurate means of measuring the shrinkage strain in steel at early ages. However, at later ages (after 60 days) a large amount of drift in the readings was observed. This has also been reported by other investigators (32).

### Carbonation and Creep:

Since a small amount of carbon dioxide was entrapped in the sealed chambers, it is believed that carbonation would have contributed a very small amount to the shrinkage readings. However, in the second investigation the specimens were stored in steel drums which were opened frequently to record the weight loss and shrinkage readings. Carbonation may have caused small error to the amount of moisture loss and shrinkage readings.

Like carbonation, creep effect was also included in the shrinkage readings. Carbonation and creep have been found to be diffusion phenomenon and consequently have no effect on the shape of the diffusion curves. The creep effect was included in the modified modulus of elasticity which was substituted in the theoretical analysis to derive the ultimate shrinkage strain in steel, and hence can be separated from the shrinkage readings, if necessary.

### ADDITIONAL FINDINGS:

From the previous discussion of the writer's experimental results, it appears that diffusion theory can be applied to the drying shrinkage of reinforced concrete. In addition, the writer

has applied diffusion theory to the shrinkage results reported by Glanville (31), and Keeton (41).

Glanville's results are presented in figures 92 and 93 where the average fractional shrinkage is plotted against  $t/b^2$ . An examination of his results shows that, the shrinkage data tends to fall on a single curve regardless of the percentage of reinforcement; water cement ratio, and the mix proportion. The scatter in his results can be attributed to the variation in the ambient relative humidity condition, which was not controlled during his experiments.

Keeton's shrinkage results of reinforced slab specimens made of normal and light weight concretes are presented in figures 94 and 95. An examination of these figures shows that the theoretical curves ( $K, K_0$ ) fit the shrinkage results regardless of the specimen size, type of concrete, and the relative humidity condition.

Thus, this provides additional confirmation that diffusion theory can provide an accurate method of predicting the drying shrinkage of reinforced concrete members. The shrinkage diffusion coefficients  $K$  and  $K_0$  appear independent of the size of member; the water-cement ratio; mix proportion; type of concrete; and the relative humidity condition.

## CHAPTER VIII

### CONCLUSIONS

#### OBSERVATIONS AND CONCLUSIONS:

The main purpose of this research investigation was to develop an accurate and more practical method of predicting the drying shrinkage of reinforced concrete. This entailed using diffusion theory to develop a method which would, adequately take into account the effects of specimen size, different bar diameters, different percentages of reinforcement and different ambient relative humidities. Also it included developing a relatively quick method of evaluating the ultimate shrinkage of plain and reinforced concrete. Based on the writer's experimental results, the following conclusions would appear to be warranted:

#### Drying Versus Shrinkage of Reinforced Concrete:

A linear relationship seems to exist between the drying shrinkage of reinforced concrete and the moisture loss, specially at later ages. The relationship appears unaffected by the reinforcement, the age of curing, or the specimen size.

The drying of reinforced concrete can be predicted by the



linear diffusion theory of constant diffusion coefficient  $K$ . The moisture diffusion coefficient for the reinforced specimens was slightly higher than that for the plain concrete ones.

Diffusion Analogy and The Shrinkage of Reinforced Concrete:

Diffusion theory seems to provide an adequate means of predicting the drying shrinkage of reinforced concrete members, taking into account the effect of reinforcement, bar diameter, specimens size, type of cement, age of curing, and the drying condition. The shrinkage diffusion coefficients  $K$  of the theoretical curves used to fit the data appear to be relatively unaffected by the variables considered in this investigation.

A better fit of shrinkage results can be obtained by considering the shrinkage diffusion coefficient  $K$  to be a function of the Fourier number ( $t/b^2$ ) of the form:

$$K = K_0 (1.0 - 0.1 \ln (t/b^2)) \dots\dots\dots(47)$$

The theoretical curves used to fit the shrinkage data tend to fall within a very narrow band that can be approximated, without introducing any significant error, by a single theoretical curve.

### Shrinkage Stress Development:

It appears that shrinkage stresses along the reinforcing bar increase gradually from the ends of the member towards the centre over a distance which is short compared with the usual length of the member. Uniform stresses are developed in the central portion.

The theoretical analysis provides a reasonably accurate method of predicting the ultimate shrinkage strain in steel for both symmetrically and eccentrically reinforced members.

Reasonably high shrinkage stresses can be developed in reinforced concrete members. The higher the percentage of reinforcement the higher the tensile stress in concrete, but the lower the compressive stresses in steel.

### Ultimate Shrinkage of Plain and Reinforced Concrete:

The ultimate shrinkage of plain concrete dried at any relative humidity condition ( $S_{UR}$ ) may be obtained by functions of the ultimate shrinkage of similar oven dried specimen ( $S_{UOV}$ ) and the relative humidity (R), of the form:

$$S_{uR} = 1.27 S_{uov} \cdot \log \frac{(105 - R)}{5} \dots\dots\dots(53)$$

for  $R \leq 55\%$

$$\text{or } S_{uR} = 1.54 S_{uov} - 0.84R \dots\dots\dots(54)$$

for  $R \leq 80\%$

The ultimate shrinkage strain in steel may be evaluated by the following theoretical equations:

$$S_{su} = \frac{A_c I_c}{I_c (nA_s + A_c) + nA_s A_c e^2} S_{uR} \dots\dots(40)$$

For eccentrically reinforced members, and

$$S_{su} = \frac{1 - P_s}{1 + (n - 1)P_s} S_{uR} \dots\dots\dots(43)$$

For symmetrically reinforced members.

RECOMMENDED METHOD OF PREDICTING DRYING SHRINKAGE:

Based on the writer's experimental results, the following method of predicting drying shrinkage of reinforced concrete is suggested:

1. The average shrinkage strain in steel in reinforced concrete members can be evaluated at any time as a ratio of the ultimate values, from figure 96 or 97. The graphs give minimum and maximum values of the fractional shrinkage strain in steel. The writer suggests average values could be used in common practical problems.
2. The ultimate shrinkage strain in steel can then be determined, using equation 40, or 43, and the properties of steel and concrete, as a function of the ultimate shrinkage of the corresponding plain concrete member.
3. The ultimate shrinkage of plain concrete at the required relative humidity, using equations 53 or 54, can be approximately determined as a function of the ultimate shrinkage of a small size specimen dried at 220°F.
4. Once the shrinkage strain in steel is calculated, the shrinkage force, moment (for eccentrically reinforced member), and deformation (warp or deflection), can be predicted using the equations derived in Chapter VI.

RECOMMENDED FUTURE RESEARCH:

From the foregoing, it appears that diffusion theory can be used to predict accurately the drying shrinkage of plain and reinforced concrete members. Since creep is believed to be a diffusion phenomenon, the writer feels that a study to apply diffusion theory, represents the most promising approach of predicting more accurately the creep of plain and reinforced concrete.

The writer also feels that diffusion analogies may be used to predict many properties of concrete, such as, strength, modulus of elasticity, hydration ..etc.

APPENDIX A

SHRINKAGE OF CONCRETE

## APPENDIX A

### SHRINKAGE OF CONCRETE

The shrinkage of concrete has been the subject of more than 1500 research papers published since the turn of the century (1). Some investigators have studied the basic mechanisms and causes, others have attempted to develop empirical methods for predicting the amount of shrinkage that might occur.

This appendix deals with the fundamentals of the shrinkage of concrete needed to understand the basic mechanisms, and the main factors affecting drying shrinkage.

#### STRUCTURE OF CONCRETE:

Concrete can be defined broadly as a two phase material consisting of inert aggregate particles embedded in a matrix of cement paste. The properties of the concrete are determined generally by the physical and chemical properties of the hardened cement paste.


The structure of cement paste can be described in terms of the following constituents: unhydrated cement; solid products of hydration (mainly tobermorite gel, but also include calcium

hydroxide crystals and crystallites); and void space containing both strongly adsorbed and capillary water and air (1).

Many investigators have studied both the gross structure and the micro-structure of cement paste, which has resulted in the development of two major models (1) (2) (3). Such studies, using electron diffraction and x-ray diffraction, have only revealed the very complex nature of the various phases of hydrated cement paste.

Powers (4), presented a simplified model of the structure of cement paste as shown on figure 1. In his model, the hydrated cement paste consists of tobermorite gel particles (represented by the cross-hatched lines) and the space between them (gel pores), and capillary cavities (the original water filled space in the paste) which are designated by the letter "C". The paste may also contain crystals of calcium hydroxide, relatively large, and usually some residue of unhydrated cement.

Figure 2, shows the model of the microstructure of cement paste proposed by Feldman and Sereda (2). This model attempts to show the structure of the sub-microscopic tobermorite gel (represented by the tobermorite sheets), the interlayer hydrate water (represented by the letter "X" between two tobermorite sheets), and the physically adsorbed water (represented by the large circles). Both interlayer hydrate and physically adsorbed water are strongly attracted to the tobermorite sheets at distances





between 0 and 30 Å. The physically adsorbed water has been described as "load bearing water" by Powers (4), and as adsorbed water by ACI Committee 209, and may be evaporated at relative humidities below 40 percent (1).

#### VOLUME CHANGES OF CONCRETE:

A number of volume changes take place in concrete from the time water is added to a dry concrete mix. These volume changes have been studied by many investigators and will be briefly reviewed here.

#### Chemical Volume Changes:

Autogenous Shrinkage and Swelling: Autogenous shrinkage may be defined, as the volume change, of cement paste as a result of hydration of cement compounds. In concrete mixes of a high water content, additional shrinkage is attributed to sedimentation in the plastic concrete. Autogenous shrinkage can be explained by the fact that the volume of hydration products is less than the initial volume of cement and water. Autogenous shrinkage can be measured in sealed specimens or in specimens stored in saturated air (5) (7). This autogenous shrinkage is usually included in the drying shrinkage measurements.

Autogenous shrinkage is important in mass structures.

Davis (5), and Ross (6), reported autogenous shrinkage of 100  $\mu$  in/in after 5 years in concretes employed in massive structures.

Swelling occurs during the hydration process when cement paste and concrete are cured continuously in water. This swelling is due to the adsorption of water by the cement gel. The water molecules act against the cohesive forces and tend to force the gel particles further apart (8). Swelling in concrete is about 100<sup>m</sup> to 150  $\mu$  in/in. This swelling is accompanied by an increase in weight of the order of 1 percent (7).

Carbonation Shrinkage: Carbonation shrinkage occurs when carbon dioxide present in the atmosphere reacts, in the presence of moisture, with the hydrated cement products, mainly calcium hydroxide and the silicates. This shrinkage is also accompanied by an increase in weight (8) (9).

Carbonation shrinkage has only recently been recognized and therefore most of the experimental data on drying shrinkage includes the effects of carbonation. The rate of carbonation depends mainly on the moisture content of the concrete and on the ambient relative humidity. Water-saturated specimens or specimens dried at a relative humidity below 30% have shown little or no carbonation shrinkage (9); in the first case the pores within the cement paste are full of water and the diffusion of carbon dioxide into the paste is very slow; in the later case

85

there is insufficient water in the pores for carbon dioxide to form carbonic acid.

Concrete specimens subjected to alternating wetting and drying in air containing carbon dioxide have shown high carbonation shrinkage (during the drying cycle). Swenson and Sereda (10), stated that the maximum carbonation shrinkage occurs when the specimens are subjected to repeated wetting and drying in a 50% relative humidity condition.

#### Drying Volume Changes:

Plastic Shrinkage of Fresh Concrete: Plastic shrinkage occurs when fresh concrete is exposed to drying, and can lead to surface cracking. Plastic shrinkage is greater the larger the cement content of the mix (7) and the earlier the stiffening of the concrete (11). It has been suggested by Shacklock (11), that a greater bleeding capacity of the concrete decreases the plastic shrinkage. Plastic shrinkage due to drying usually includes the effect of autogenous shrinkage. Additional shrinkage is also attributed to sedimentation in concrete mixes (8). More information about plastic shrinkage can be found in references 12, 13, and 14.

Drying Shrinkage of Hardened Concrete: Drying shrinkage occurs when concrete is subjected to relatively dry atmospheres. This is due to the movement of water out of the pore system of the cement

gel. The loss of free water, which takes place first, causes little or no shrinkage. As drying continues, adsorbed water is removed and a partial collapse in the gel structure occurs accompanied by a reduction in the volume of cement paste (8). Part of the shrinkage on first drying is irreversible due to the partial collapse of the gel structure. It has been found that the tobermorite phase is responsible for most of the shrinkage of cement paste (9).

Many theories have been presented on the mechanism of drying shrinkage. The most acceptable theory is the one suggested by Powers (3), in which he considered drying shrinkage to be caused by three different mechanisms:

1. Change in surface tension of the colloidal gel particles.
2. Change in pressure between the gel particles.
3. Change in capillary tension.

1. Change in Surface Tension of the Colloidal Gel Particles: A solid body consists of many particles held together by inter-particle forces of attraction and repulsion in a state of static equilibrium. The surface of a solid body is always in tension while the bulk of the body is in compression. The surface tension of a solid is reduced and the solid expands when the surface interacts with another substance either chemically or physically (9).

A change in surface tension of the colloidal gel particles.

occurs due to adsorption or desorption of water molecules in or out of the gel system, causing swelling or drying shrinkage of the cement paste. It has been found by Powers (3) that the change in surface tension of the colloidal gel particles can account for approximately 10 to 20% of the total amount of drying shrinkage.

2. Change in Pressure Between the Gel Particles: It has been found (9), that the average distance between particles in cement gel is about  $24 \text{ \AA}$  which is about 6.6 times the estimated diameter of a water molecule in the adsorbed state. Any two surfaces spaced that closely are subjected to mutual forces of attraction. The forces are known as Van Der Waals attraction. If water is adsorbed on the surfaces, the attractive force between the solid surfaces is reduced and an overall expansion of the cement paste occurs. Adsorption, on an open surface in saturated vapor, can build up a layer 5 molecules thick. This is more than the gel pores can accommodate. Therefore, at saturation pressure, the adsorbed water is under considerable pressure in order to be in thermodynamic equilibrium with the surrounding, thus causing further expansion of the cement paste.

Change in pressure between the gel particles is believed to be responsible for the major part of drying shrinkage.

3. Change in Capillary Tension: When concrete is prepared with a

water-cement ratio higher than 0.38, the cement paste will contain a certain number of capillaries after hardening. When the concrete is subjected to drying, part of the water diffuses out and/or reacts with the unhydrated cement and tension tends to build up in the remaining water due to capillary action. As a result the paste will be compressed, and hence a reduction in the volume occurs. As the cement paste dries out, more and more of the capillary pores are emptied of water and can no longer sustain the hydrostatic tension (9).

When the relative humidity is as low as 40 to 50% all capillary pores are empty and the capillary mechanism does not contribute to the drying shrinkage of concrete. Hansen (9), suggested that capillary tension in cement paste having a water-cement ratio of 0.50 contributes no more than 20 to 30% of the total amount of shrinkage.

Figure 3, shows the estimated individual contributions of each mechanism to the total drying shrinkage (9). It should be noted however that in concrete members, the internal relative humidity at various points in the cross-section may vary from zero percent at the surface to 100 percent in the interior. As a result while capillary tension may be the mechanism that causes the most shrinkage at the interior points of the member, surface tension and pressure between the gel particles may cause the major portion of shrinkage at some other points close to the surface.

DRYING OF CONCRETE:

It is generally accepted that diffusion theory can be applied to the drying process in concrete (15) (16) (17).

Pihlagavaara (16), studied the drying of plate-shaped mortar specimens. He concluded that the moisture diffusion coefficient is moisture content dependent and takes the form:

$$K = K_e (1 - nU^v) \dots\dots\dots (55)$$

where

$$U = C/C_0$$

n, v, and  $K_e$  are assumed constants.

Becker (15), investigated the drying of concrete in more detail. Figure 4, shows the average moisture loss versus the Fourier number to an arbitrary scale for concrete made with type I and type III cements. He concluded that the moisture diffusion coefficient is not influenced significantly by the specimen size or by the moisture content of the concrete. He suggested that the diffusion coefficient is a linear logarithmic function of the fourier number, such that

$$K = K_0 (1 - K_1 (\text{Ln } K_0 t/b^2)) \dots\dots\dots (56)$$

The best fit to his results was obtained by assuming that  $K_1 = 0.50$  in<sup>2</sup>./day.

It is generally believed that drying shrinkage is primarily due to loss of moisture. Many investigators (15) (17) (18) have studied the relationship between these two in order to apply diffusion theory to the phenomenon of drying shrinkage. Figure 5 shows the relationship between shrinkage and water loss for a series of specimens ranging from neat cement to a mixture composed of 25 percent cement and 75 percent pulverized silica. While the relationship is linear for neat cement paste, it gradually becomes nonlinear, especially at early drying, as the silica content is increased. This nonlinearity has been attributed to the increase in capillary cavities known to be associated with the increase in rock-flour content (18). Becker (15), studied such a relationship for plain concrete specimens. An example of his results is shown in figure 6. He concluded that, at early ages, a relatively large moisture loss is associated with a small amount of drying shrinkage, and a reasonably linear relationship seems to exist at later ages.

Unfortunately, there is no available information regarding the relationship between moisture loss and drying shrinkage of reinforced concrete.

#### FACTORS AFFECTING DRYING SHRINKAGE OF CONCRETE:

Many factors influence the rate and amount of drying shrinkage. The amount of ultimate shrinkage is determined



primarily by the concrete constituents, but is also affected by the curing conditions and the drying environment. The rate of shrinkage can be affected by the size and shape of the member, drying environment, etc.. The most important factors affecting shrinkage as reported in the technical literature will be briefly reviewed here.

#### Concrete Constituents:

Cement and Water: From the forgoing discussion, it can be seen that, cement gel is responsible for most of the drying shrinkage in concrete. The type, composition and fineness of cement can produce cement gel of varied physical and chemical properties and consequently affects shrinkage. The cement content in a concrete mix is reflected in the amount of gel produced. Therefore, a large cement content tends to increase the drying shrinkage.

Kreijger (19), reported that the fineness of cement increased the drying shrinkage. Using mortar mixes (1:3 by weight) and a constant water-cement ratio, he found that increasing the Blaine fineness of the cement from 3000  $\text{cm}^2/\text{g}$  to 5500  $\text{cm}^2/\text{g}$  produced an increase in the drying shrinkage of 10 to 25%.

The composition of cement has also been shown to influence the drying shrinkage of concrete. It has been found (19) that the greater the  $\text{C}_3\text{S}$  content the lower the drying shrinkage.

while an increase in  $C_3A$  and  $C_4AF$  contents resulted in an increase in shrinkage. The effect of other trace compounds in the cement on the shrinkage seems to be insignificant<sup>(20)</sup>.

The water content has a significant influence on the drying shrinkage. It has been found<sup>(8)</sup> that a high water content (water-cement ratio) produces low drying shrinkage at early ages but higher ultimate shrinkage.

Aggregates: Drying shrinkage of cement paste is substantially reduced by the presence of aggregate particles. The restraining effect<sup>(21)</sup> of the aggregate particles depends mainly on the aggregate content and the elastic properties of the aggregates, and is presented in figure 7. It can be seen that the higher the aggregate content and the rigidity of the aggregates the lower the drying shrinkage.

The size and grading of aggregate has little influence on the amount of drying shrinkage. However, a larger aggregate size usually permits the use of a leaner mix and hence results in a lower shrinkage.

Pickett<sup>(22)</sup>, presented the following equation of the effect of aggregate content on drying shrinkage:

$$S_f = S_p (1 - a)^n \dots \dots \dots (57)$$

where,

$S_f$  = Drying shrinkage of concrete

70

a = the aggregate content

n = constant

The experimental values of n varied between 1.2 and 1.7 (8).

Many investigators have presented different empirical formulae for predicting the drying shrinkage of plain concrete taking into account the effect of aggregate on a similar basis to that of Pickett. These formulae are reviewed in more detail in Chapter II.

Admixtures: The use of admixtures in concrete mixes has increased in recent years in order to improve certain properties of concrete, such as durability, strength, workability...etc.

The commonly used admixtures have showed a varied influence on the drying shrinkage of concrete. An admixture which increases the water requirement of a concrete mix is generally expected to increase the drying shrinkage. The converse is not necessarily true (1). Air entraining admixtures have been found to have no significant affect on shrinkage (8).

The addition of calcium chloride increases the drying shrinkage by 10 to 50% (8). This is probably because a finer cement gel is produced. The use of blast furnace slag in portland cement generally increases the drying shrinkage.

Pozzolans, when used as a partial replacement of cement in concrete mixes, have shown lower shrinkage at early ages but higher

ultimate shrinkage. However, fly ash of low carbon content tends to reduce the ultimate drying shrinkage (1).

The effect of many other admixtures on drying shrinkage has not yet been established and still requires experimental evaluation.

#### Curing and Drying Environment:

The properties and the amount of cement gel produced, immediately after casting, depend largely on the curing condition, which in turn affects the drying shrinkage.

Steam curing has been found (23) to reduce the drying shrinkage of concrete by as much as 50%. This is due to the fact that a coarser cement gel is produced. The reduction in shrinkage is dependent on the temperature and duration of steam-curing.

The effect of moist-curing on shrinkage is small but rather complex. Cement pastes subjected to prolonged curing show higher shrinkage on drying. This is due to a reduction in the volume of unhydrated cement grains which restrain the shrinkage. However, Neville (8) has reported some contradictory results on the effect of moist-curing on drying shrinkage of concrete. But in general, the length of the moist-curing period has little influence on the ultimate drying shrinkage.

The ambient relative humidity has been reported (24) to

influence the rate and the magnitude of drying shrinkage as shown on figure 8. Concretes subjected to low relative humidities have shown higher drying shrinkage. Dutron (25) and many other investigators have suggested formulae to predict drying shrinkage taking into account the effect of ambient relative humidities. These formulae will be reviewed in detail in chapter II .

Ross (26) studied the effect of ambient temperature on drying shrinkage. He considered temperatures ranging from 68 to 212 °F. He found that, within 60 days of drying, shrinkage increased with an increase in temperature as a result of an increase in the rate of hydration. It has been reported (1), that the extent of hydration in saturated concrete is approximately proportional to the integral of temperature versus time, referred to a datum temperature of 11° F at which the rate of hydration is negligible.

#### Size and Shape of Member:

The rate of drying shrinkage is largely affected by the size and shape of the concrete member. It has been reported by many investigators that an increase in the size of member results in slower shrinkage development. Since the diffusion of moisture out of a large member proceeds more slowly, the regions near the surface are subjected to tensile stresses while the core is subjected to balancing compressive stresses (27).

Ross (28), Hansen and Matock (29), suggested that drying shrinkage is proportional to the volume to surface ratio.

Becker (15), treated drying shrinkage as a diffusion process and found that shrinkage for different sizes and shapes can be determined accurately by the Fourier number to an arbitrary scale ( $t/b^2$ ).

The effect of size and shape of member on the prediction of drying shrinkage will be reviewed in detail in chapter II .

#### Reinforcement:

The presence of steel reinforcing bars in concrete leads to a reduction in the overall drying shrinkage of the member. Troxell, et al., (30), stated that the effect of reinforcement in reducing drying shrinkage is proportional to the percentage of steel introduced in the concrete member. The restraining effect induces compressive stresses in the steel and tensile stresses in the concrete. Glanville (31), found that the distribution of the compressive stresses along the reinforcing bar proceeds from the ends of the bar towards the centre. A gradually increasing compressive stress is developed in the bar by a practically uniform bond stress over a length which is short compared with the usual length of reinforced concrete member. Over the remaining central portion there is no bond stress and the steel stress is uniform as shown in figure 9. He stated

that, the length over which bond stresses are developed at the ends does not depend appreciably on the age of the concrete.

Beyer, (32) studied the drying shrinkage of reinforced concrete members using an electrical strain gage technique. The members (7x7x48 in.) were reinforced with one centrally located bar (1 in round bar, or 1½ in square bar). Immediately after pouring, an initial strain reading was taken. The readings were taken for a period of about three months. He found that compressive stresses (up to 1200 psi) were induced in the reinforcing bar during the first day after casting. For the next day or so the compressive stresses in the steel were relieved and became tensile stresses (1200 psi). He explained that such results were due to the formation of new hydration solids from the water held in the pores of the hardened concrete as free water and consequent expansion of the gel. At later ages the hydration process utilizes all of the free water in the pores and then draws water held by the gel to continue the hydration of the cement particles. This caused the gel to shrink and the concrete to undergo a decrease in volume which caused a continuous increase in the compressive stresses in the steel for about two days after casting. After nearly three months the stresses were 7500 psi compression in the steel and 118 psi tension in the concrete.

Beyer's results after two days seem to agree with the fact that shrinkage induces compressive stresses in steel and tensile

stresses in the concrete. However, his results during the first two days seem to be questionable since he did not consider the effect of heat of hydration in his readings.

When the reinforcement is located eccentrically with respect to the concrete section, the restraining action tends to cause additional shrinkage deformation (warp or deflection). Shrinkage curvature as high as 30 to 35 x 10<sup>-6</sup>/in. have been observed in singly reinforced beams (40).

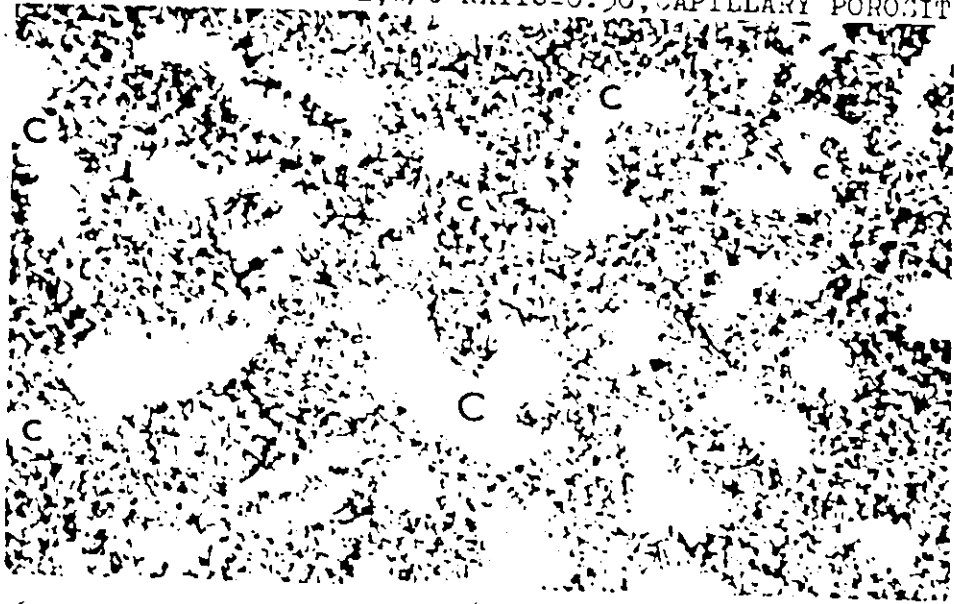
The effect of reinforcement on the prediction of drying shrinkage of reinforced concrete members is reviewed in detail in chapter III



APPENDIX B

FIGURES

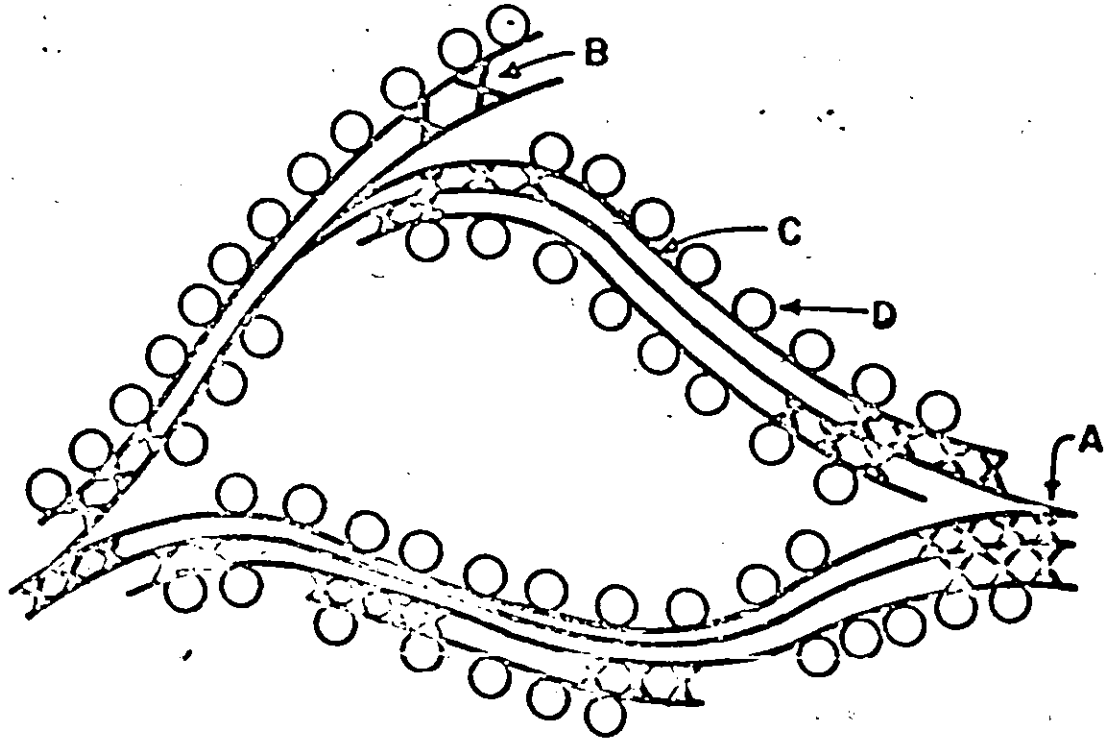
MATURE CEMENT PASTE, W/C RATIO=0.50, CAPILLARY POROSITY=20%



NEARLY MATURE CEMENT PASTE, W/C RATIO=0.30, POROSITY= 7%



Figure 1 (Powers)



- A - INTERPARTICLE BONDS
- B - INTERLAYER HYDRATE WATER
- C - TOBERMORITE SHEETS
- D - PHYSICALLY ADSORBED WATER.

Figure 2 ( Feldman and Sereda)

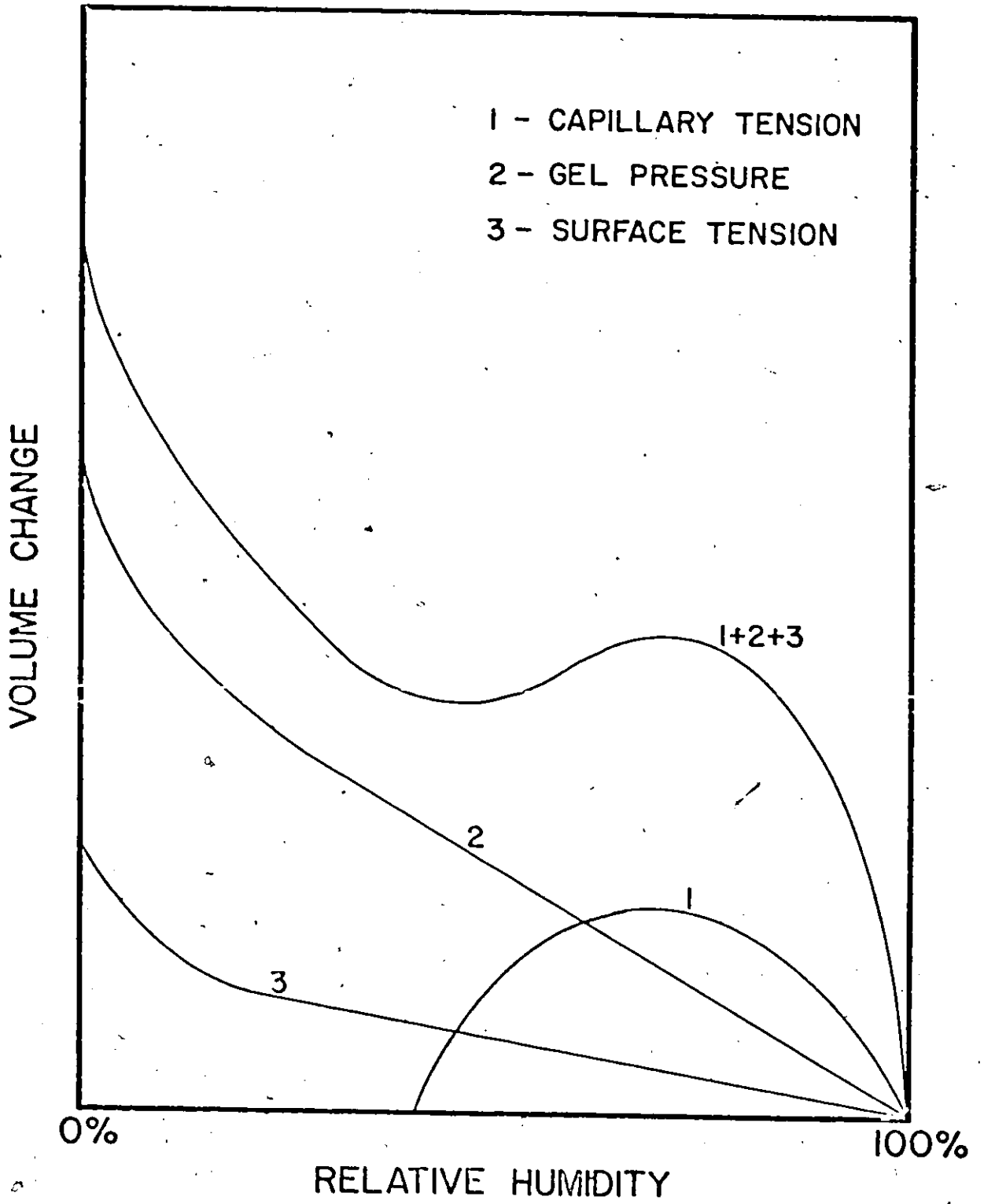


Figure 3 (Hansen)

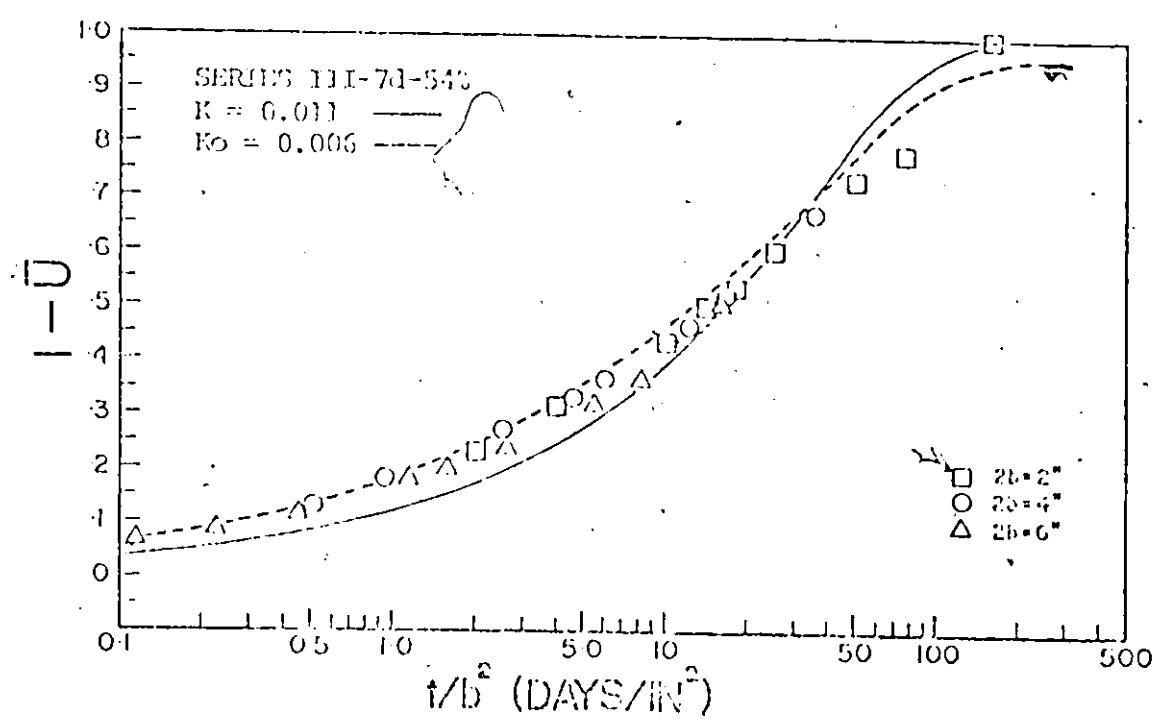
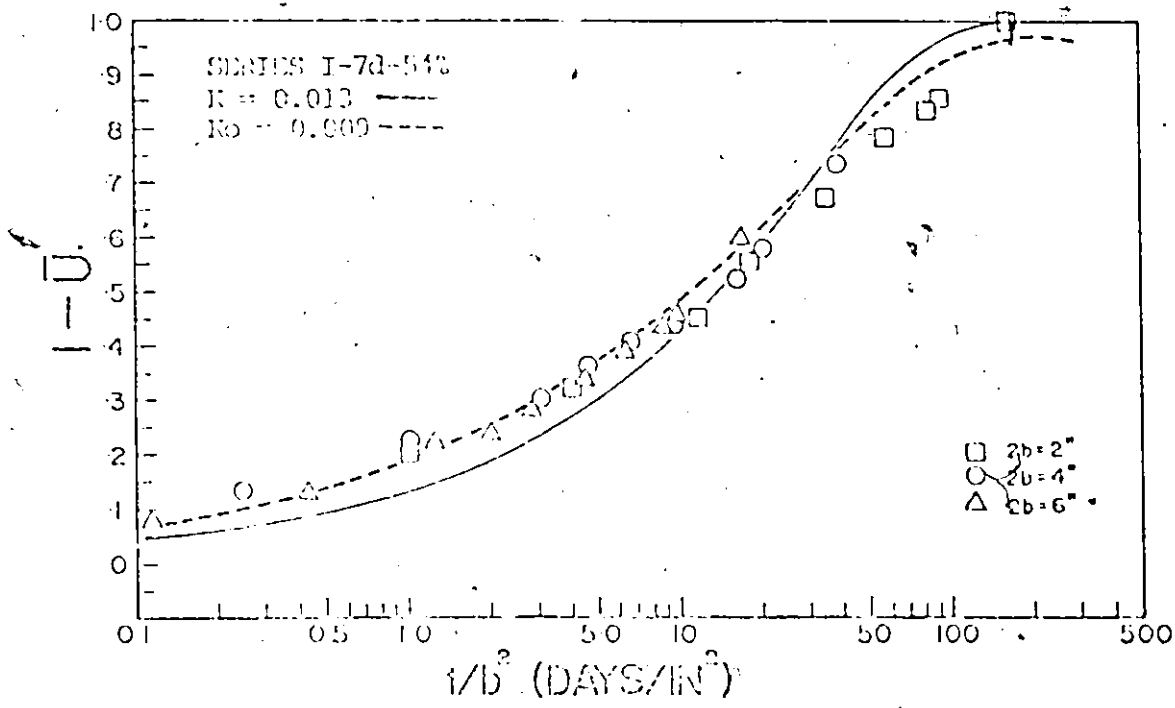


Figure 4 (Becker)

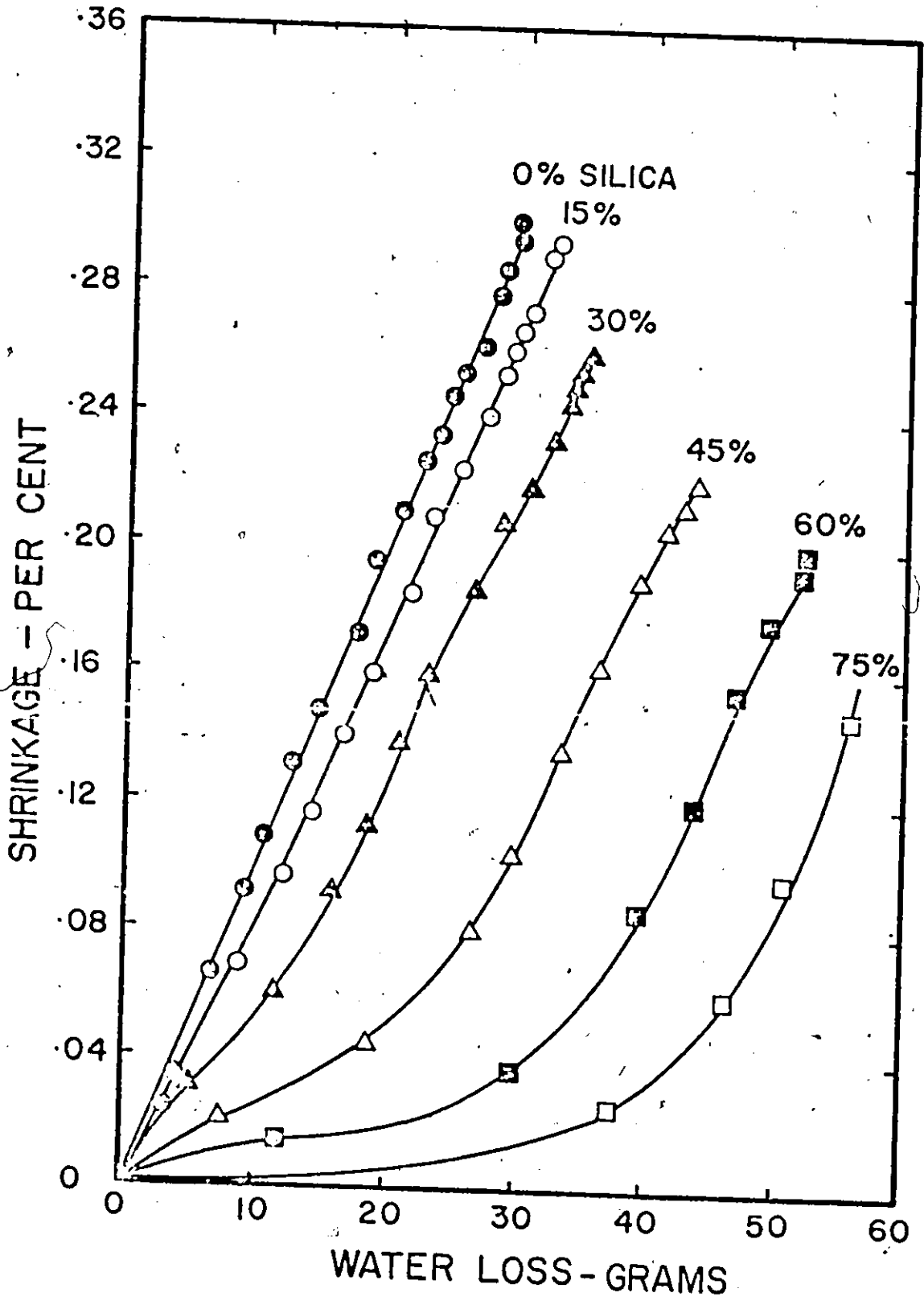


Figure 5 (Powers)

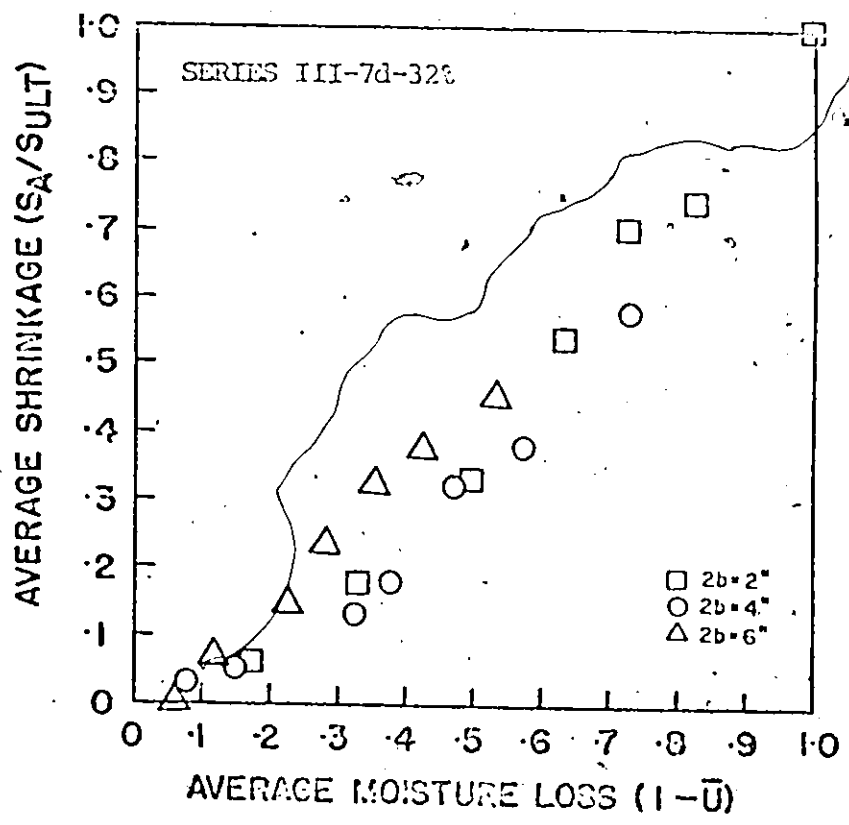
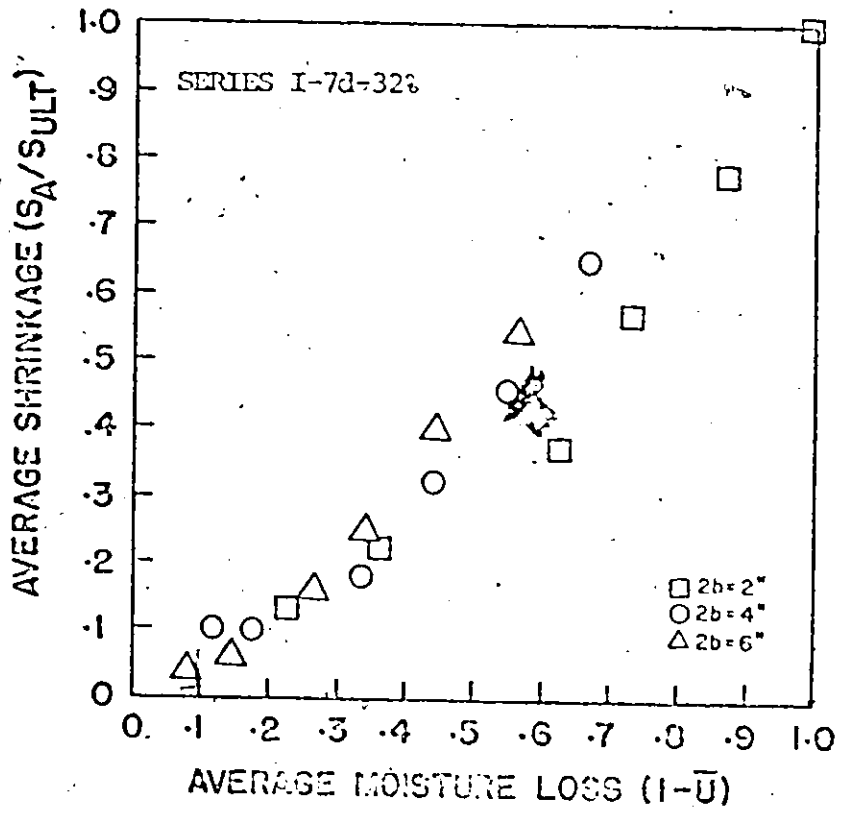


Figure 6 (Becker)

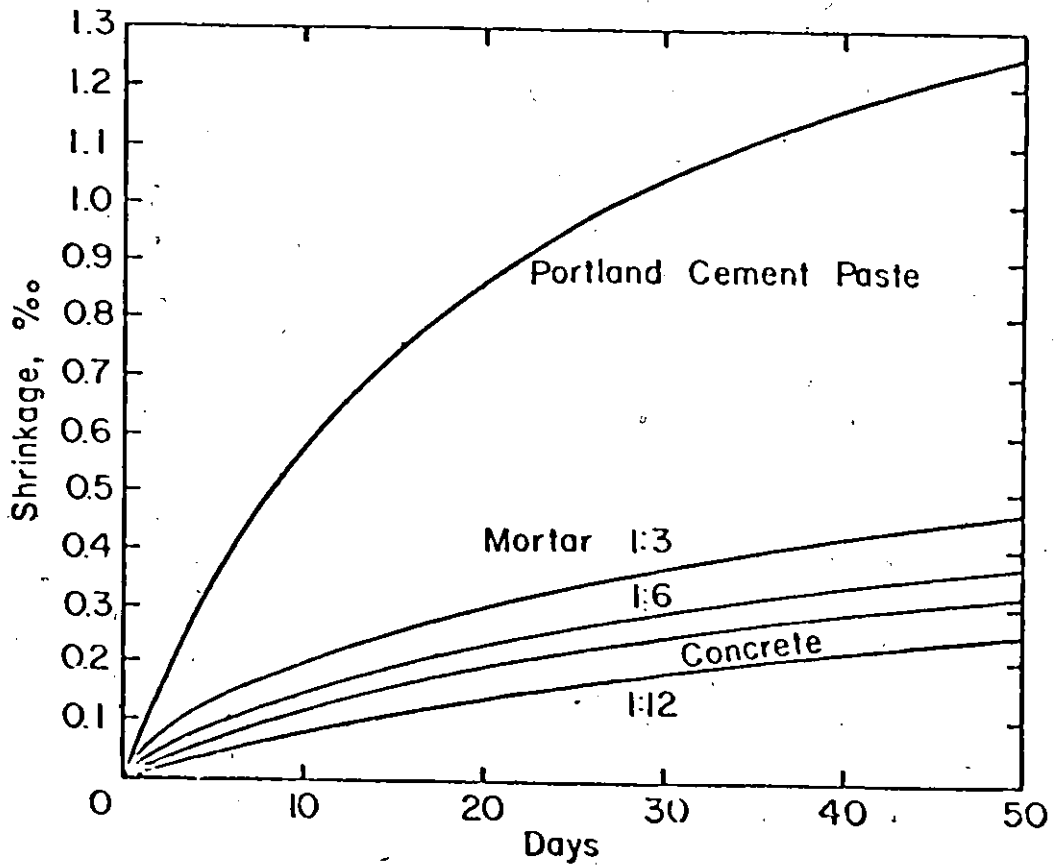
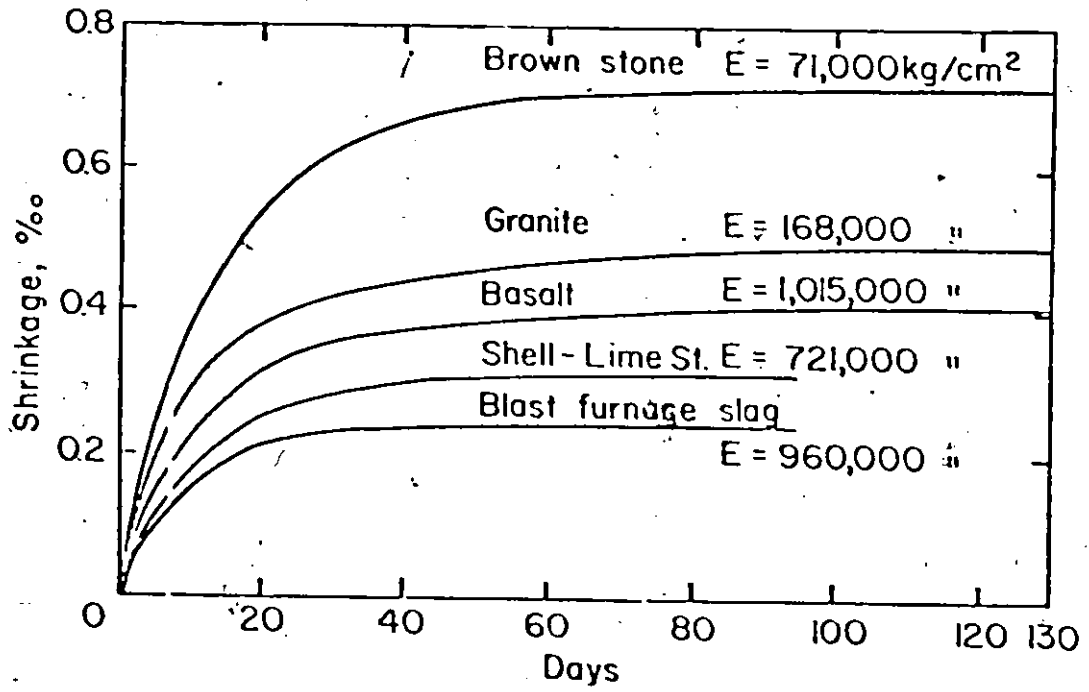


Figure 7 (Rostasy)



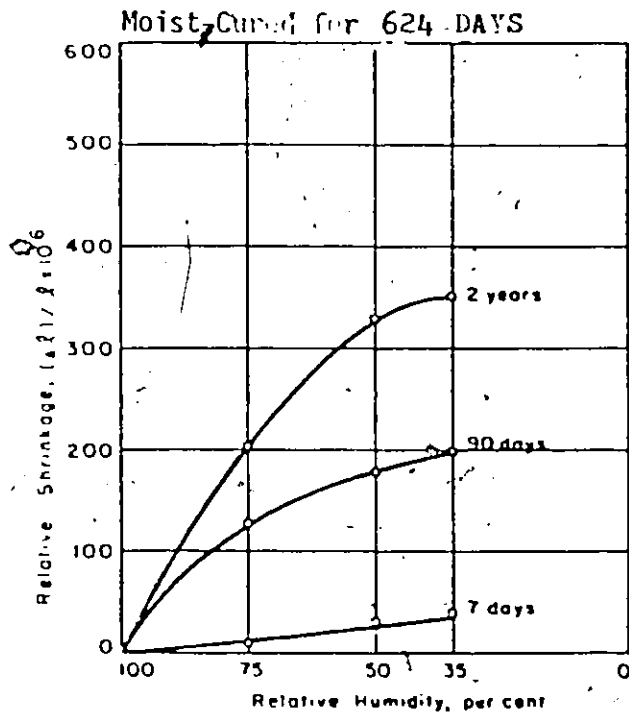
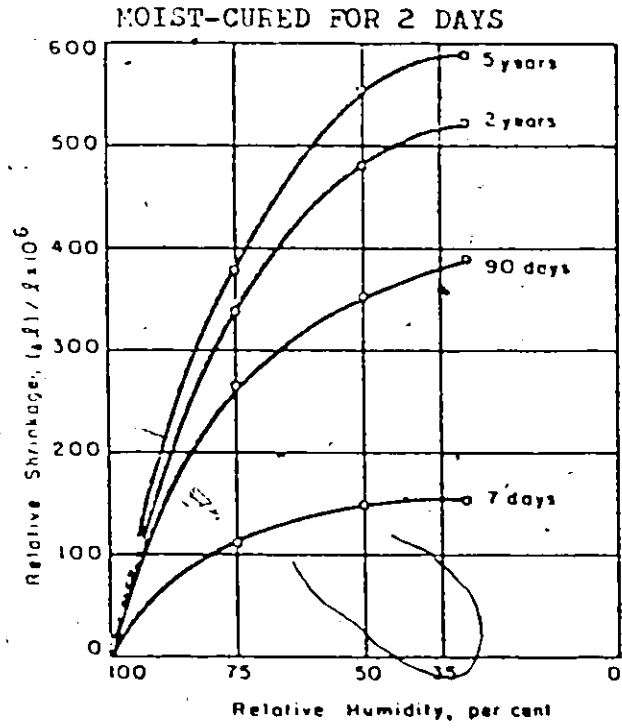


Figure 8 (L'Hermite and Mamillan)

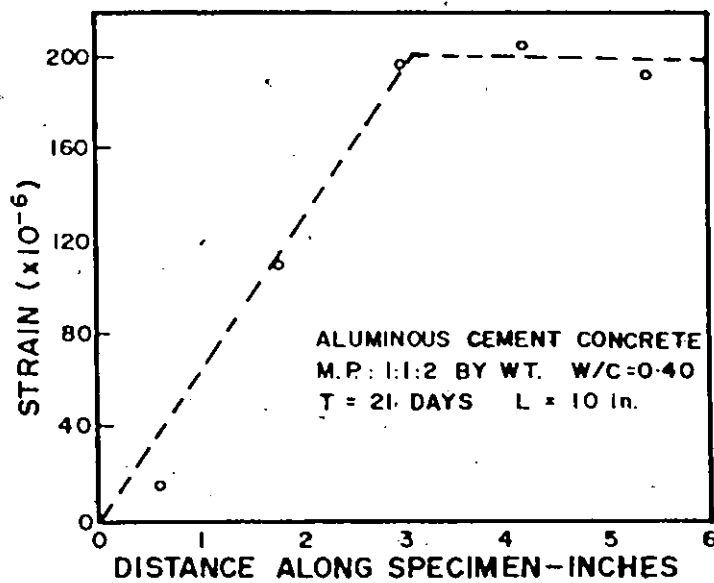
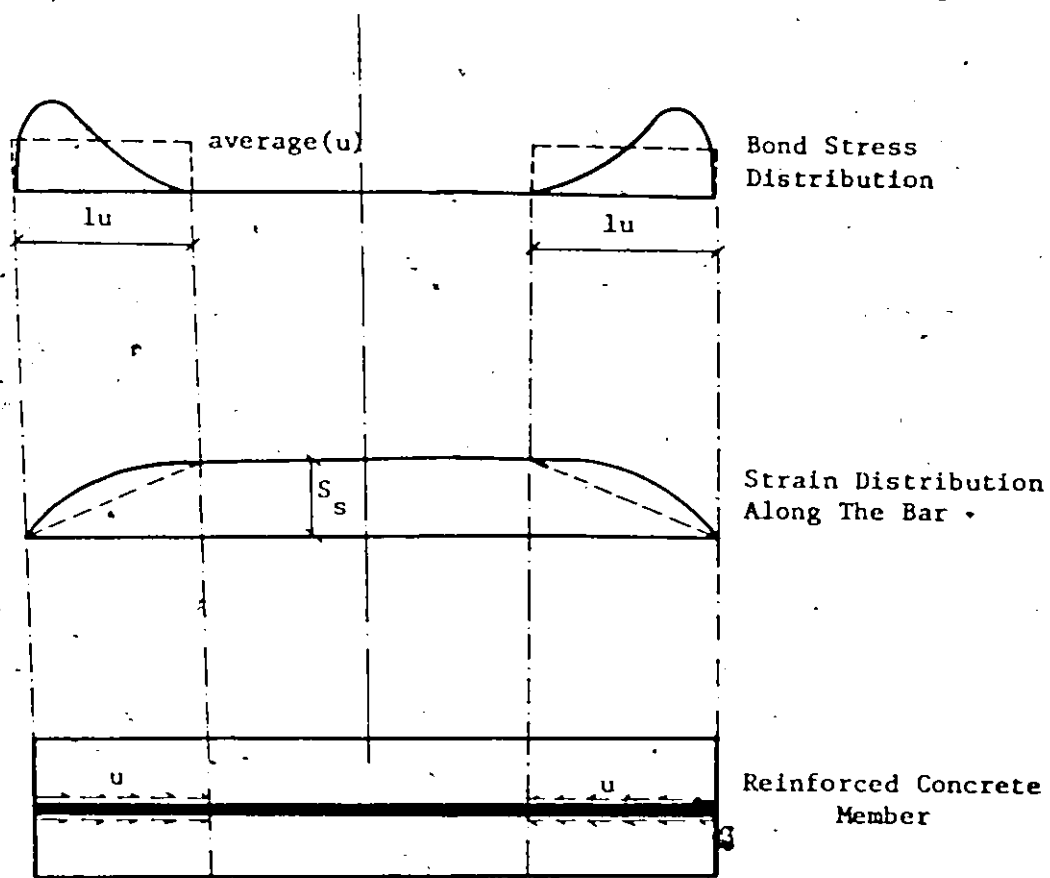


Figure 9 (Glanville)

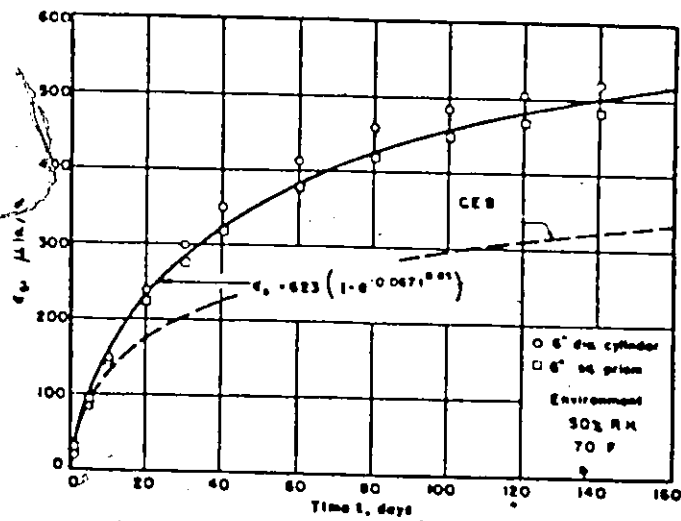
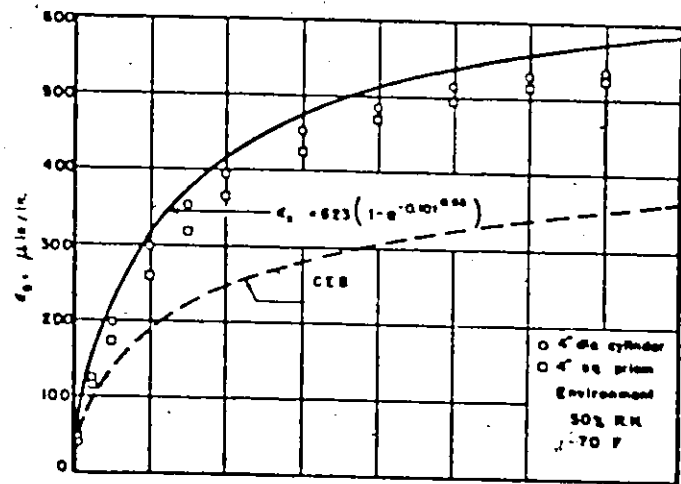
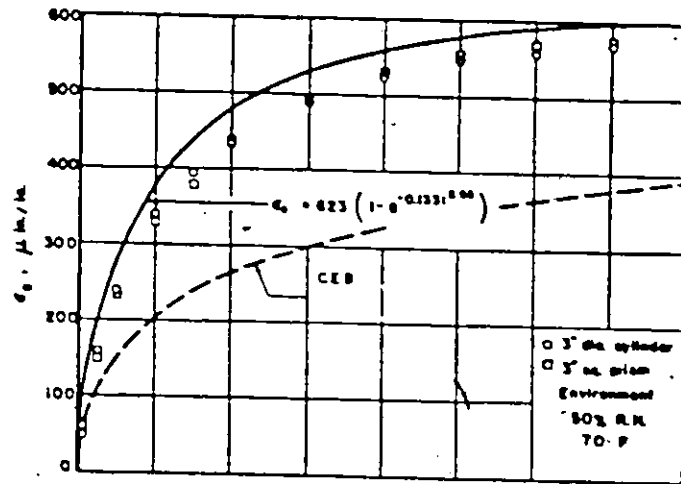
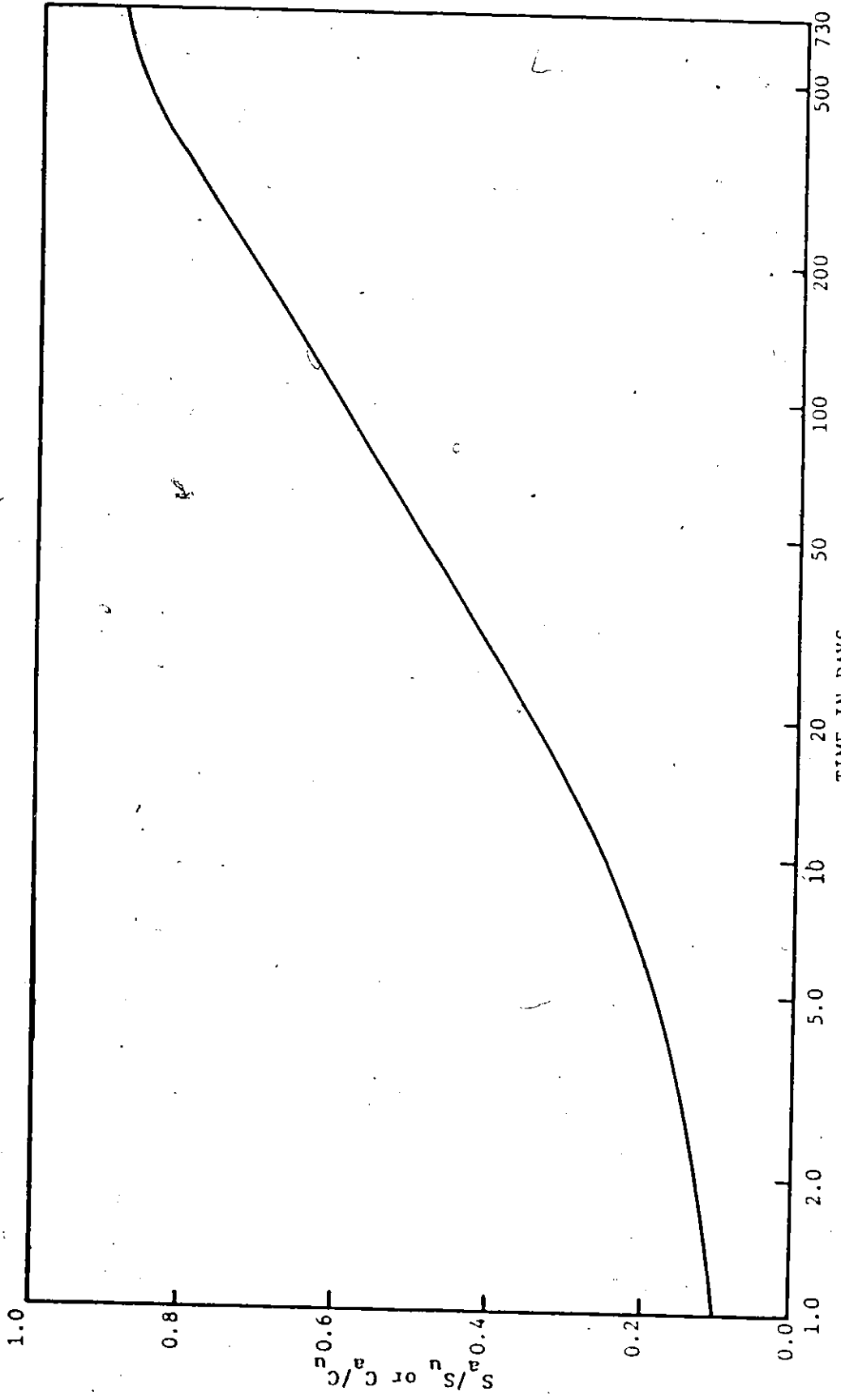


Figure 10 (Wallo)



Fractional shrinkage or creep versus time (Fintel and Khan)

Figure 11

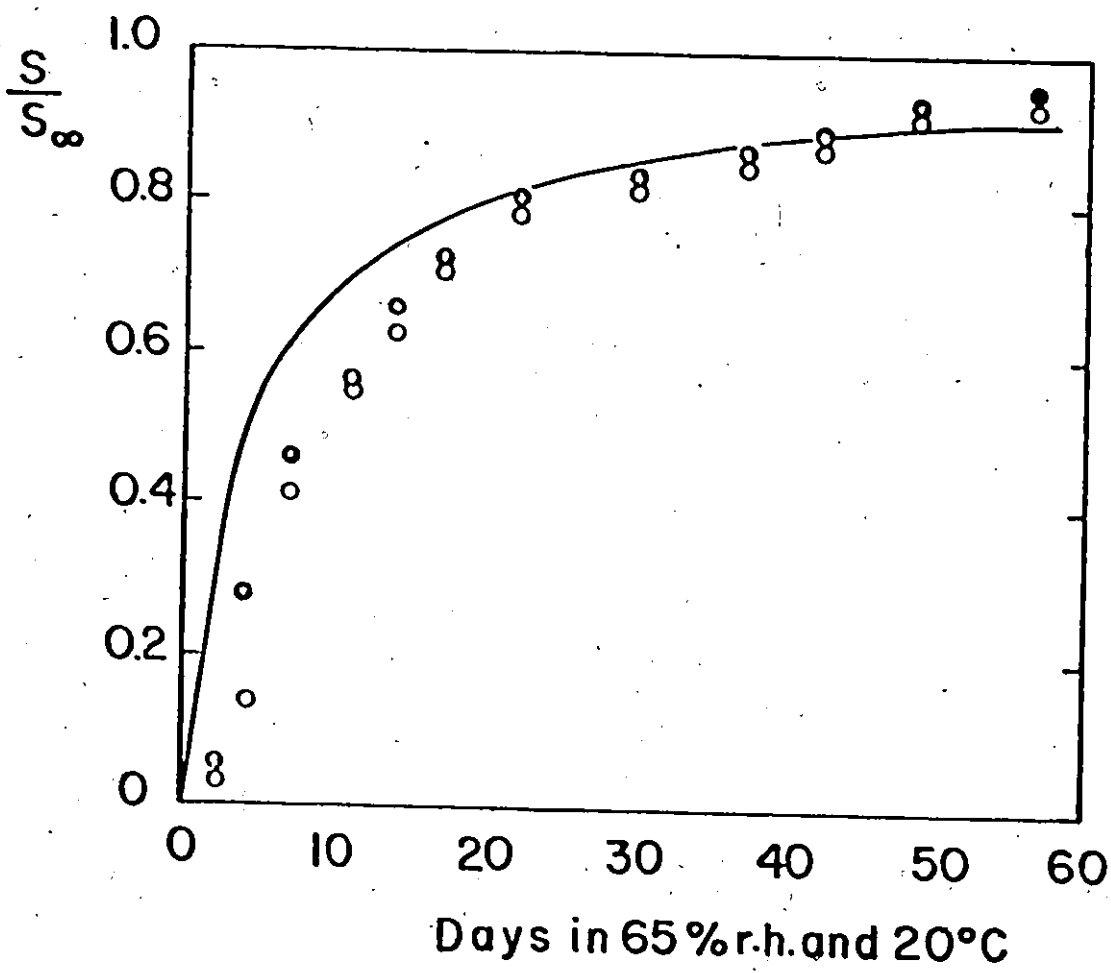
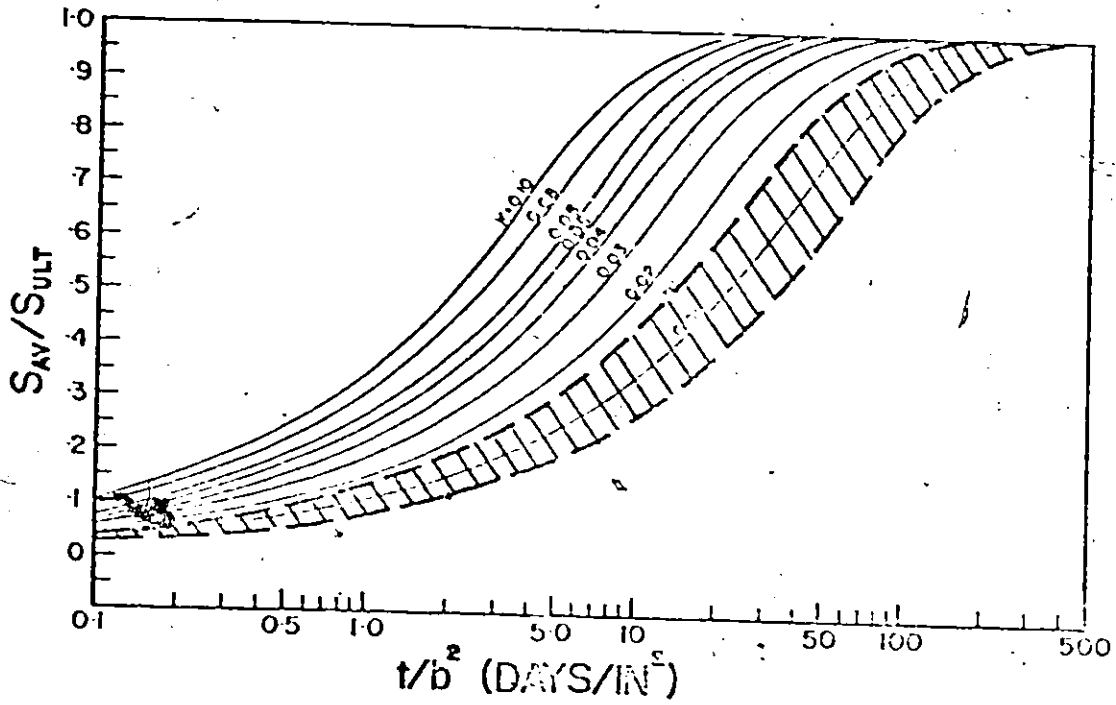
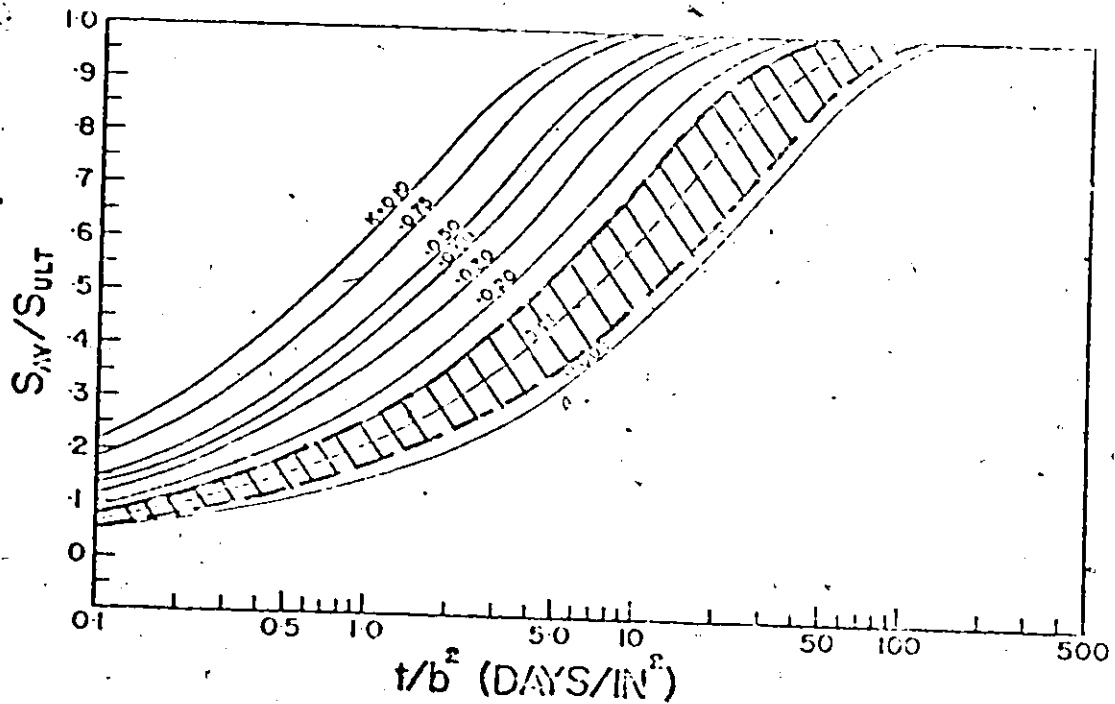


Figure 12 (Rostasy)

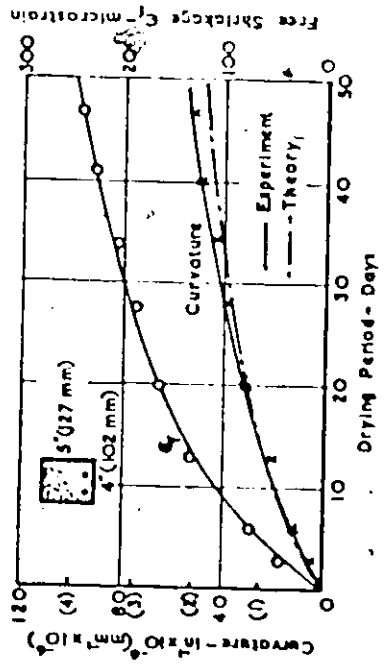


- A graphical representation of the scatter of theoretical curves needed to fit the experimental results for drying slabs.

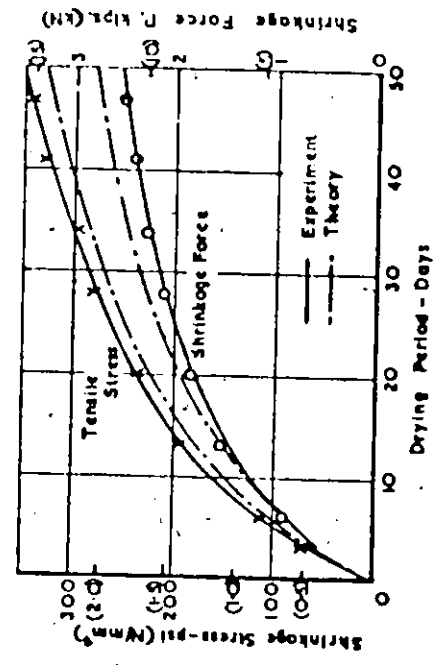


- A graphical representation of the scatter of theoretical curves needed to fit the experimental results for drying cylinders and square beams.

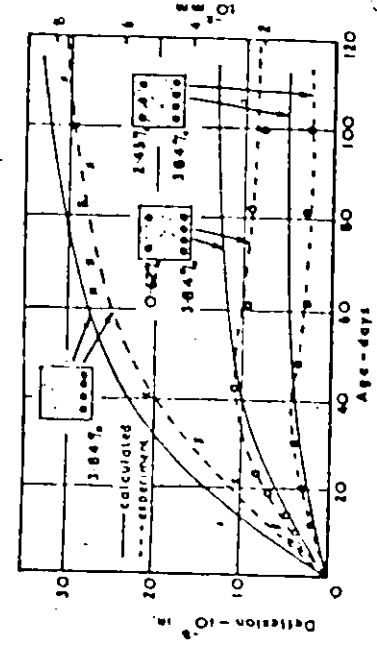
Figure 13 (Becker)



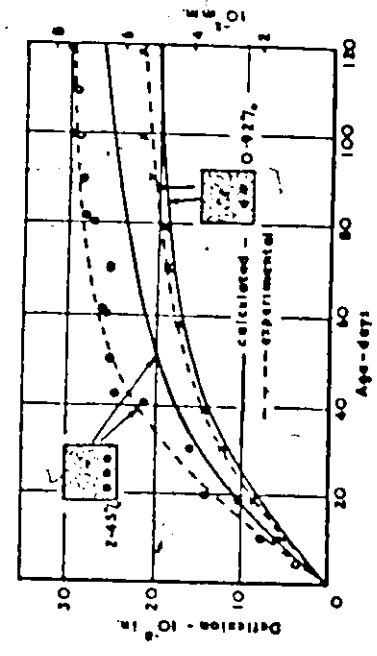
—Free shrinkage and curvature of test beams in the preliminary group (each point on the graph is the mean of two results)



—Shrinkage force and stress in concrete at the level of the steel in the preliminary tests



—Comparison between observed and theoretical deflections for beams in main group of tests



—Comparison between observed and theoretical deflections for singly-reinforced beams in main group of tests

Figure 14 (Elvery and Shaff1)

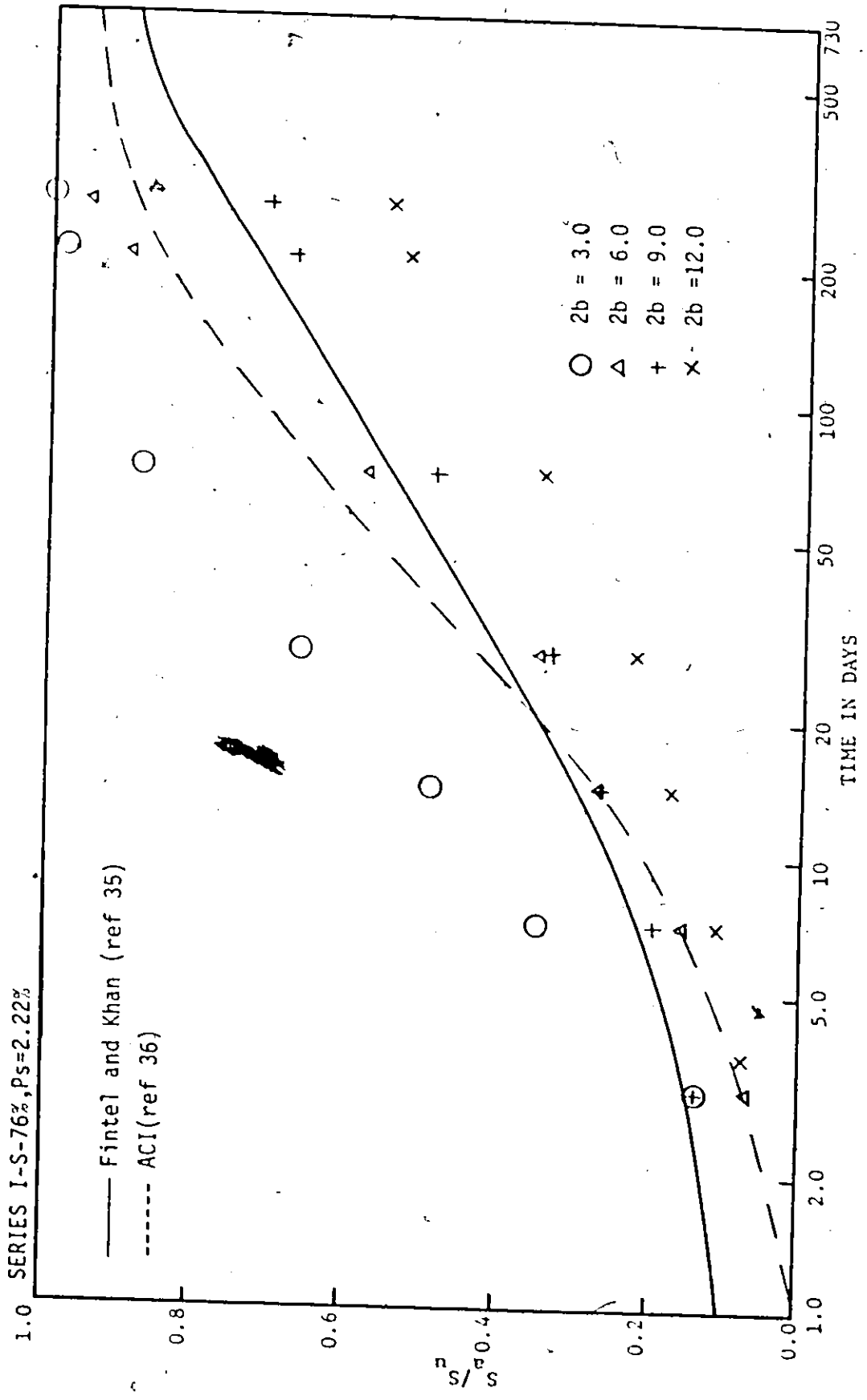


Figure 14a



THEORETICAL SHRINKAGE CURVES  
SLABS DRYING FROM 1 OR 2 SIDES

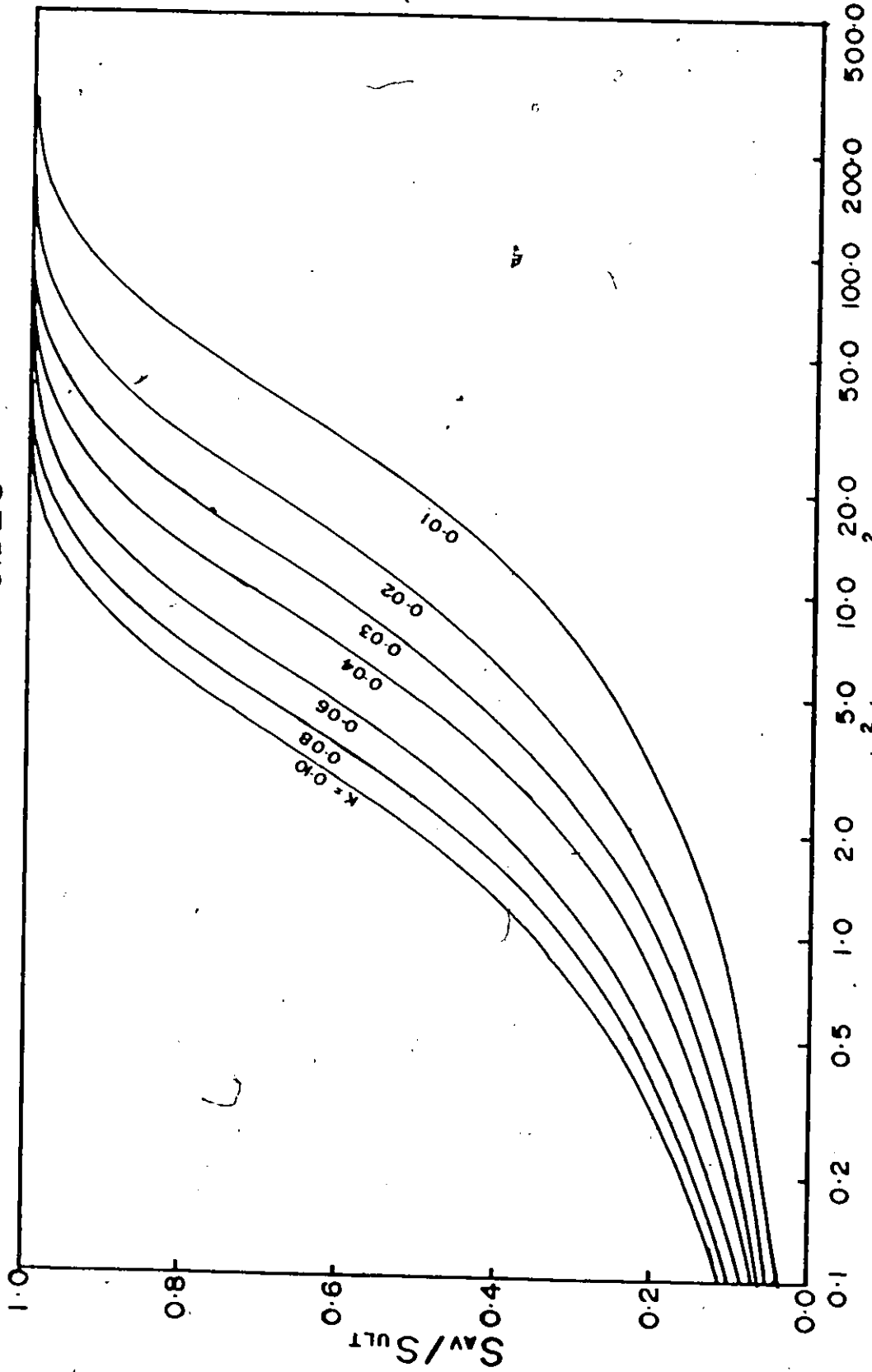


Figure 15.4

THEORETICAL SHRINKAGE CURVES  
SQUARE BEAMS OR COLUMNS DRYING FROM 4 SIDES

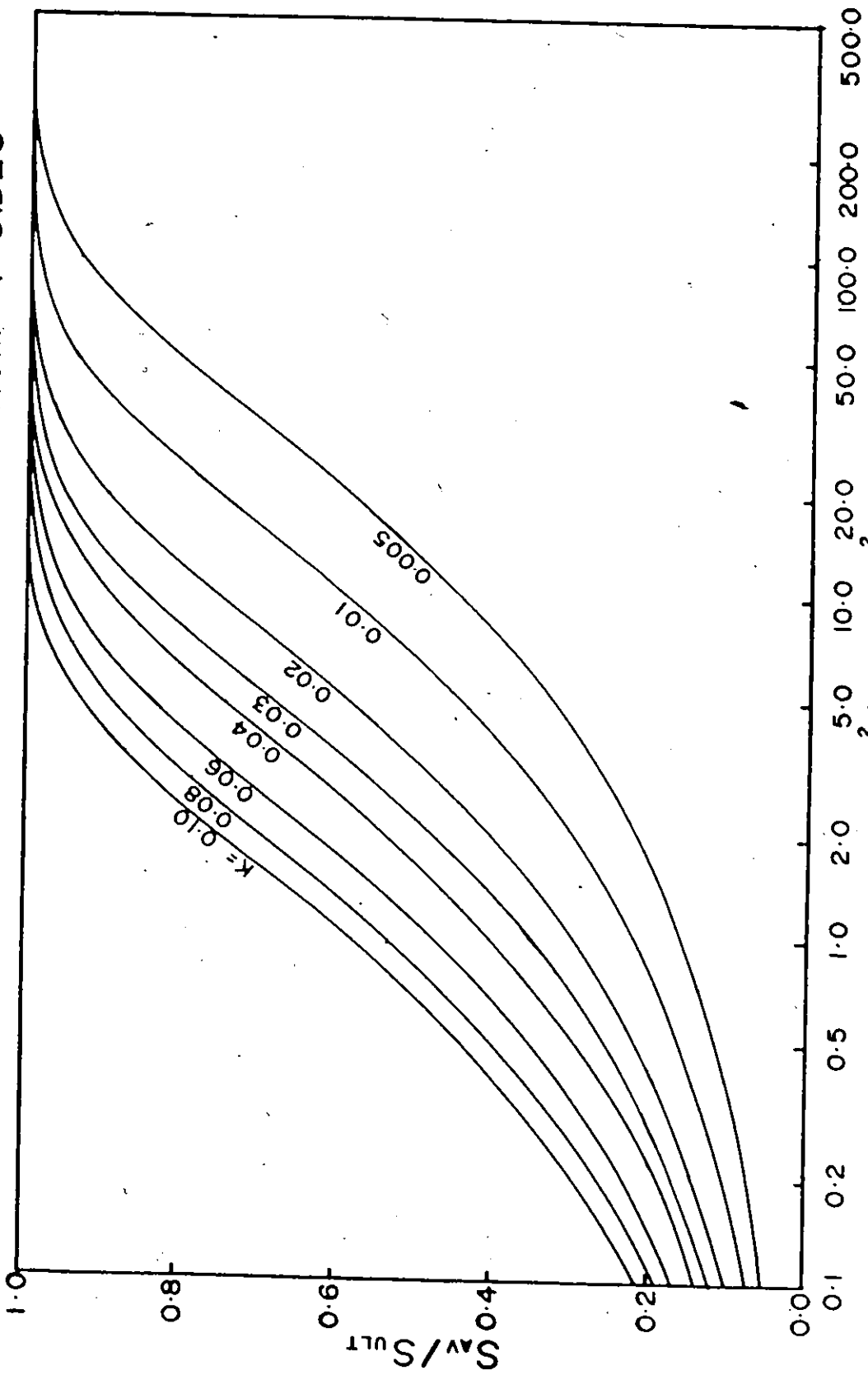


Figure 16

THEORETICAL SHRINKAGE CURVES  
RECTANGULAR BEAMS DRYING FROM 4 SIDES

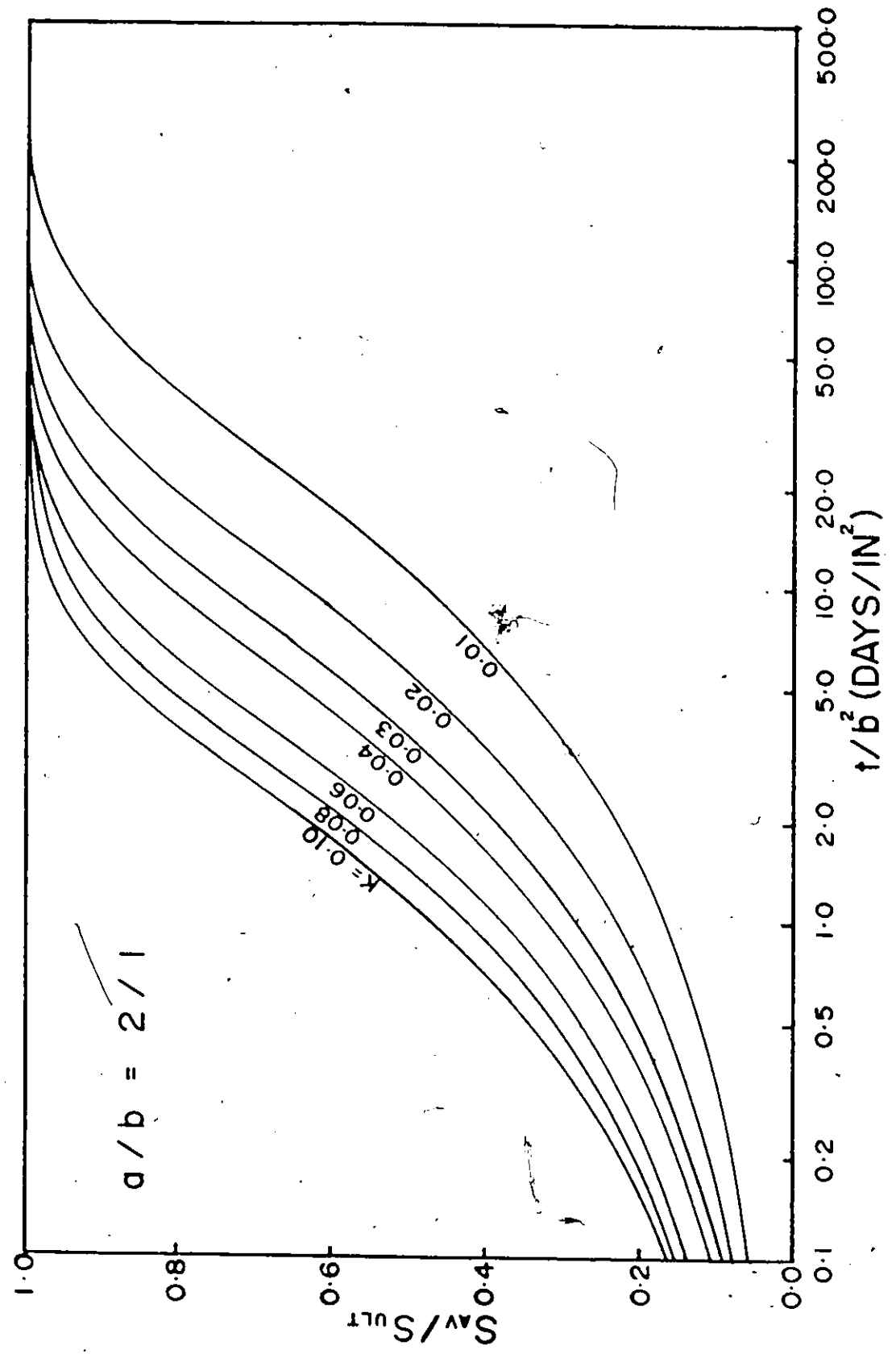


Figure 17

THEORETICAL SHRINKAGE CURVES  
RECTANGULAR BEAMS DRYING FROM 4 SIDES

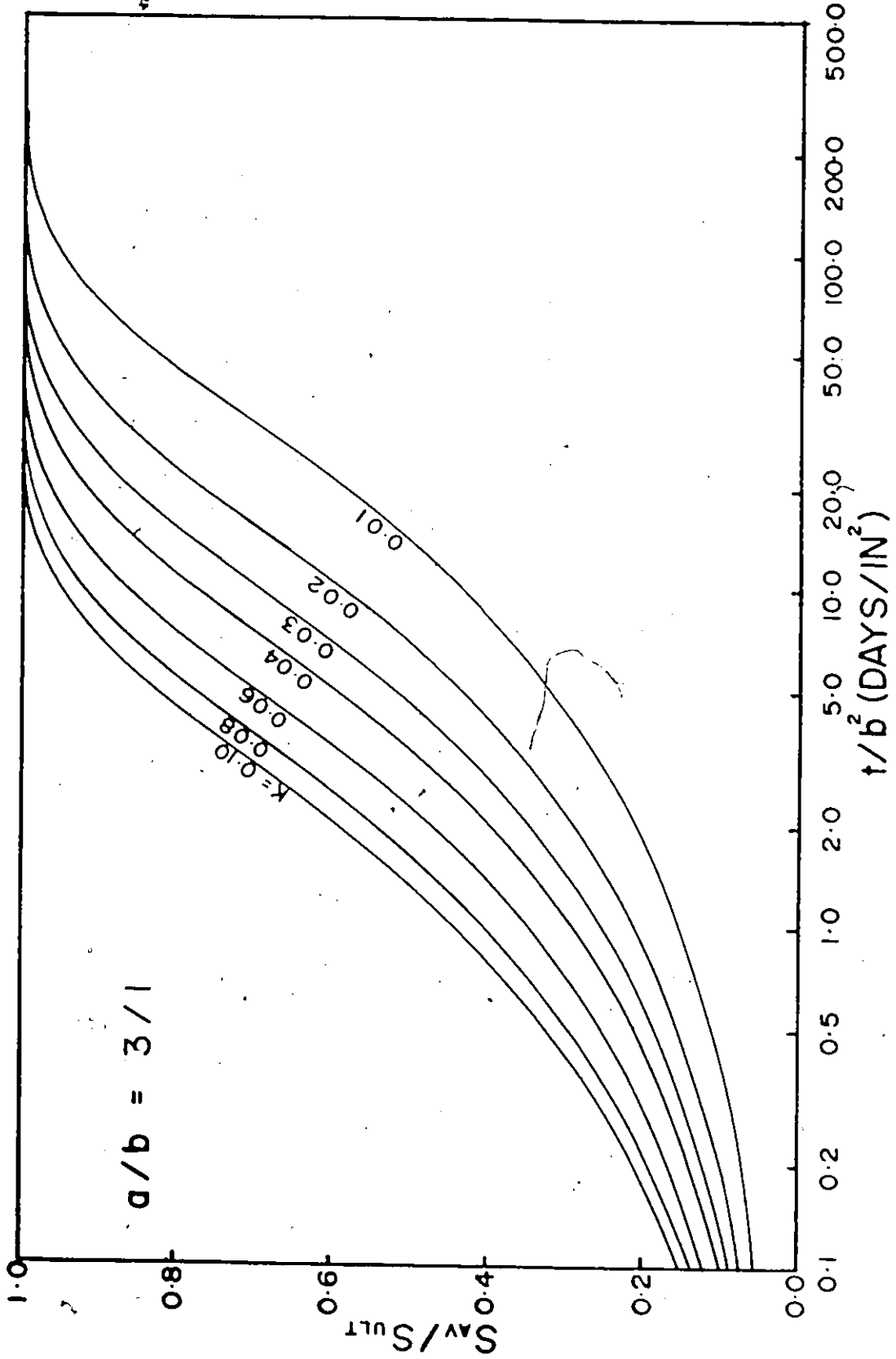


Figure 18

THEORETICAL SHRINKAGE CURVES  
RECTANGULAR BEAMS DRYING FROM 4 SIDES

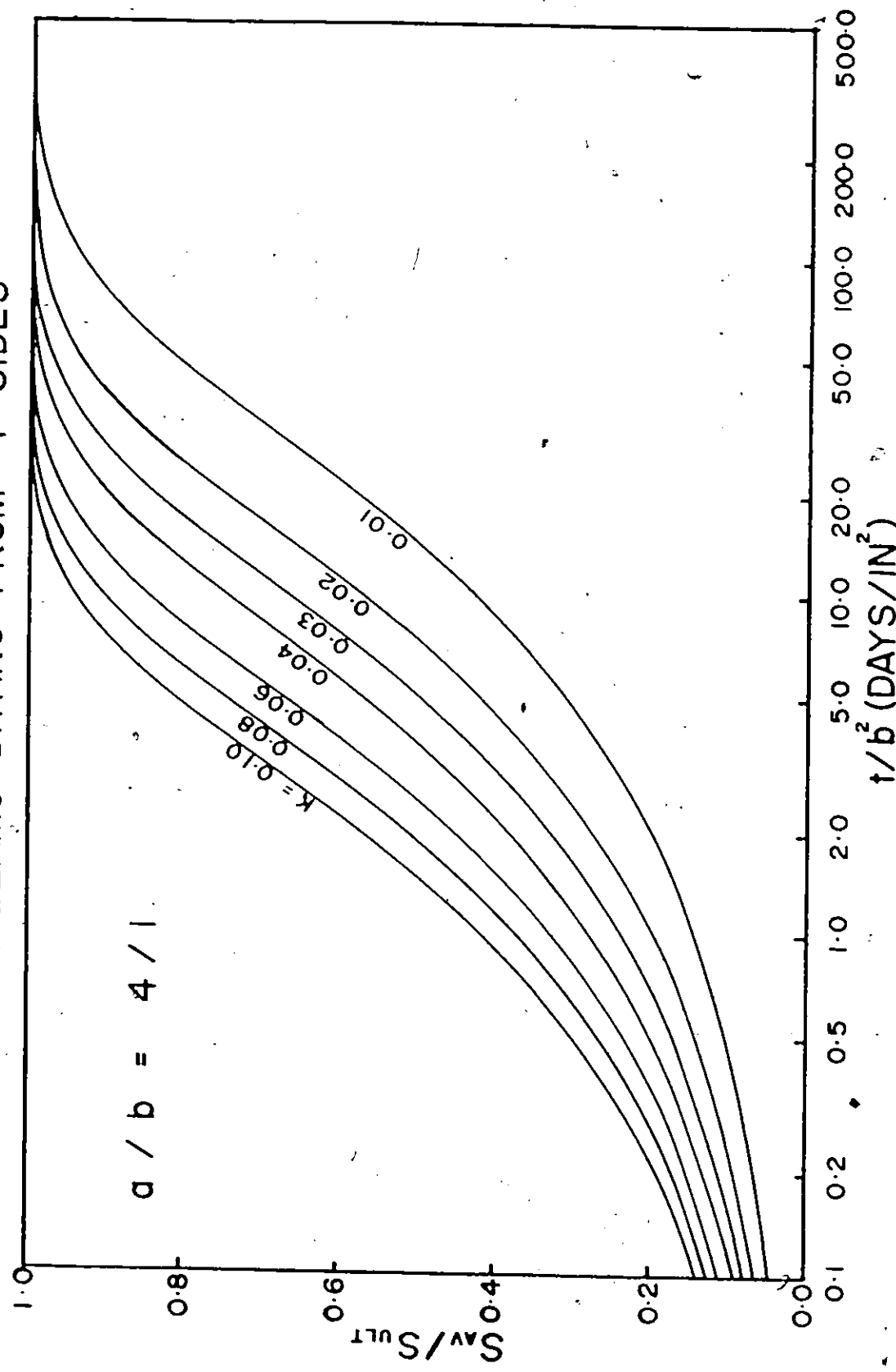
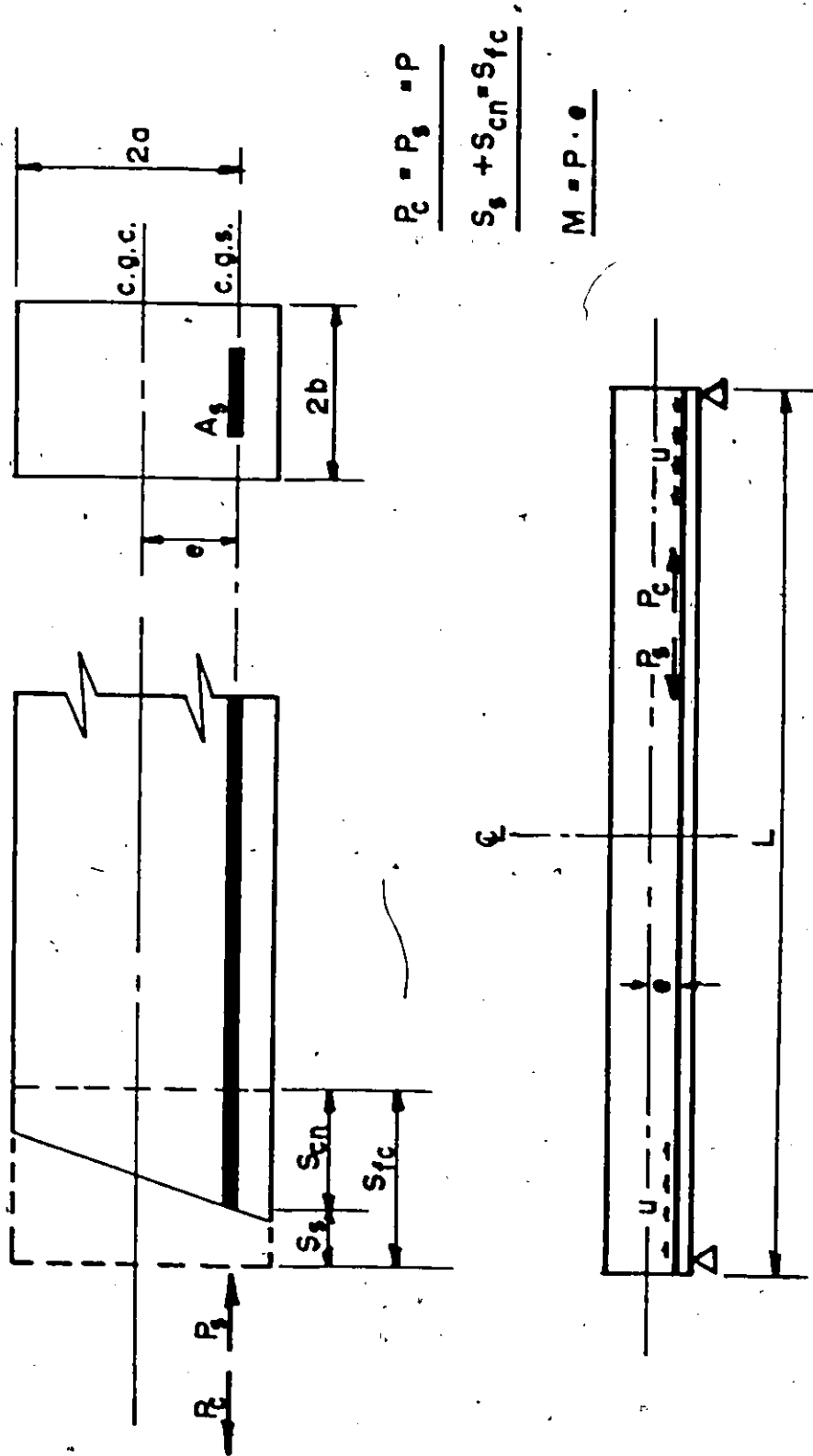
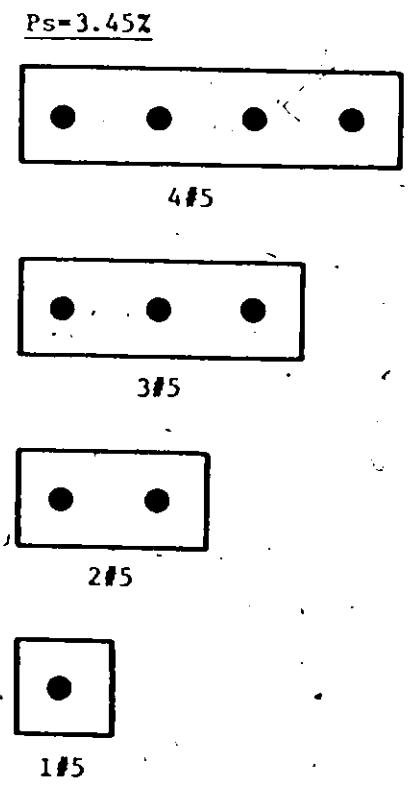
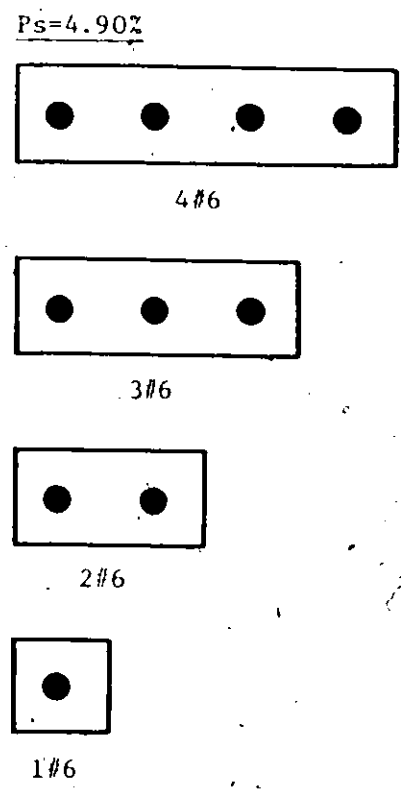
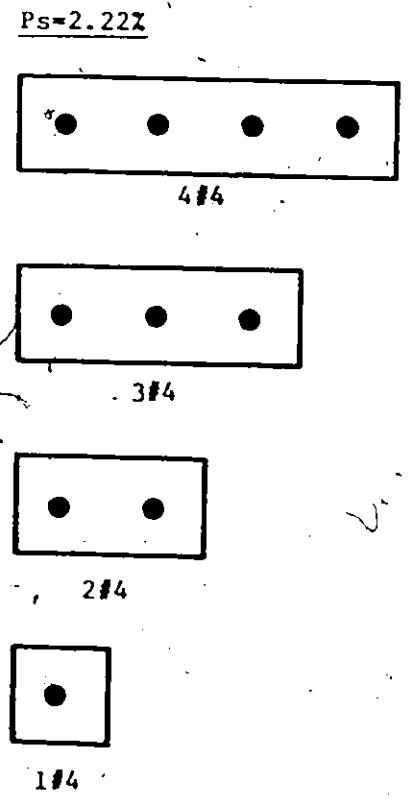
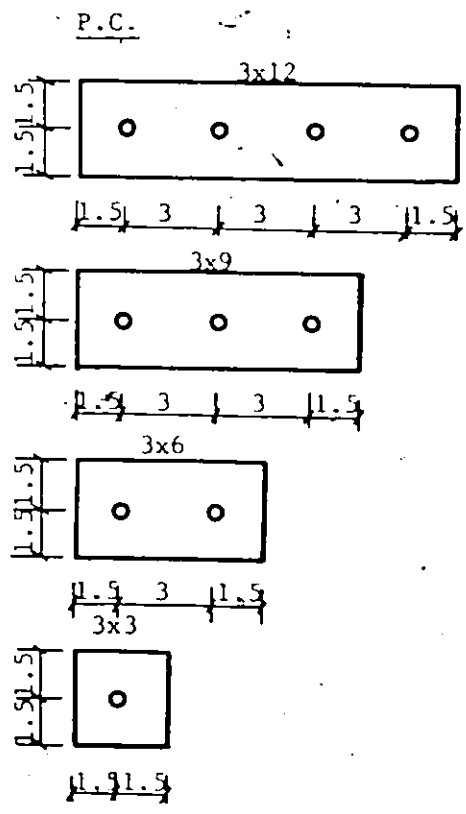


Figure 19



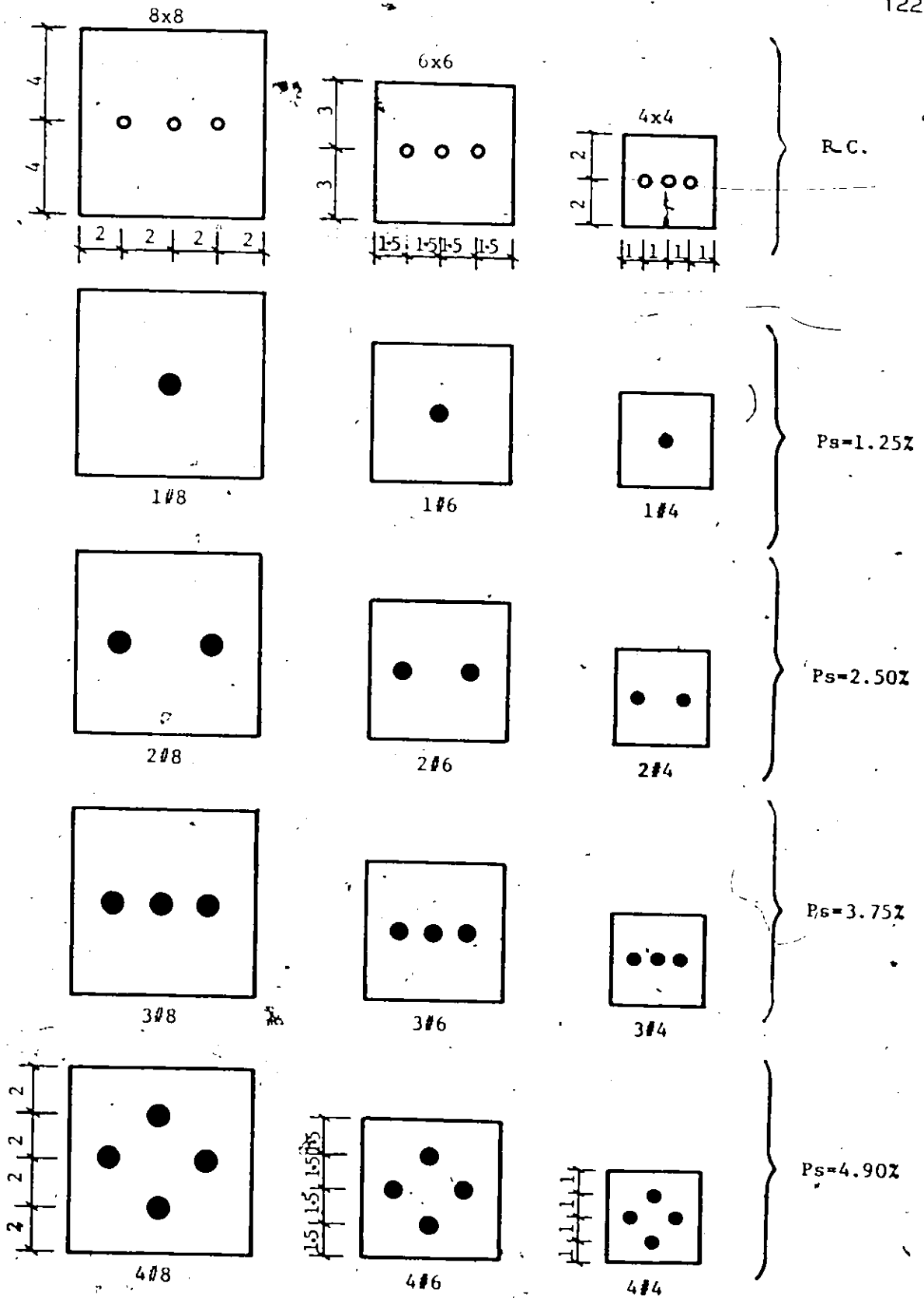
**EQUILIBRIUM CONDITIONS**

Figure 20



SLAB AND BEAM SPECIMENS

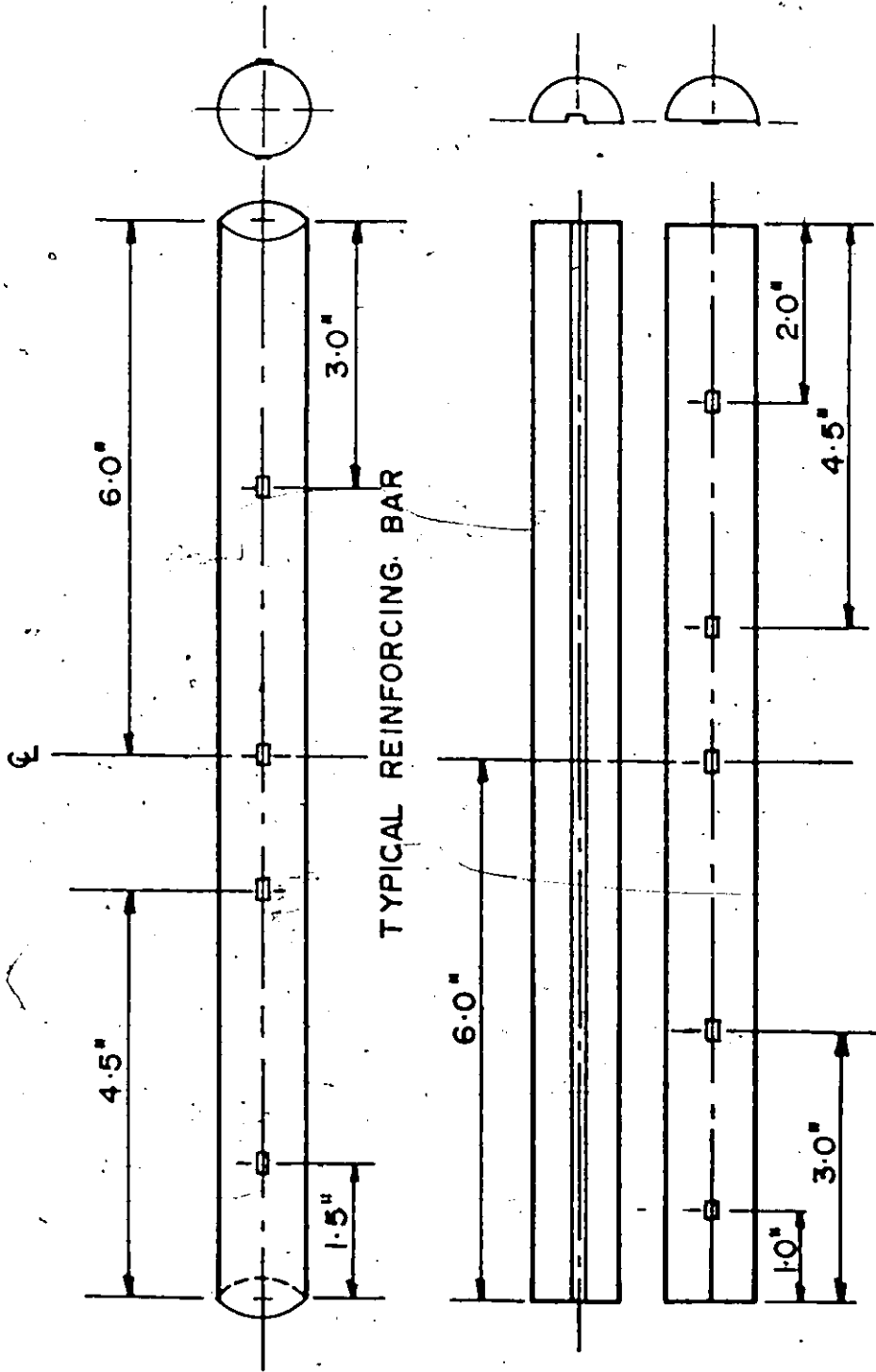
Figure 21



COLUMN SPECIMENS

Figure 22





MODIFIED REINFORCING BAR

Figure 23

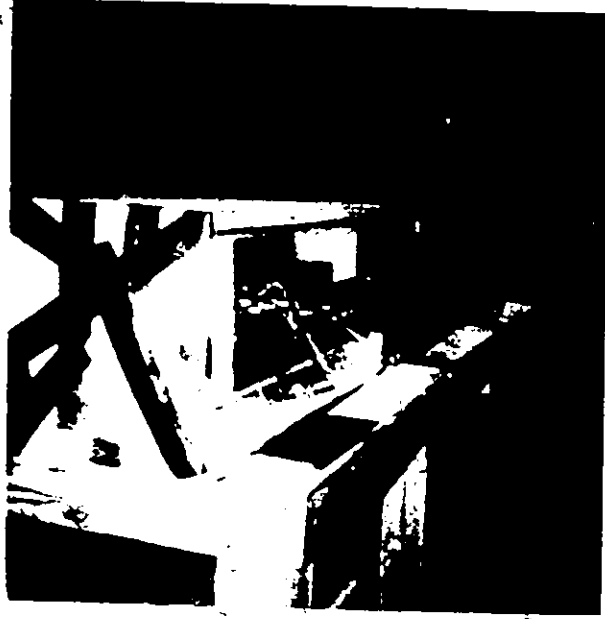


Figure 24

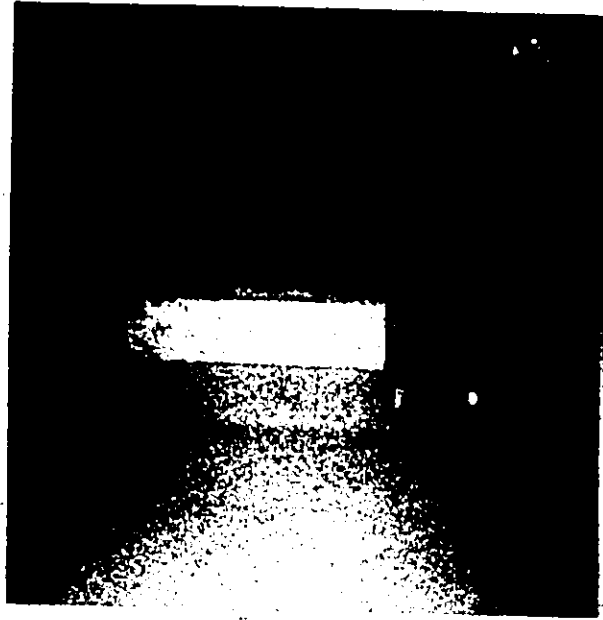


Figure 25

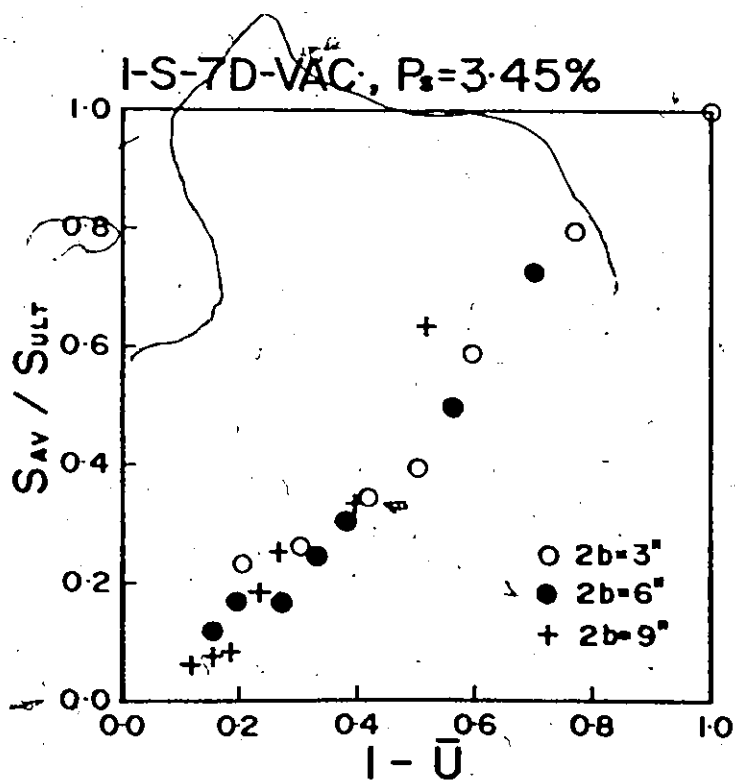
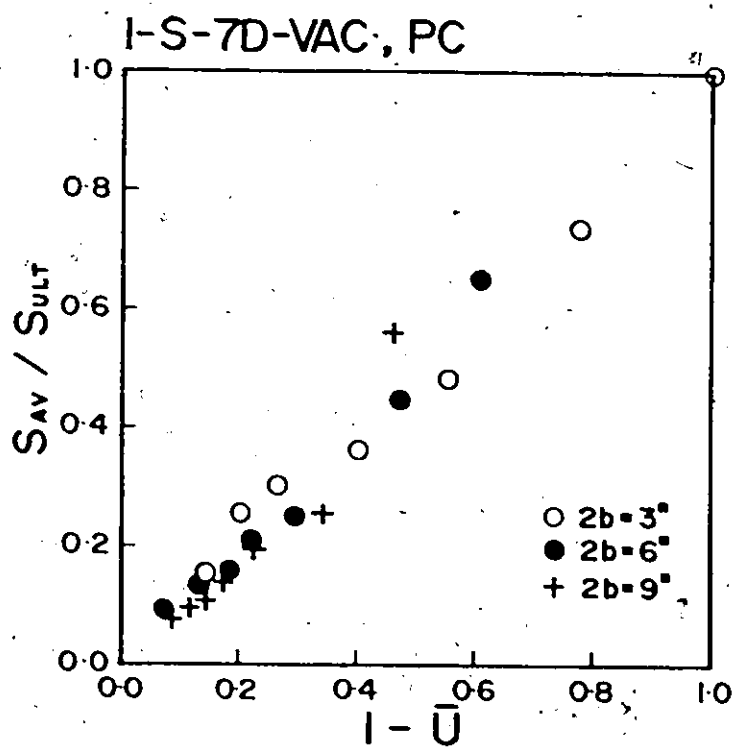


Figure 26

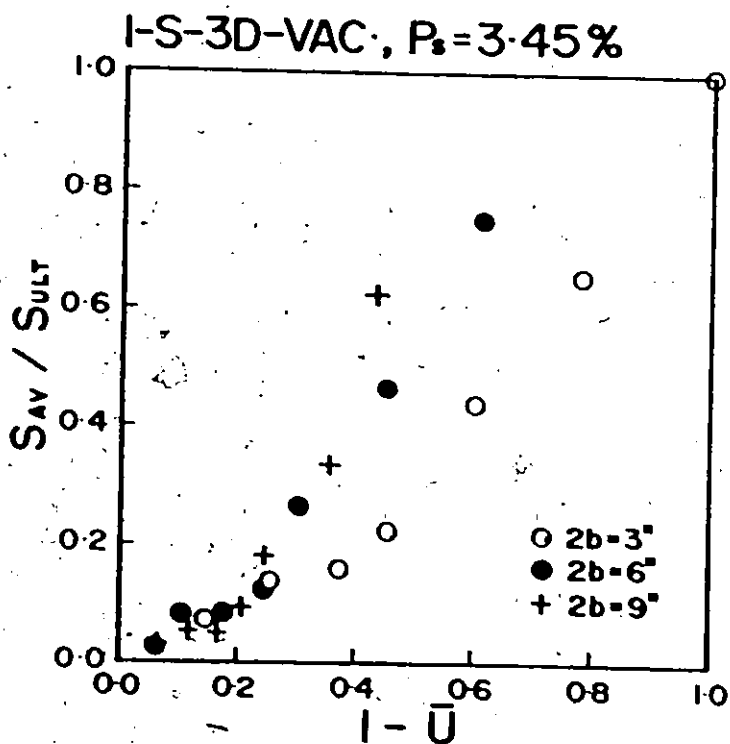
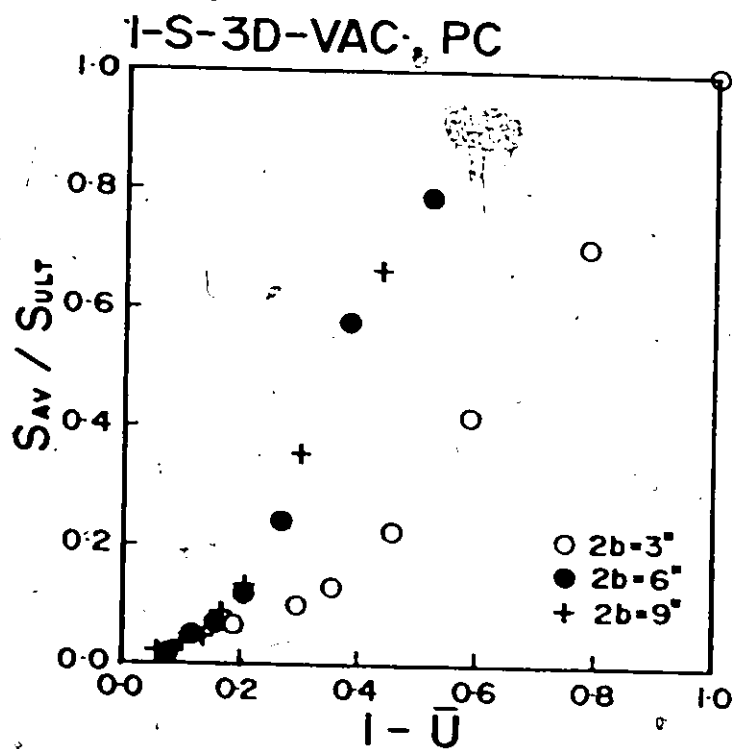


Figure 27

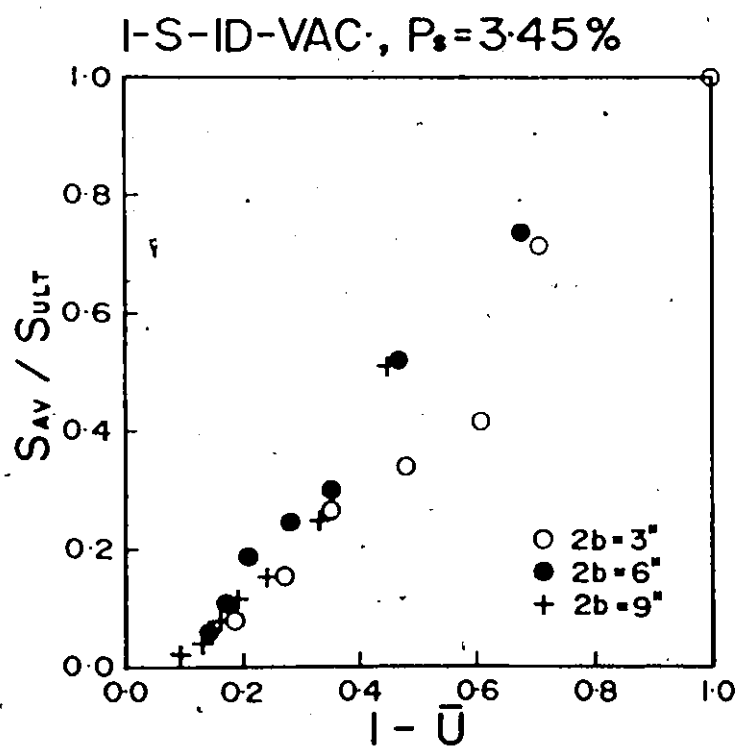
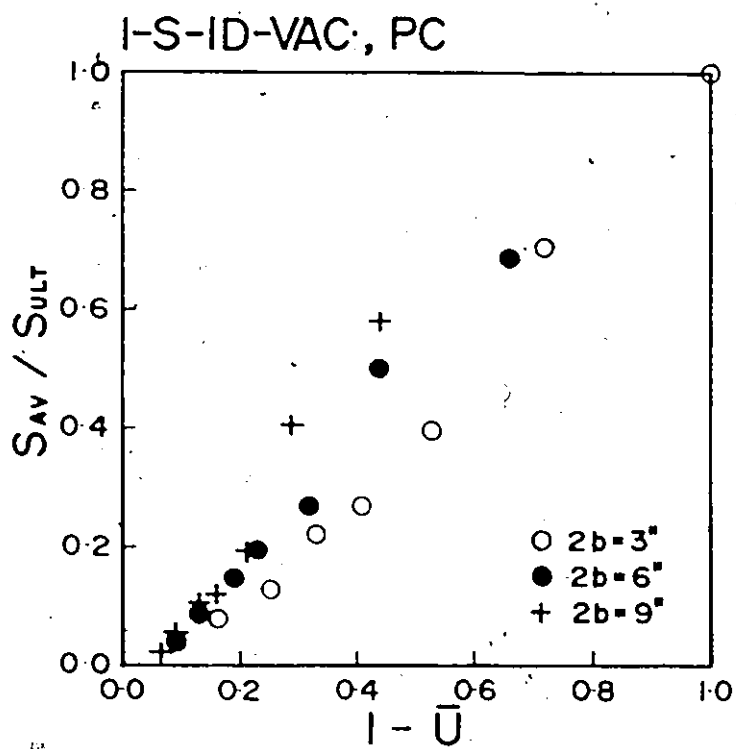


Figure 28

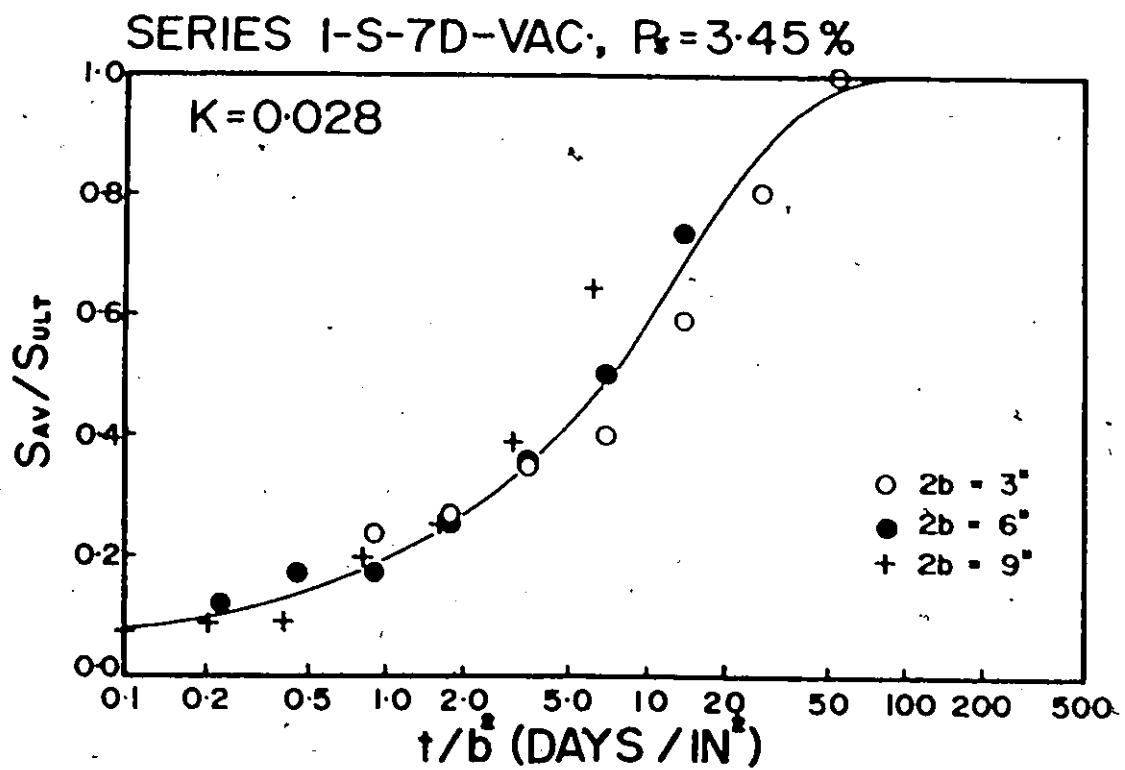
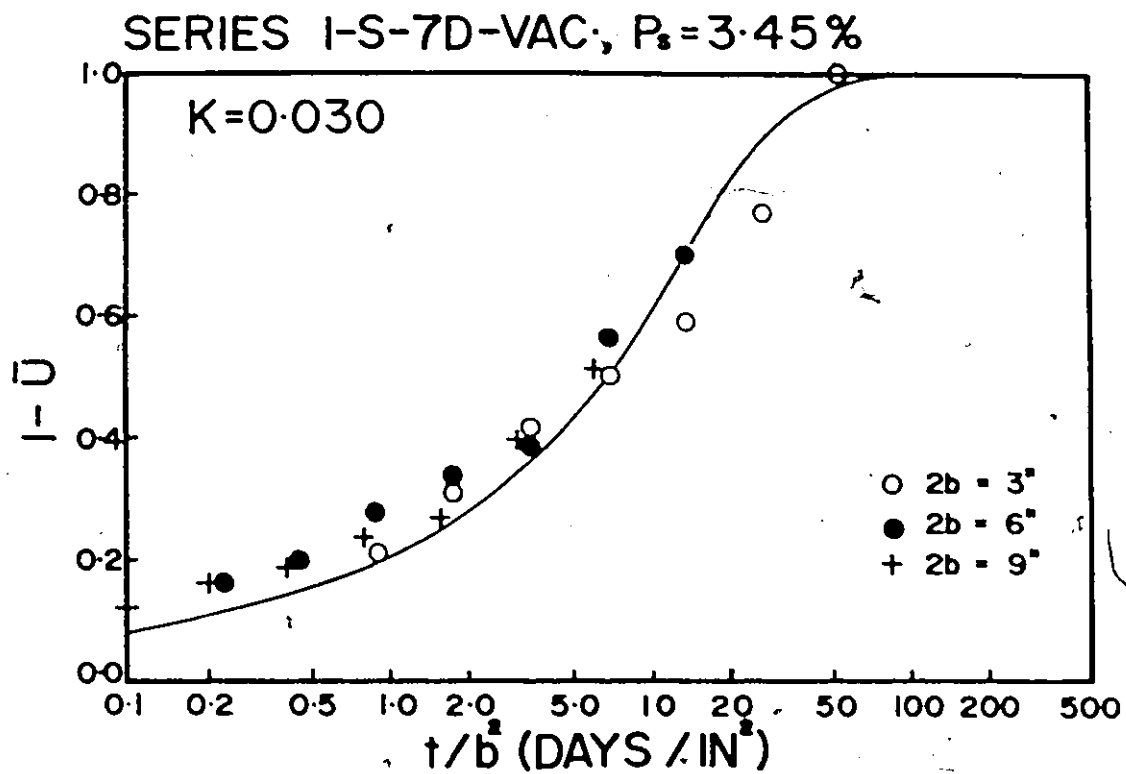


Figure 29

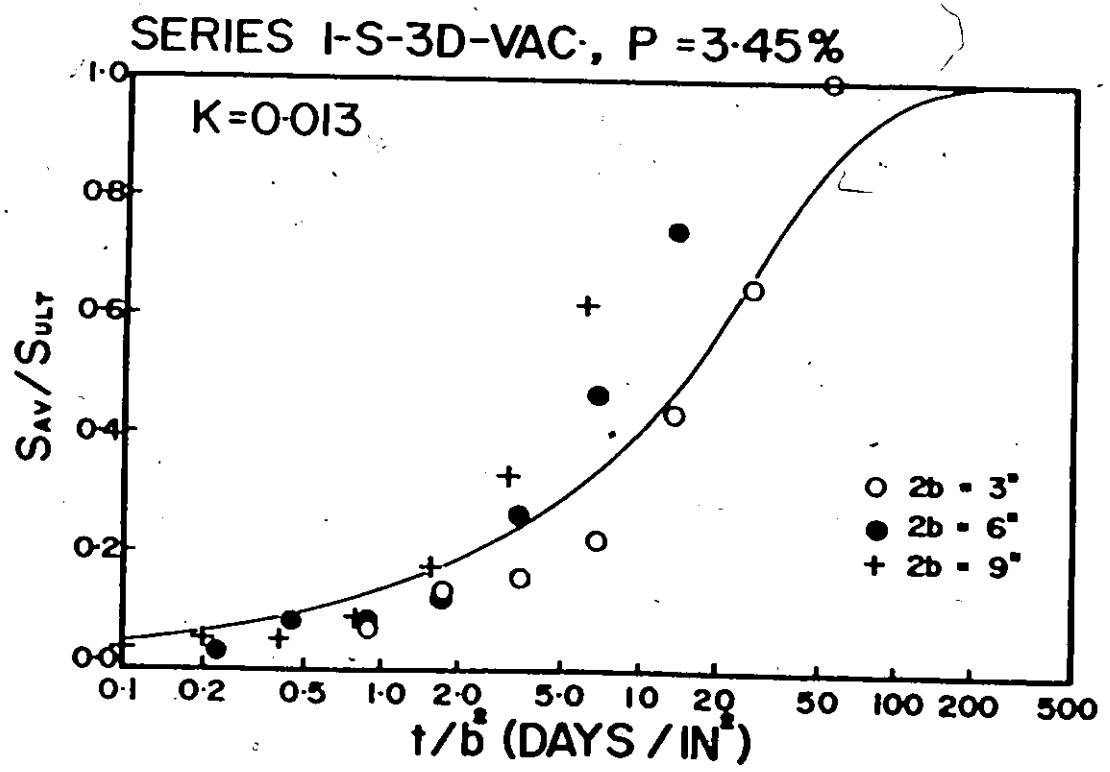
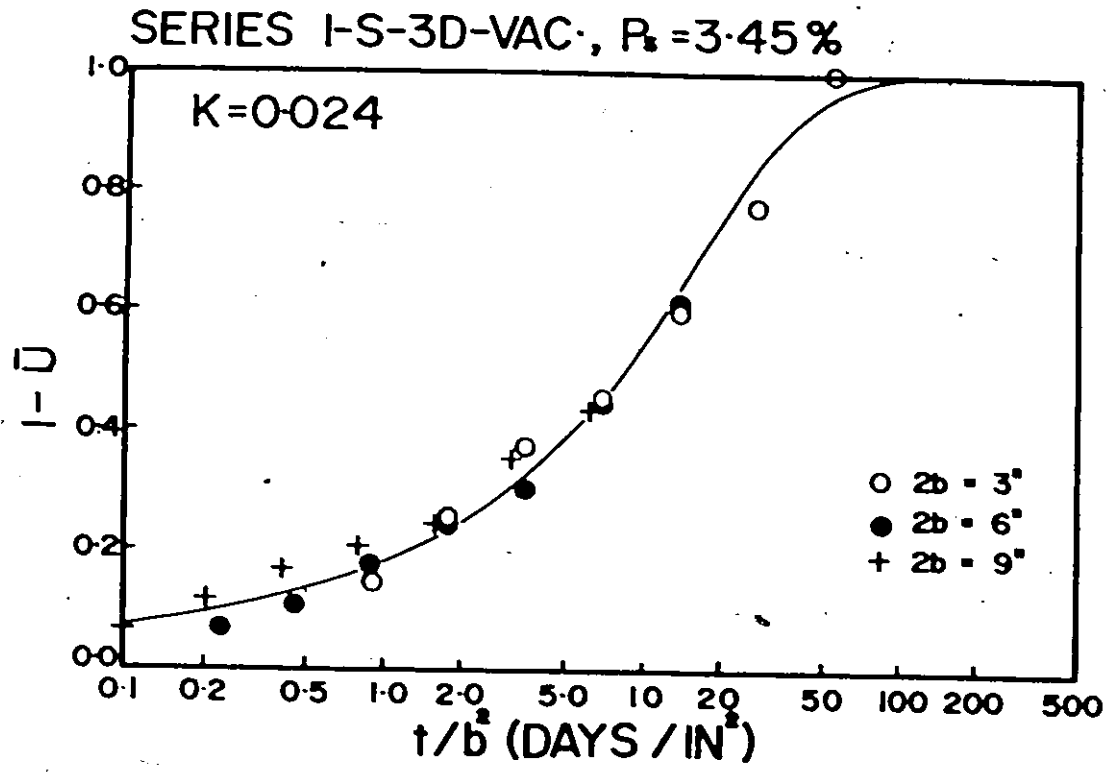


Figure 30

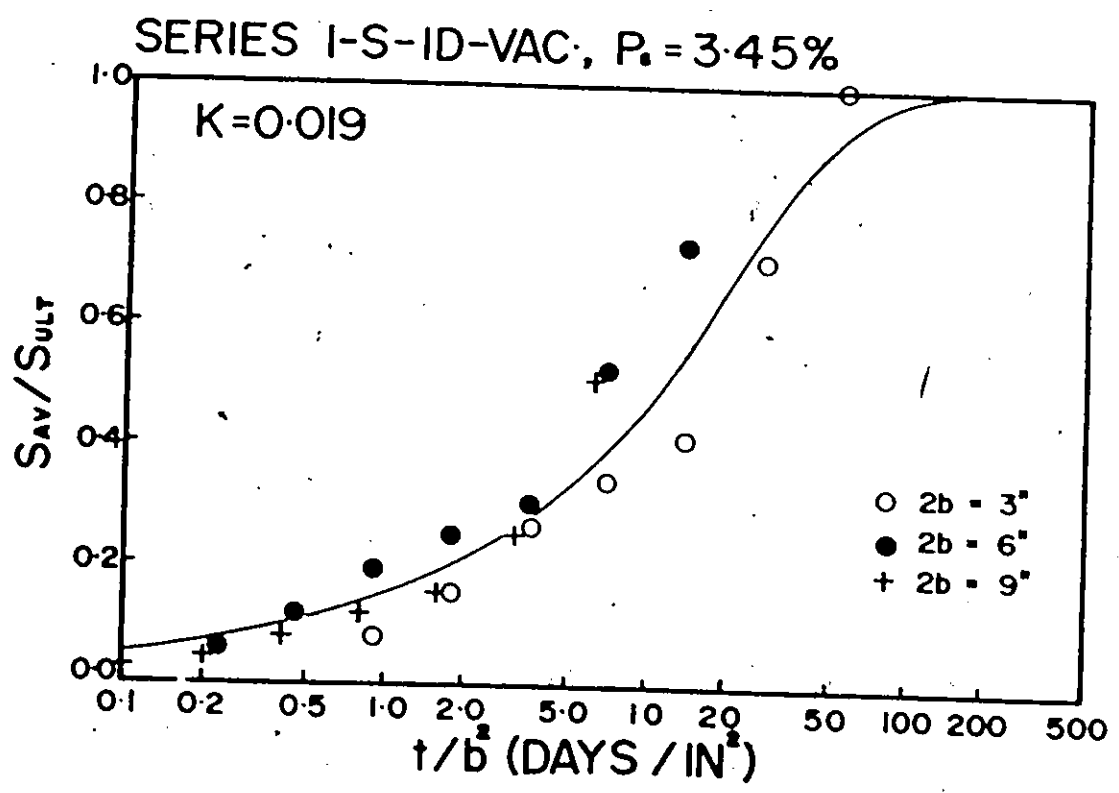
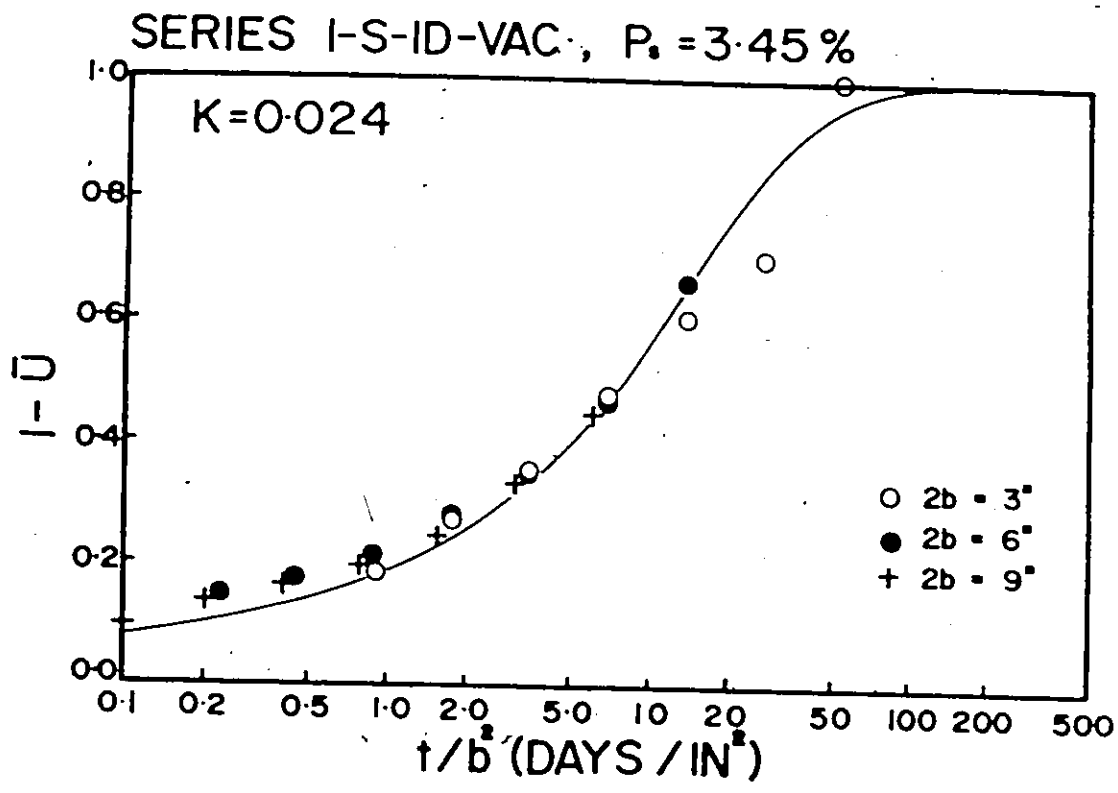


Figure 31



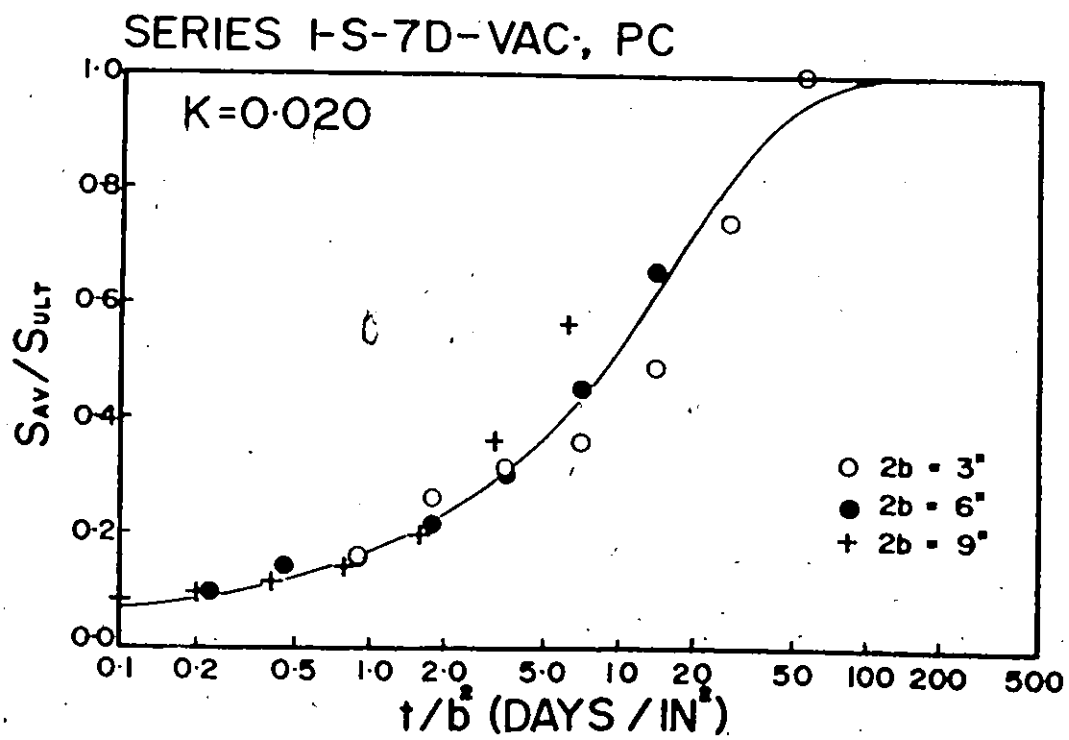
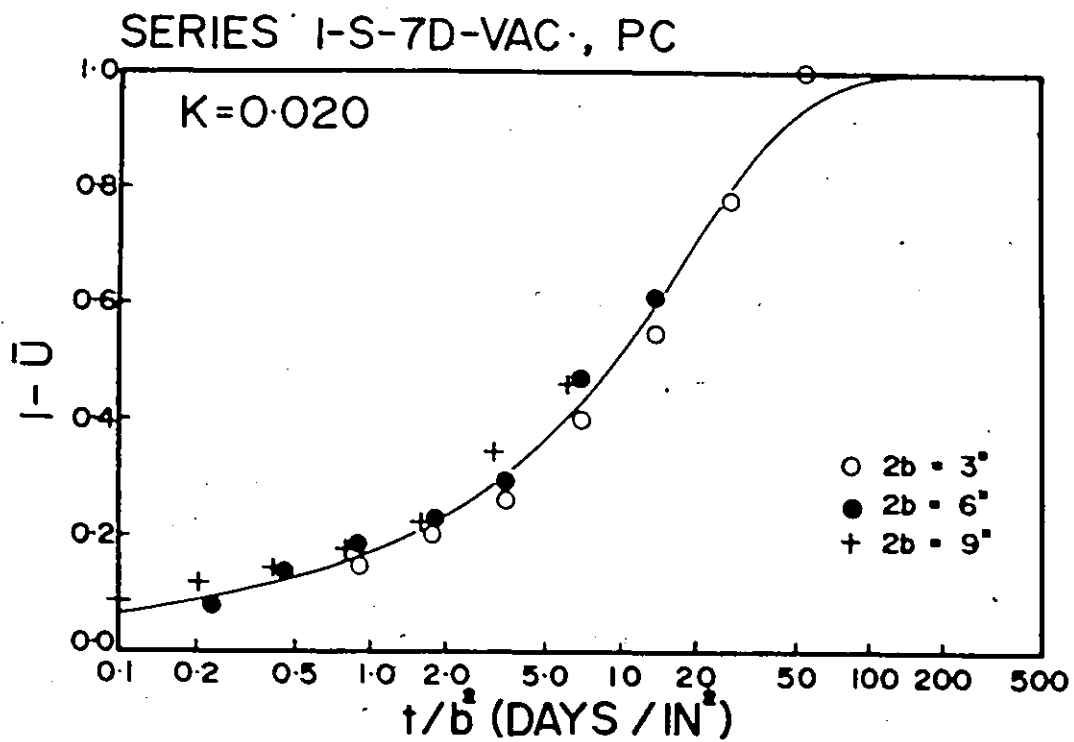


Figure 32

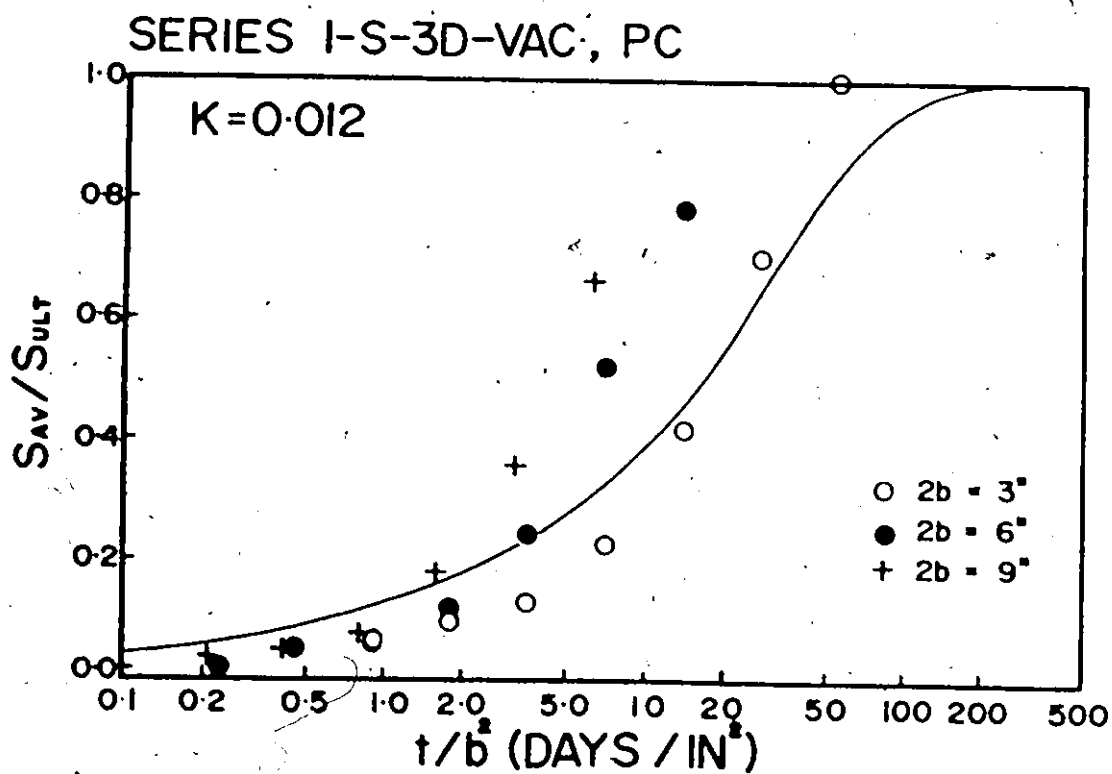
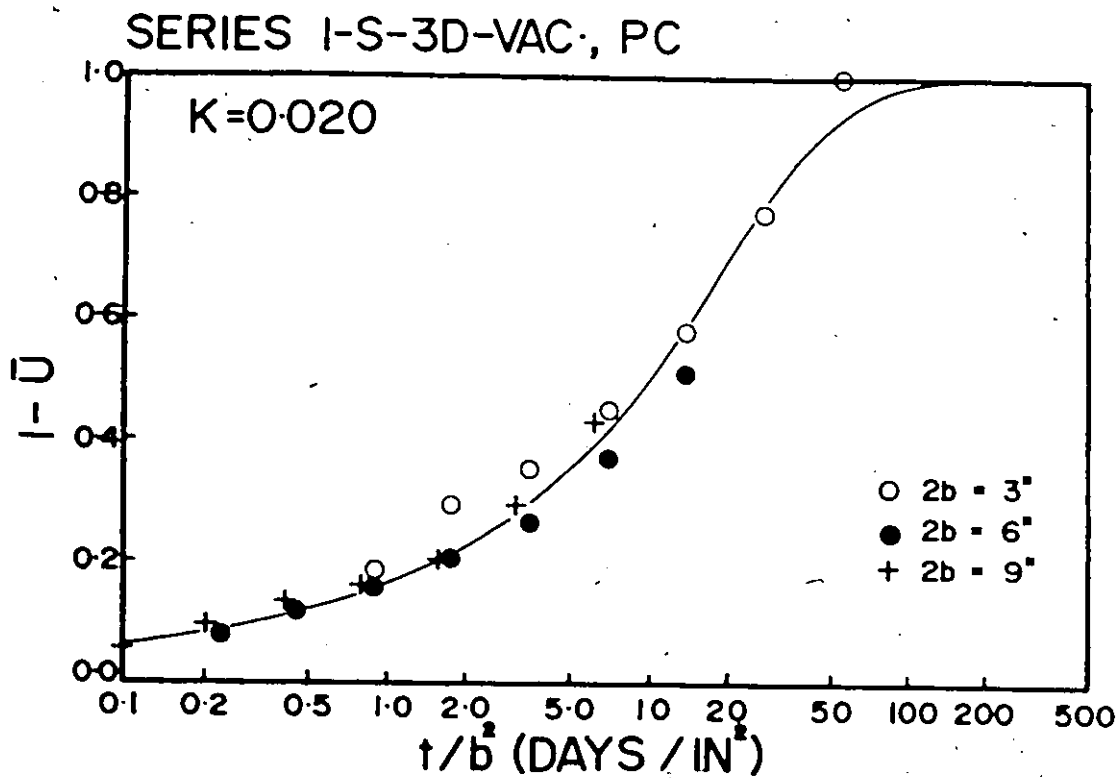


Figure 33

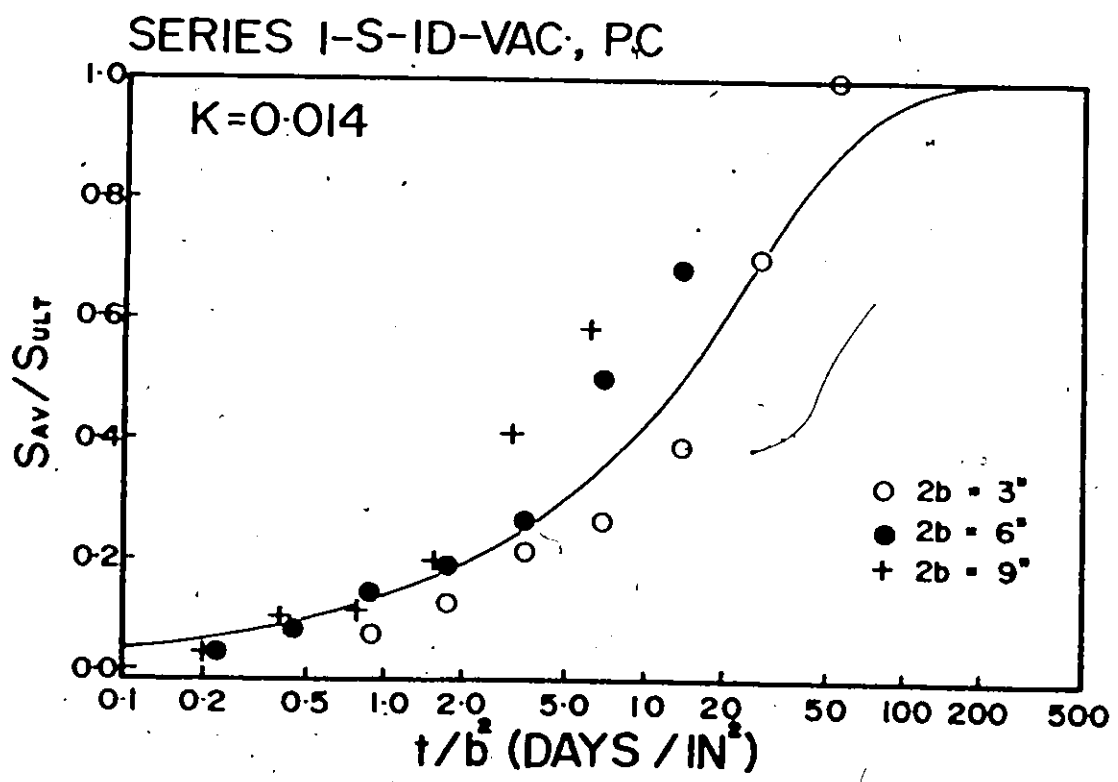
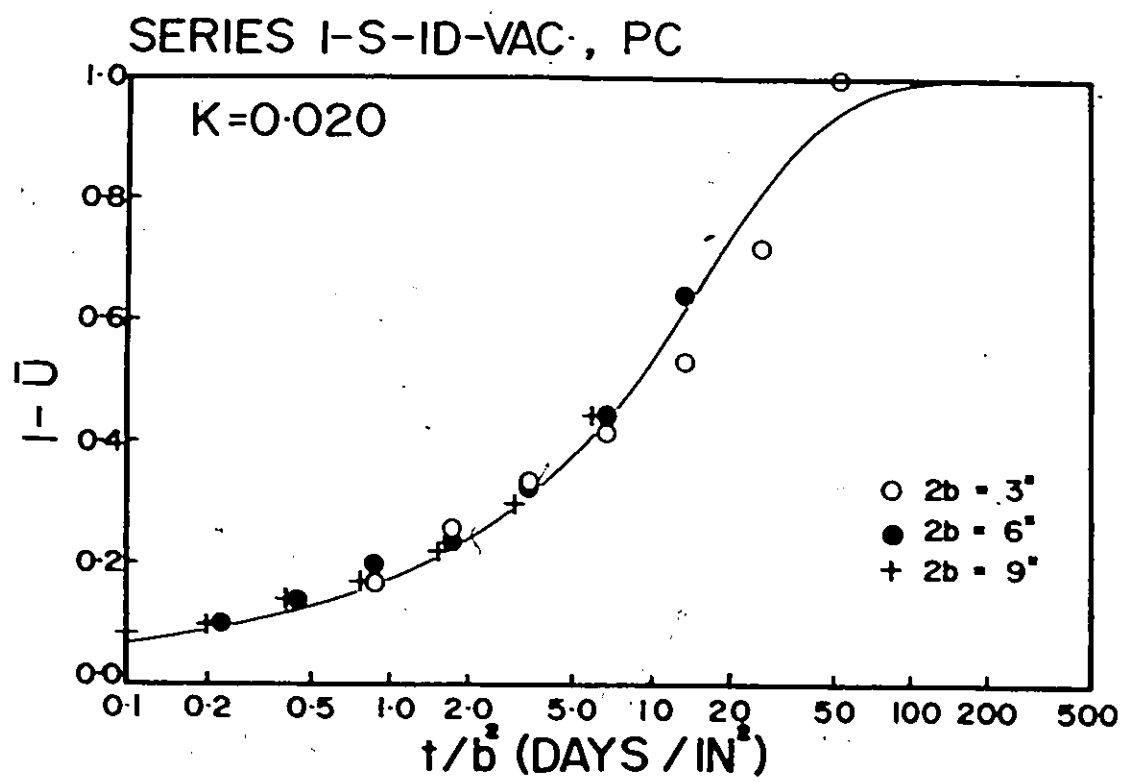


Figure 34

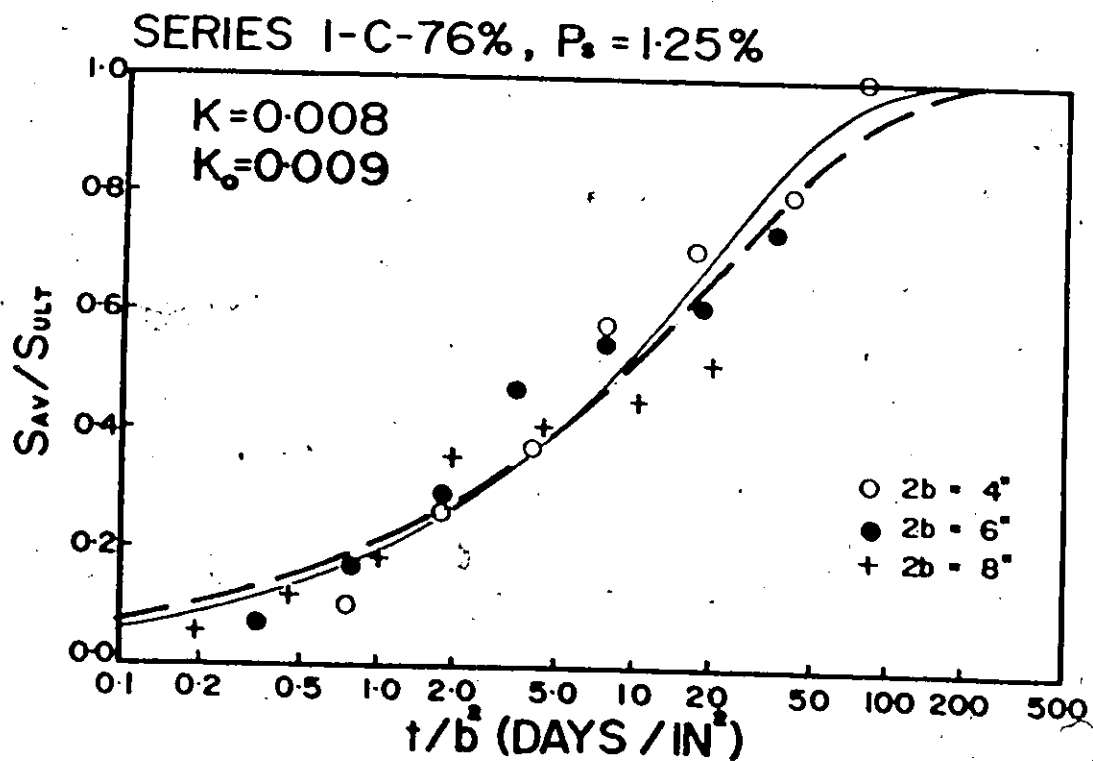
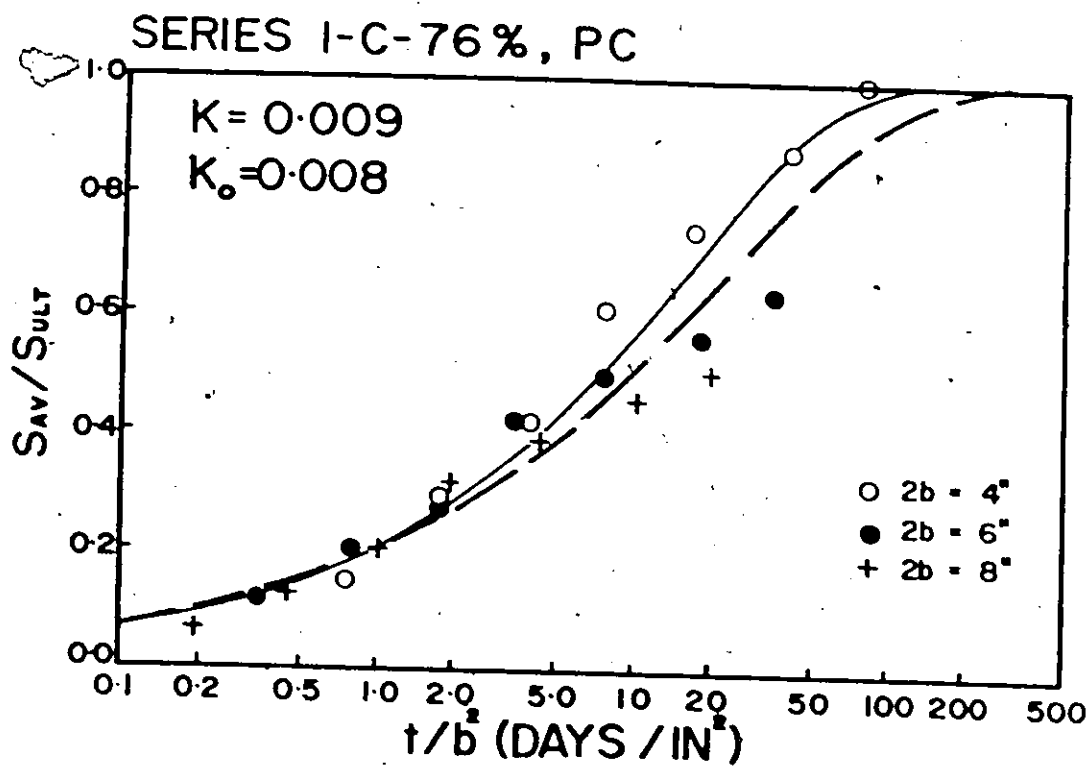


Figure 35

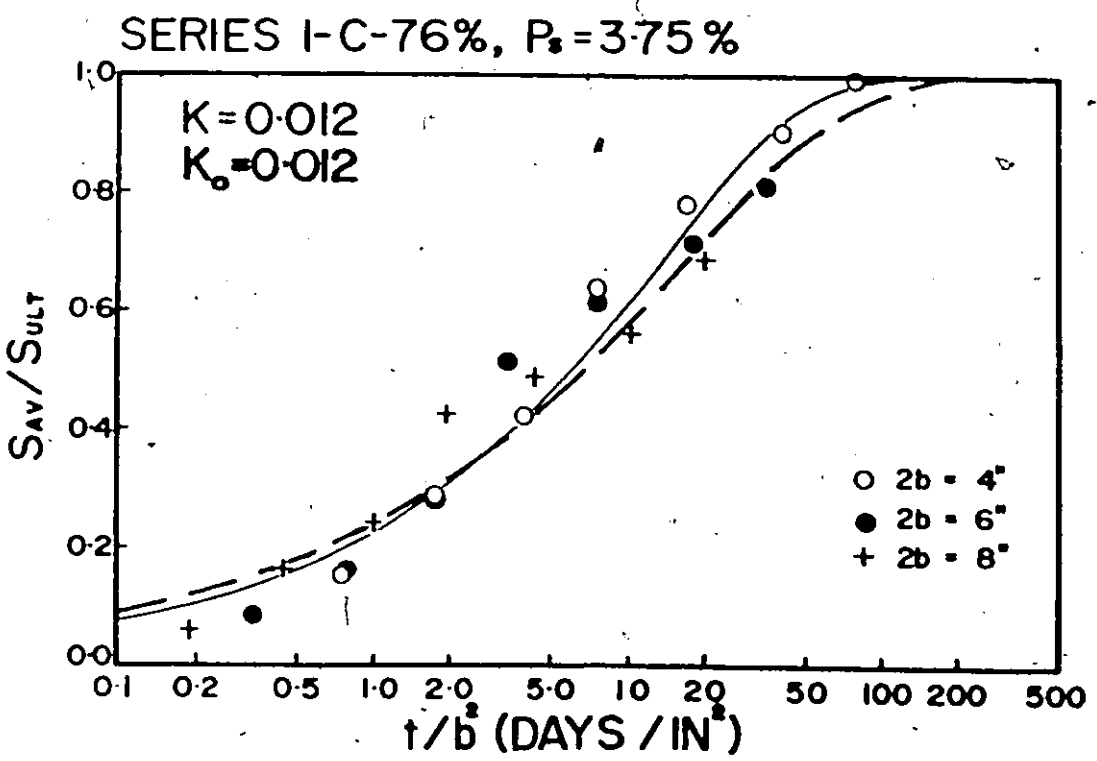
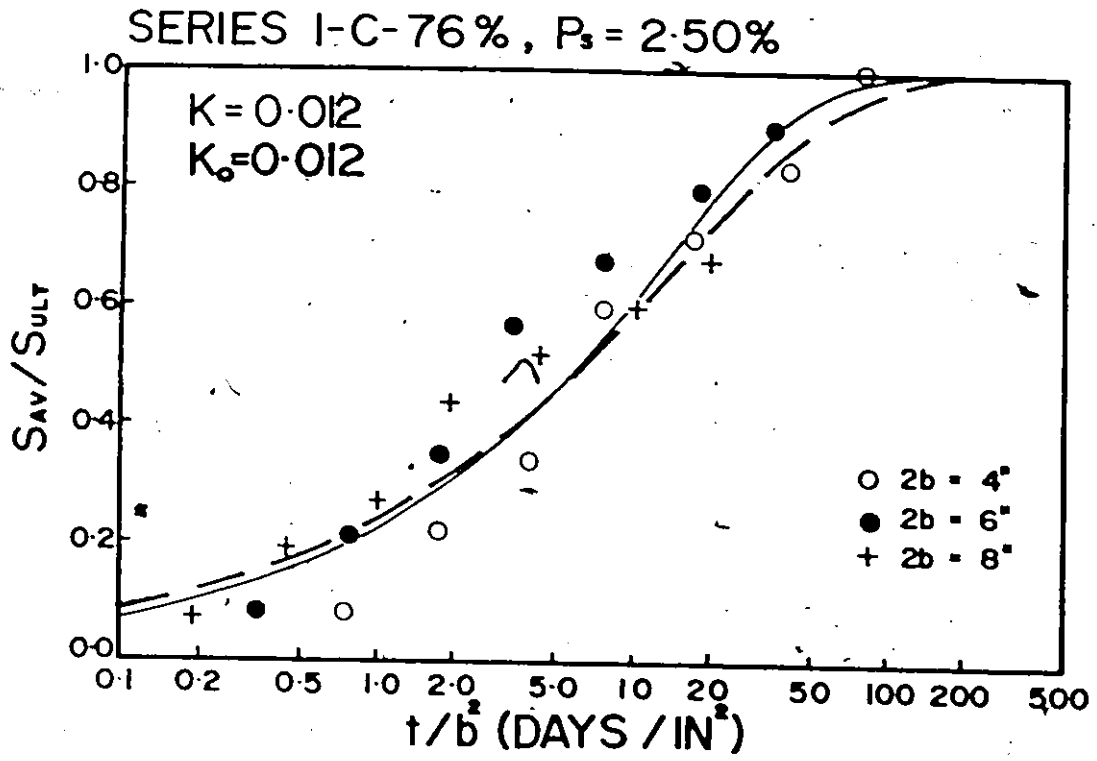


Figure 36

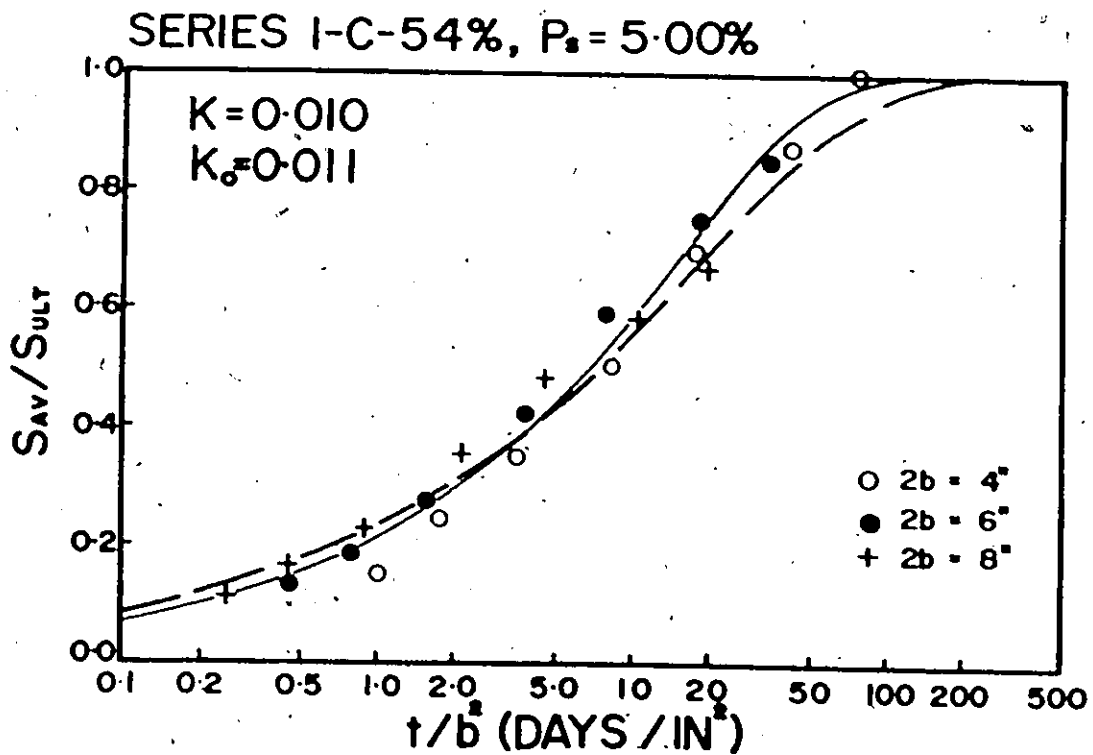
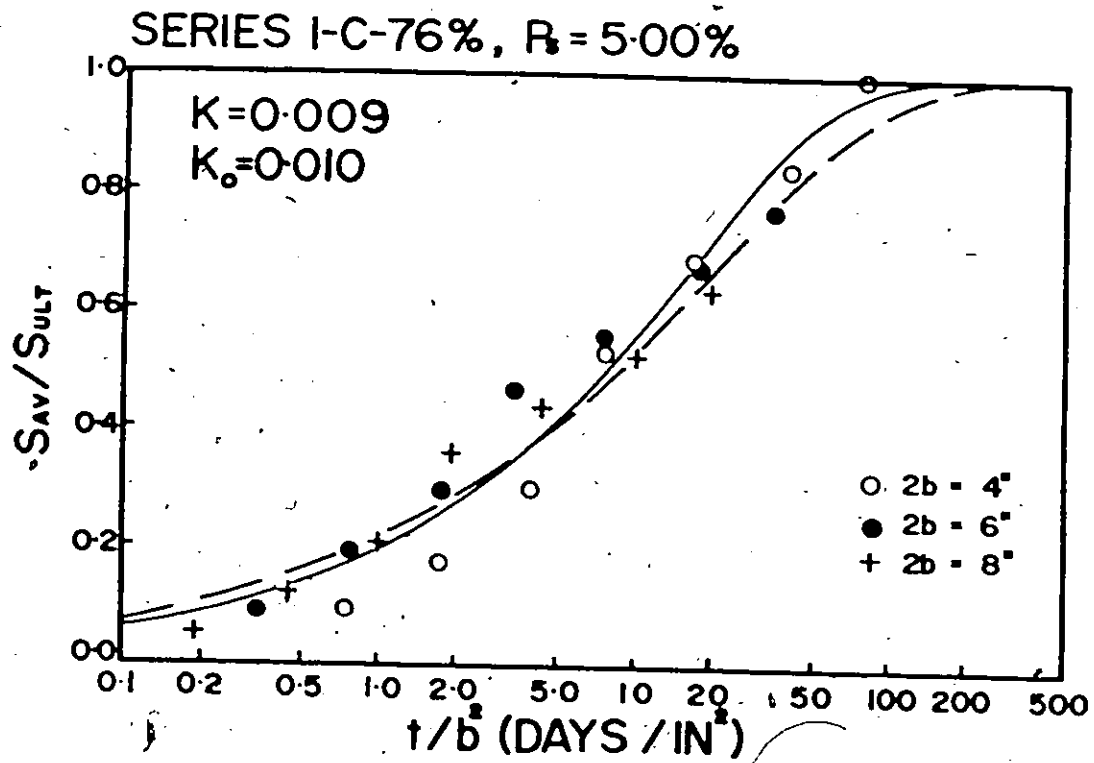


Figure 37

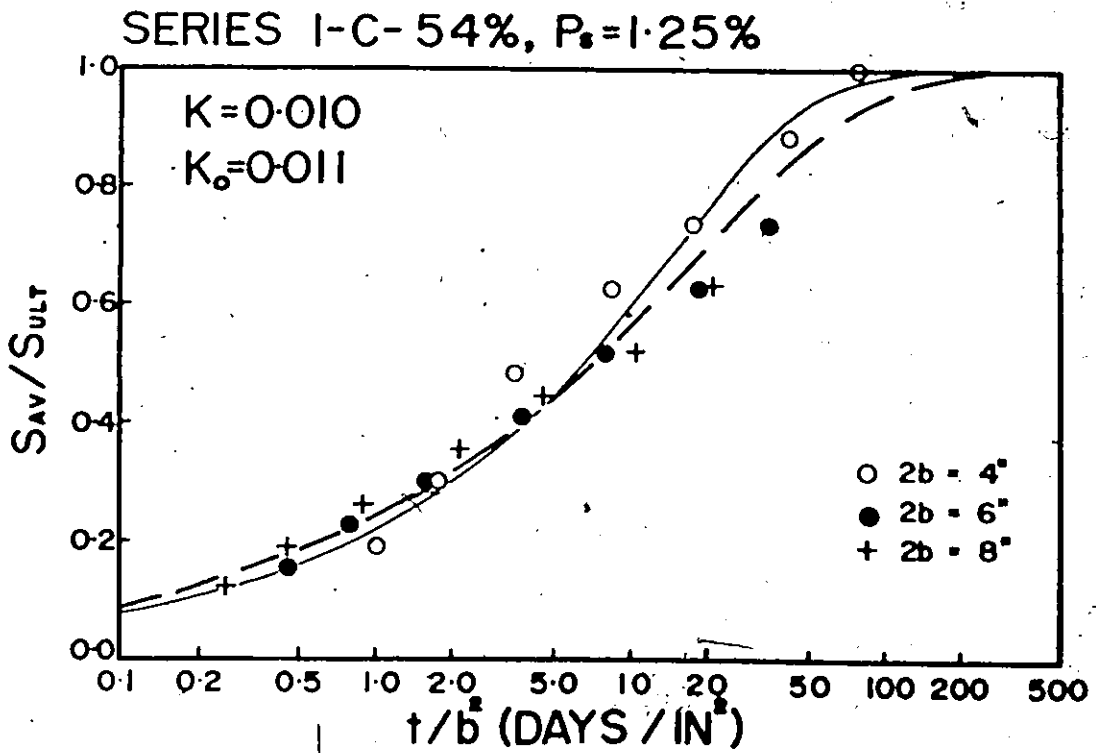
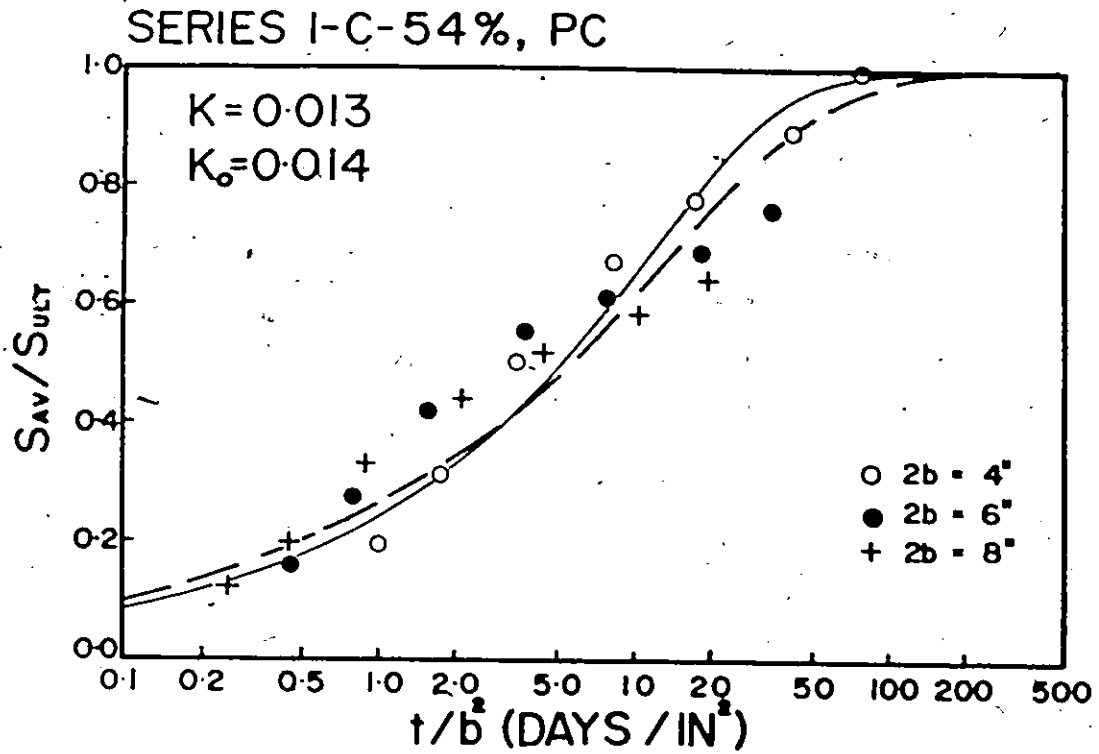


Figure 38.

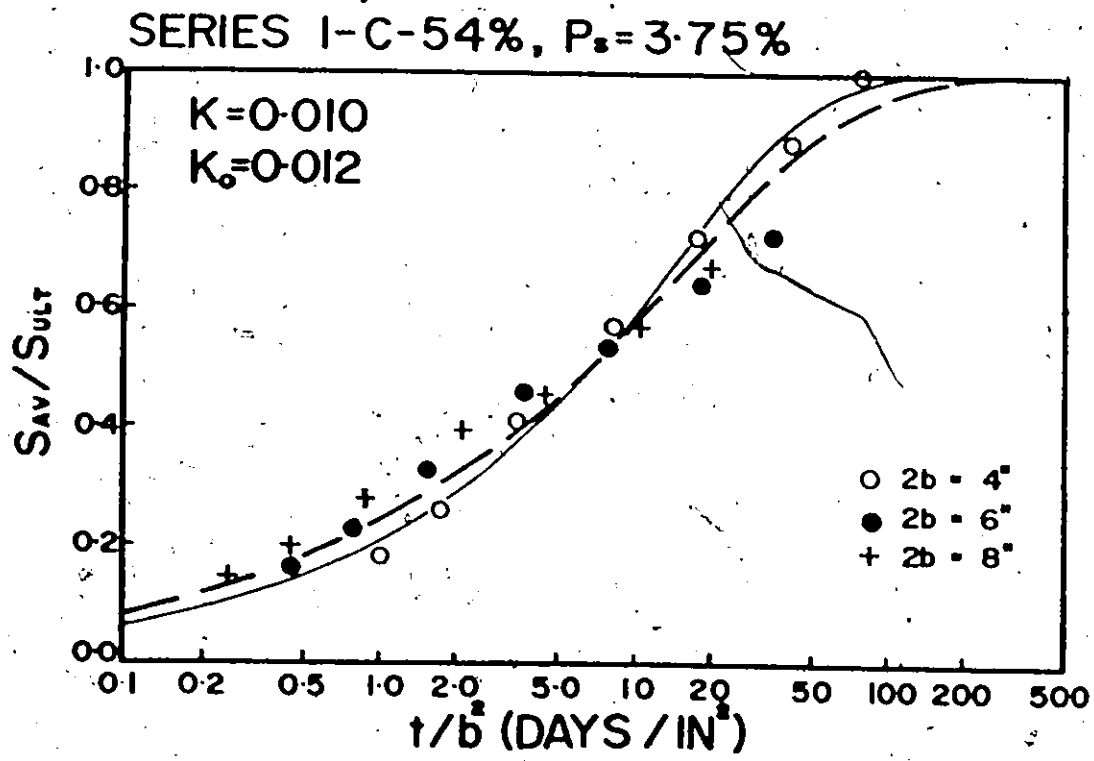
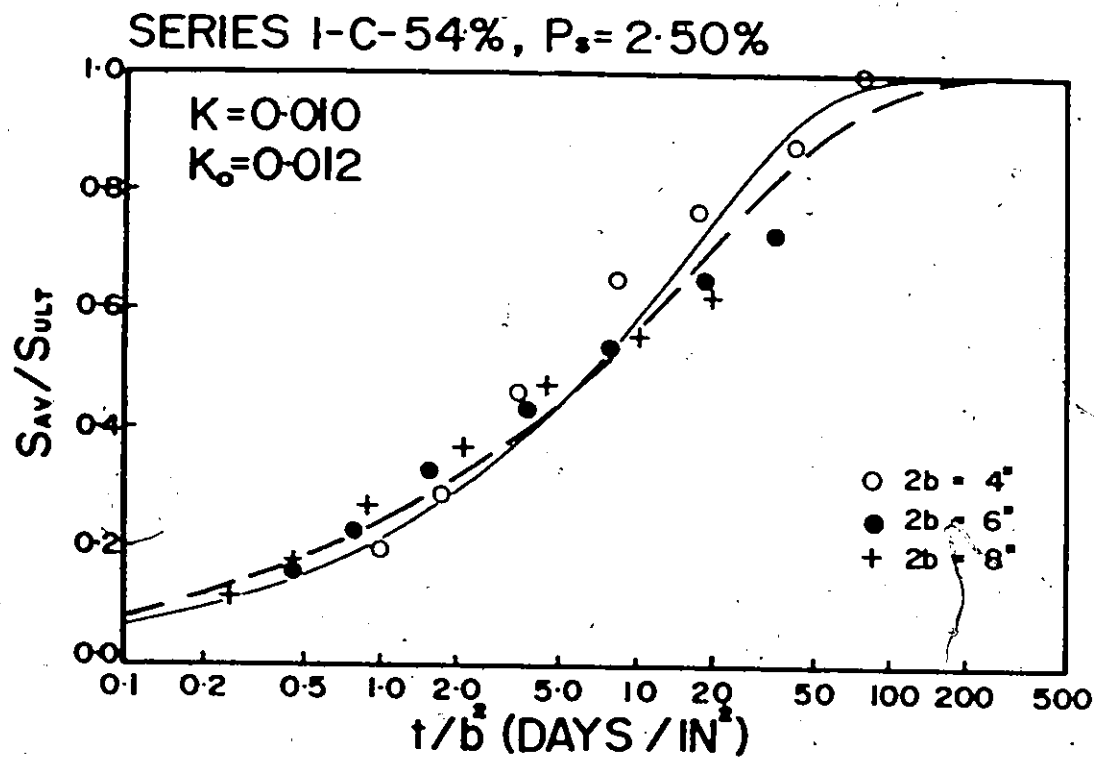


Figure 39



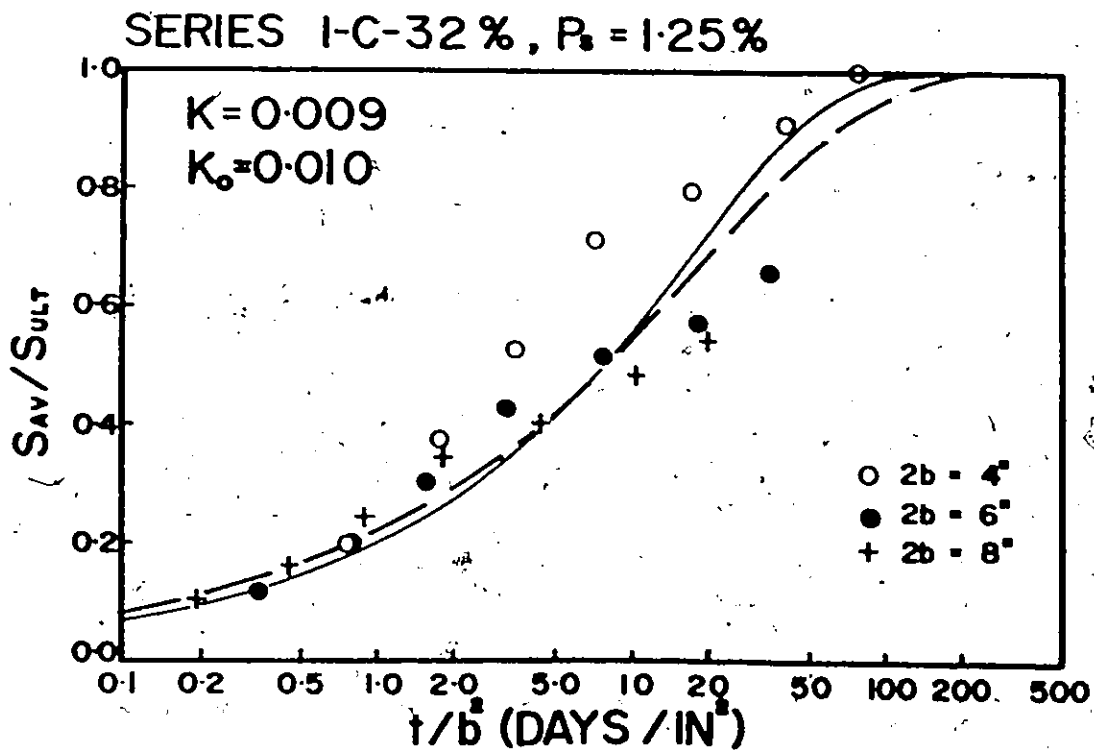
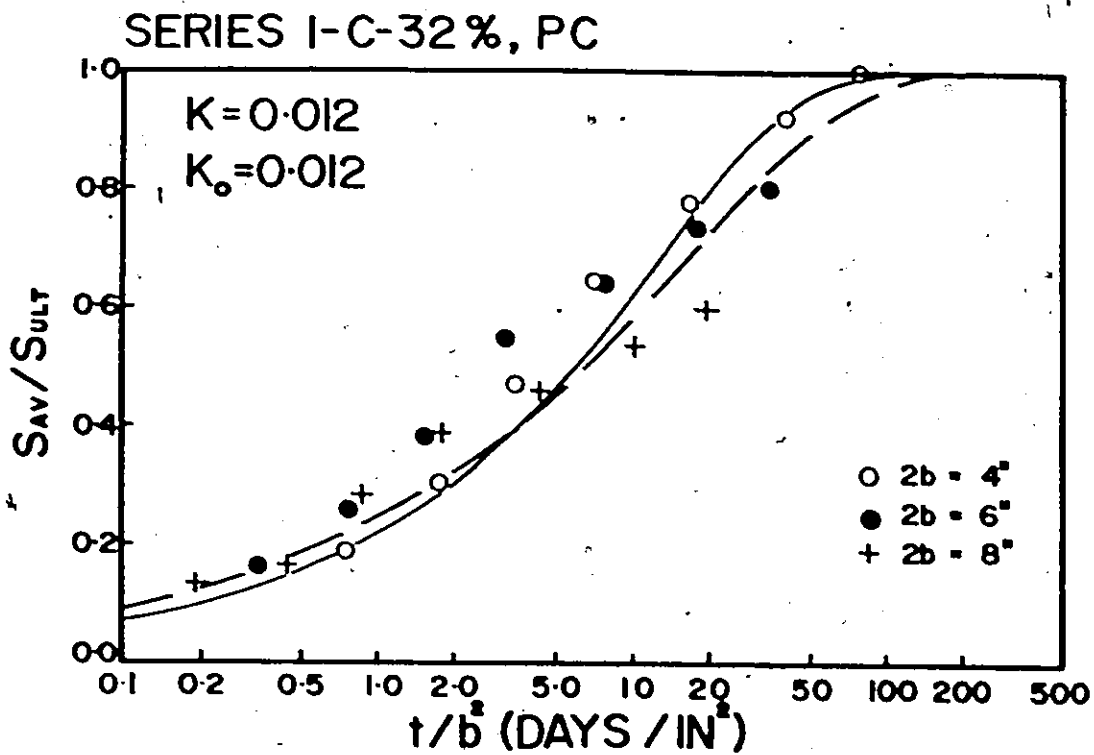


Figure 40



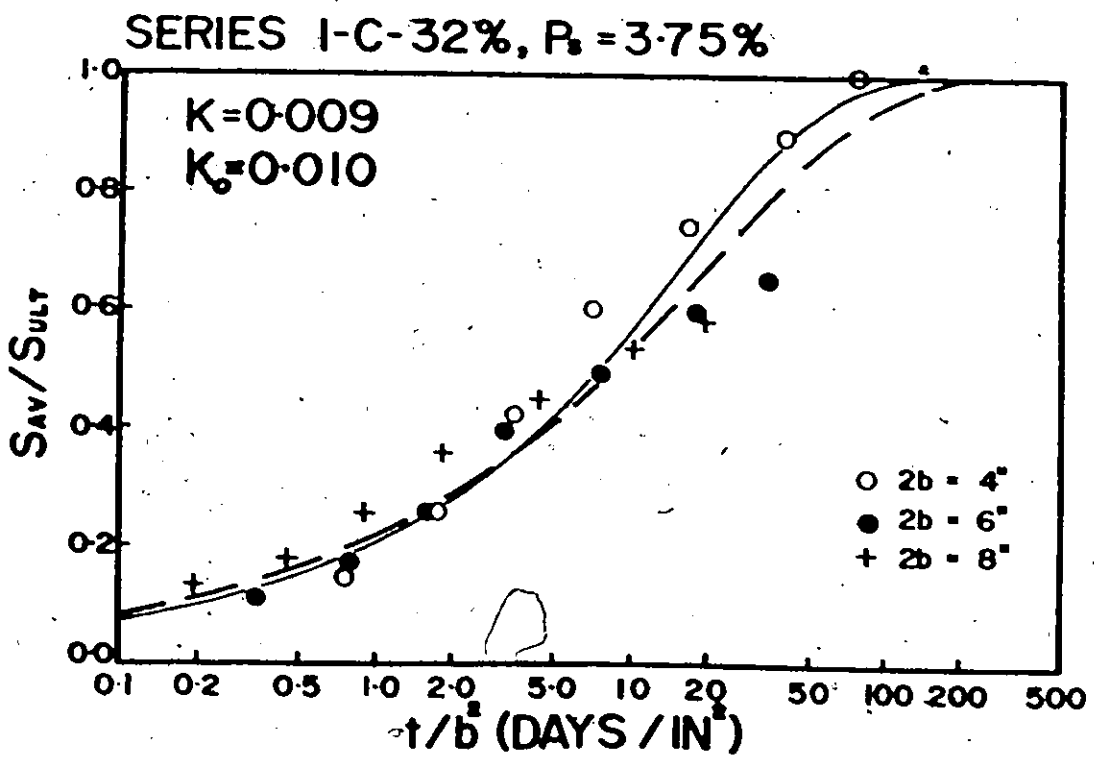
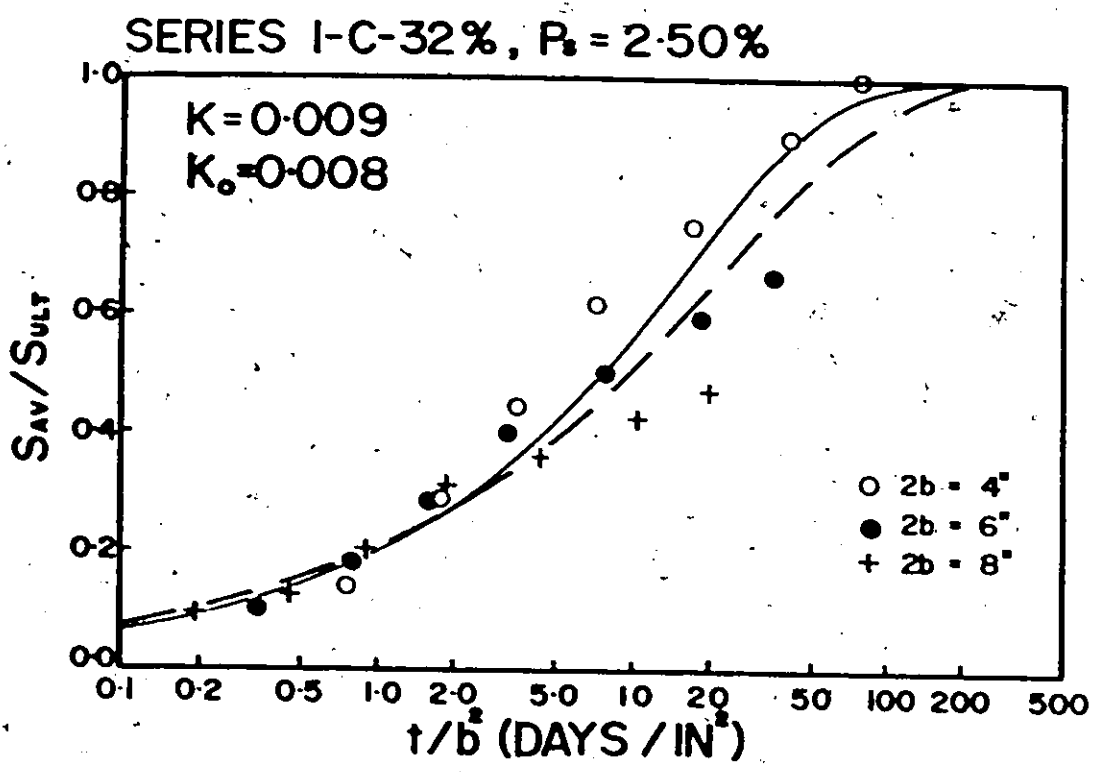


Figure 41

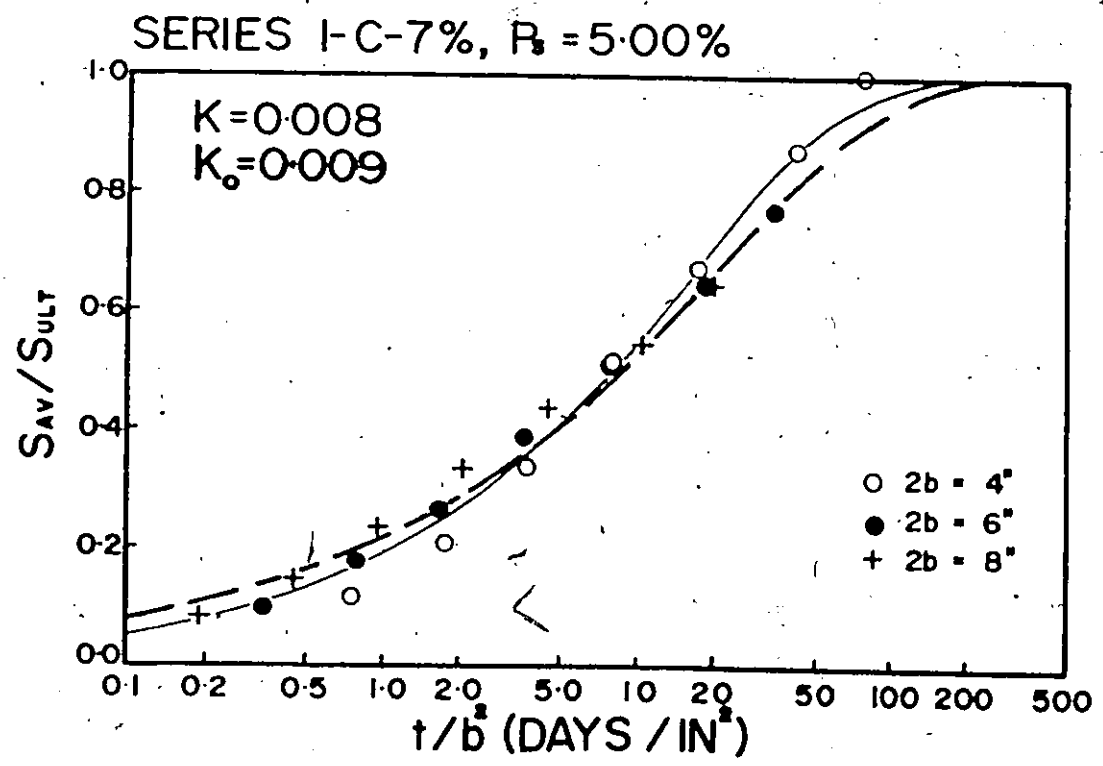
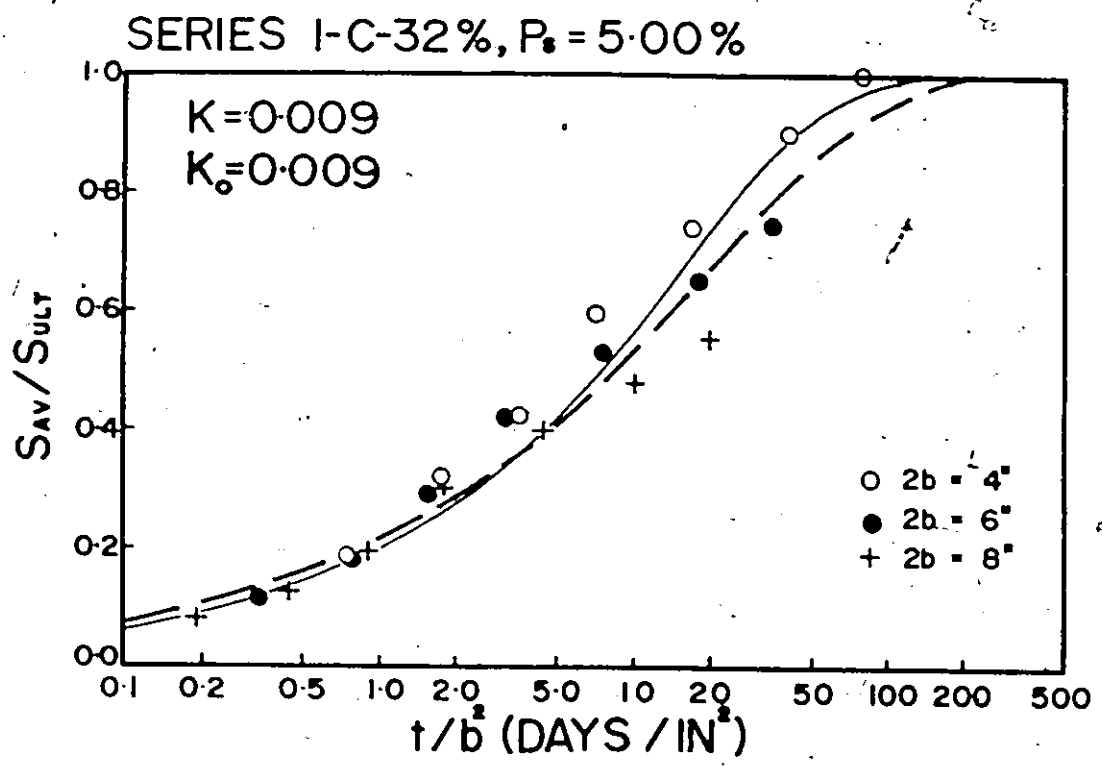


Figure 42

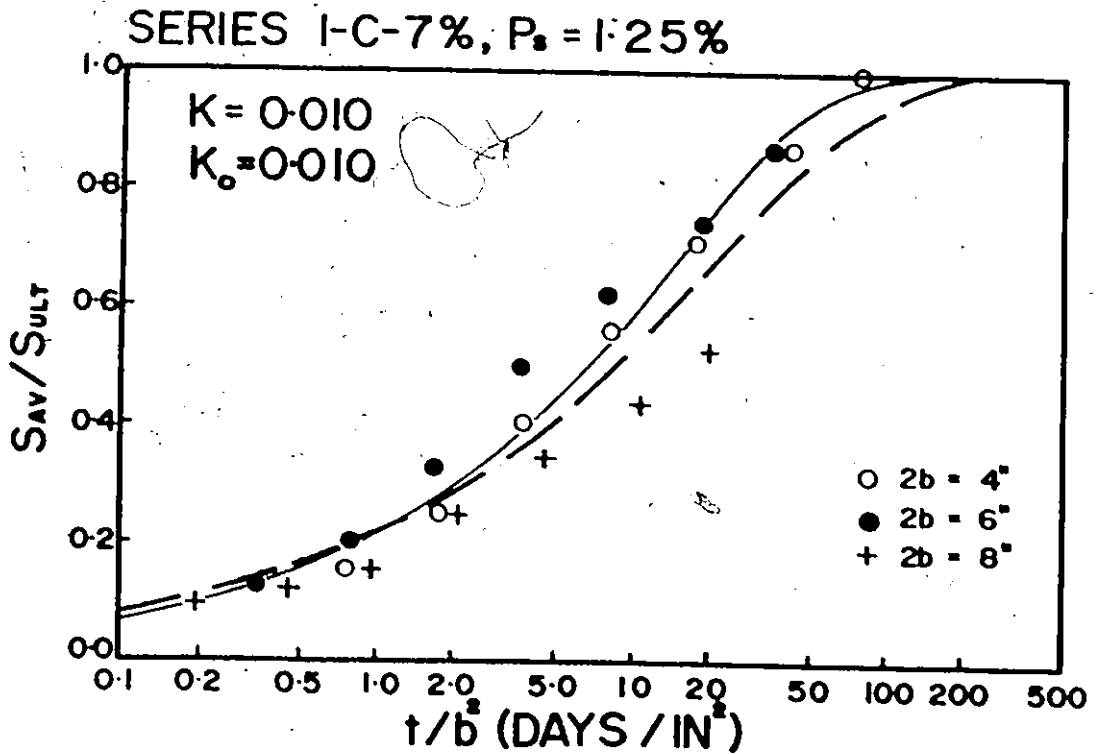
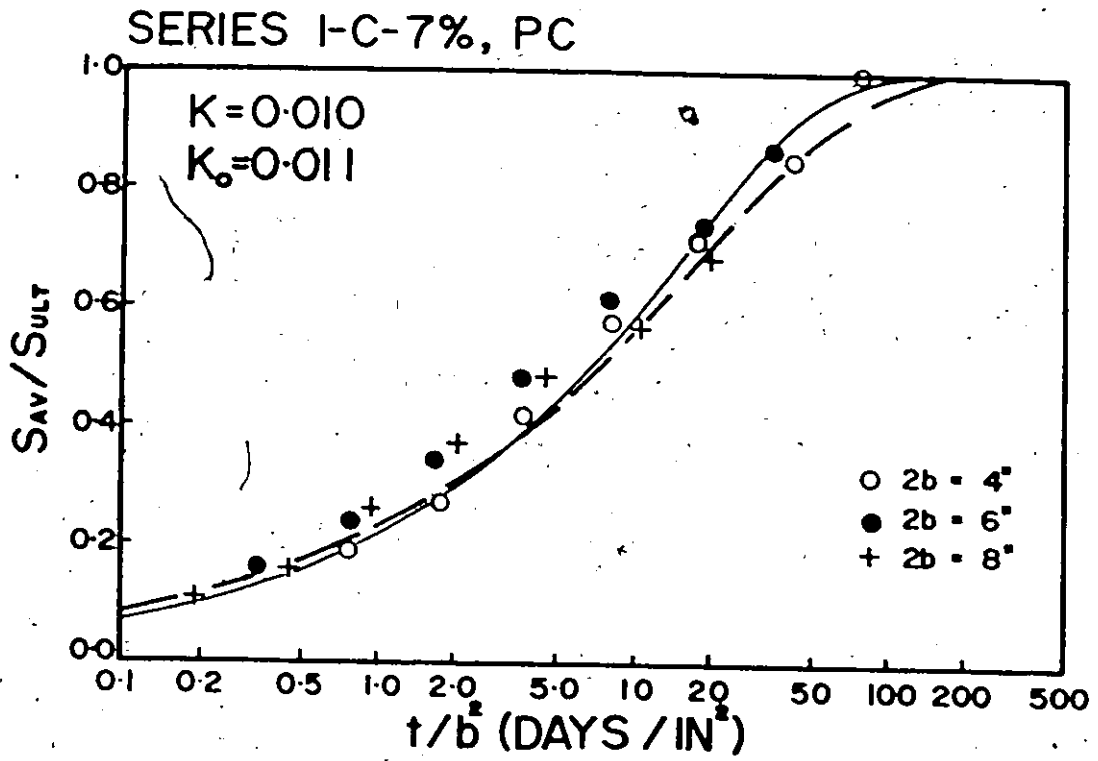


Figure 43

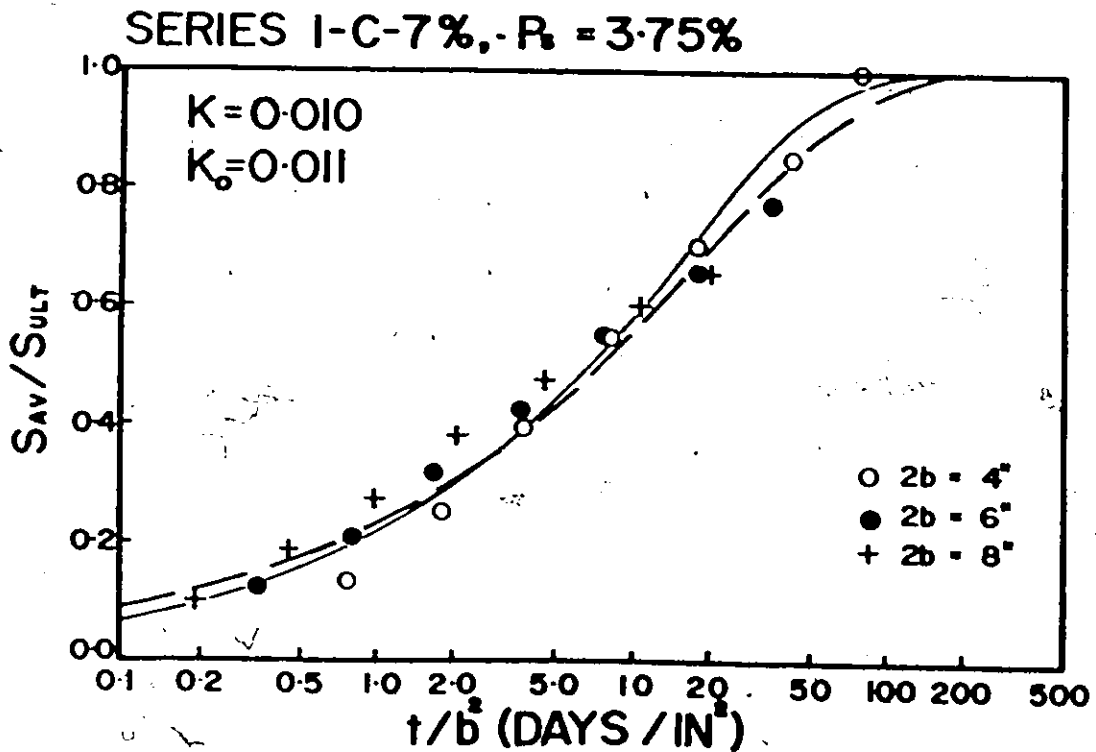
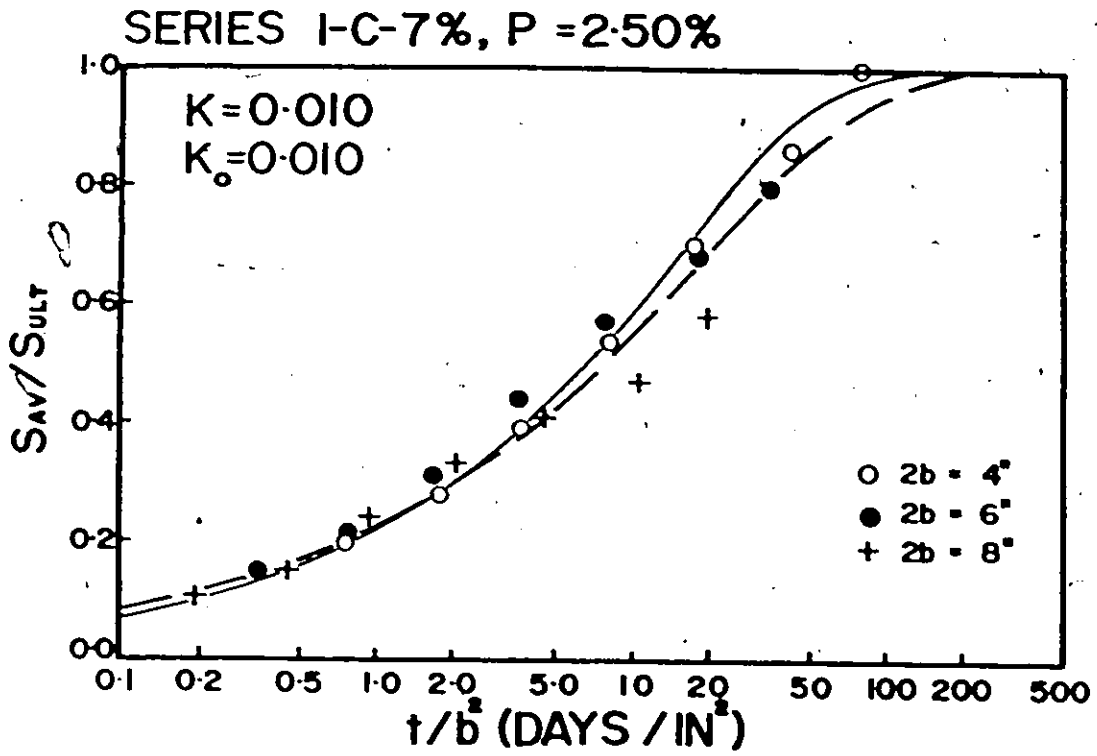


Figure 45

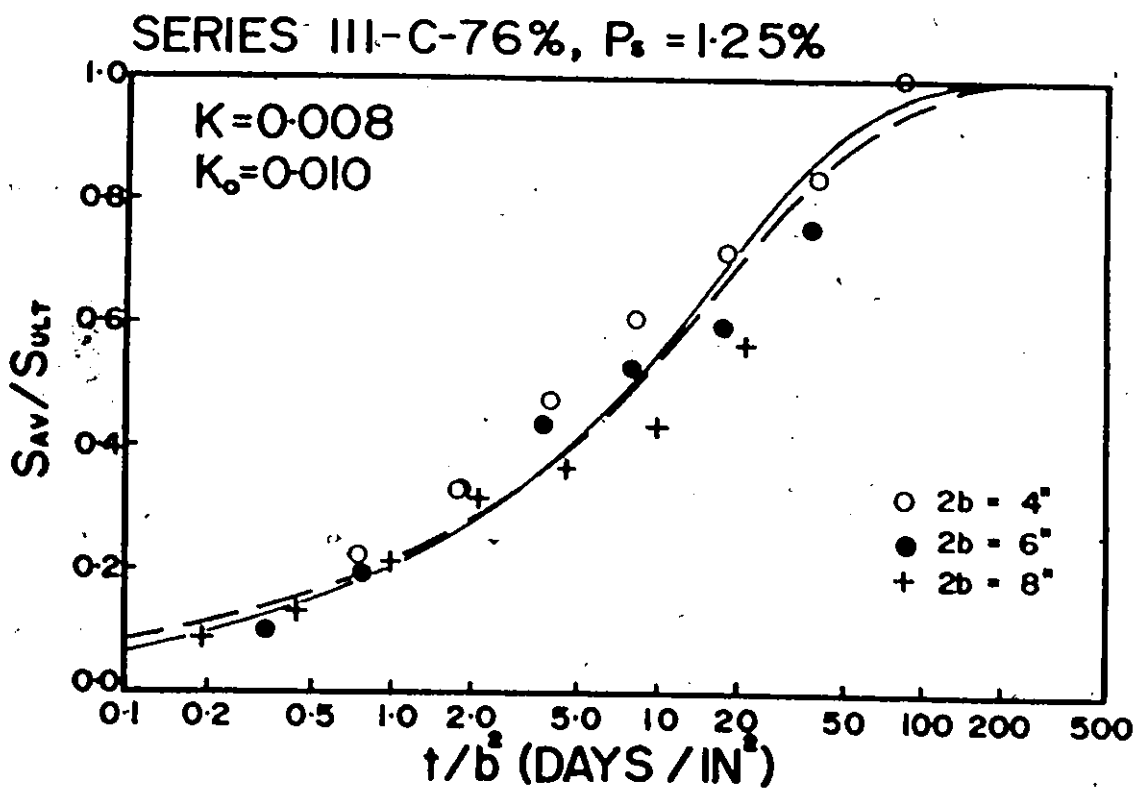
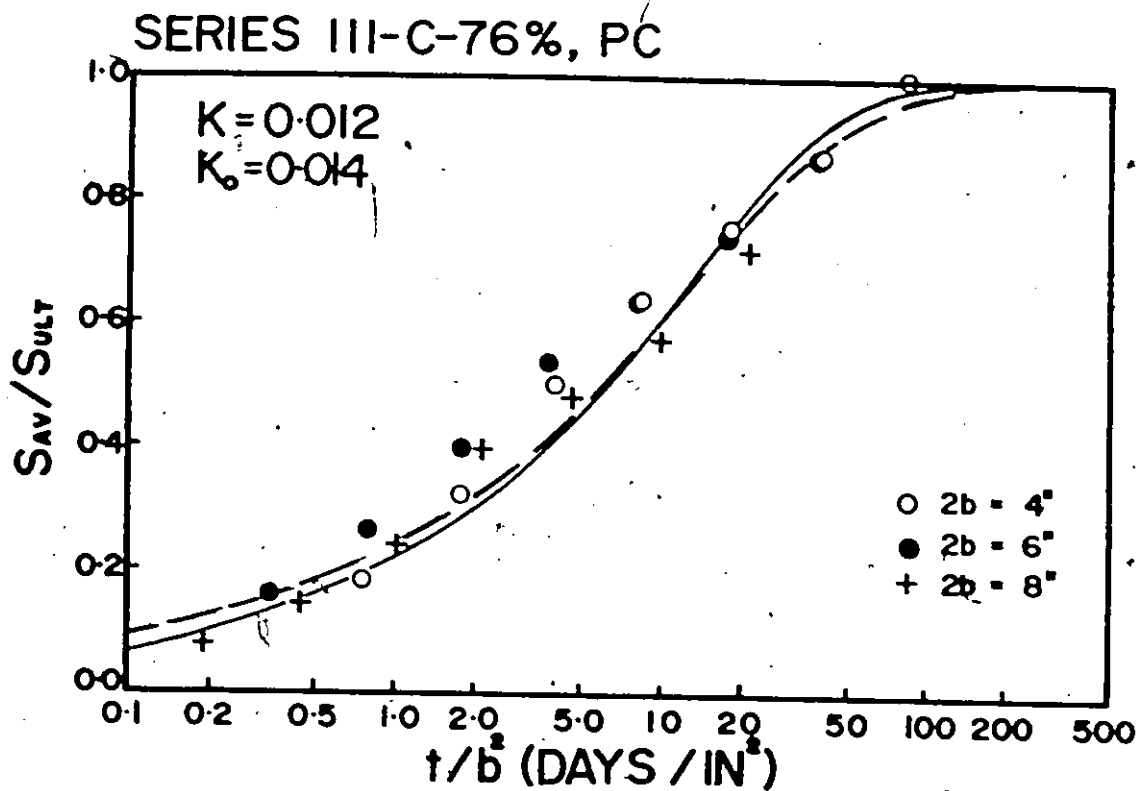


Figure 45

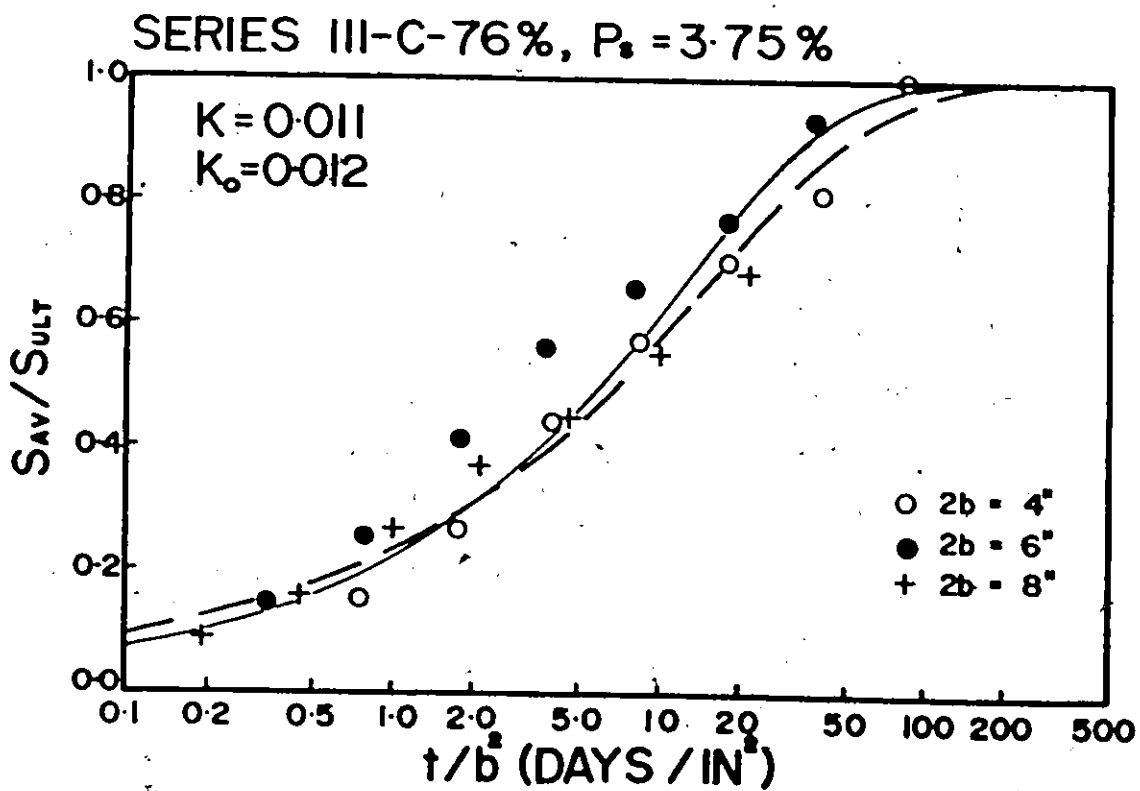
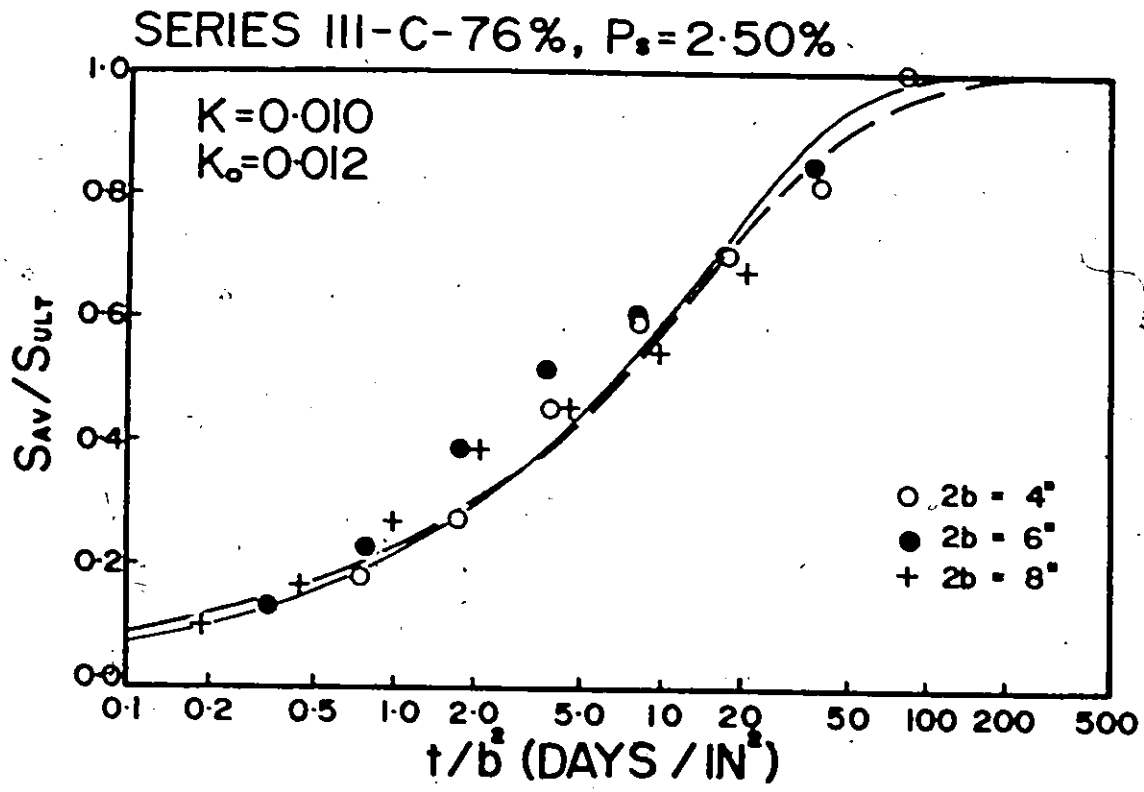


Figure 46

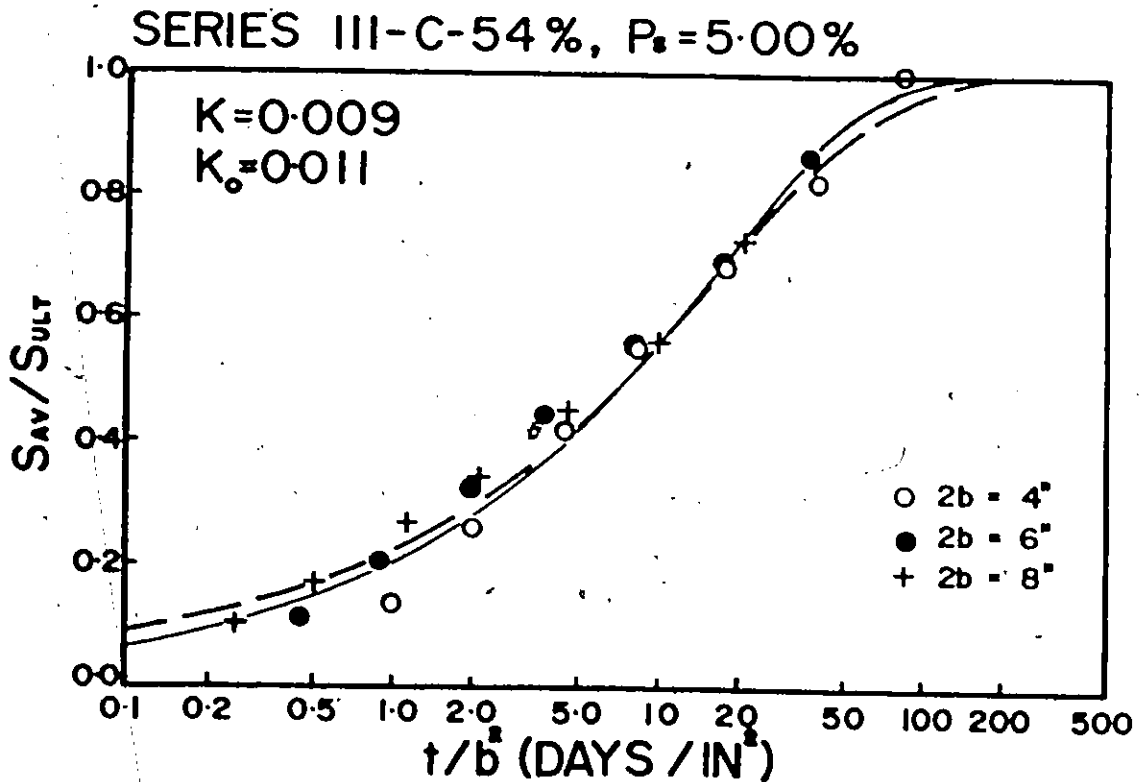
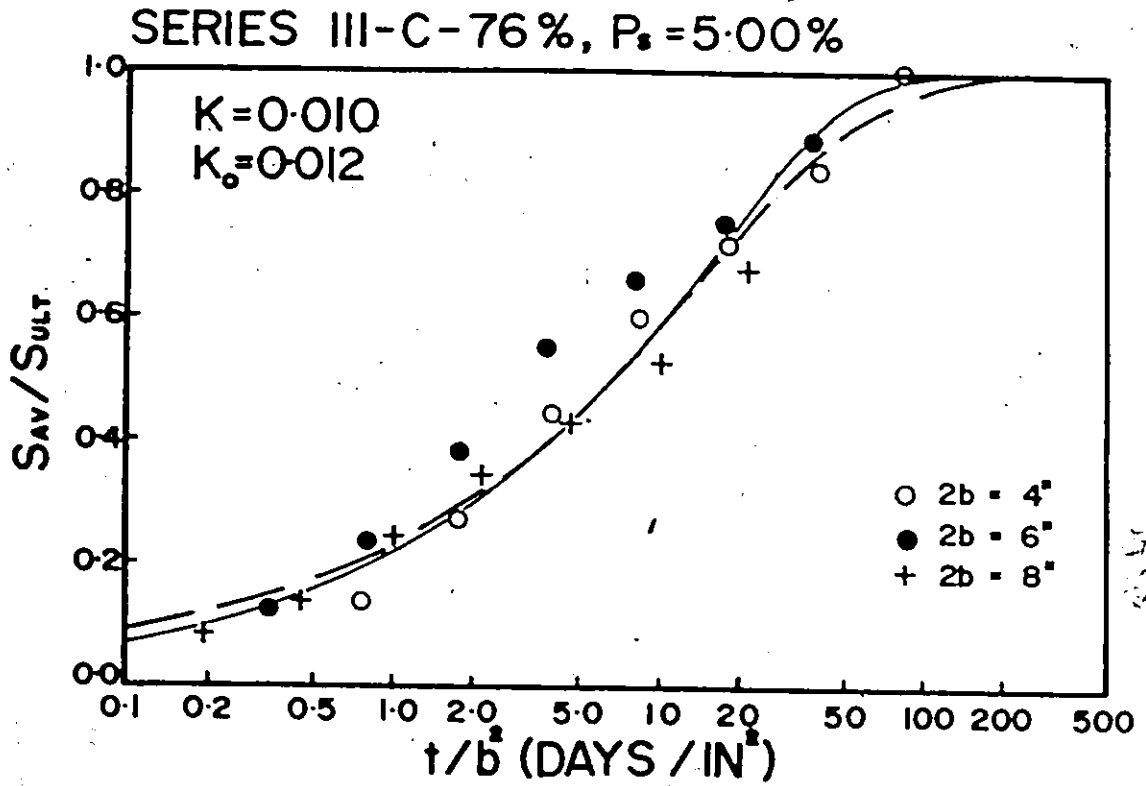


Figure 47



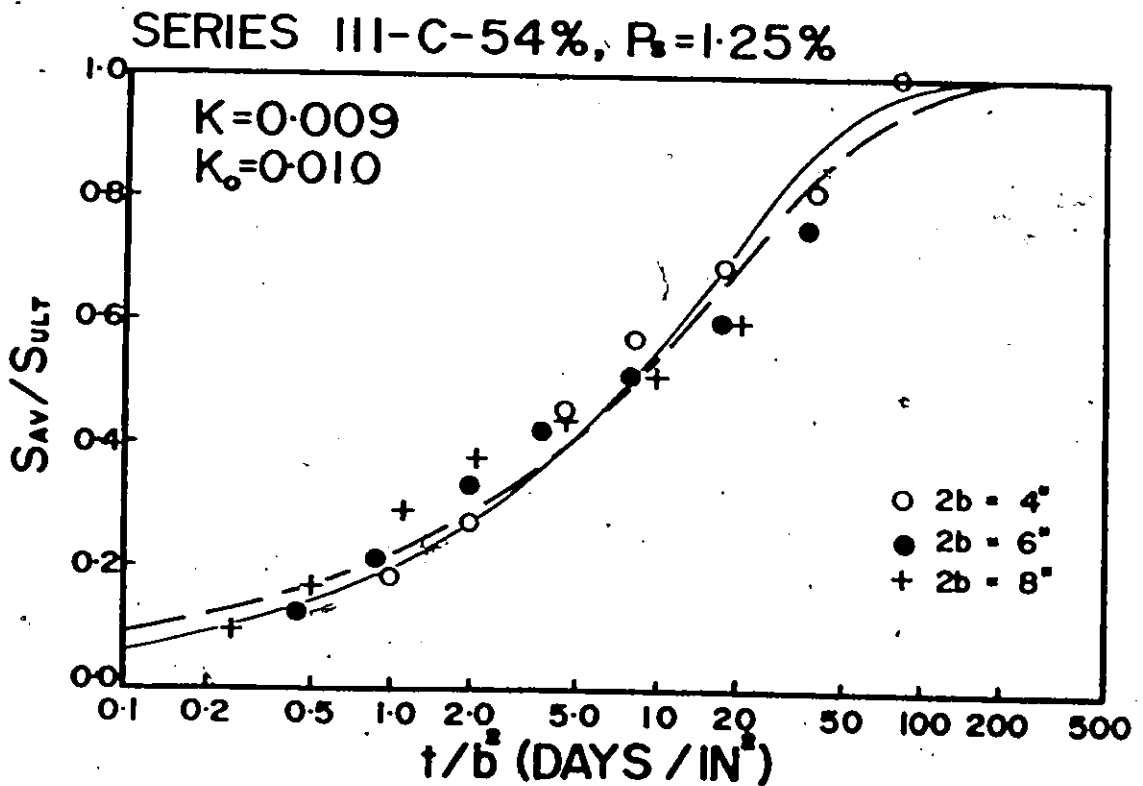
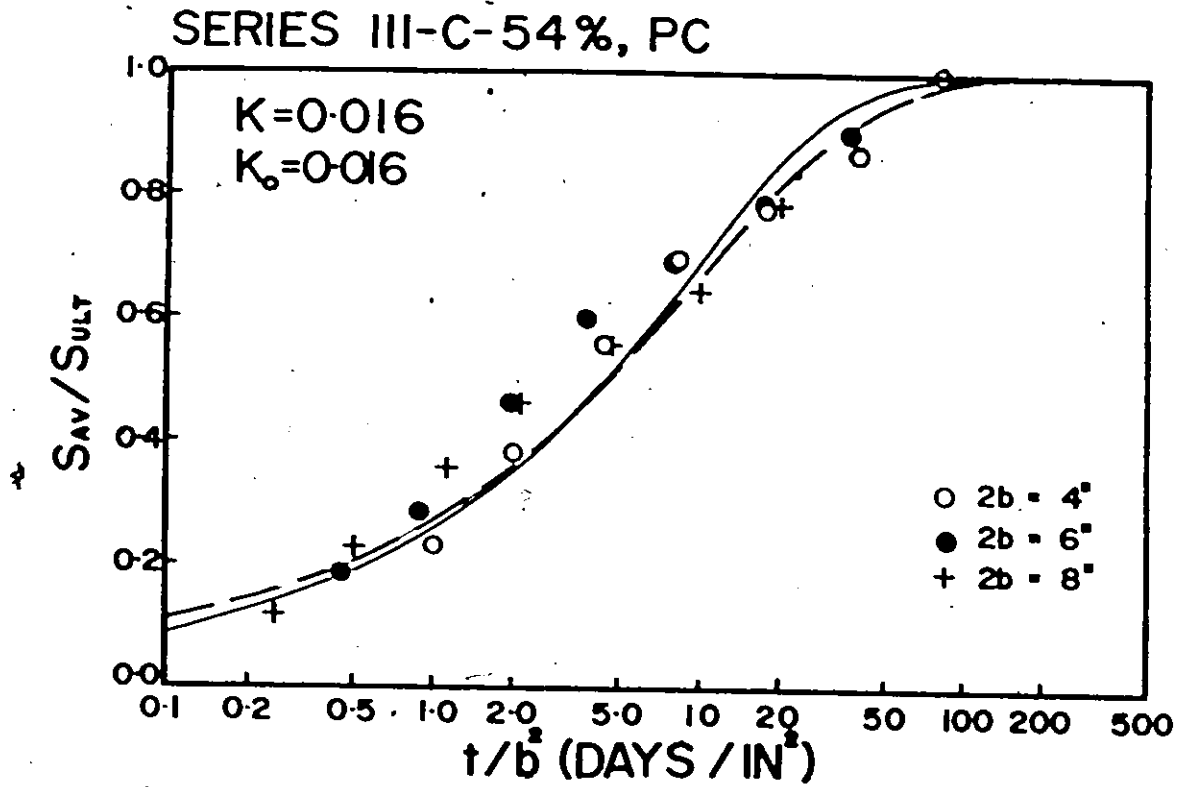


Figure 48

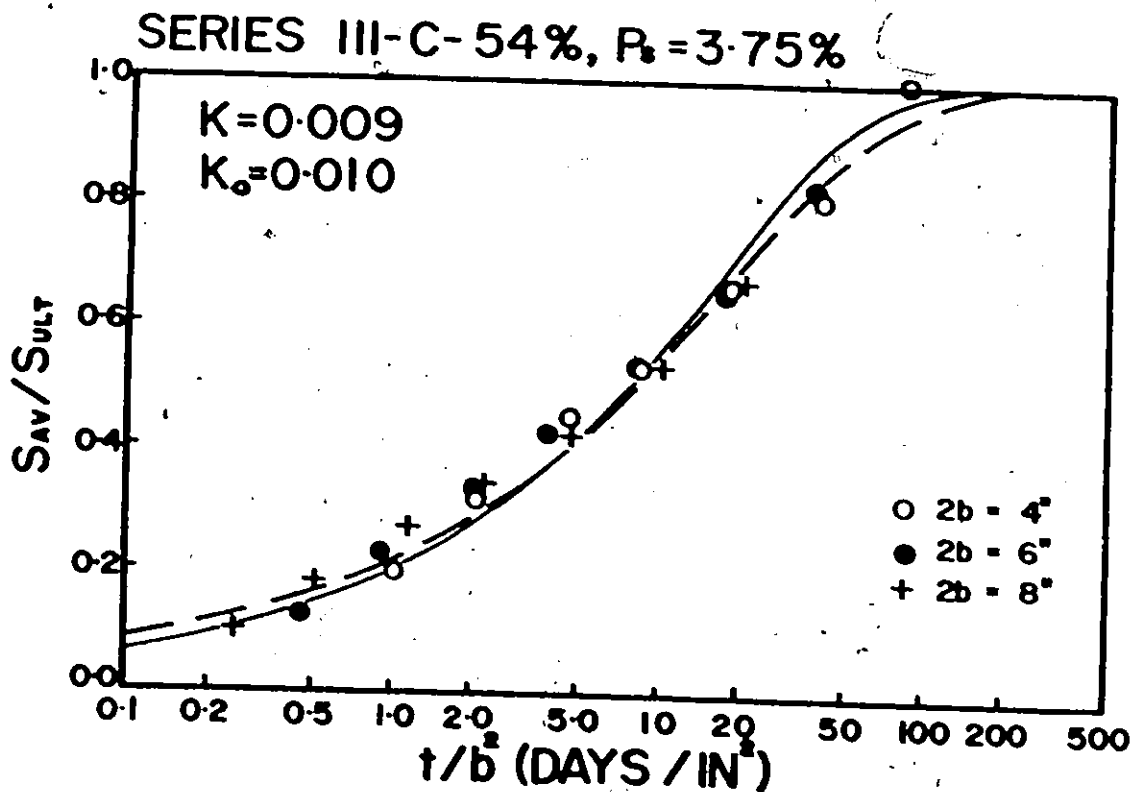
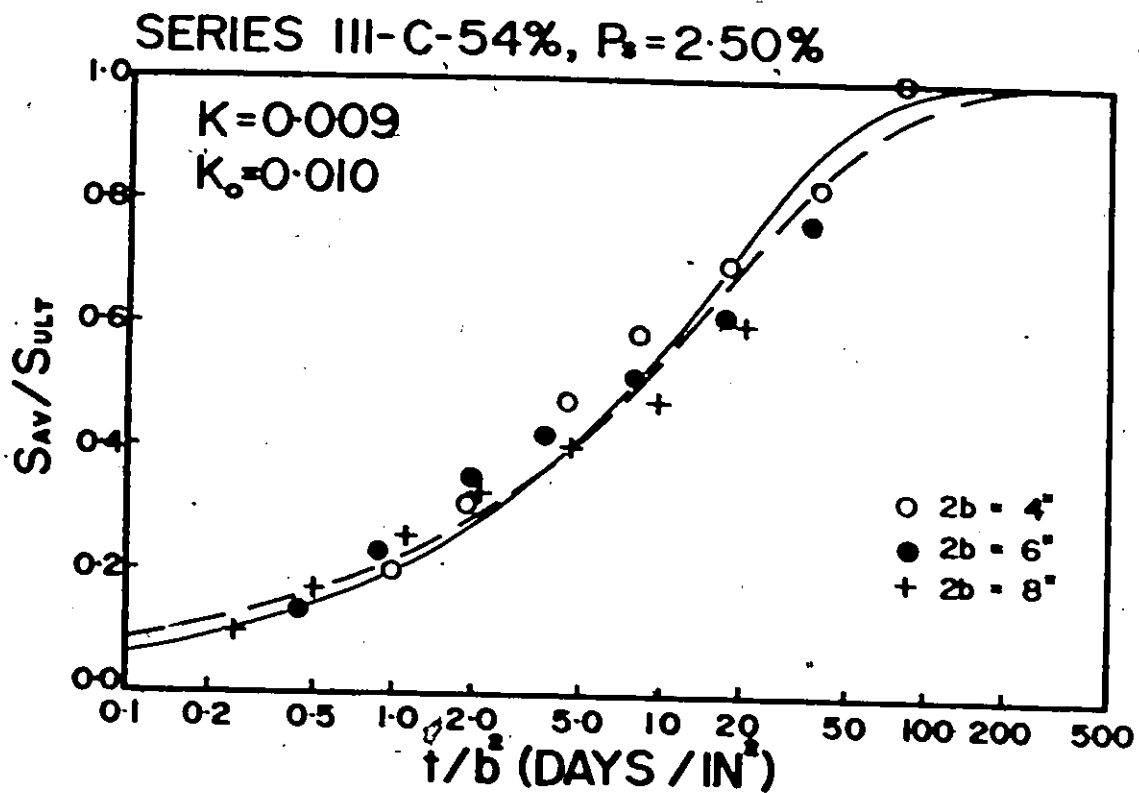


Figure 49

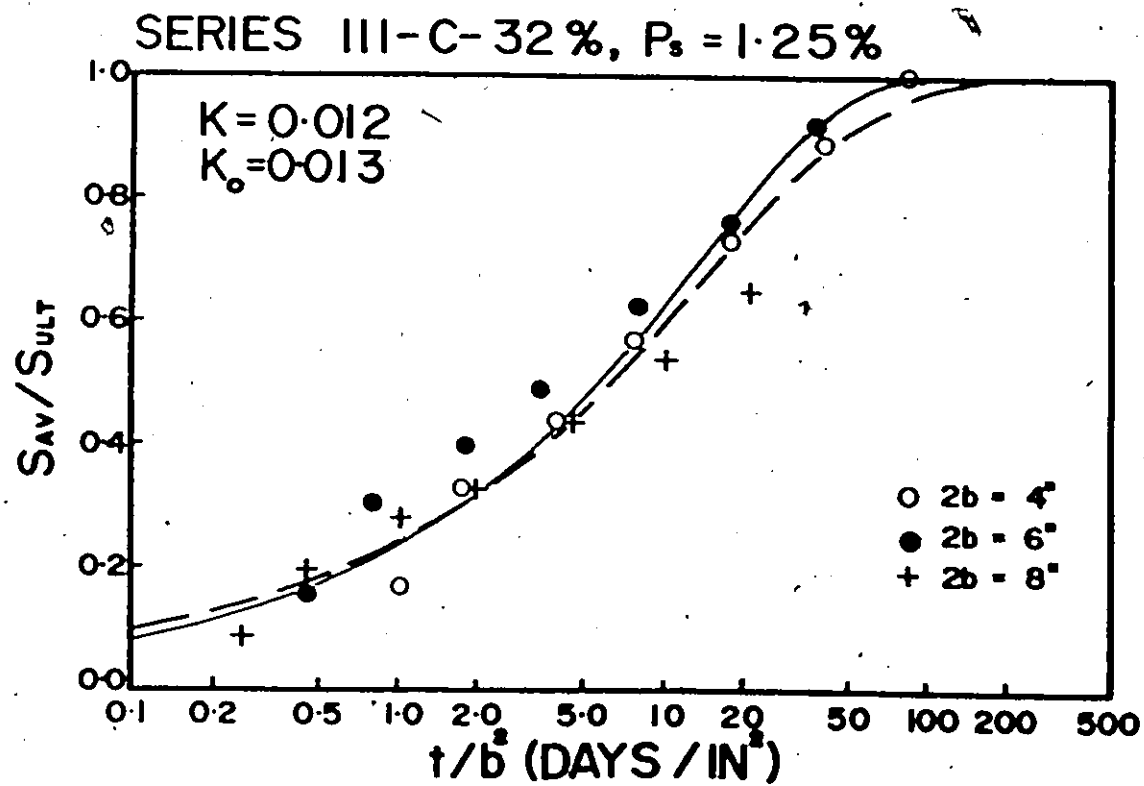
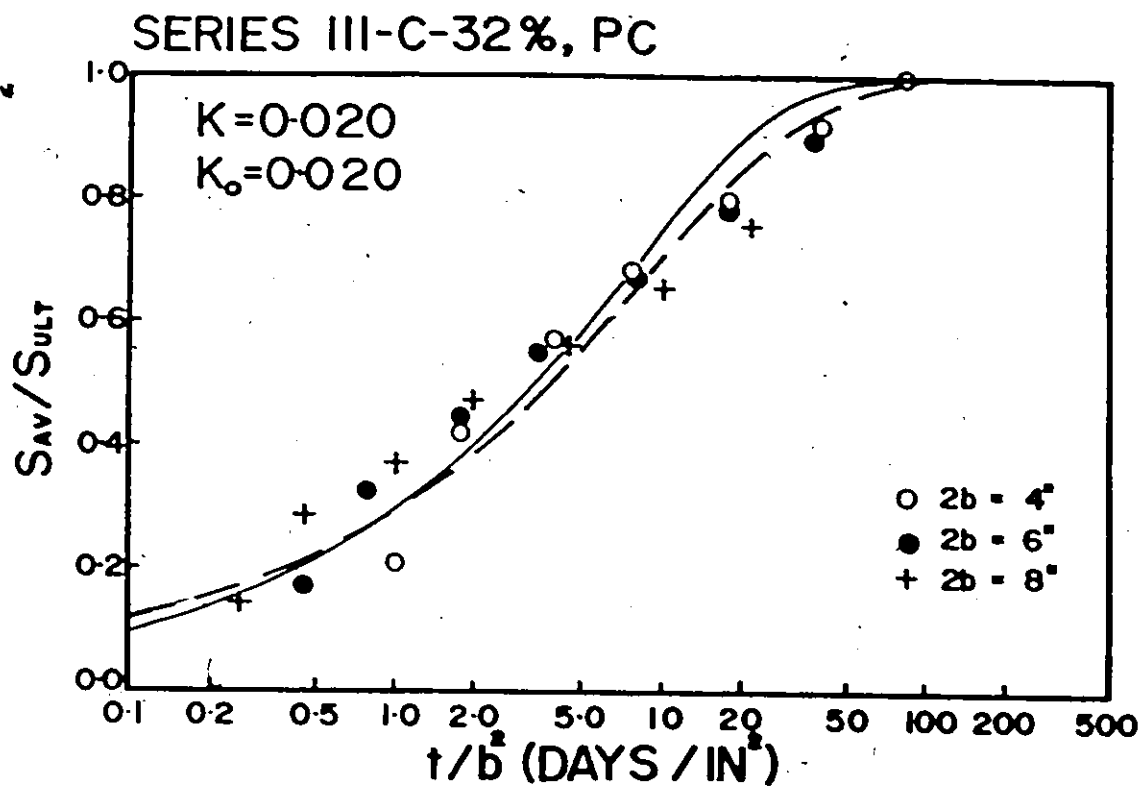


Figure 50

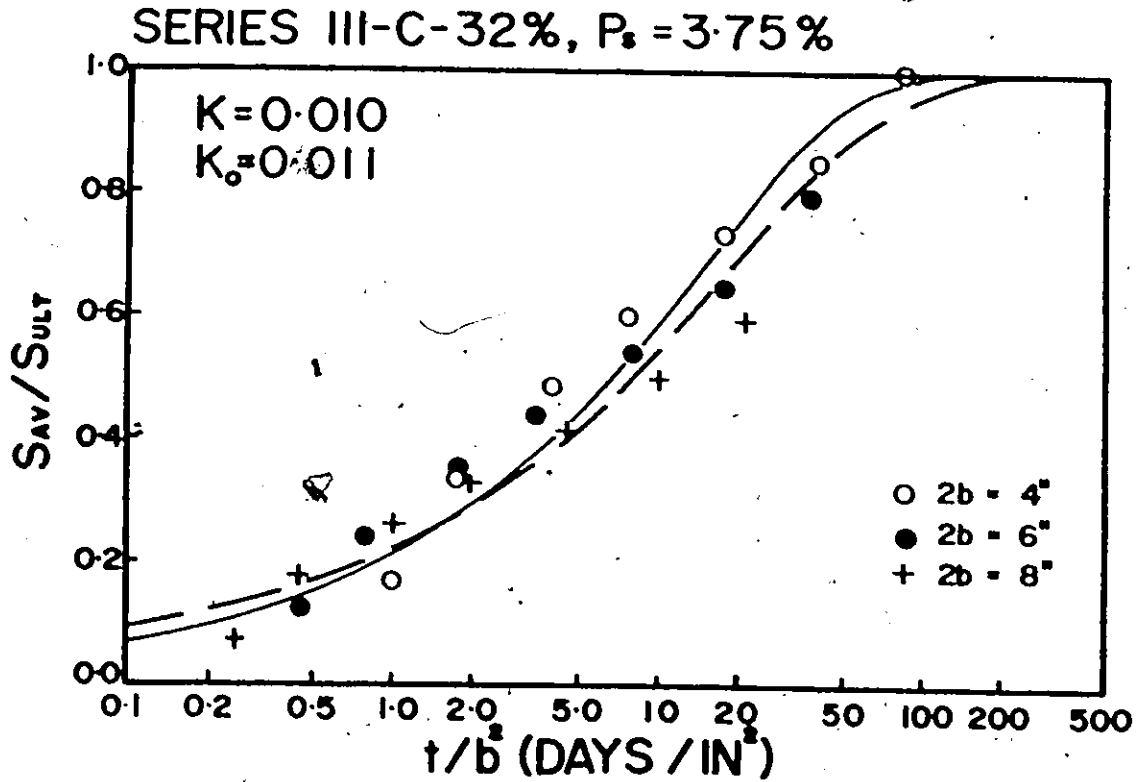
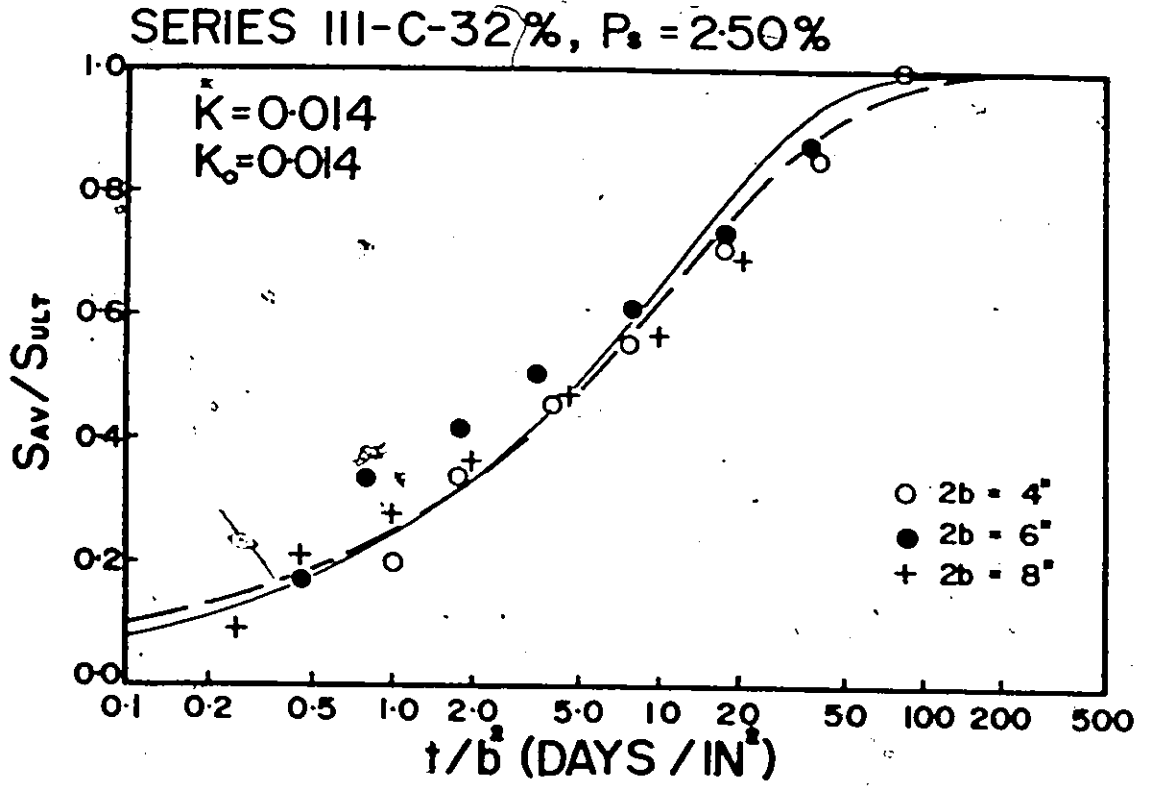


Figure 51

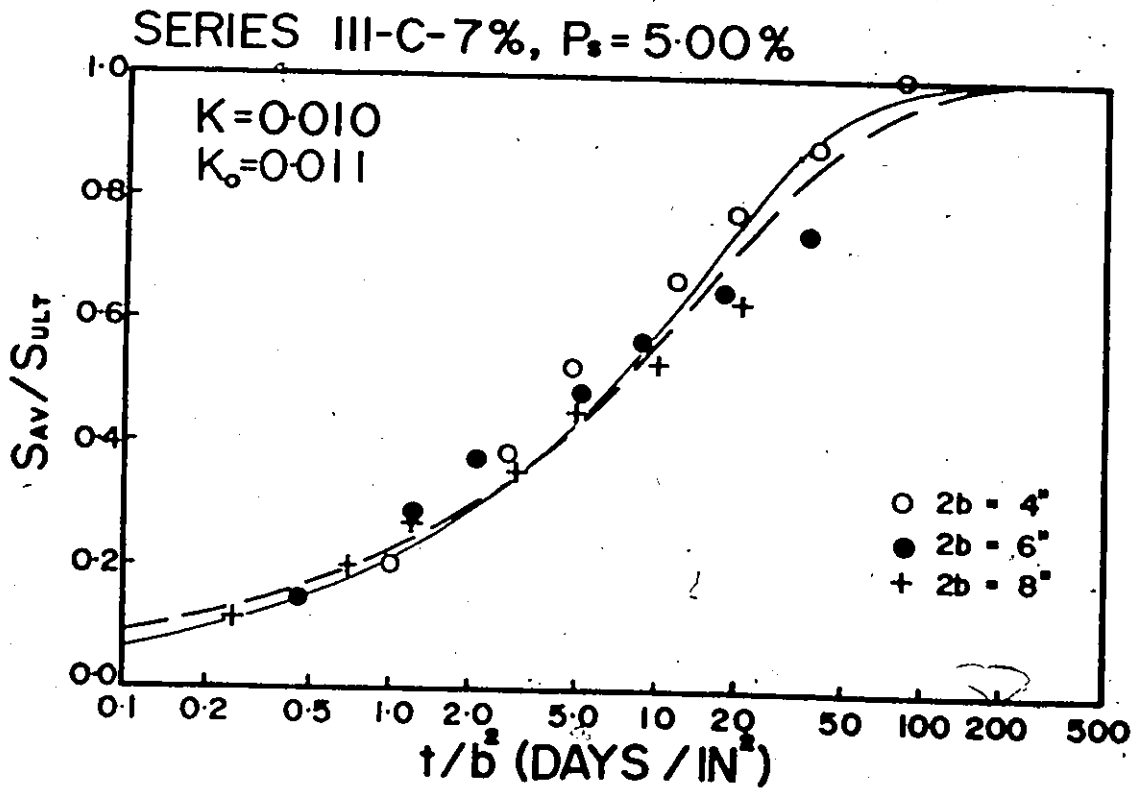
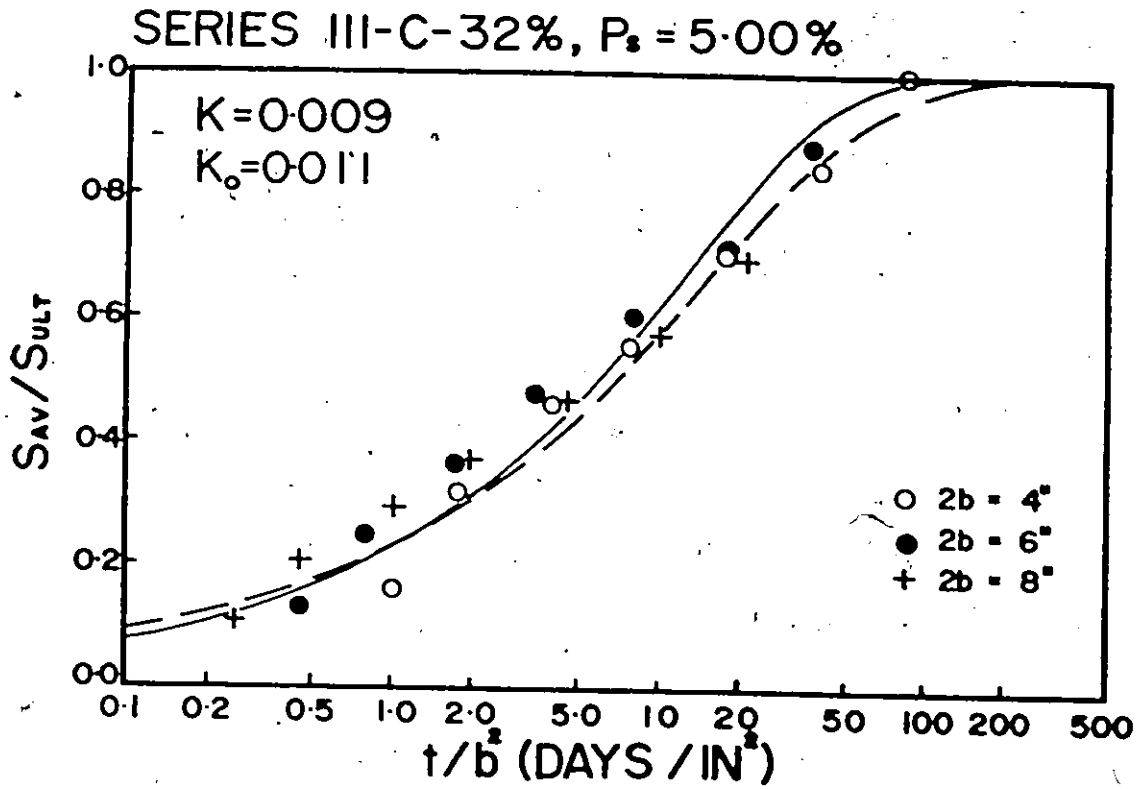


Figure 52

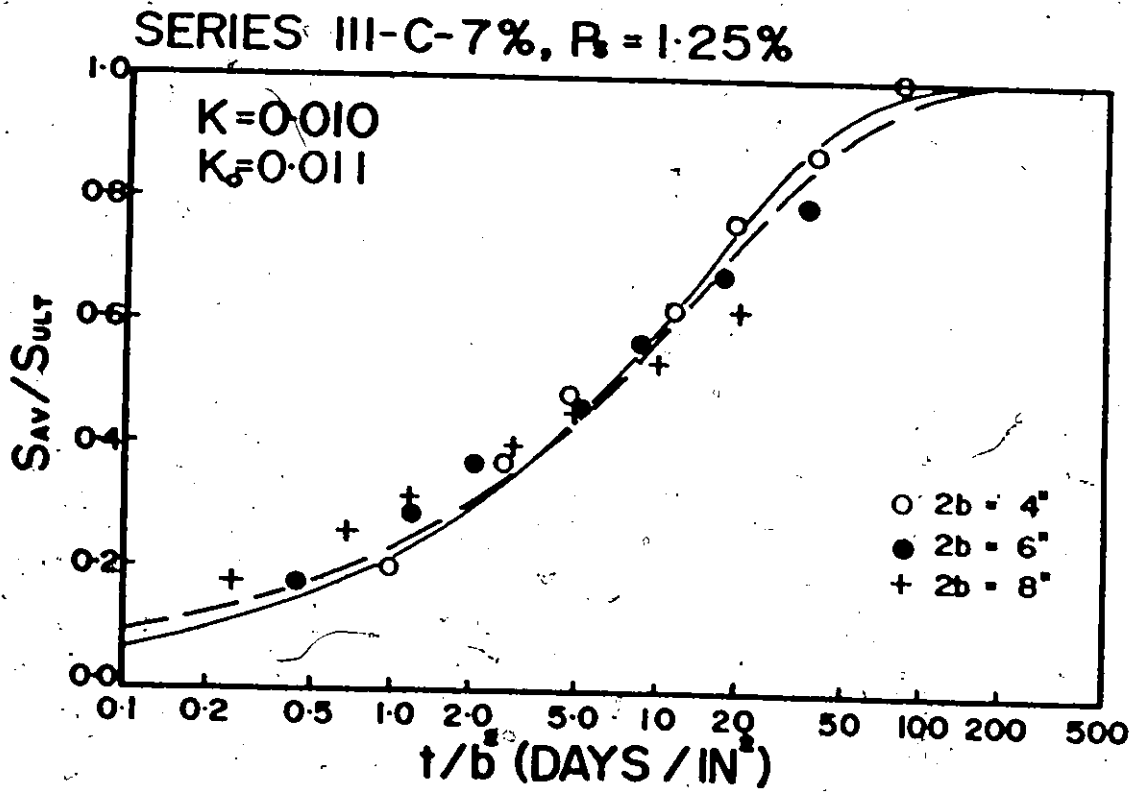
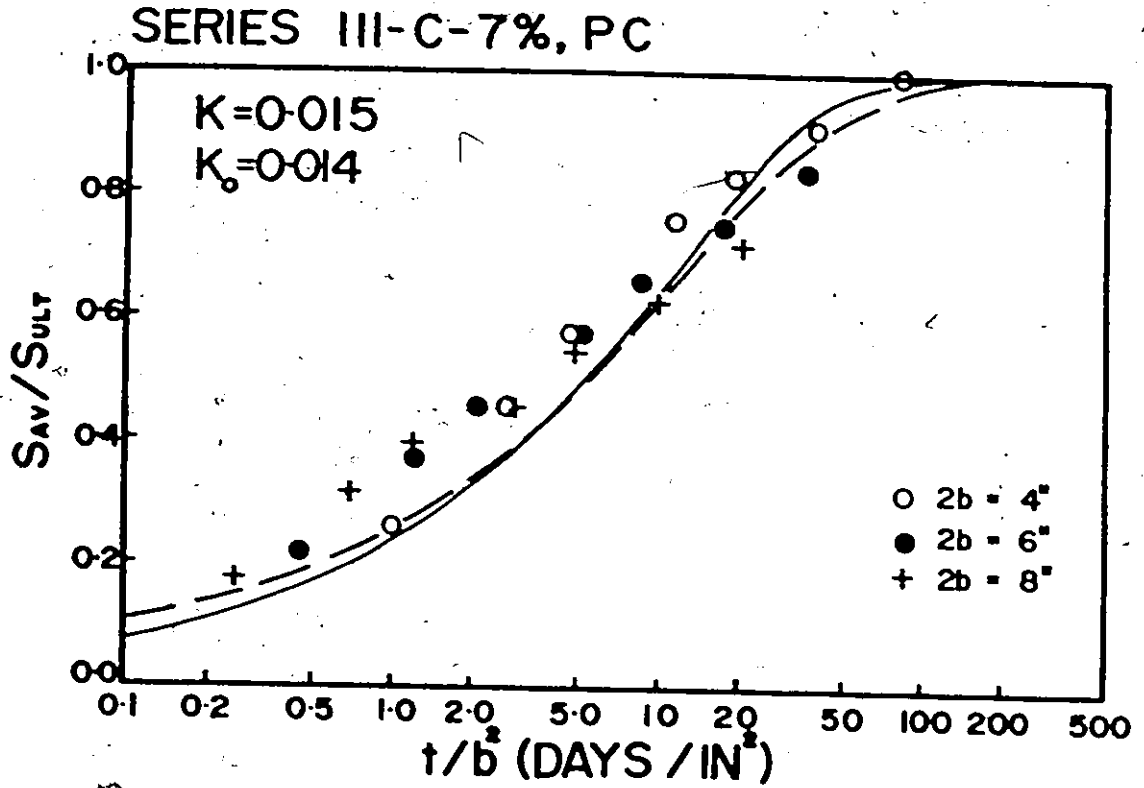


Figure 53

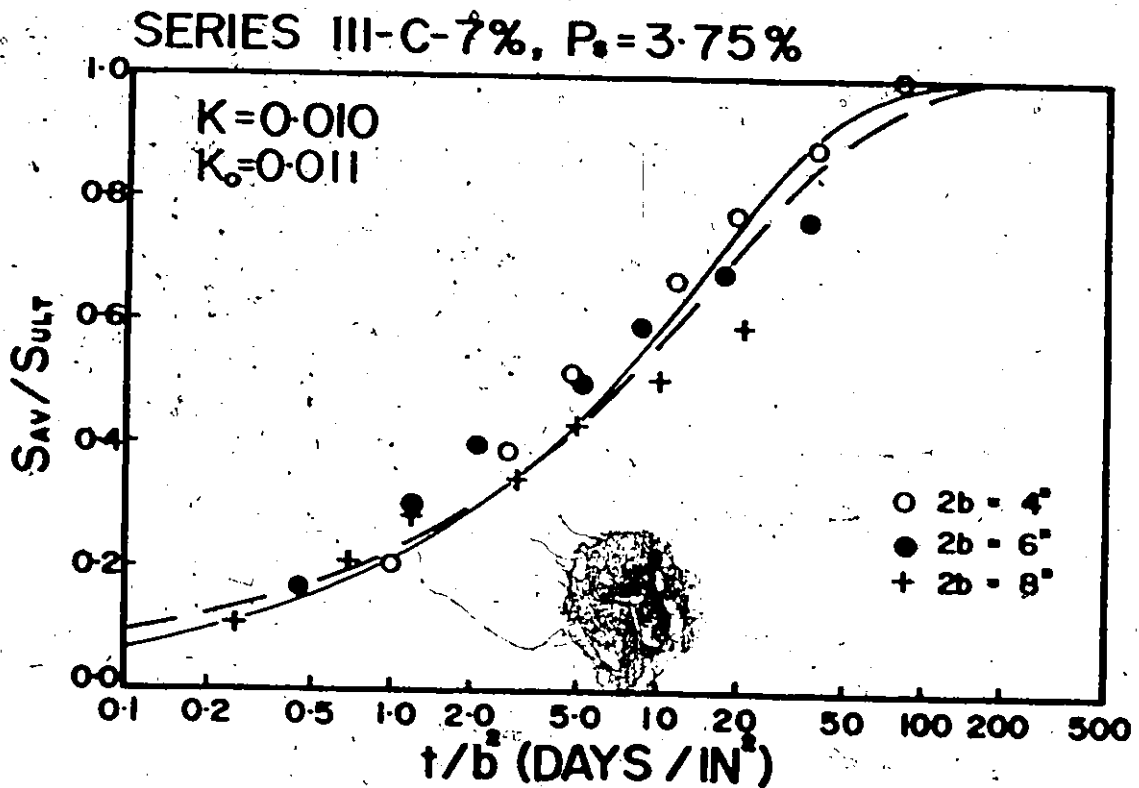
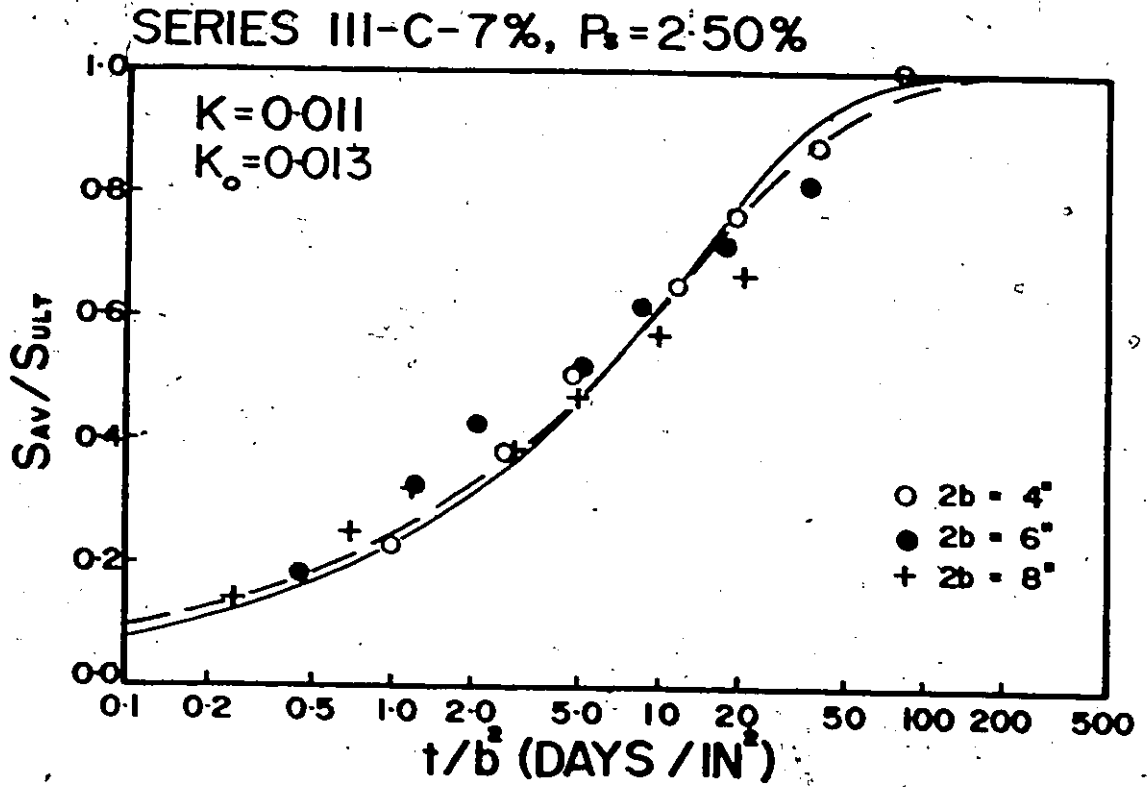


Figure 54

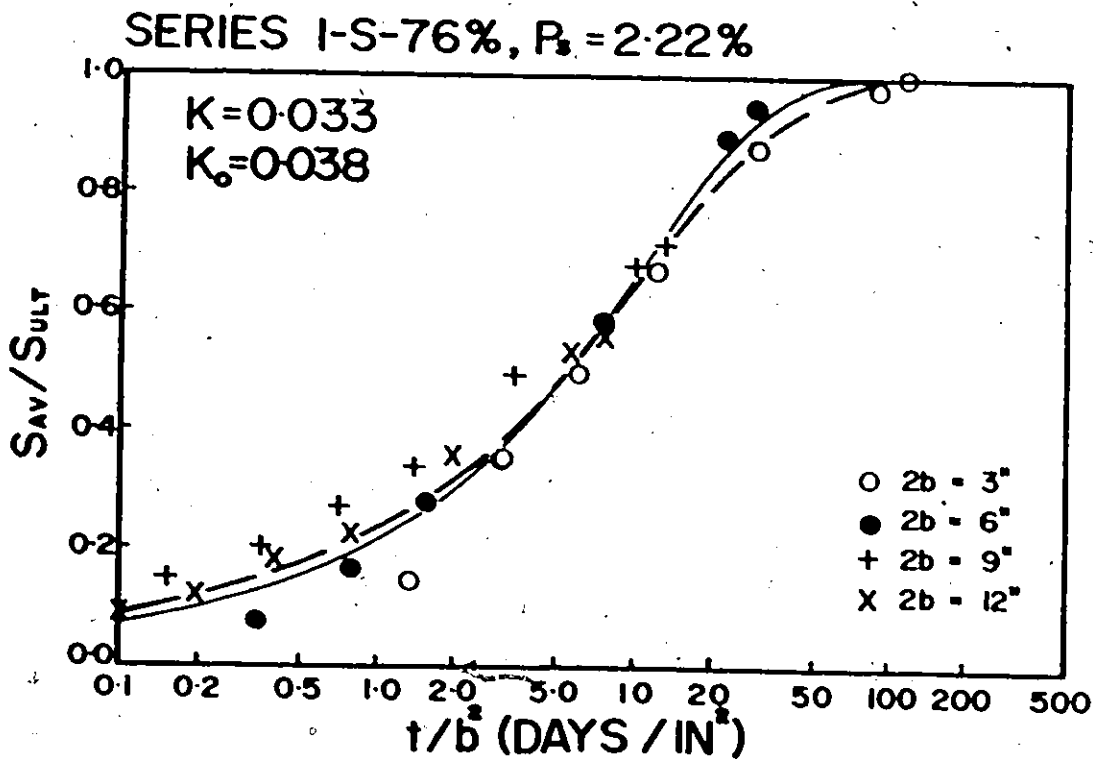
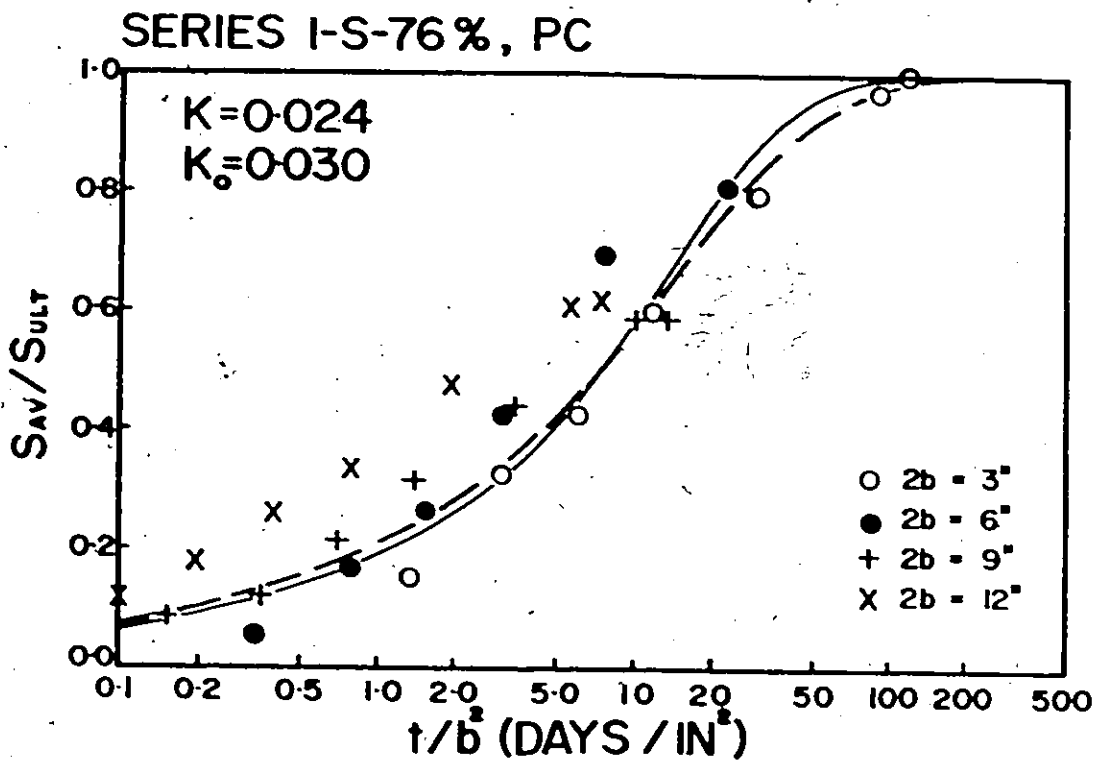


Figure 55



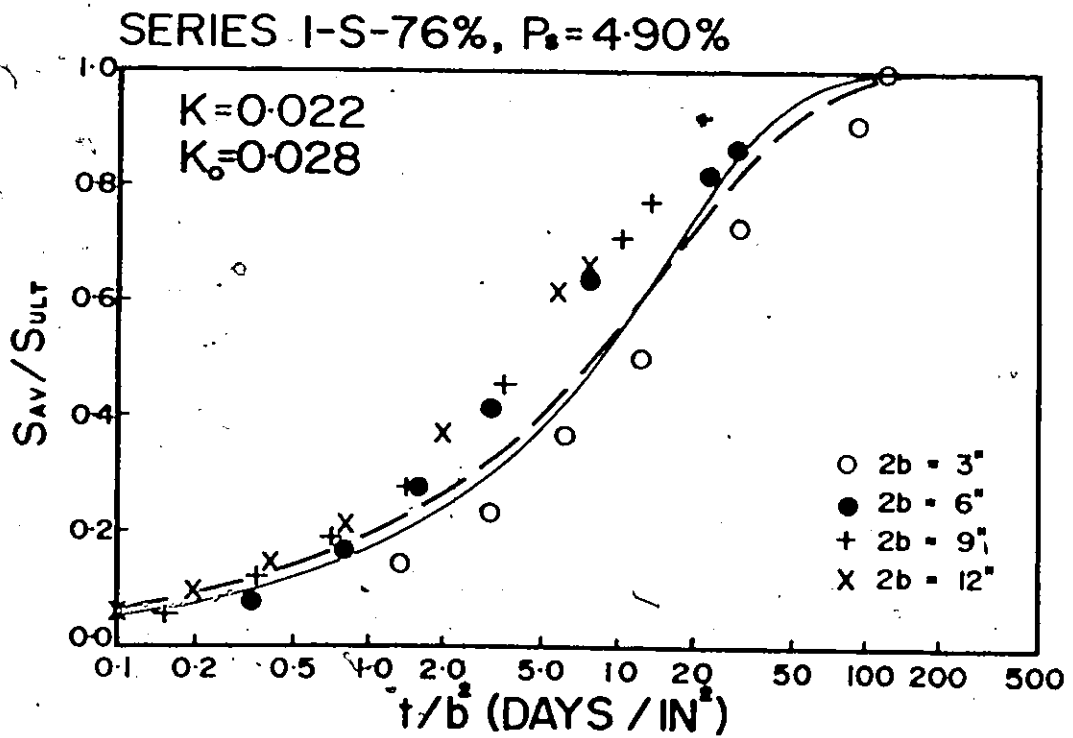
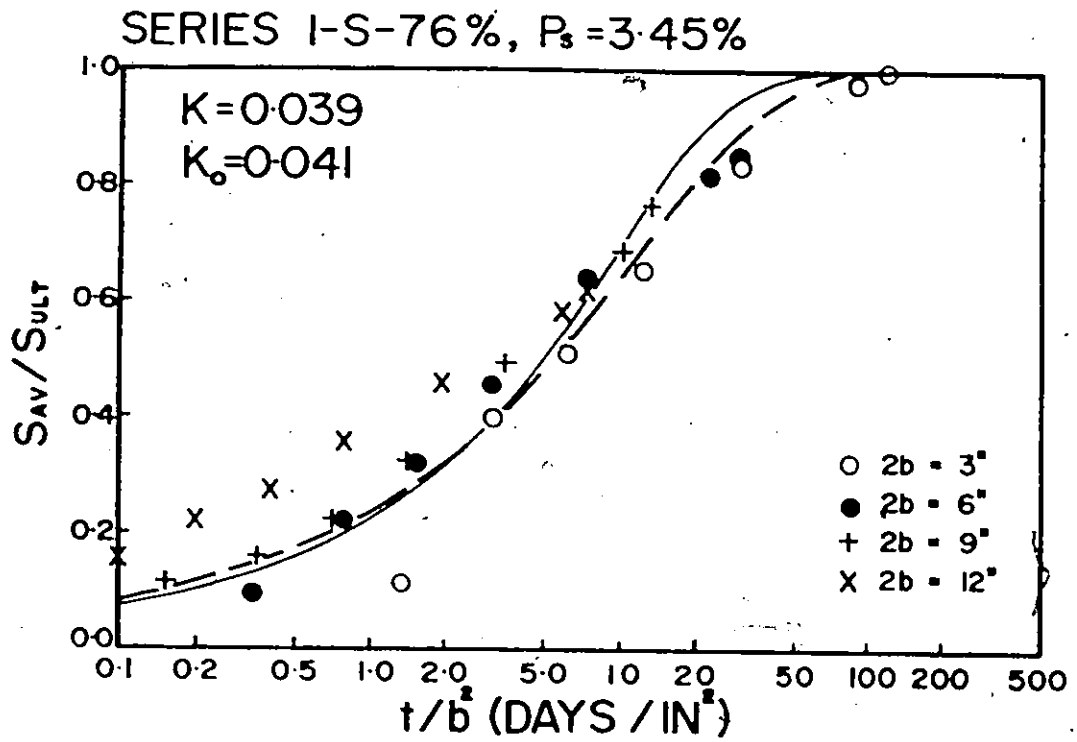


Figure 56

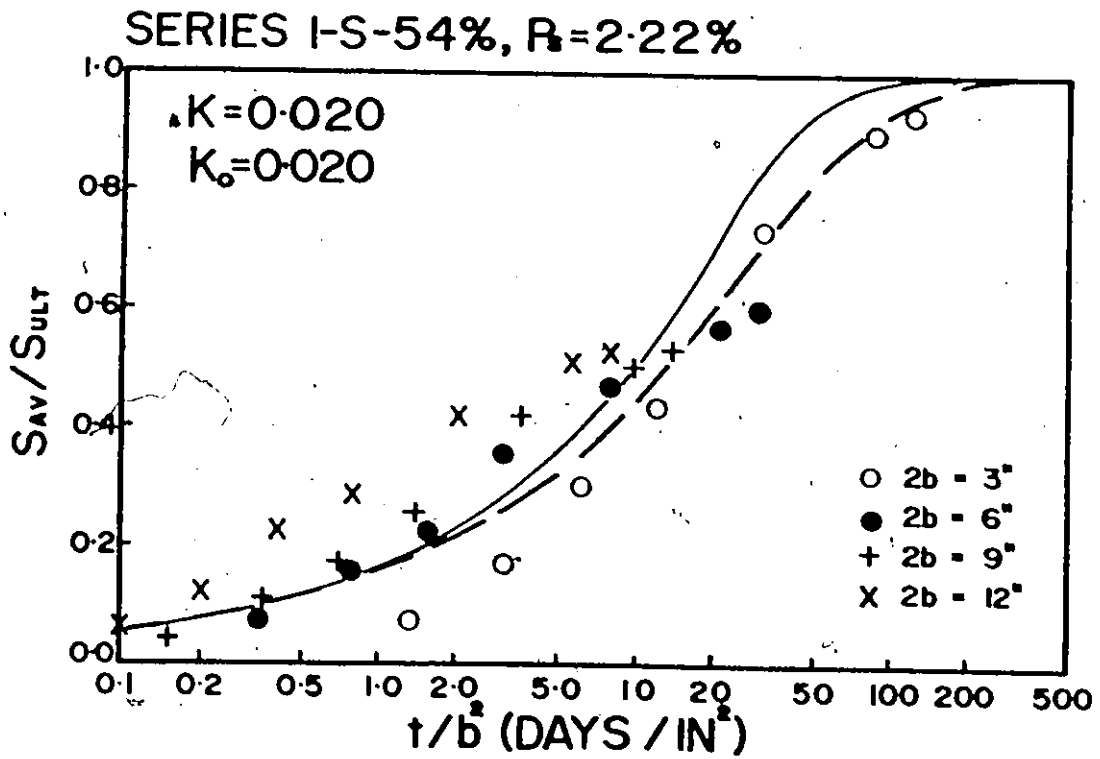
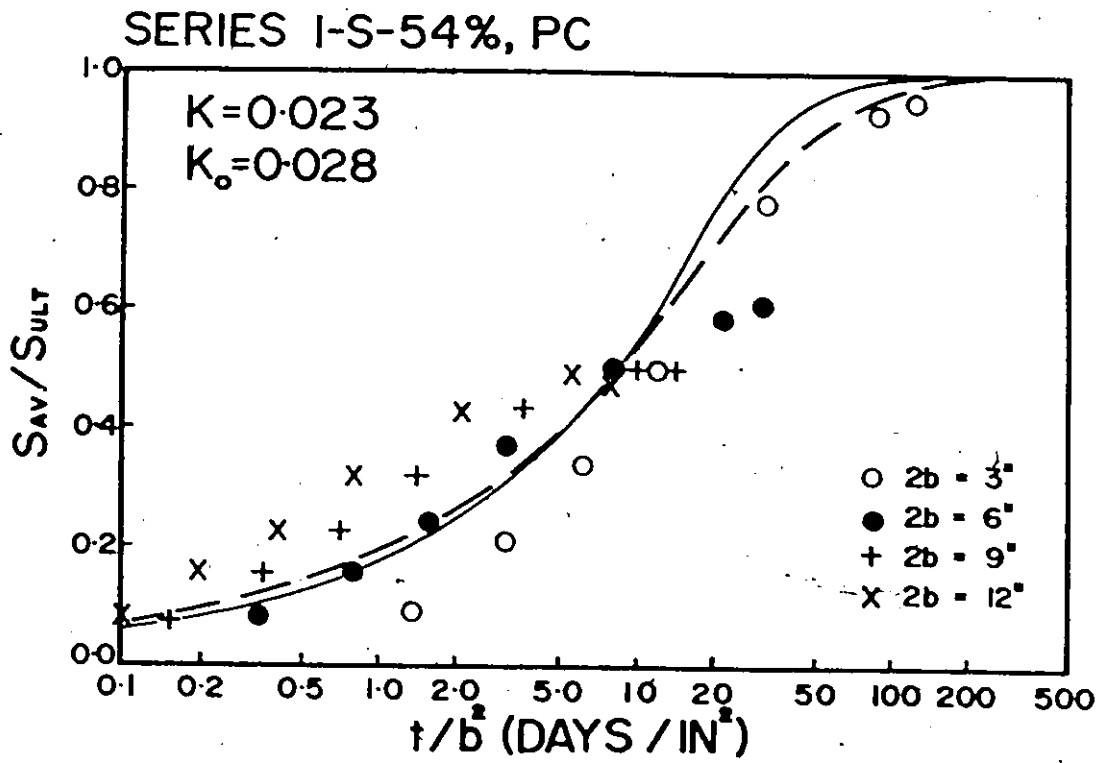
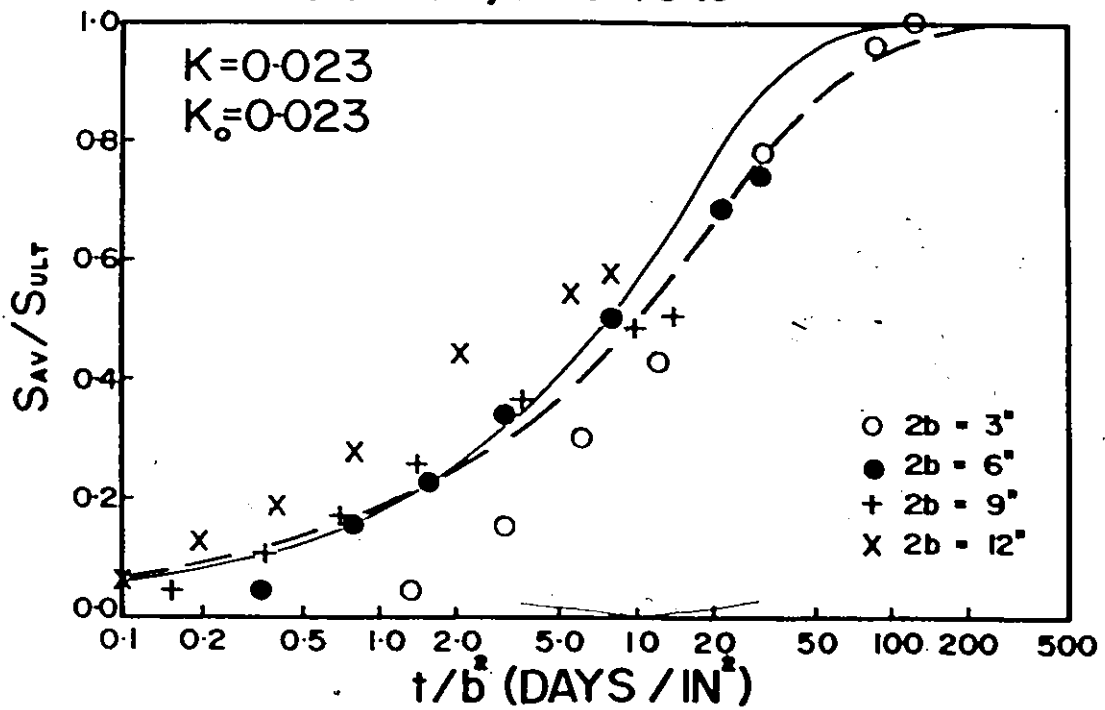


Figure 57

SERIES I-S-54%,  $R_s=3.45\%$



SERIES I-S-54%,  $R_s=4.90\%$

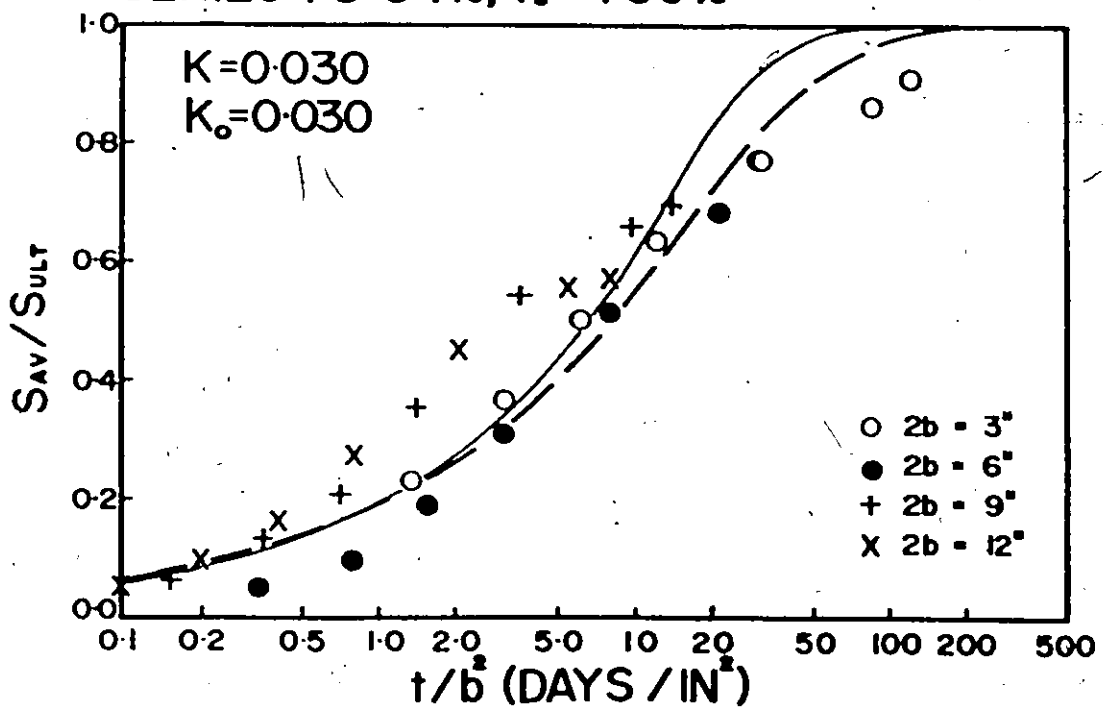


Figure 58

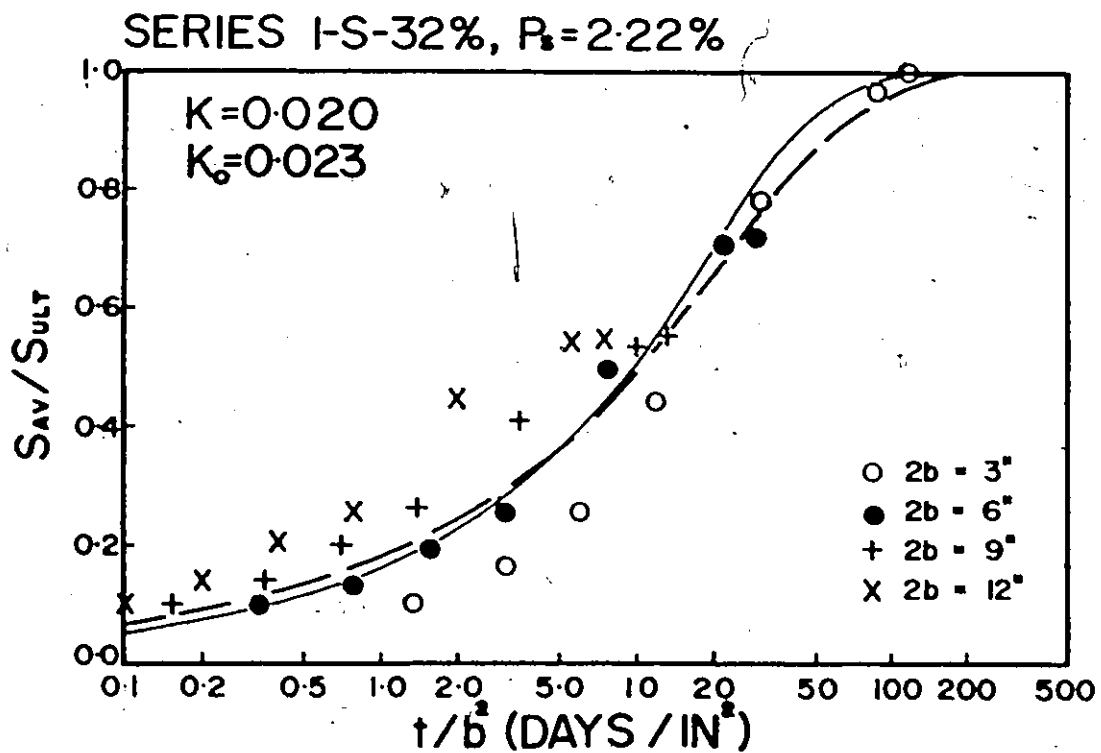
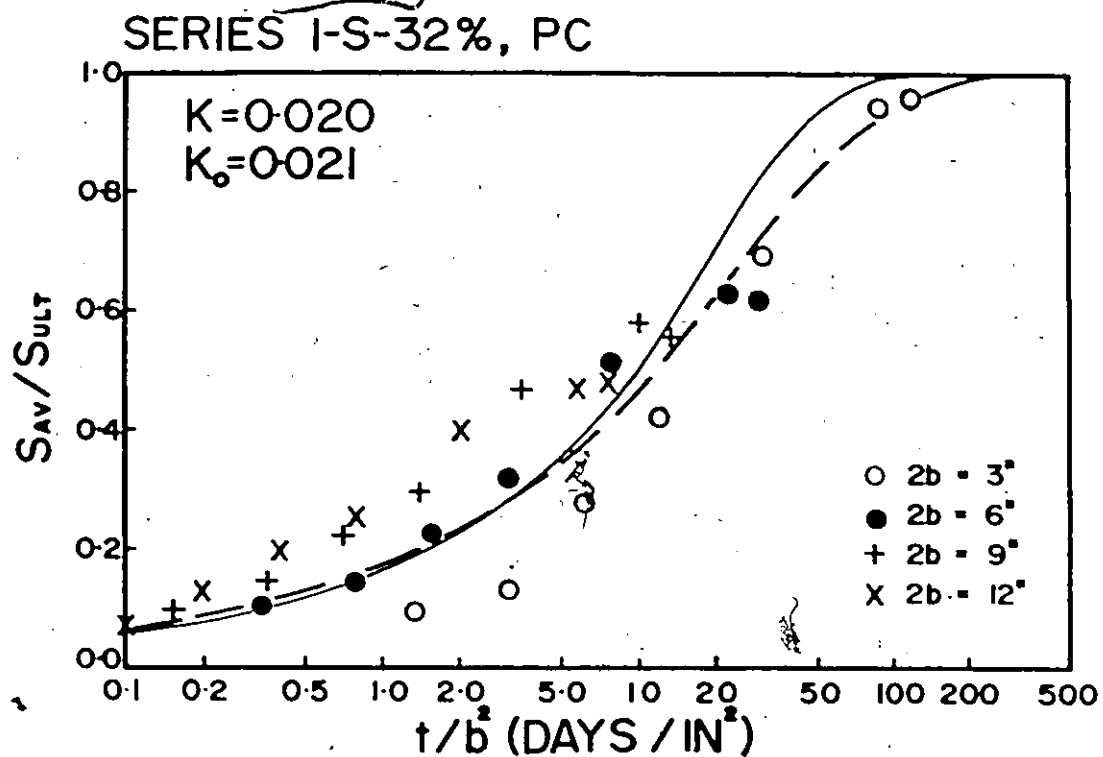
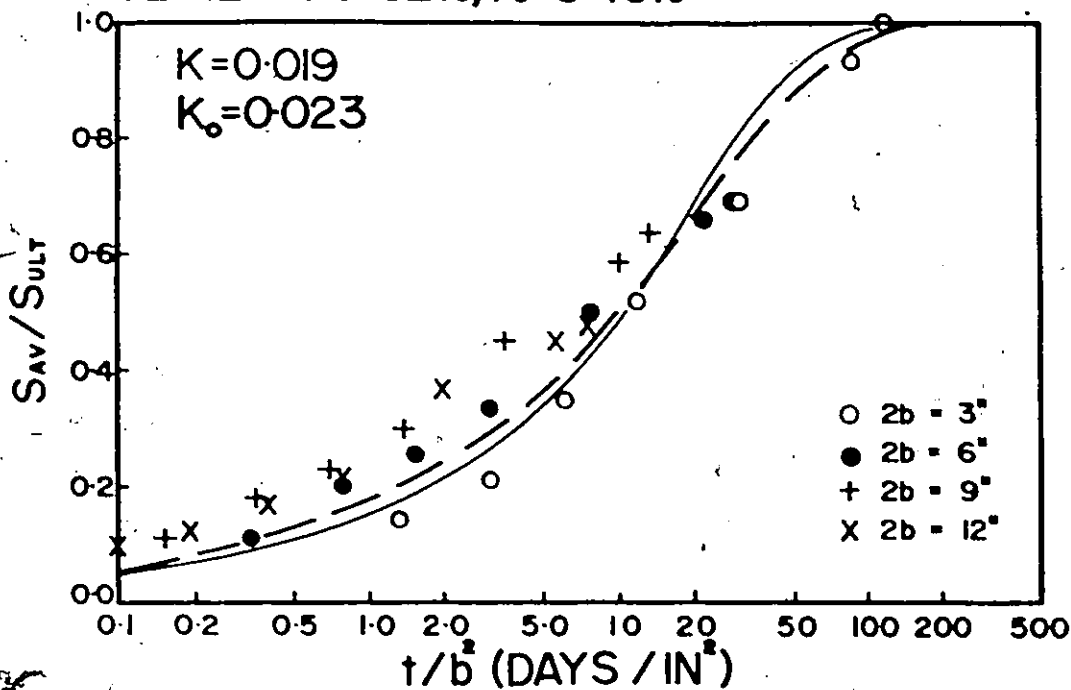


Figure 59

SERIES I-S-32%,  $P_s=3.45\%$



SERIES I-S-32%,  $P_s=4.90\%$

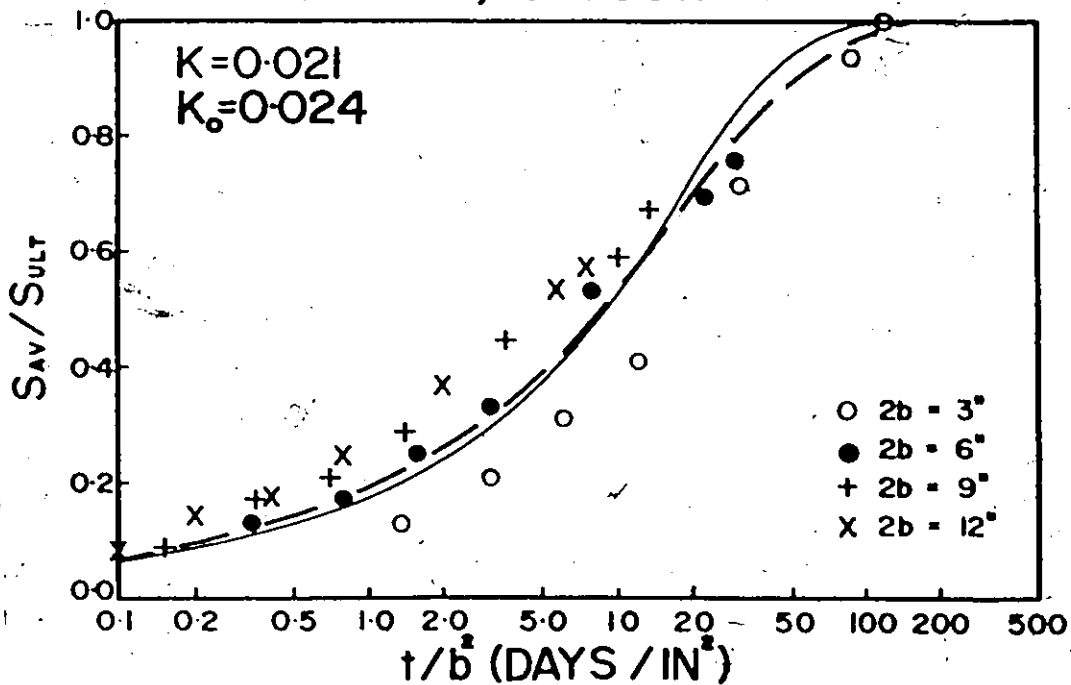


Figure 60

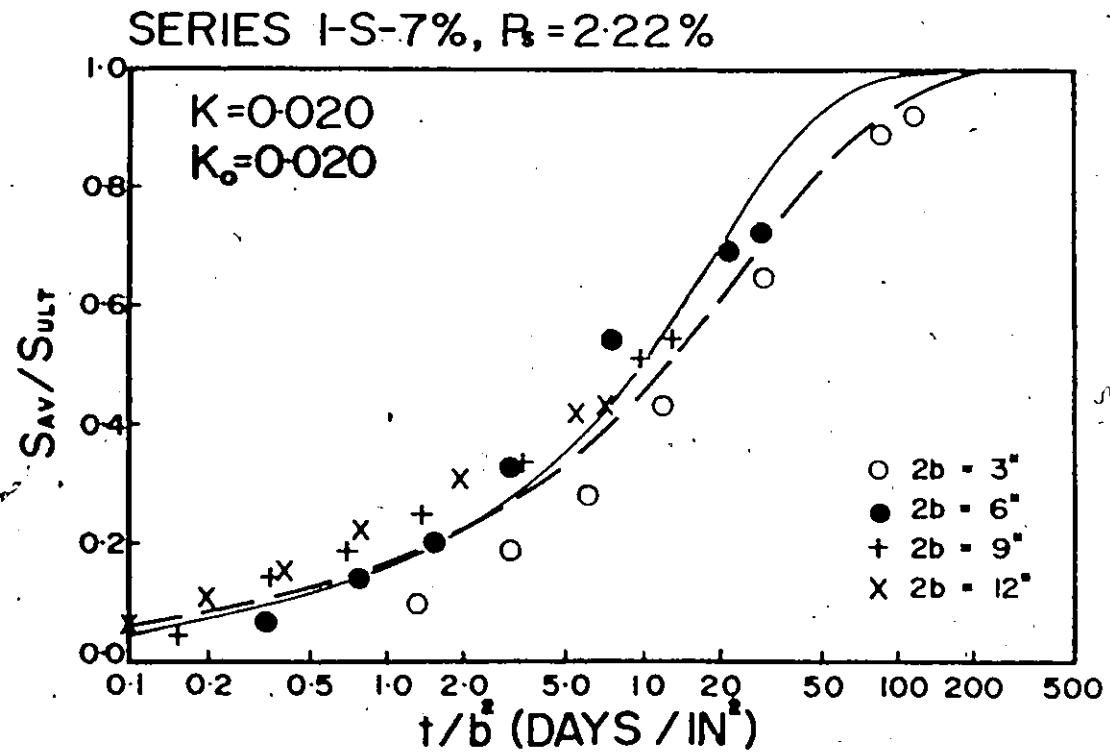
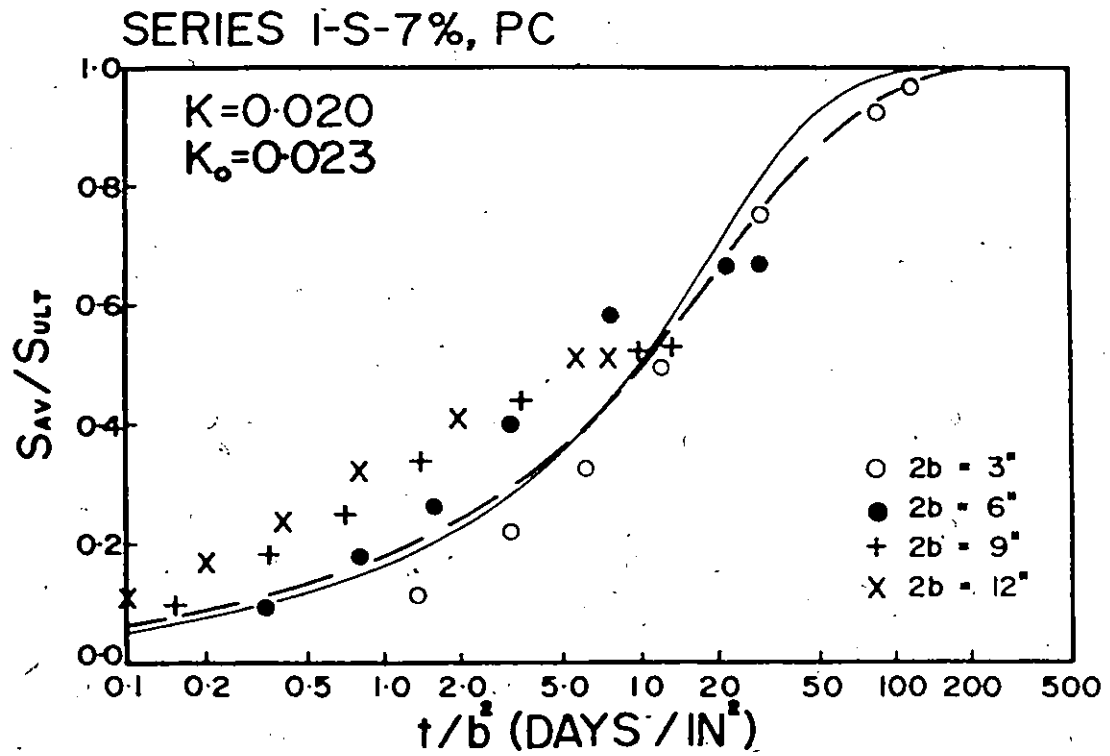


Figure 61

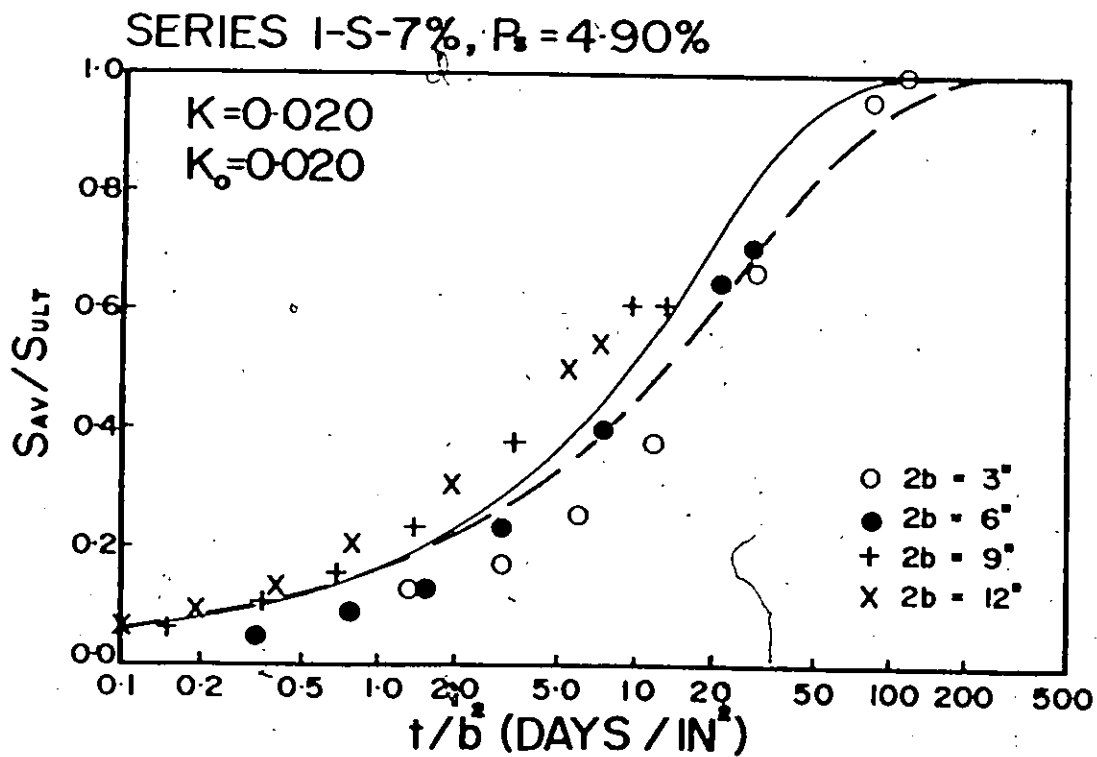
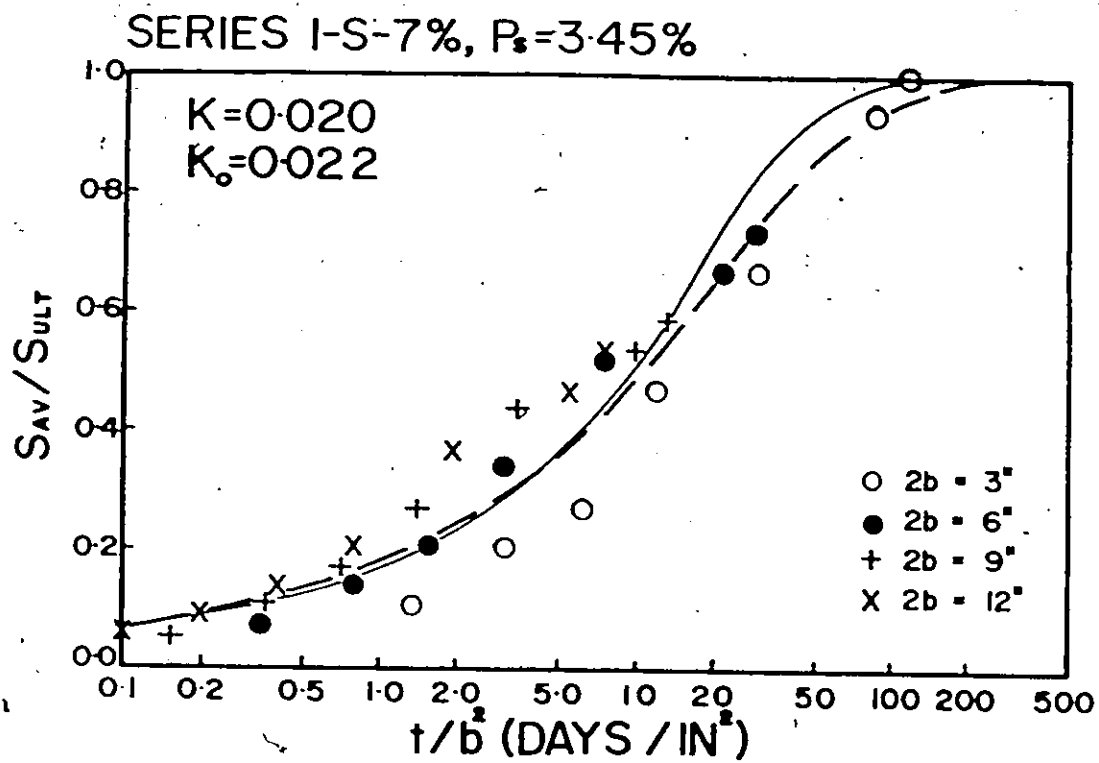


Figure 62

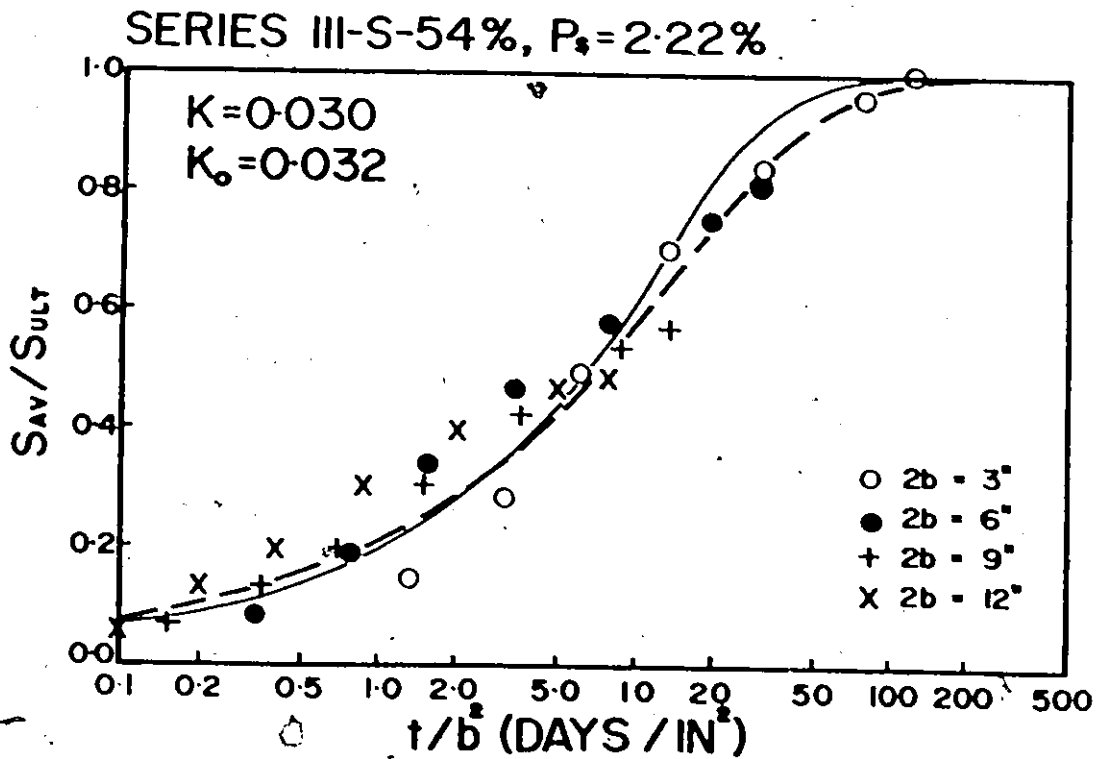
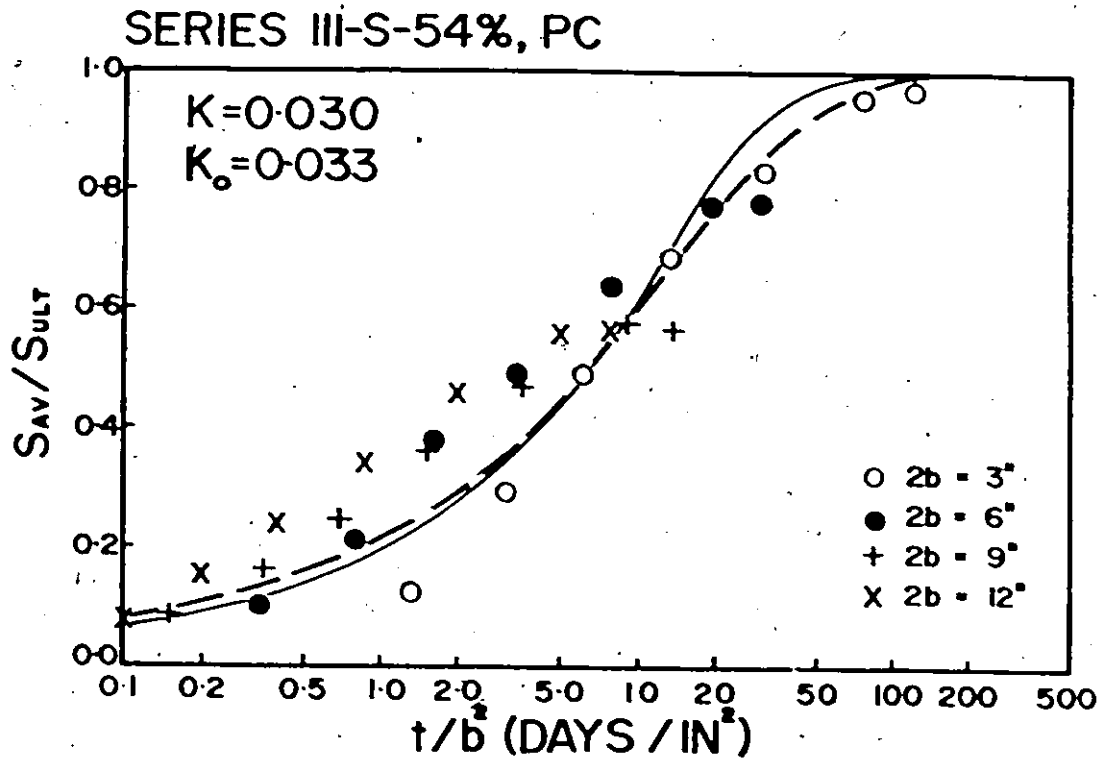


Figure 63



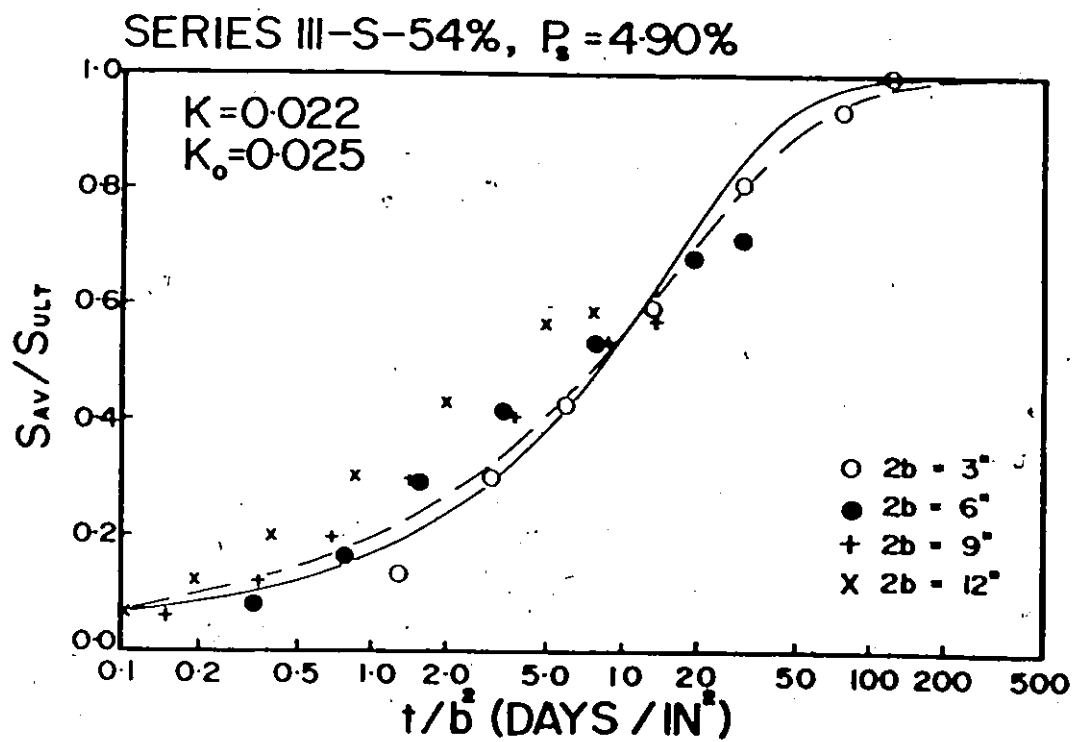
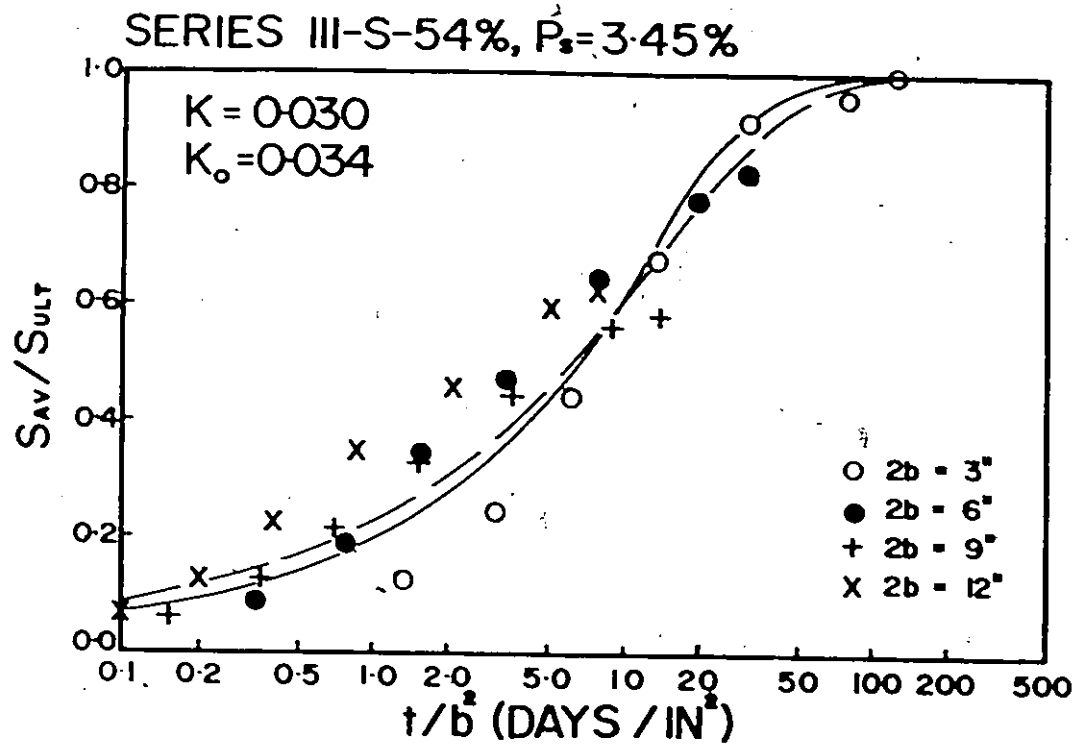


Figure 64

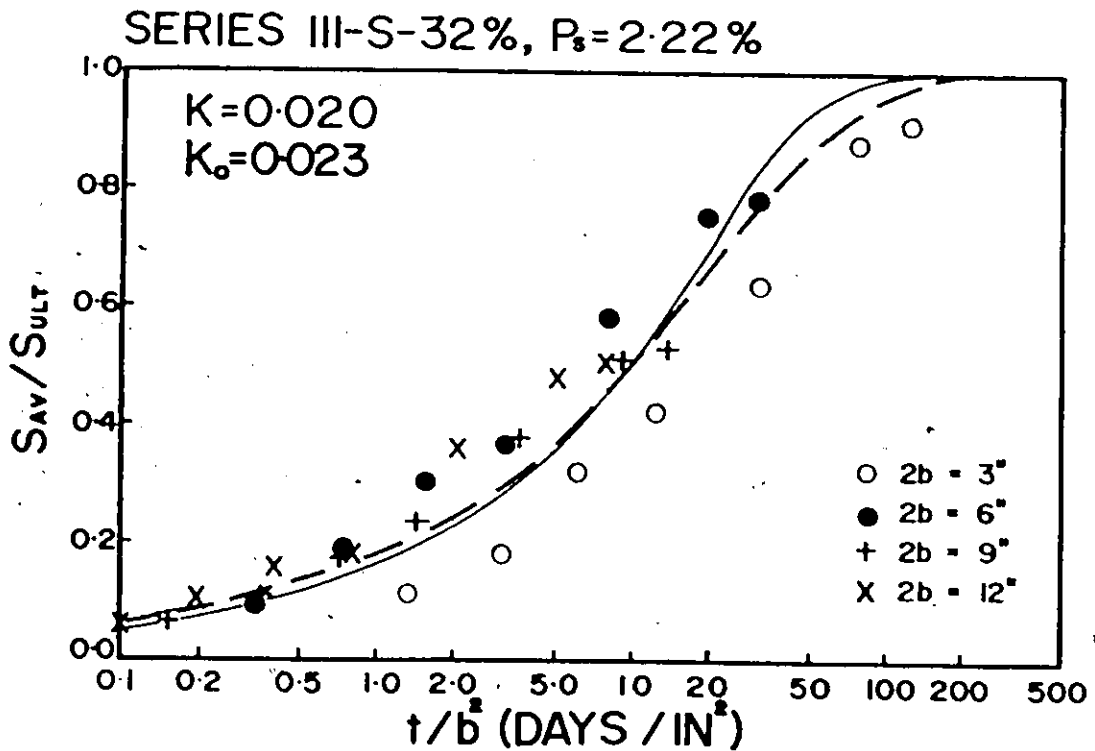
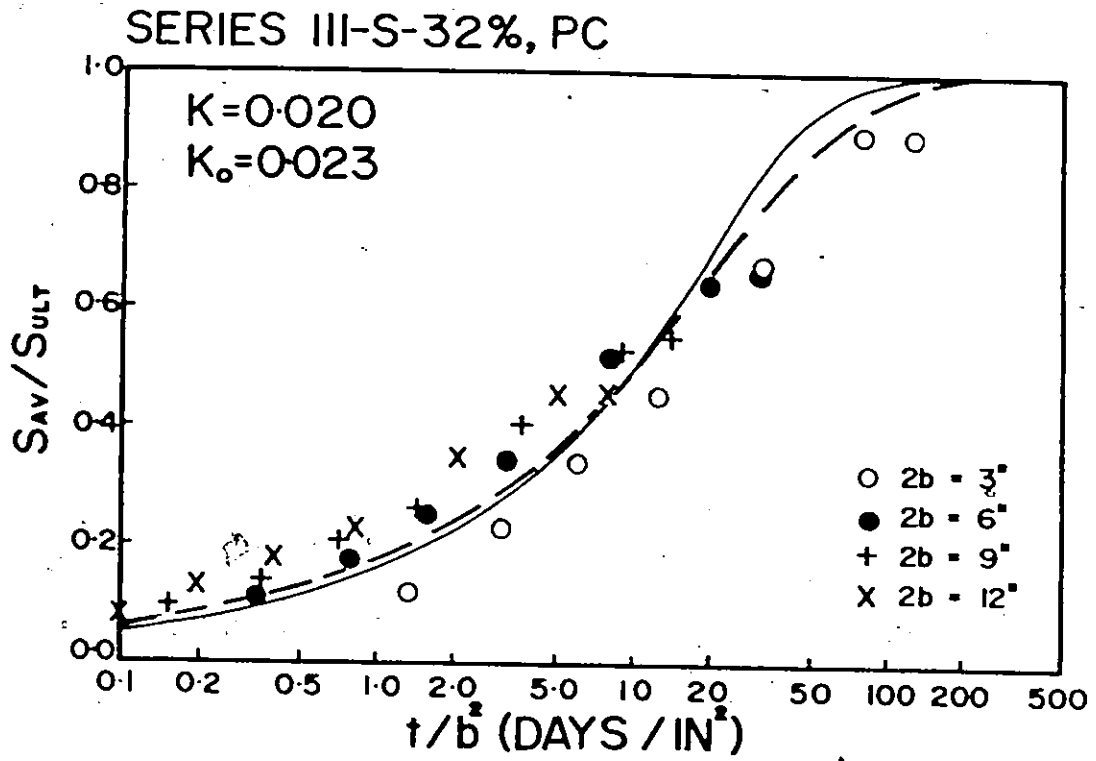


Figure 65

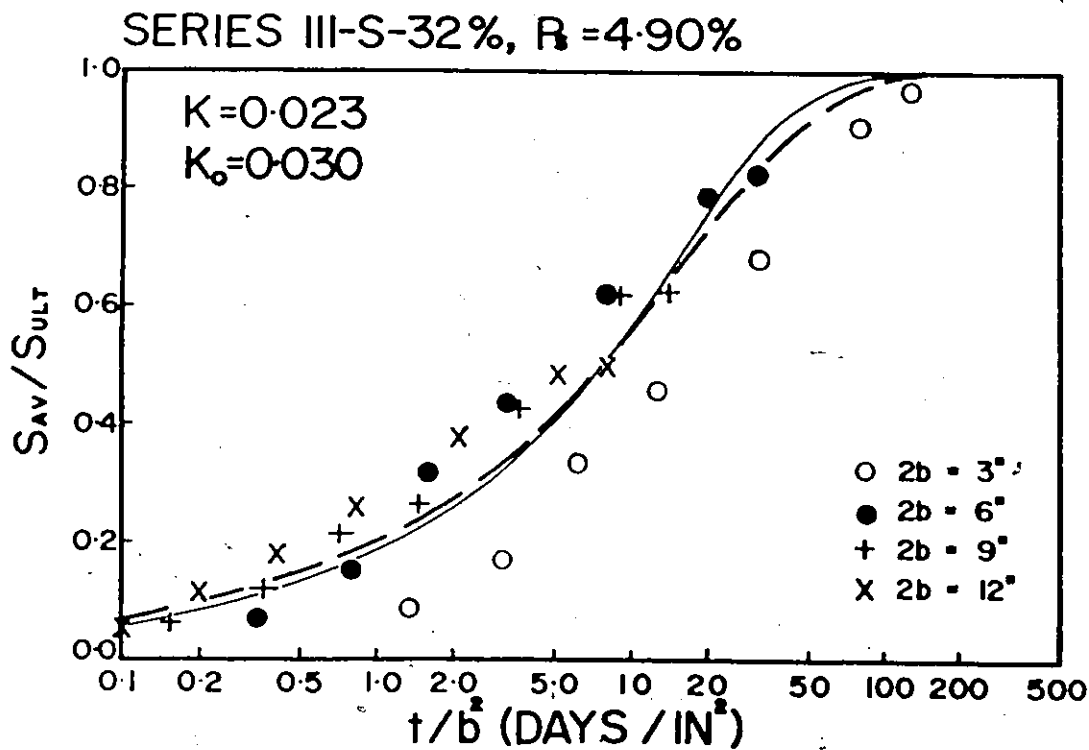
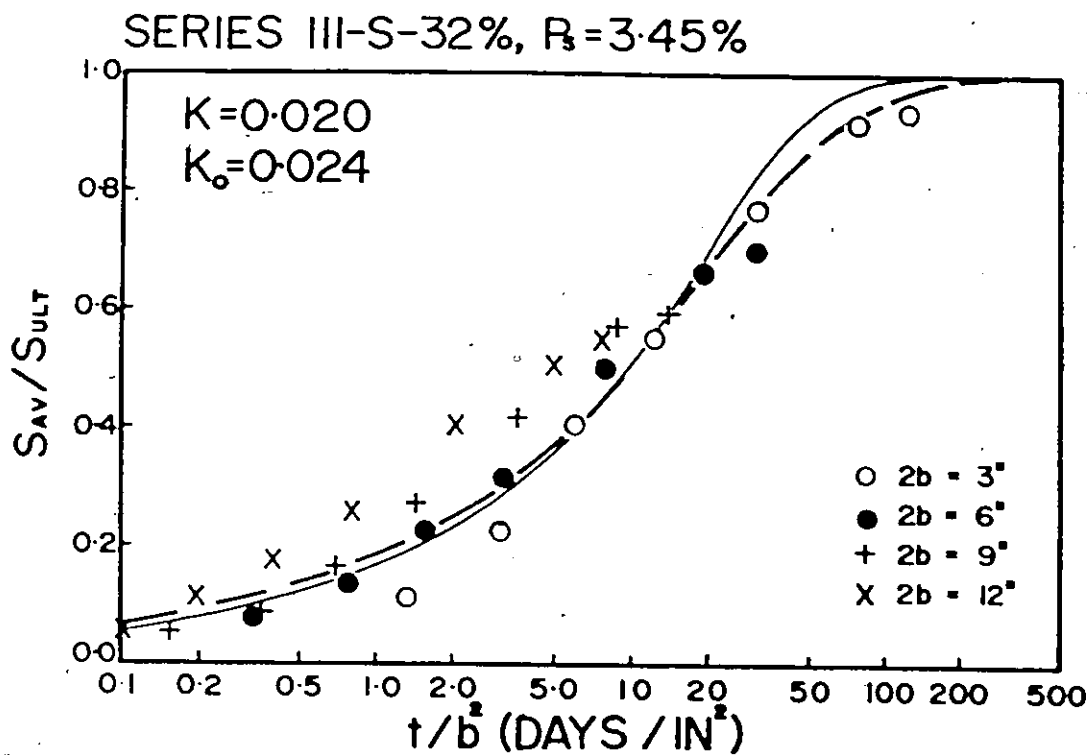


Figure 66

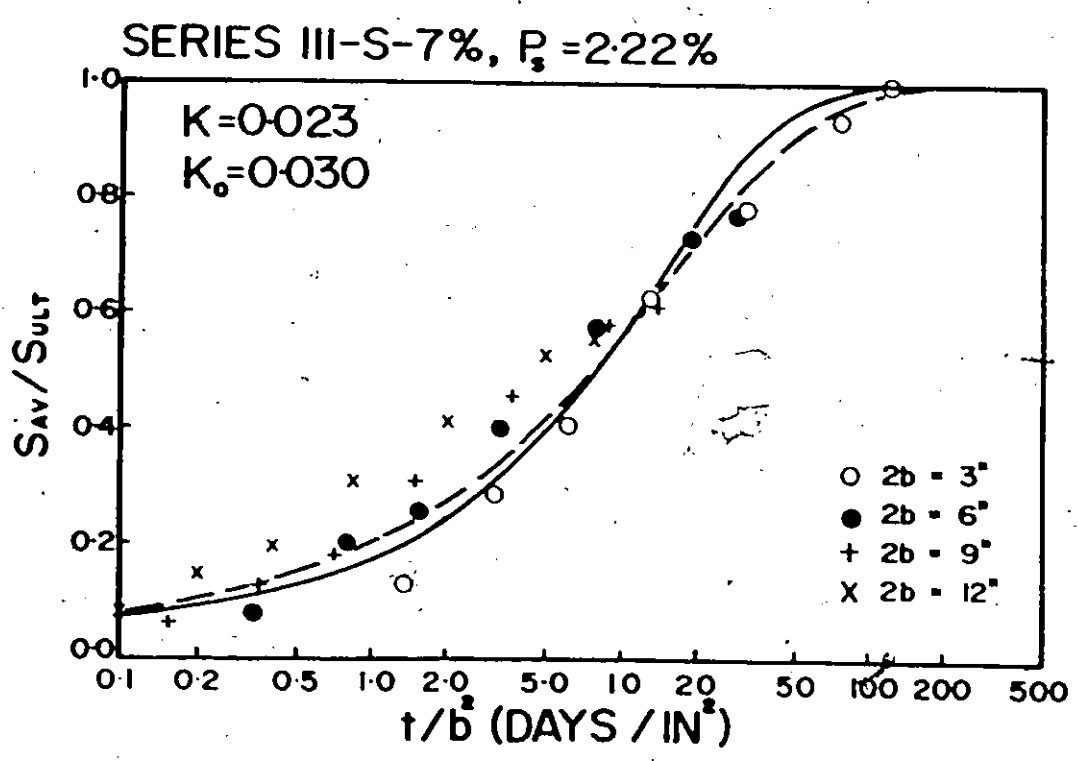
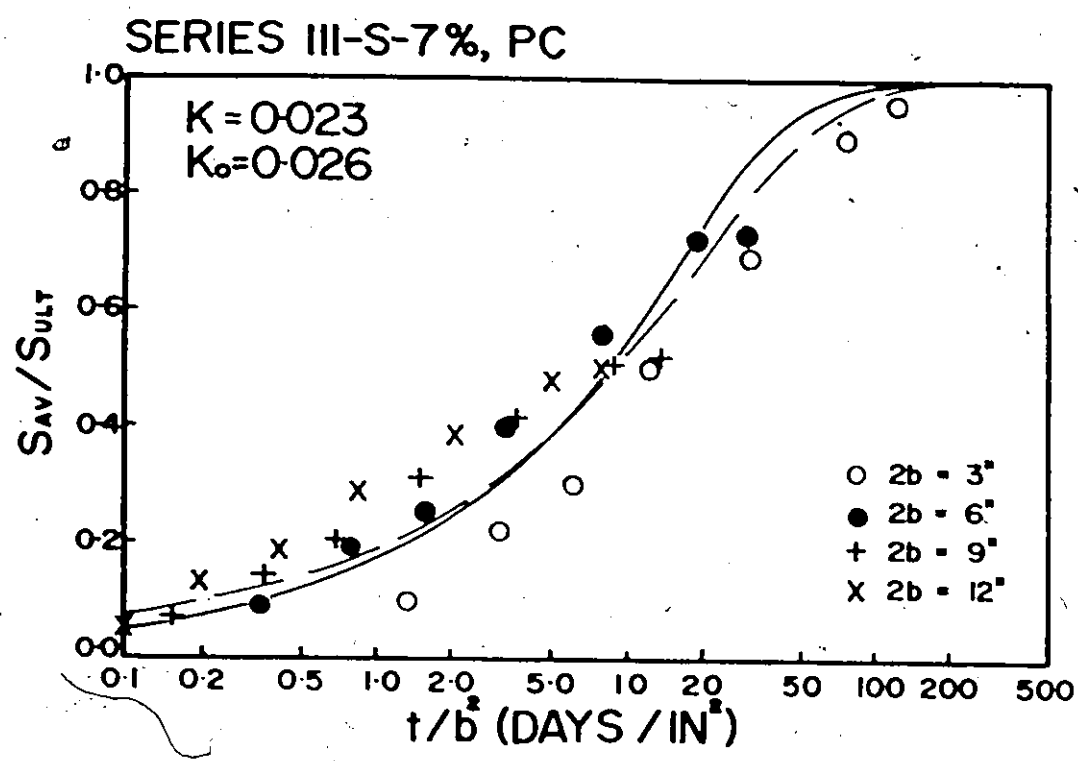


Figure 67

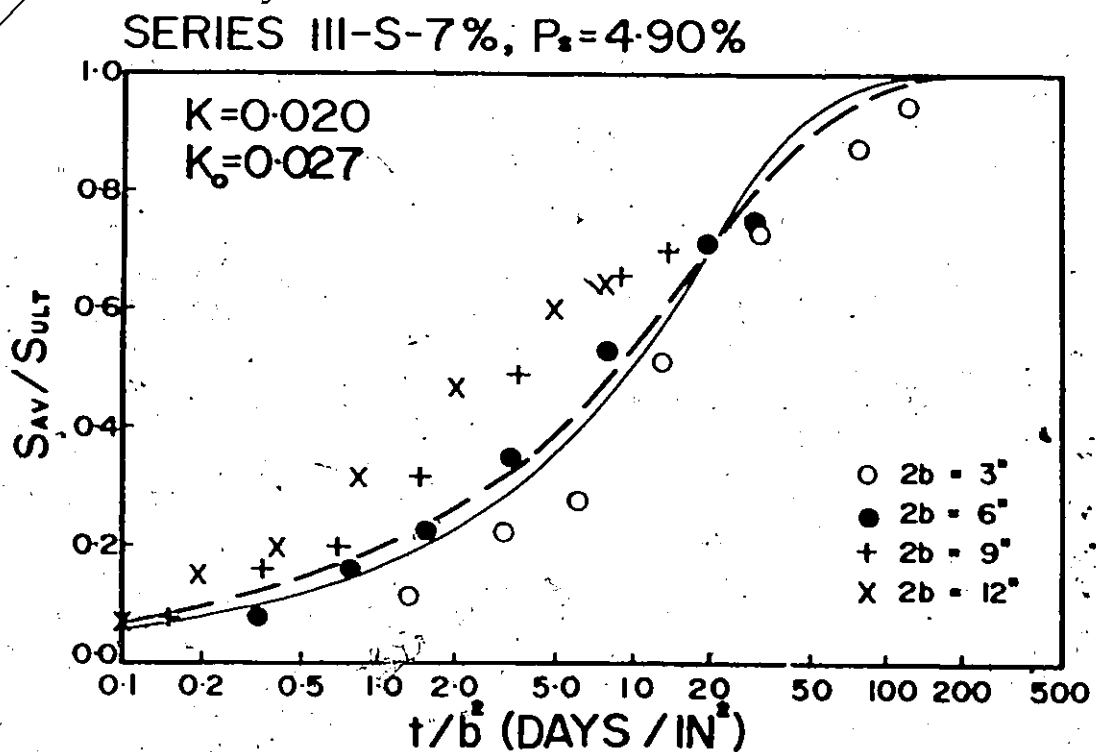
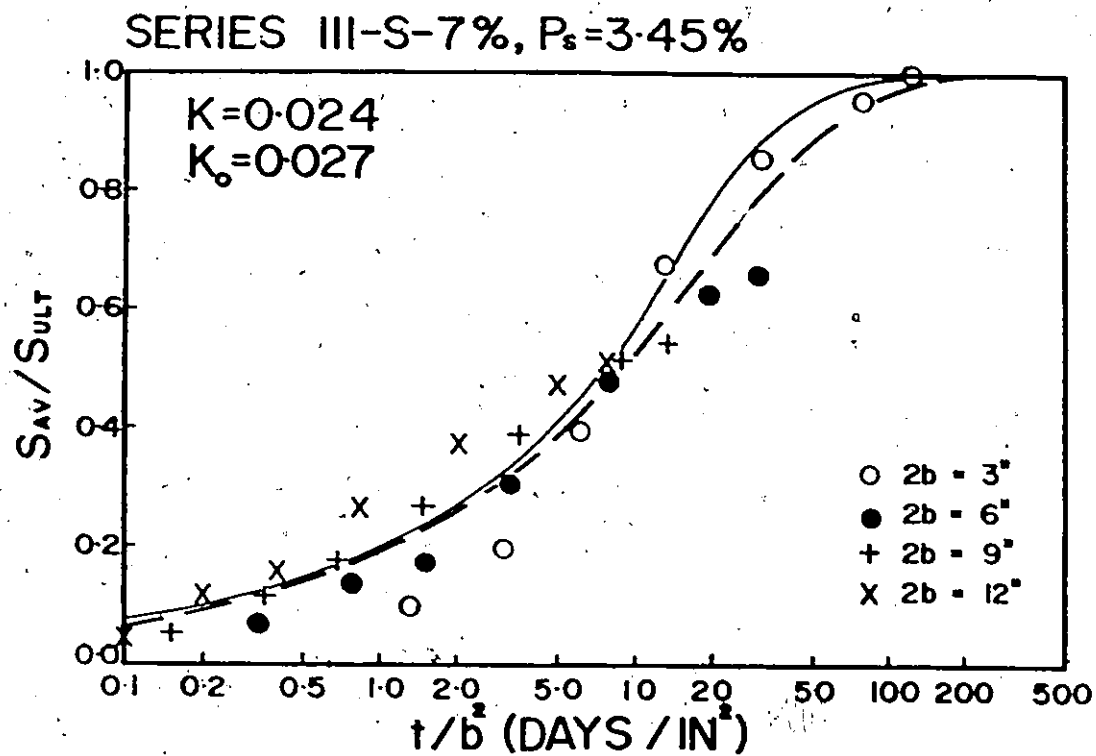


Figure 68

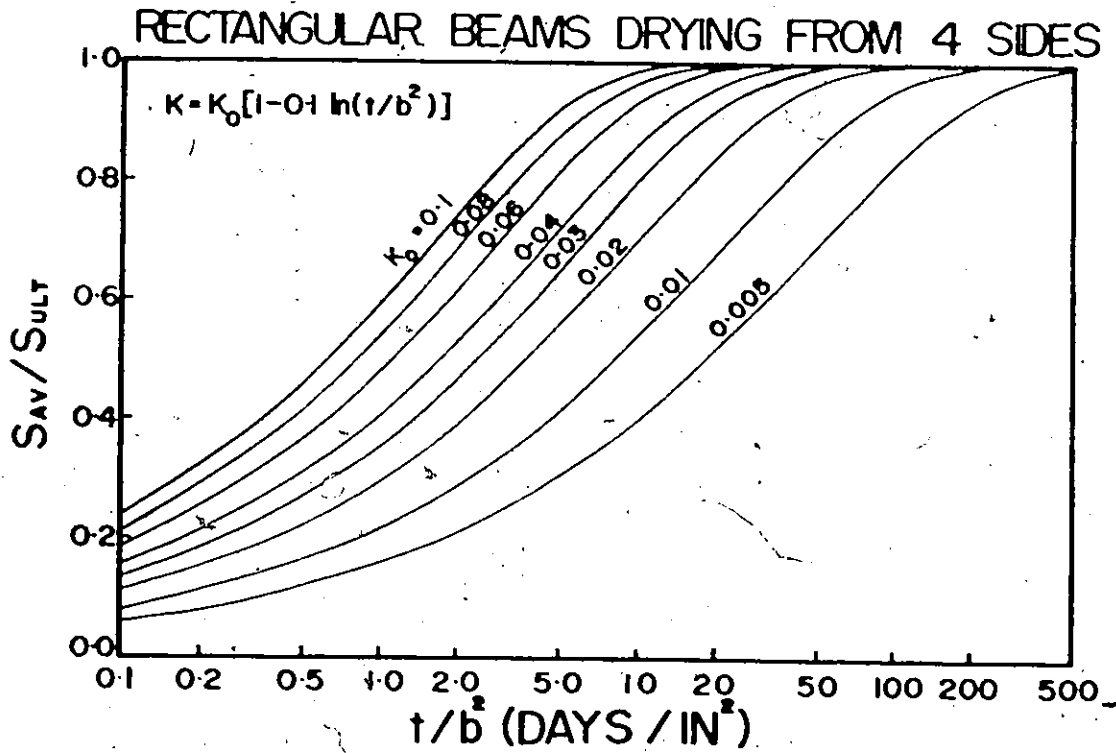
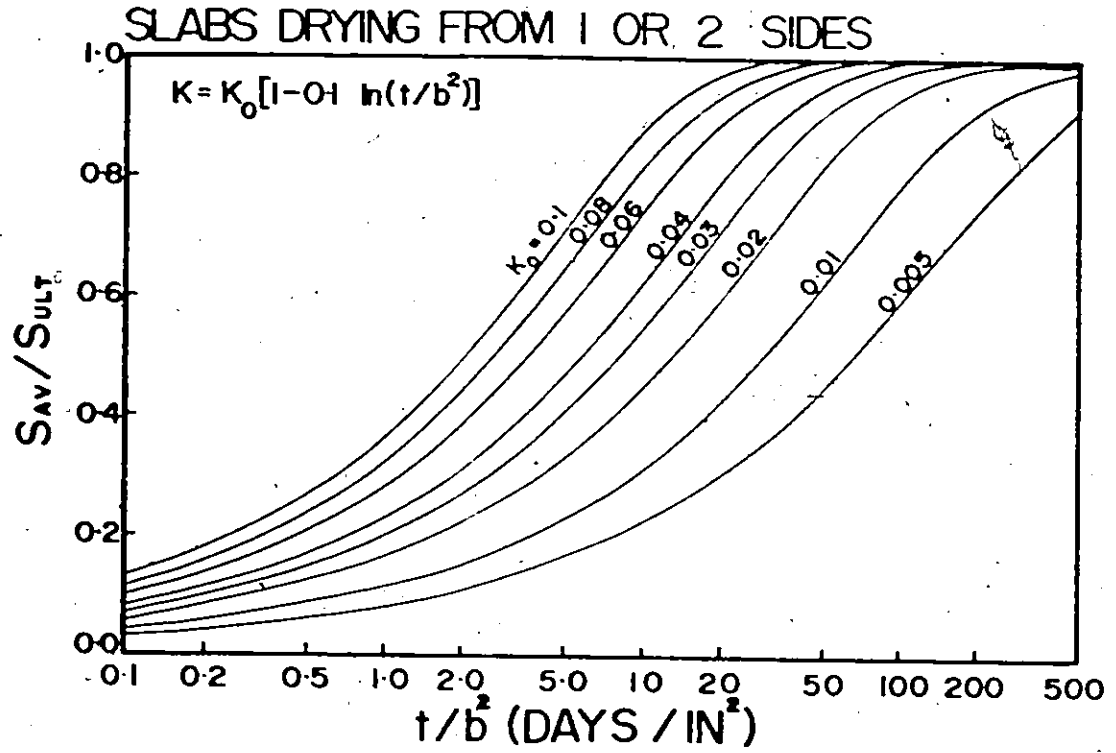


Figure 69

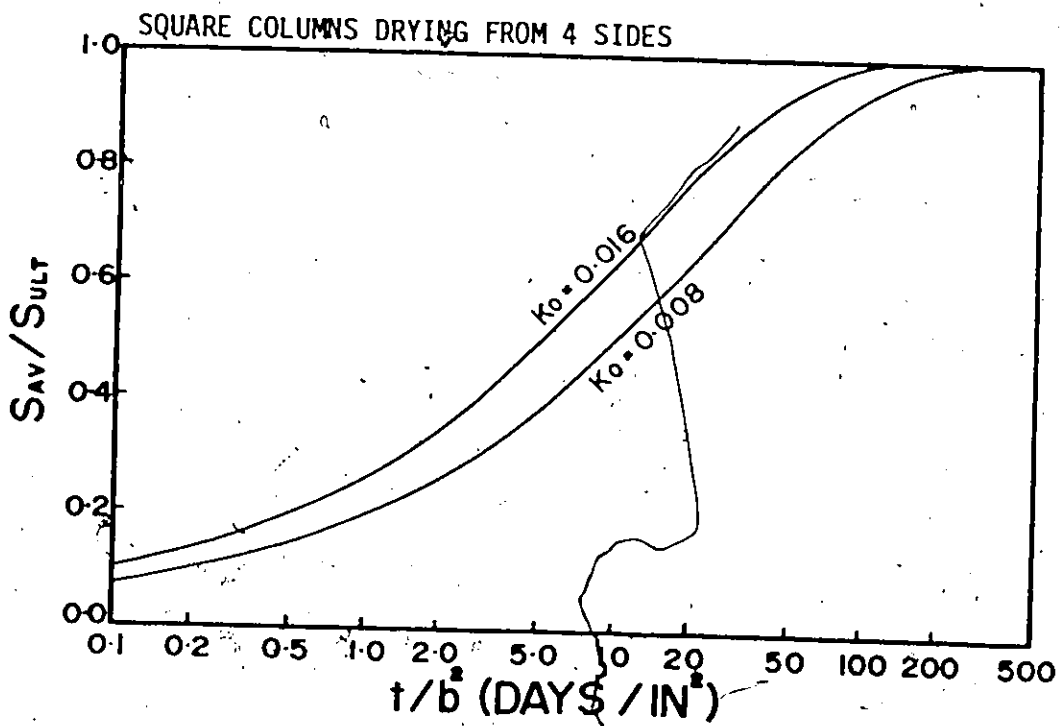
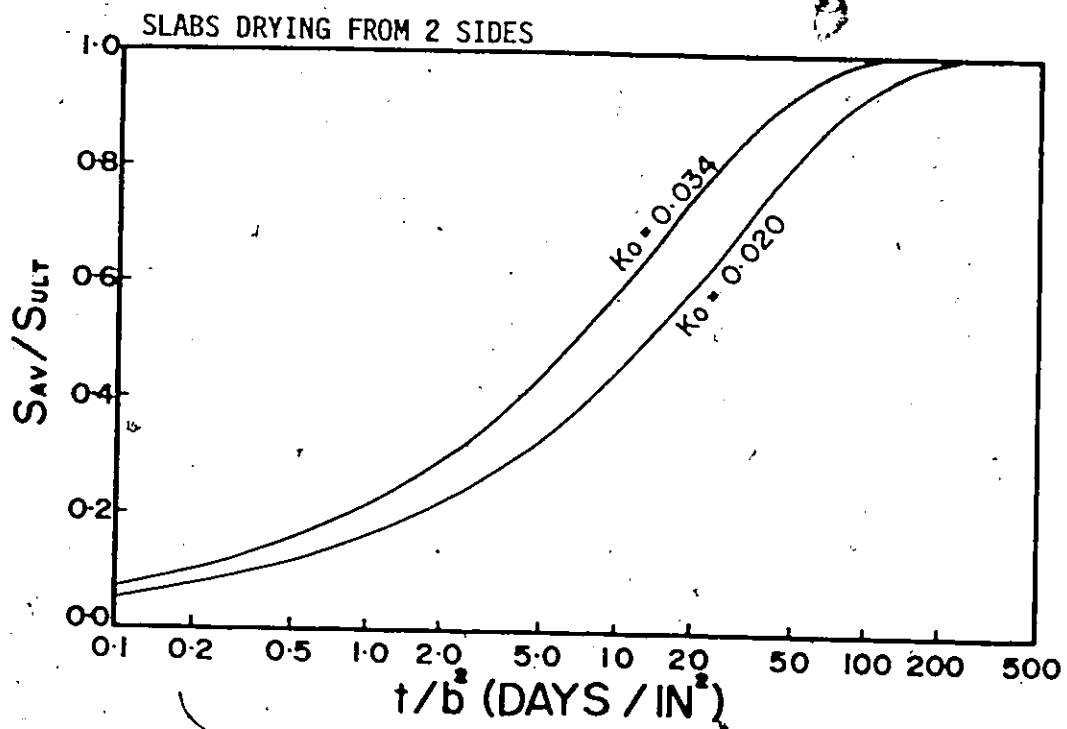


Figure 70

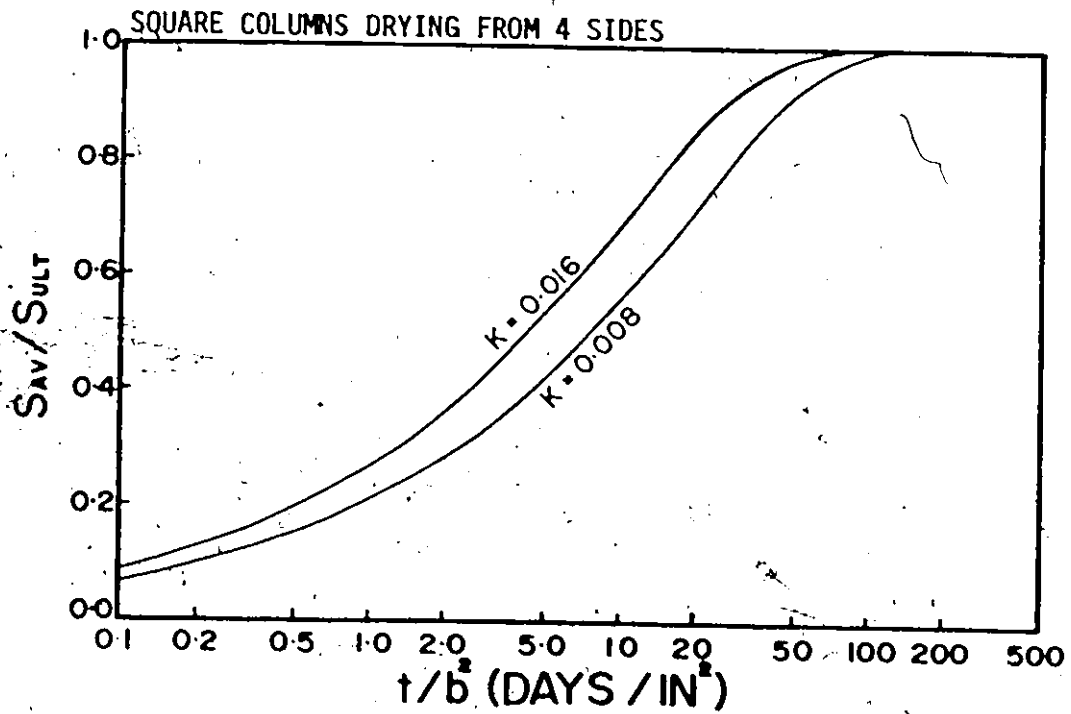
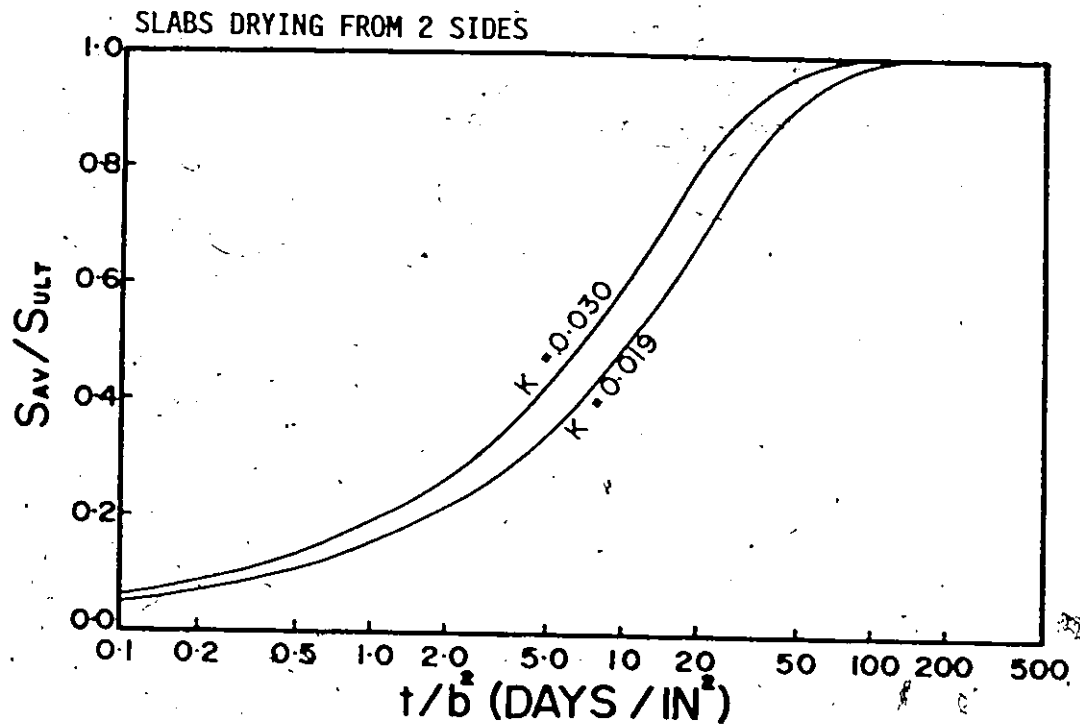


Figure 71



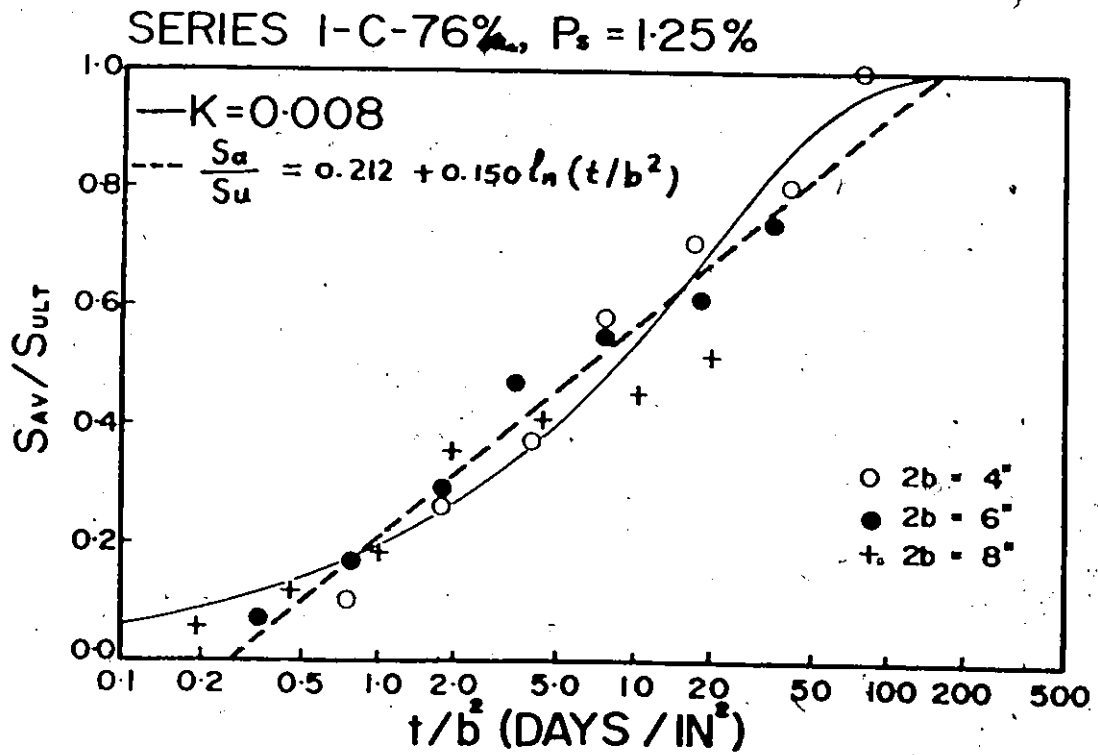
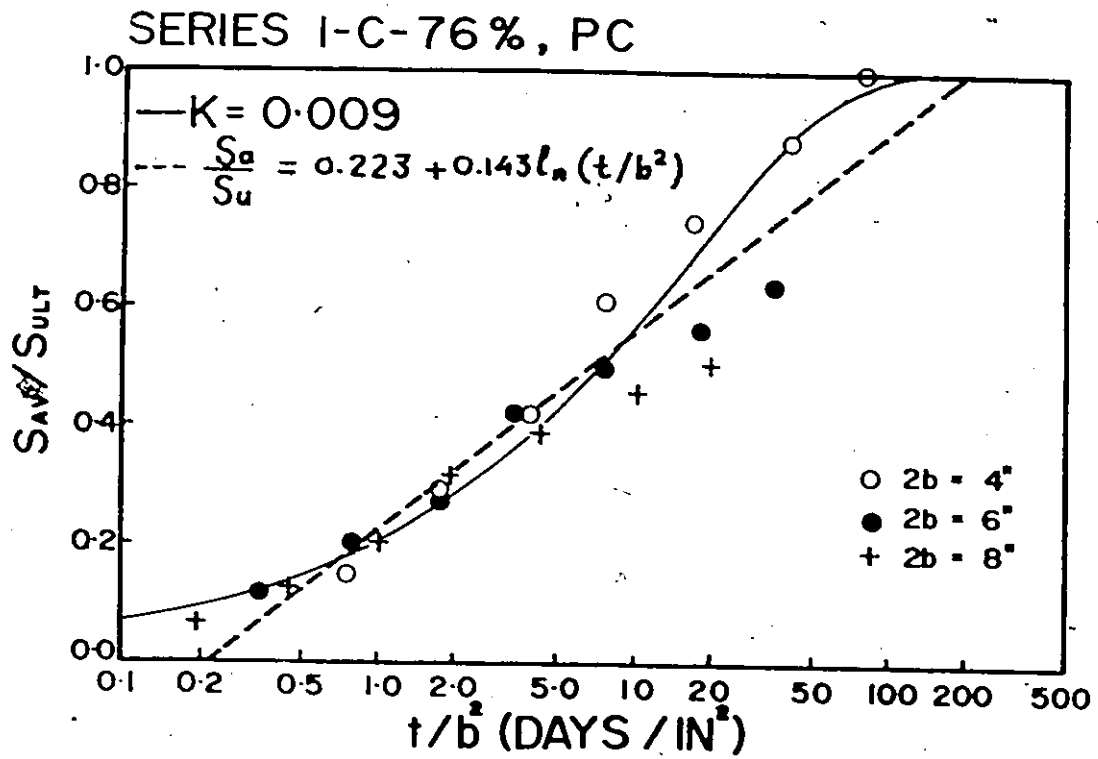


Figure 72

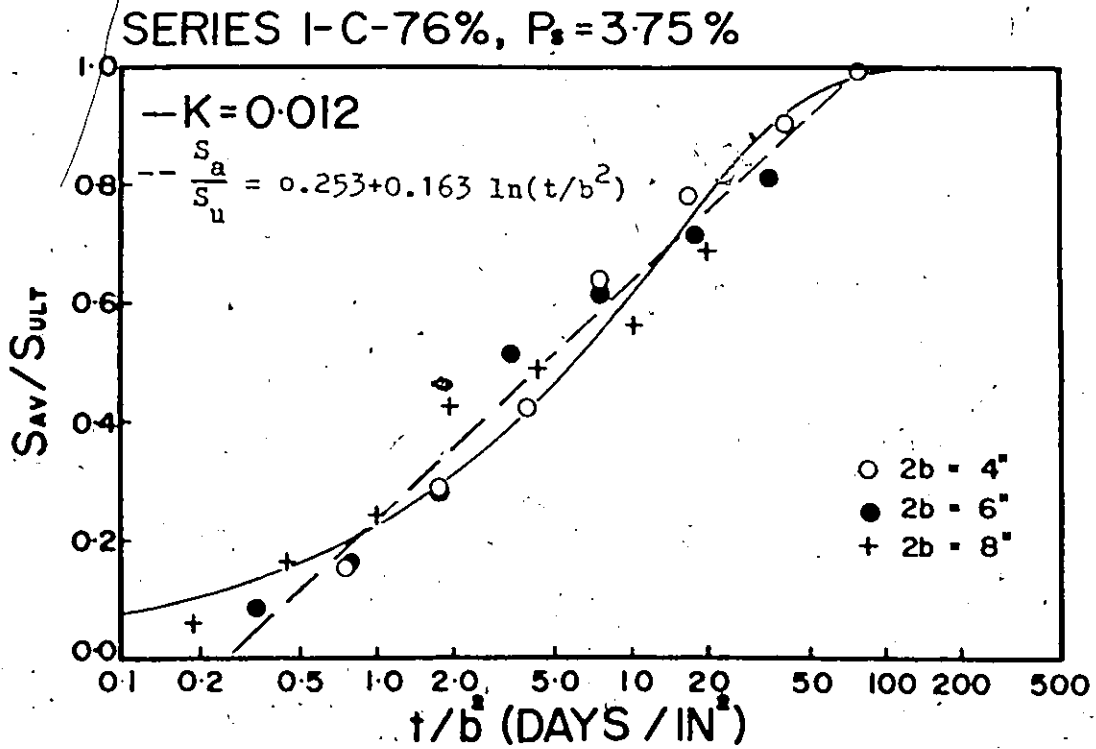
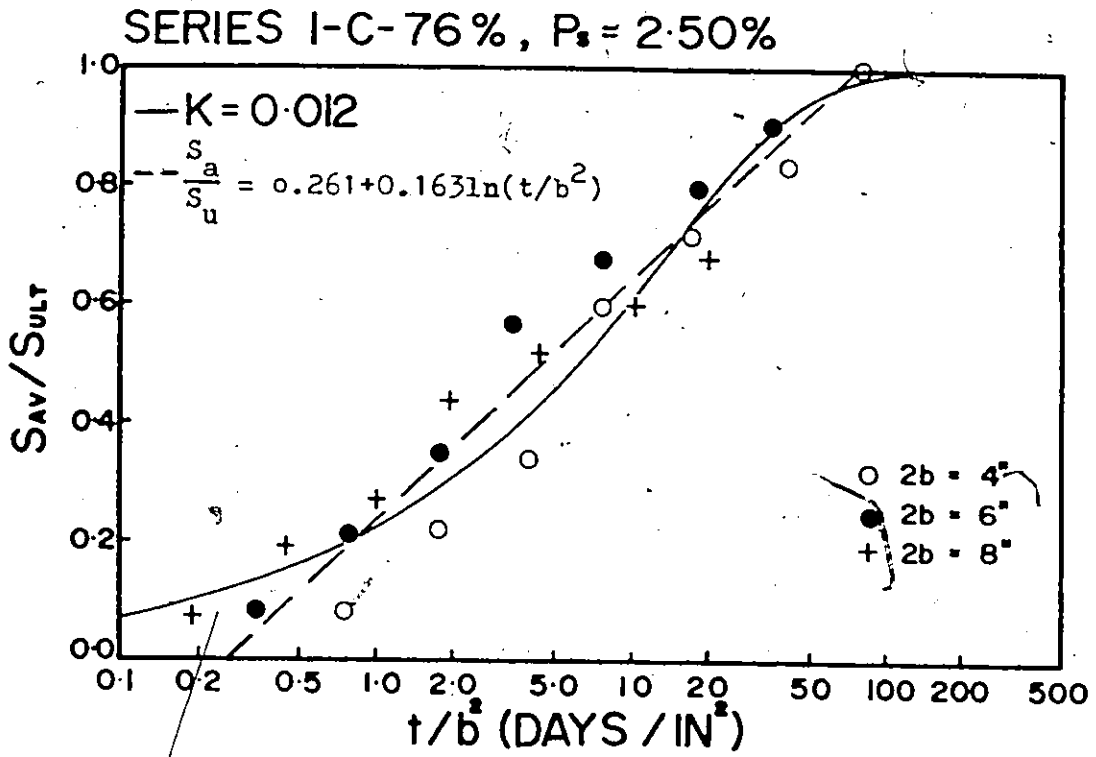


Figure 73

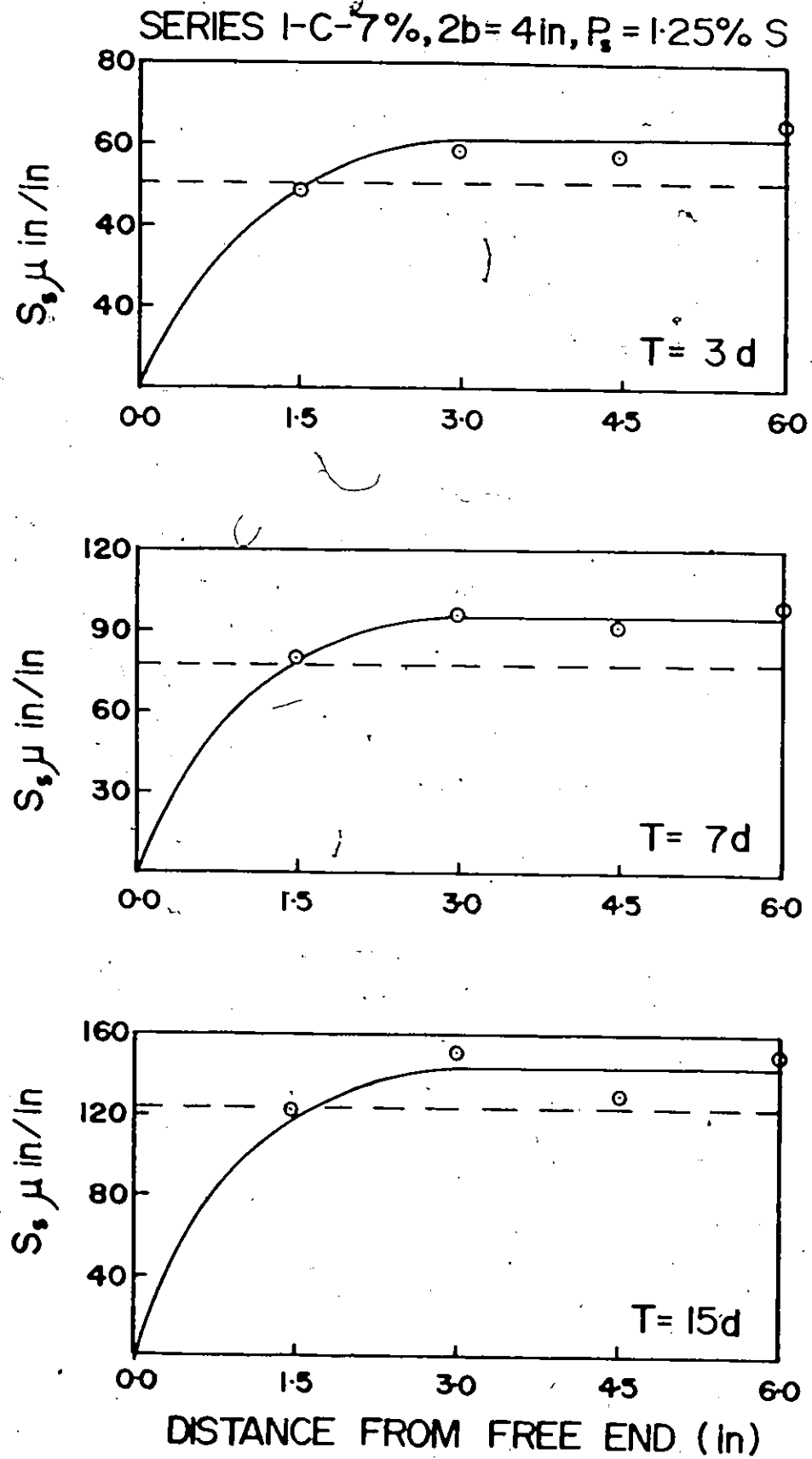


Figure 74

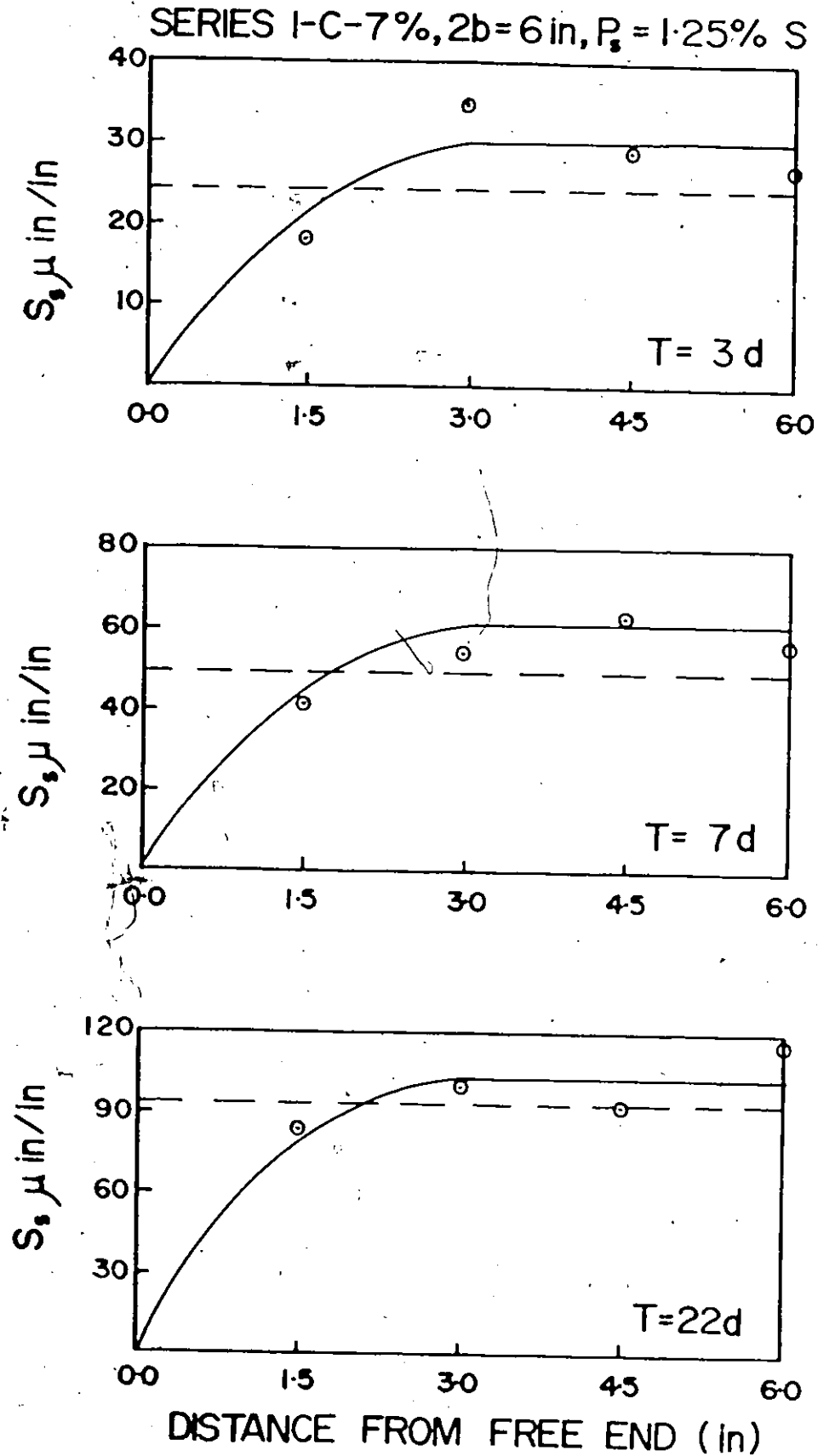


Figure 75

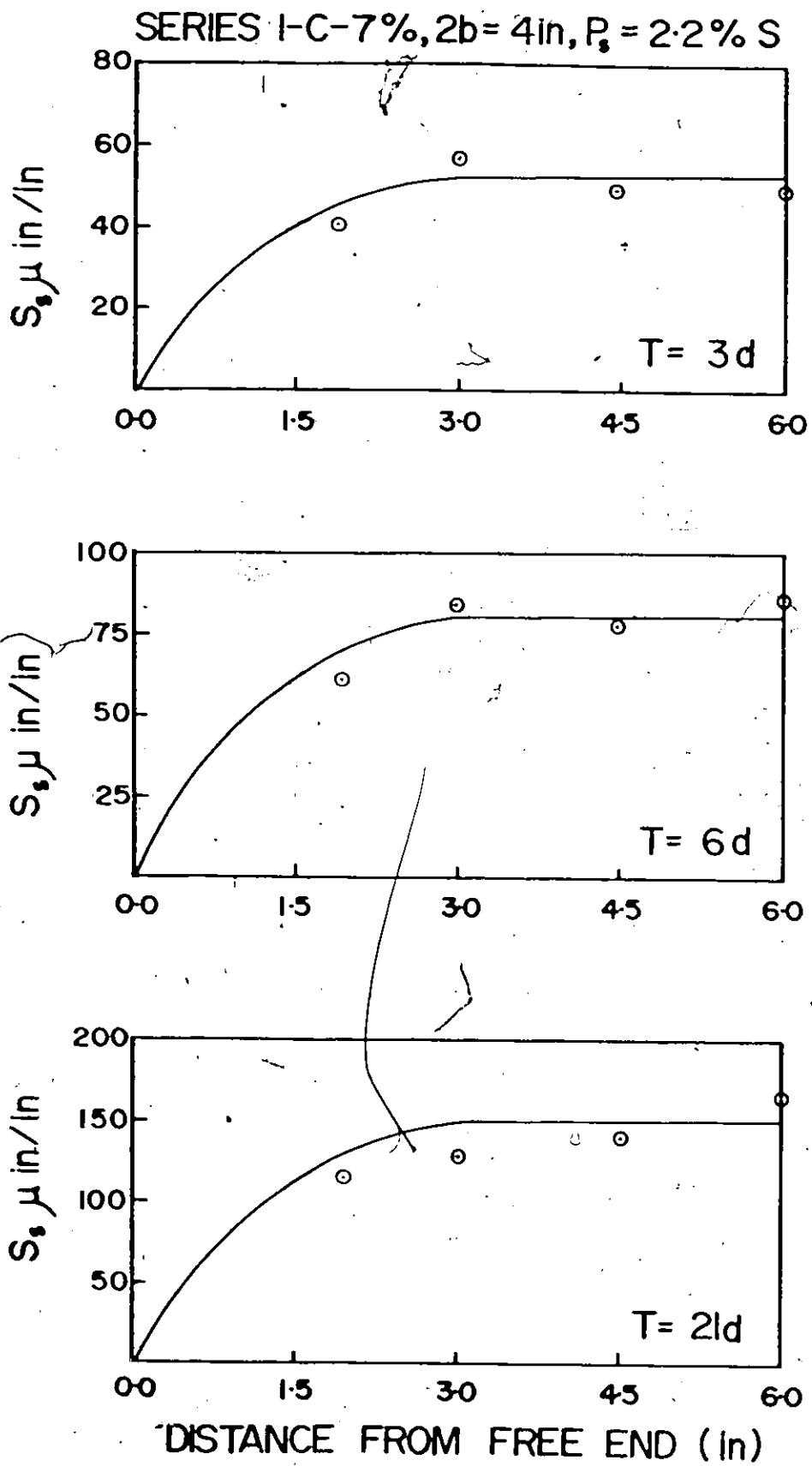


Figure 76

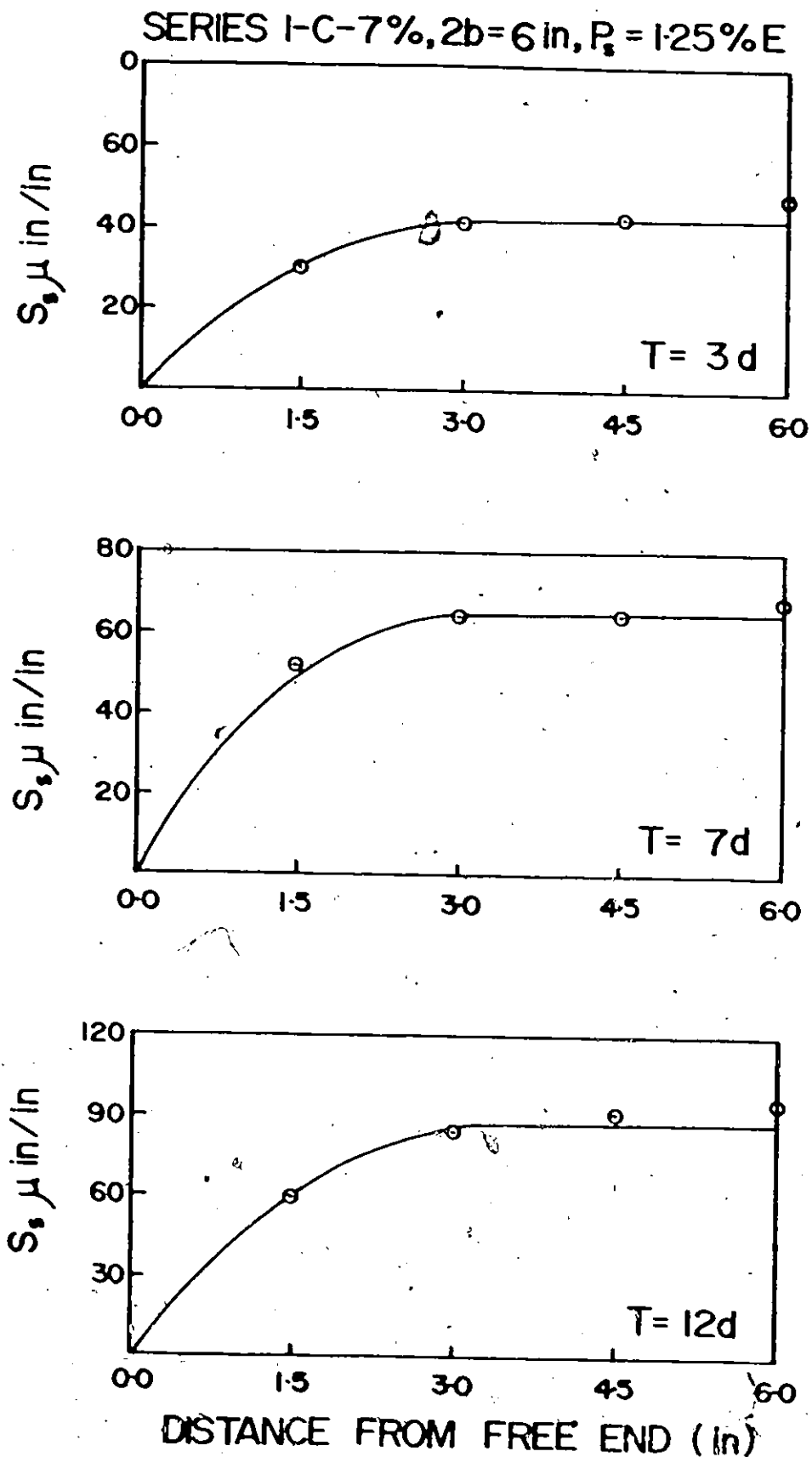
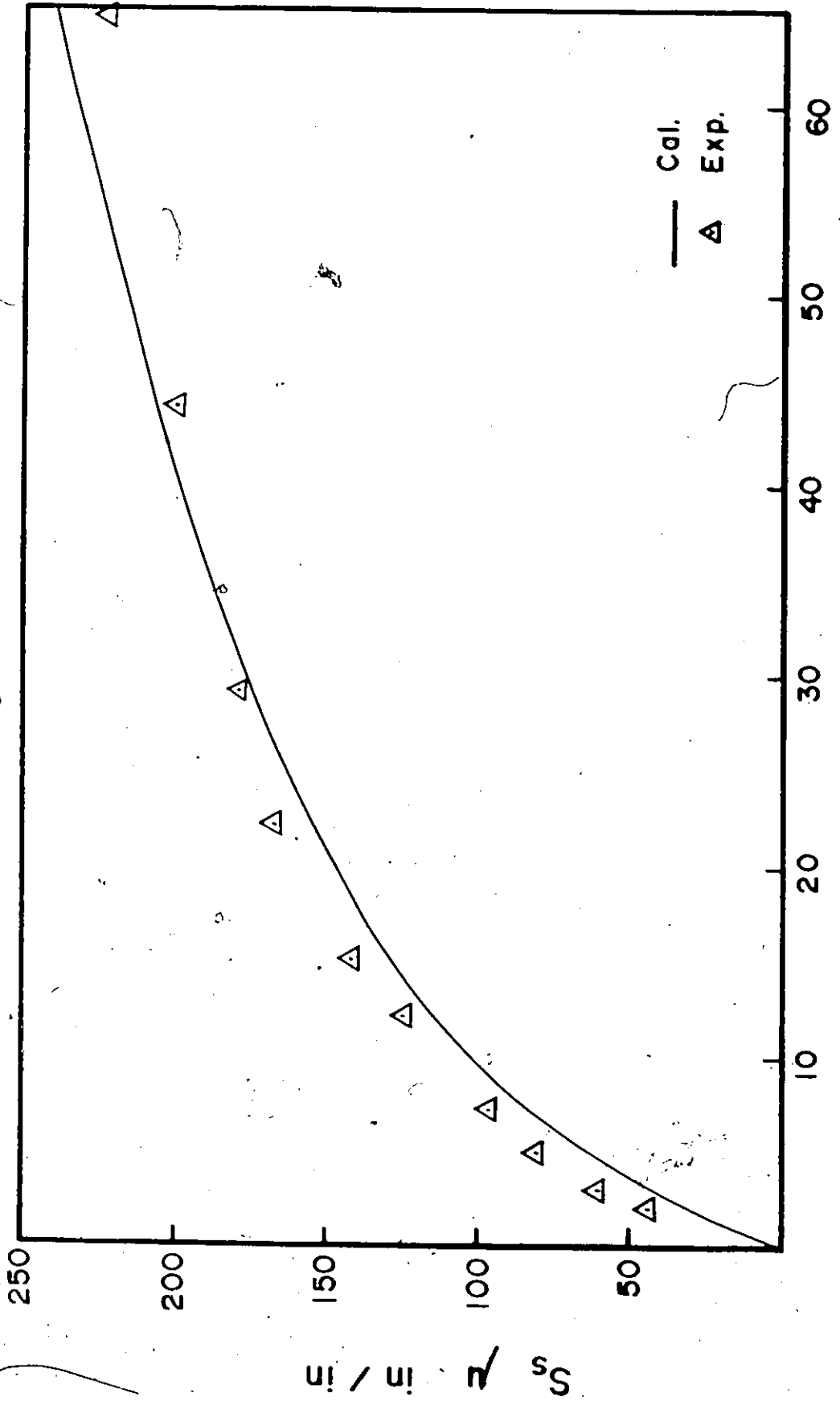


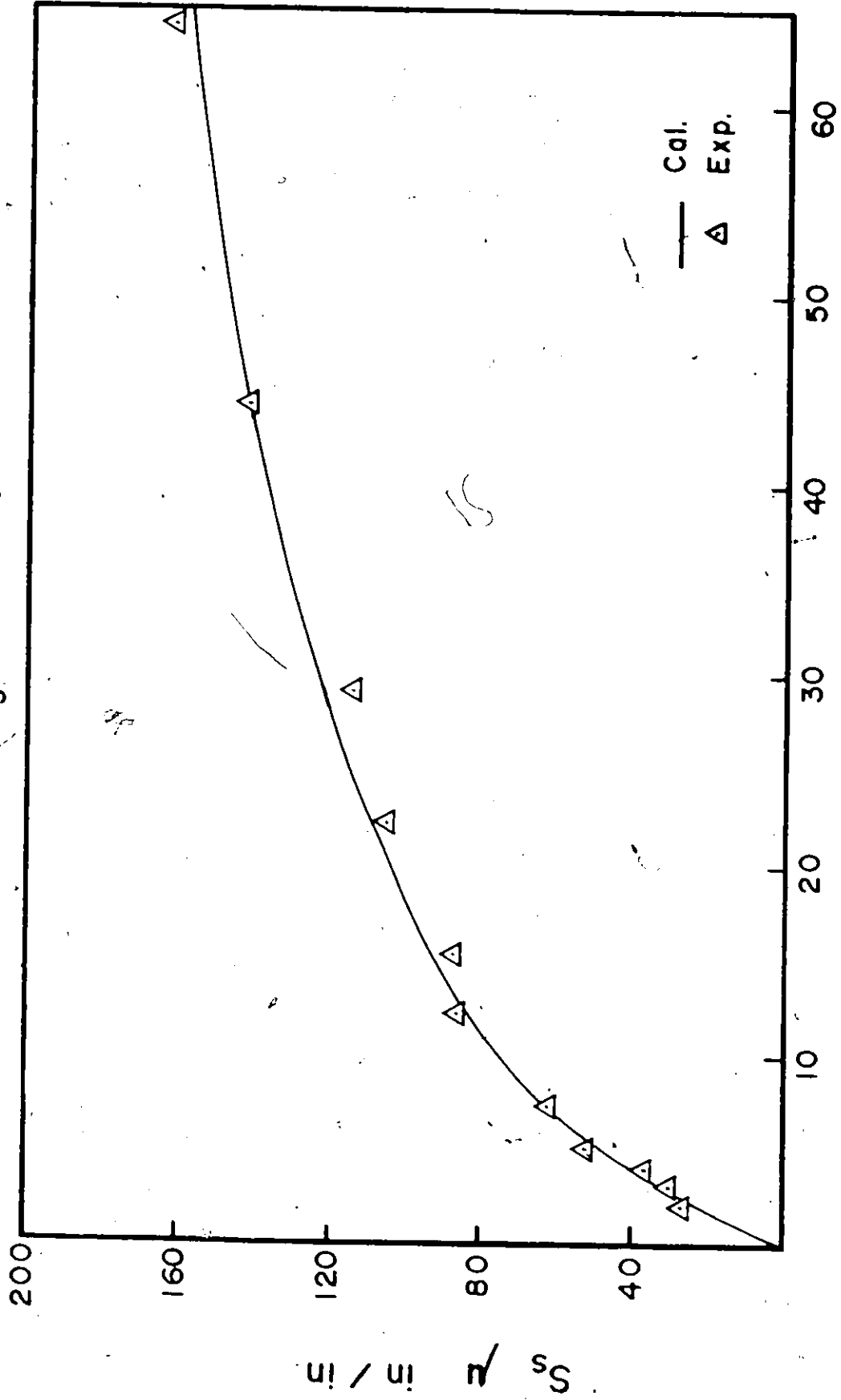
Figure 77

SERIES I-C-7%, 2b = 4 in,  $P_s = 1.25\%$ , Sym.



Time in Days  
Figure 78

SERIES I-C-7%, 2b = 6 in,  $P_s = 1.25\%$ , Sym.



Time in Days  
Figure 79



SERIES I-C-7%, 2b = 8 in, P<sub>s</sub> = 1.25%, Sym.

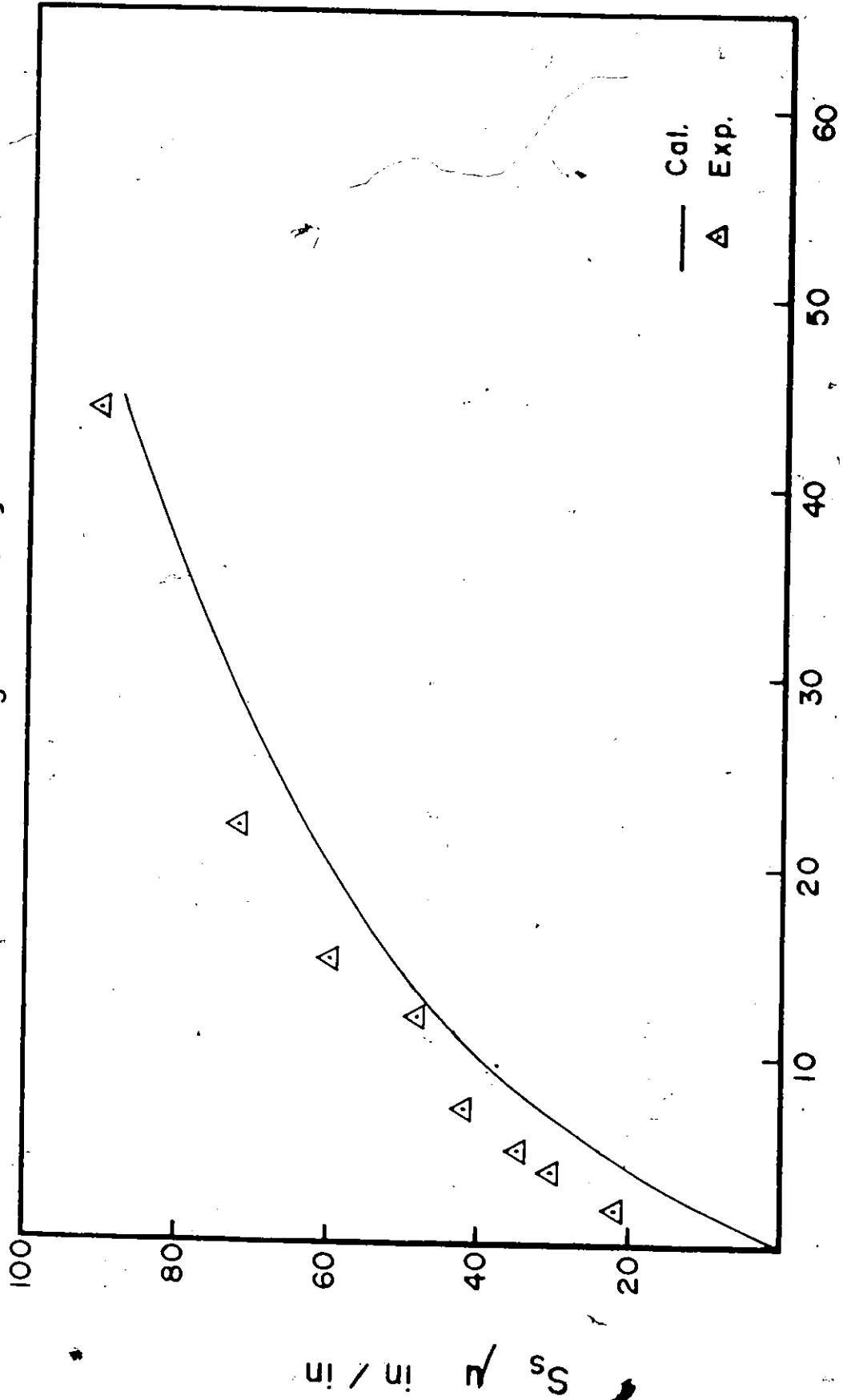
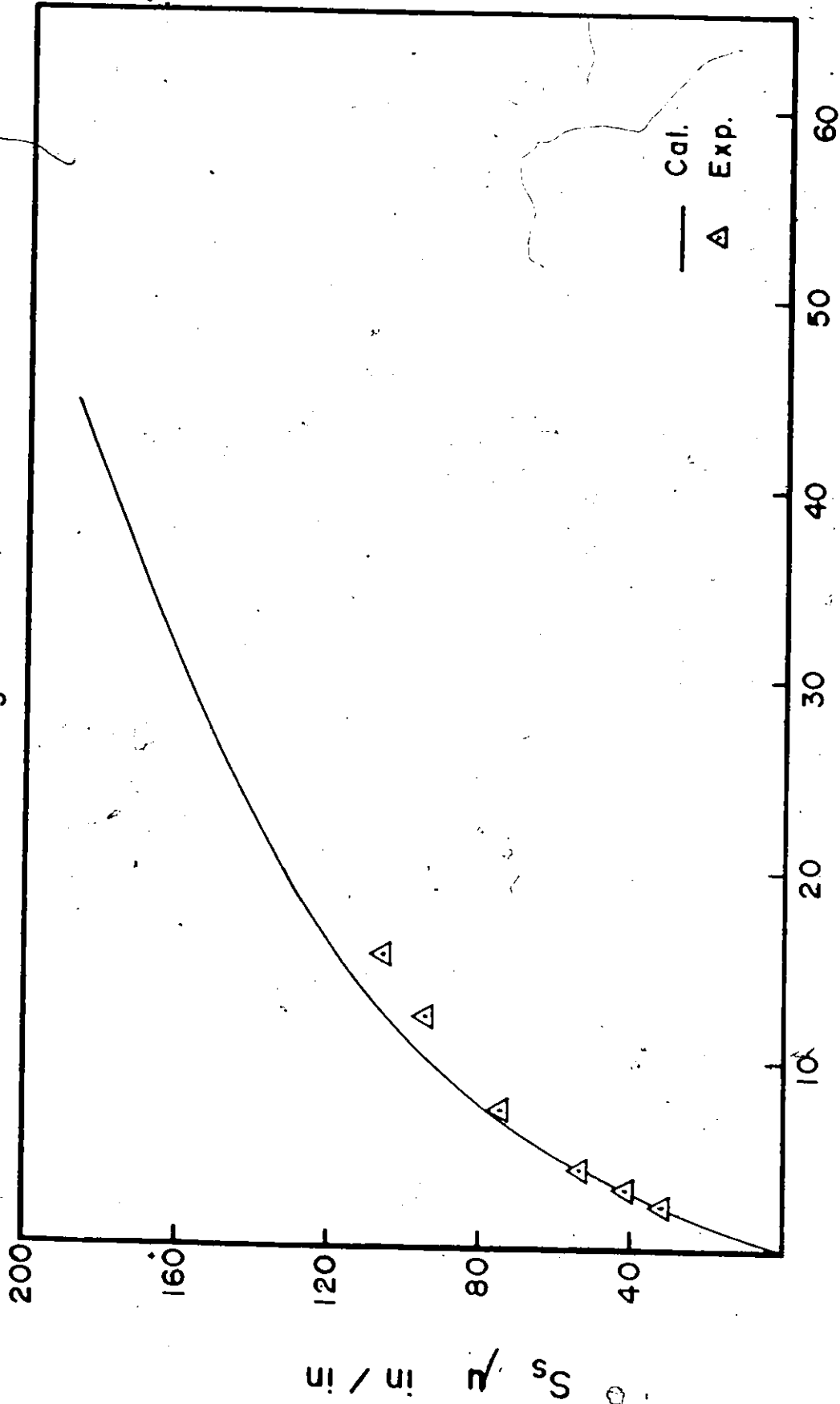


Figure 80

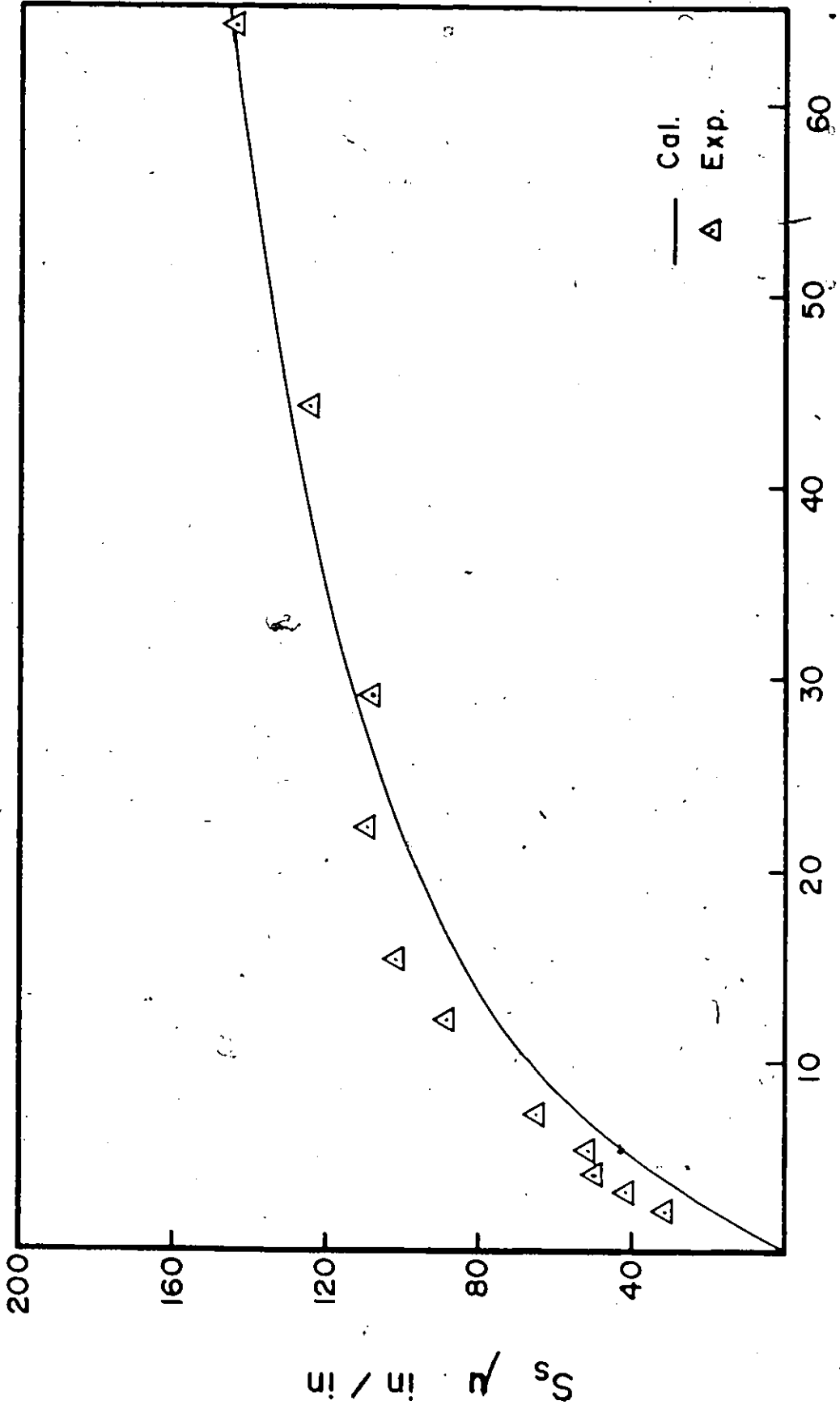
SERIES 1-C-7%, 2b = 4 in, P<sub>s</sub> = 1.25%, Ecc. = b/2



Time in Days

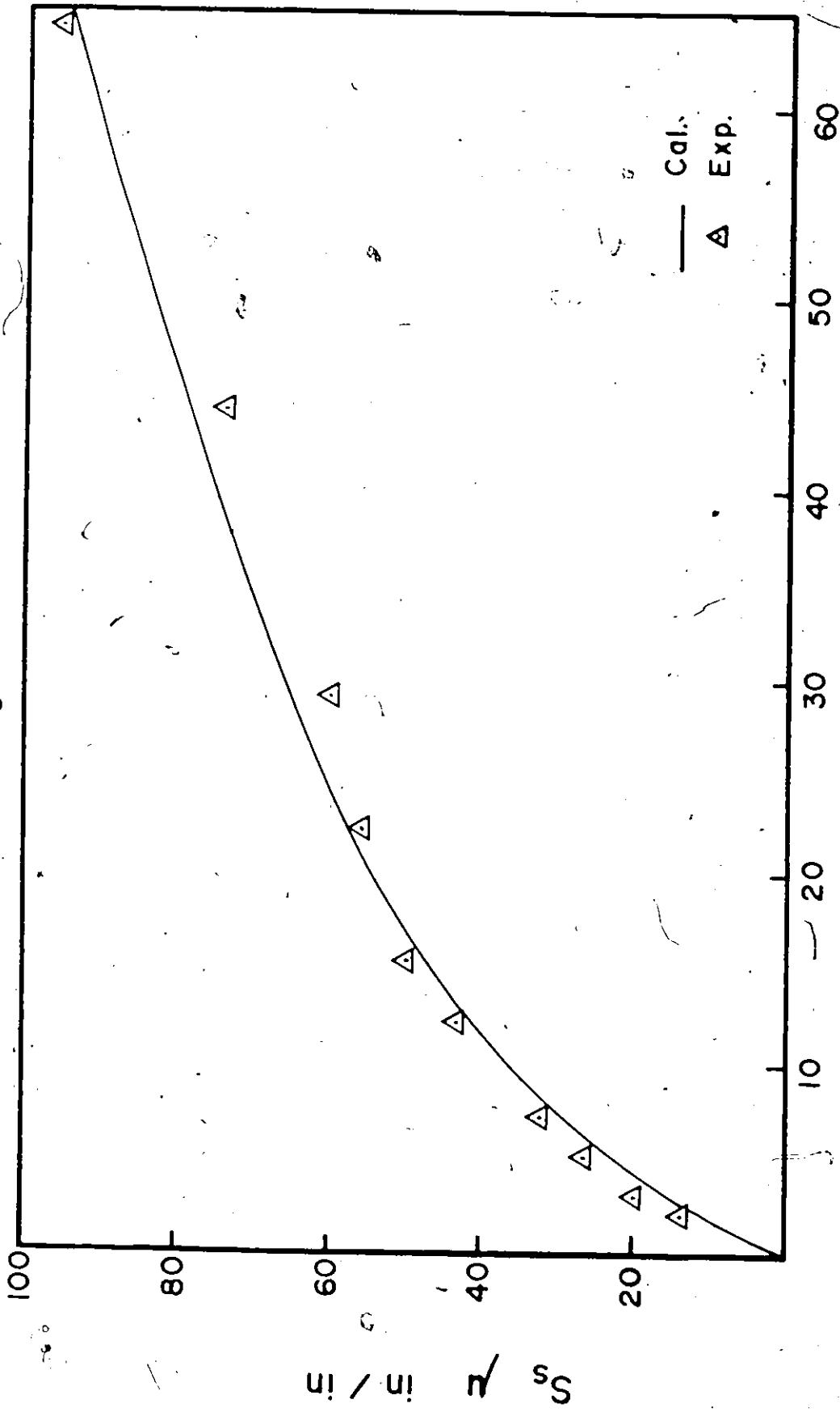
Figure 81

SERIES I-C-7%, 2b = 6in,  $P_s = 1.25\%$ , Ecc. =  $b/2$



Time in Days  
Figure 82

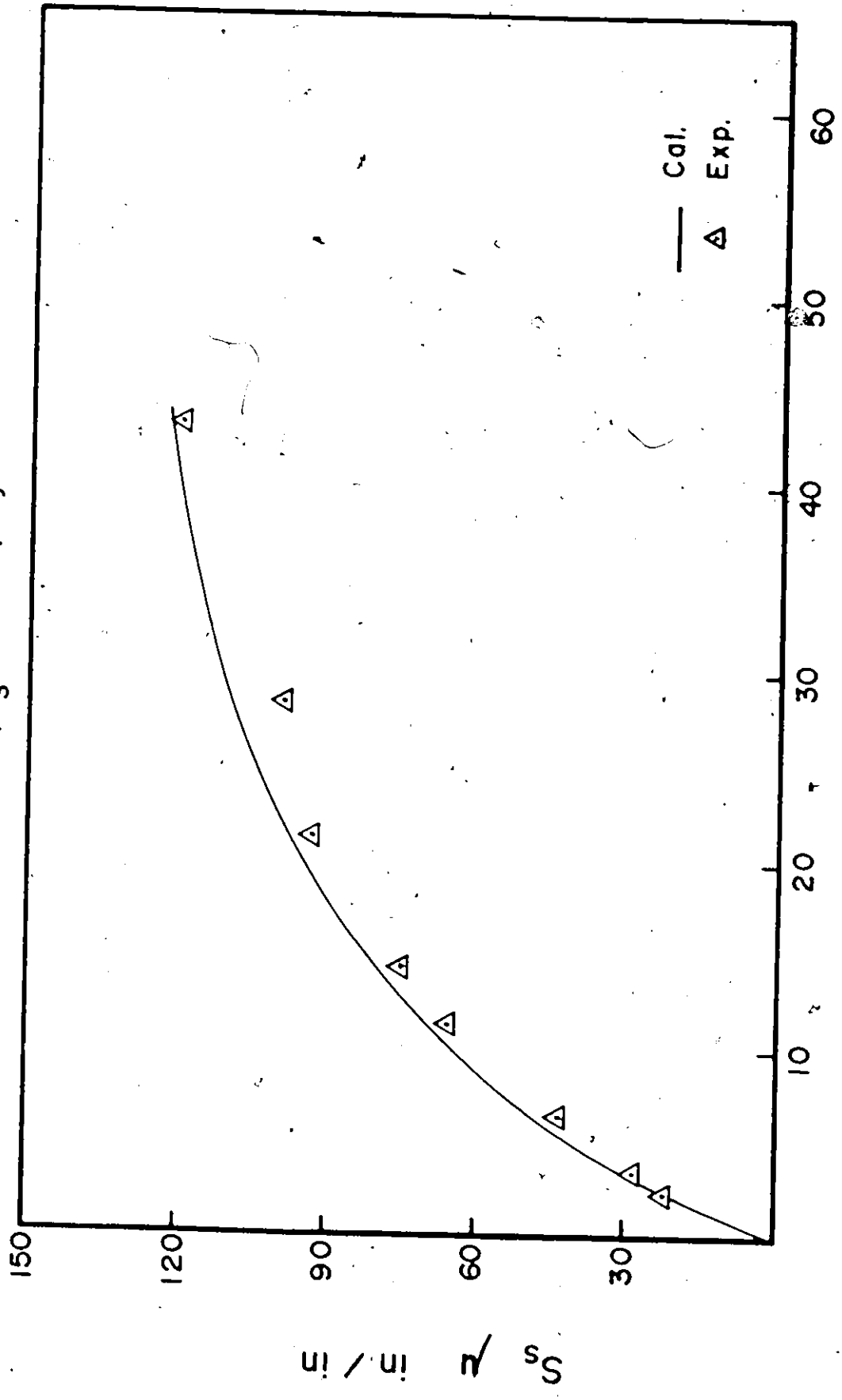
SERIES 1-C-7%, 2b = 8 in, P<sub>s</sub> = 1.25%, Ecc. = b/2



Time in Days

Figure 83

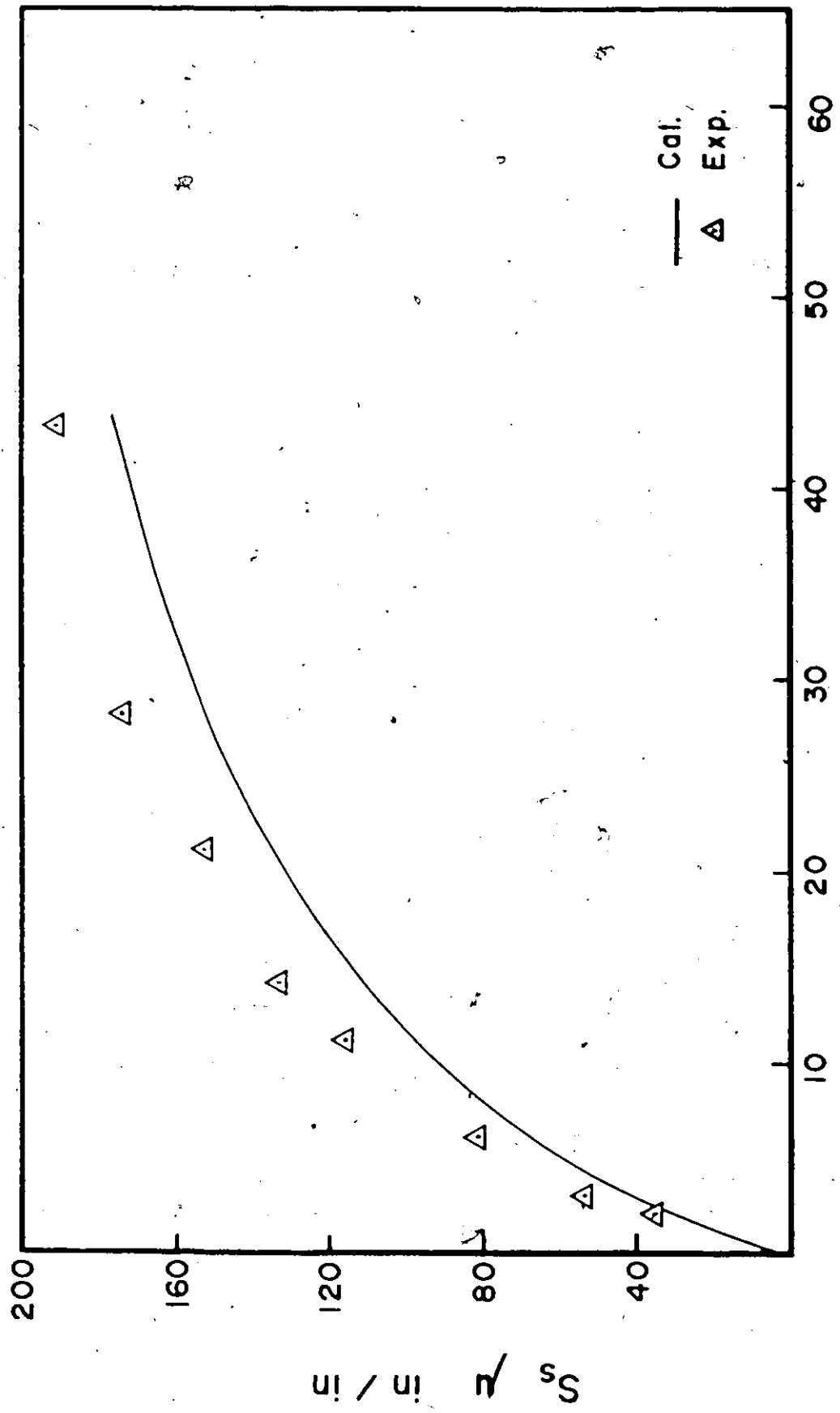
SERIES I-C-7%, 2b = 6in, P<sub>s</sub> = 1.86%, Sym.



Time in Days

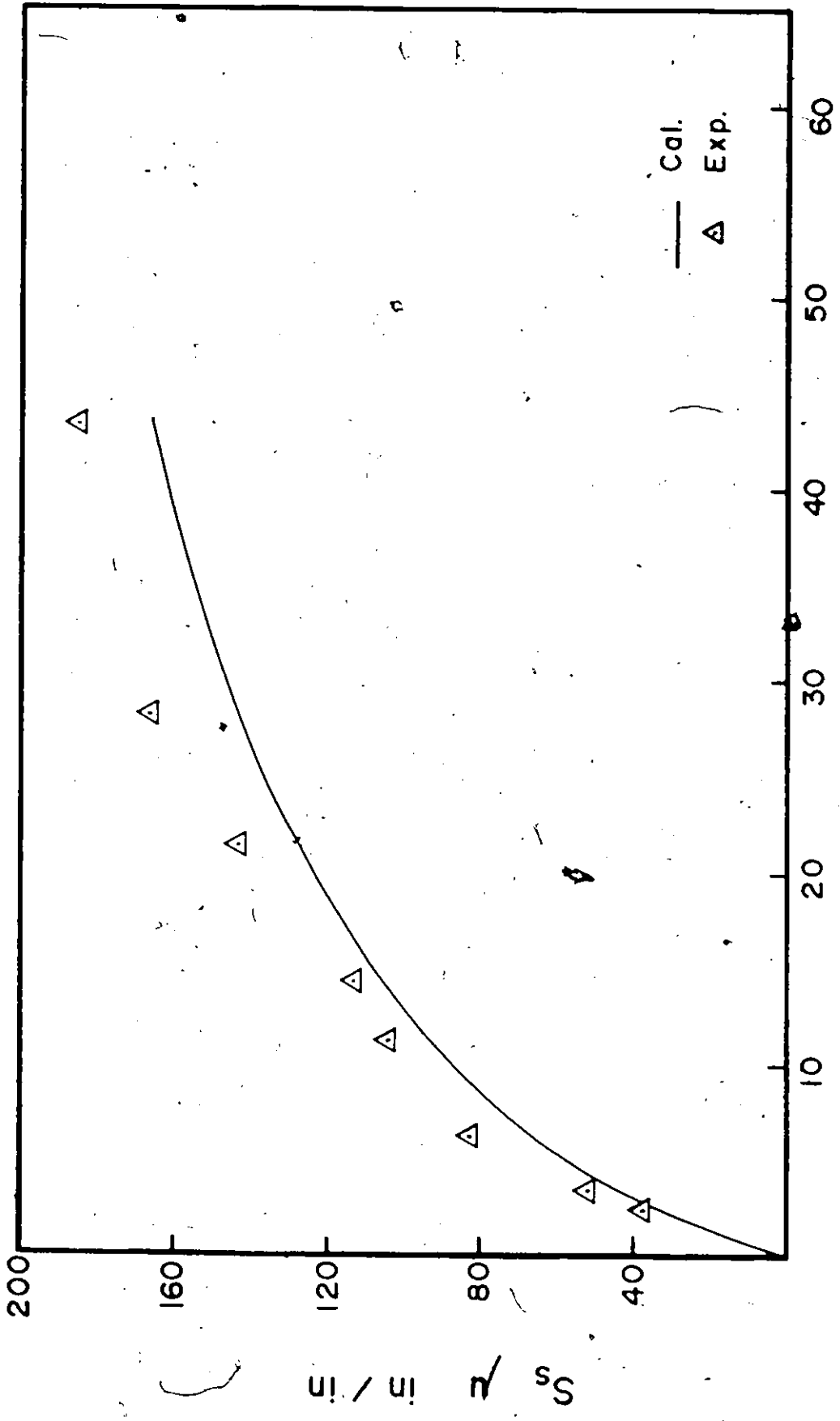
Figure 84

SERIES 1-C-7%, 2b = 4in, P<sub>s</sub> = 2.2%, Sym.



Time in Days  
Figure 85

SERIES 1-C-7%, 2b = 4in, P<sub>s</sub> = 2.75%, Sym.



Time in Days

Figure 86

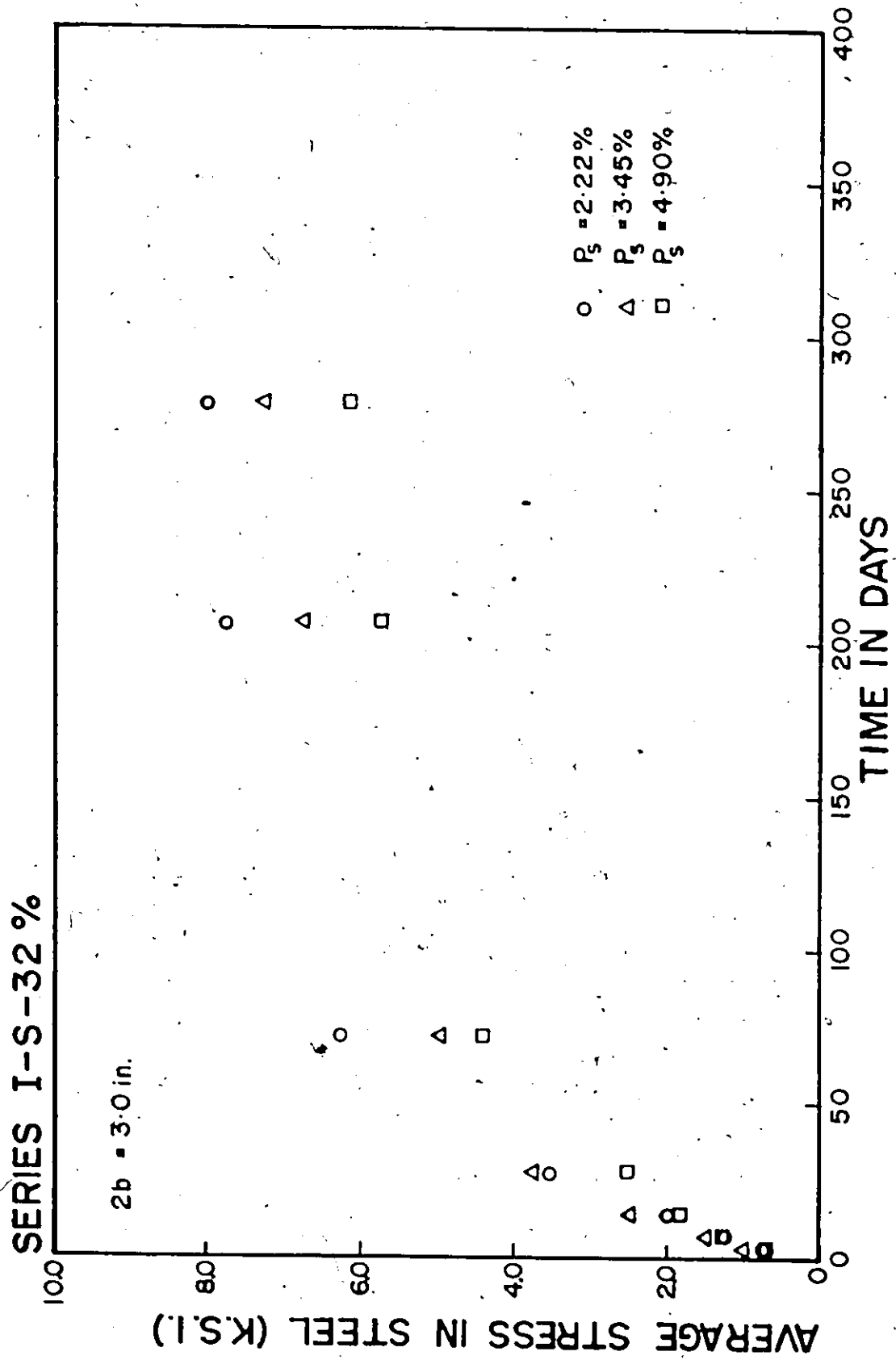


Figure 87



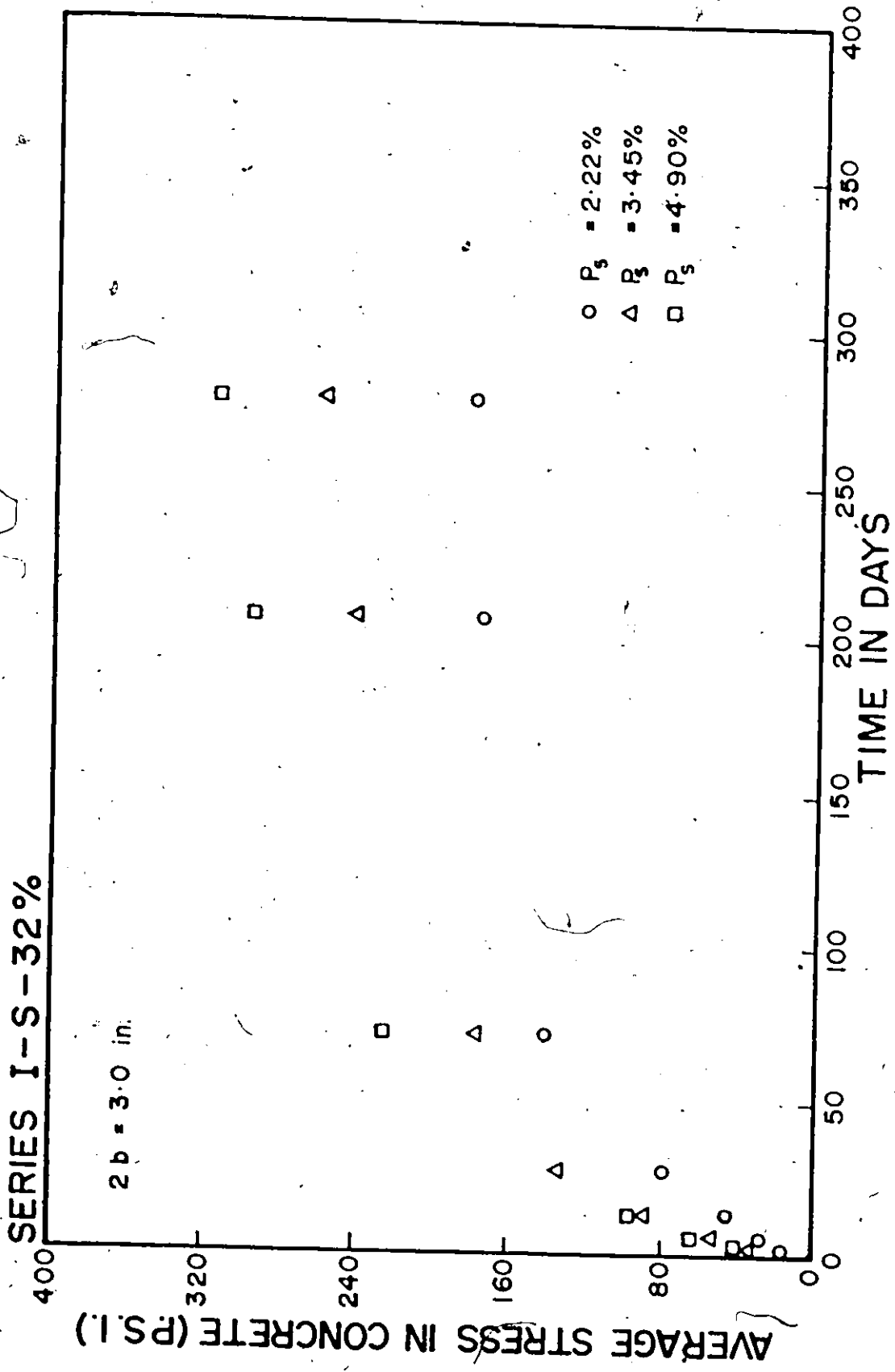


Figure 88

SERIES I-C, TEMP. = 220°F, 2b = 4"

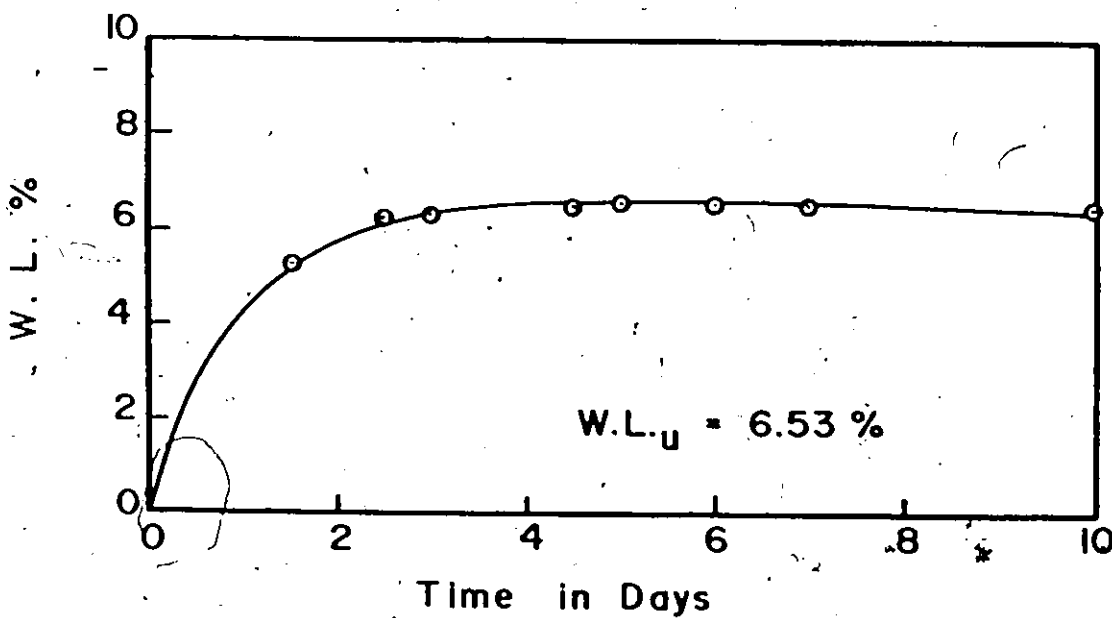
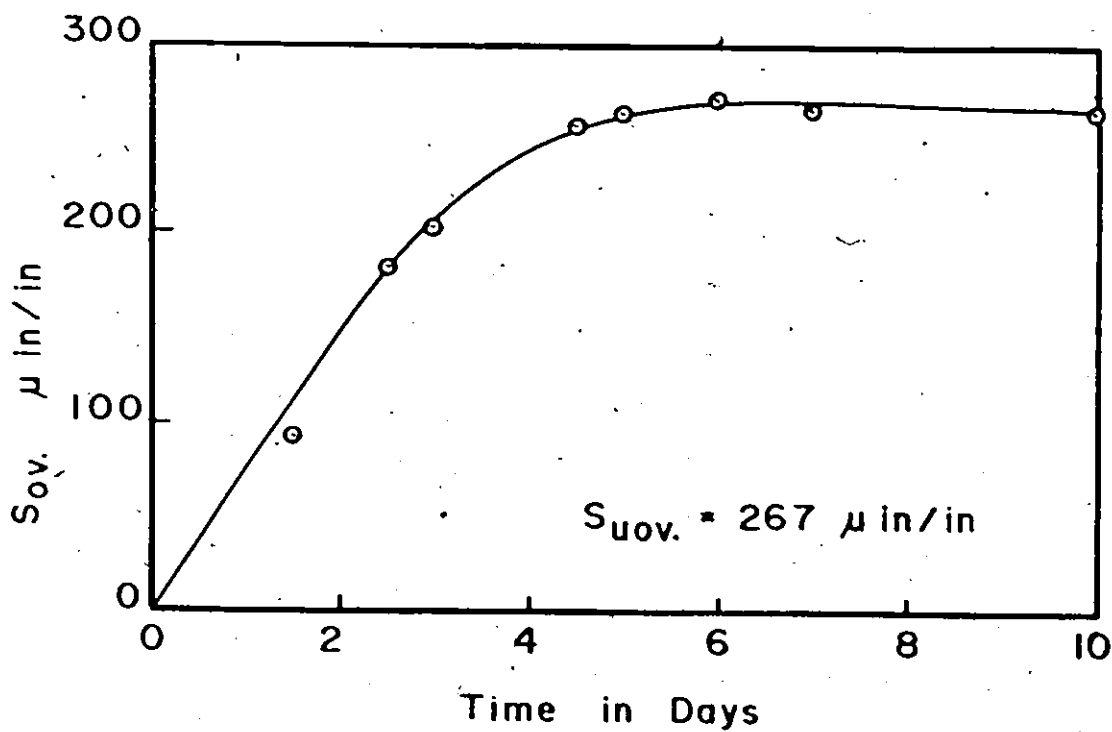


Figure 89

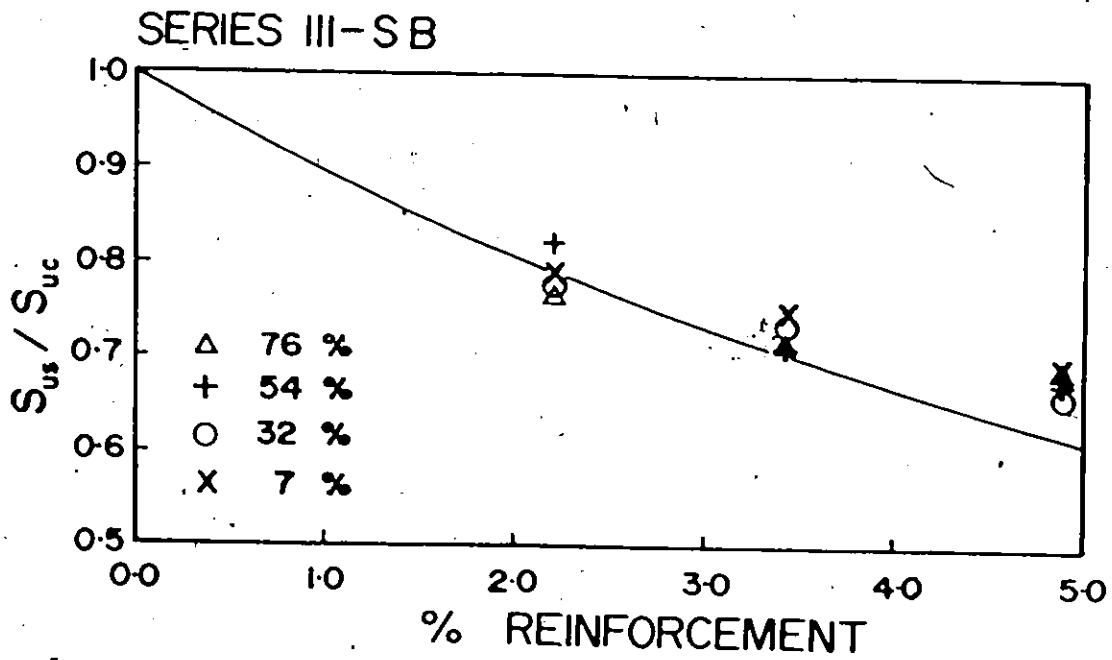
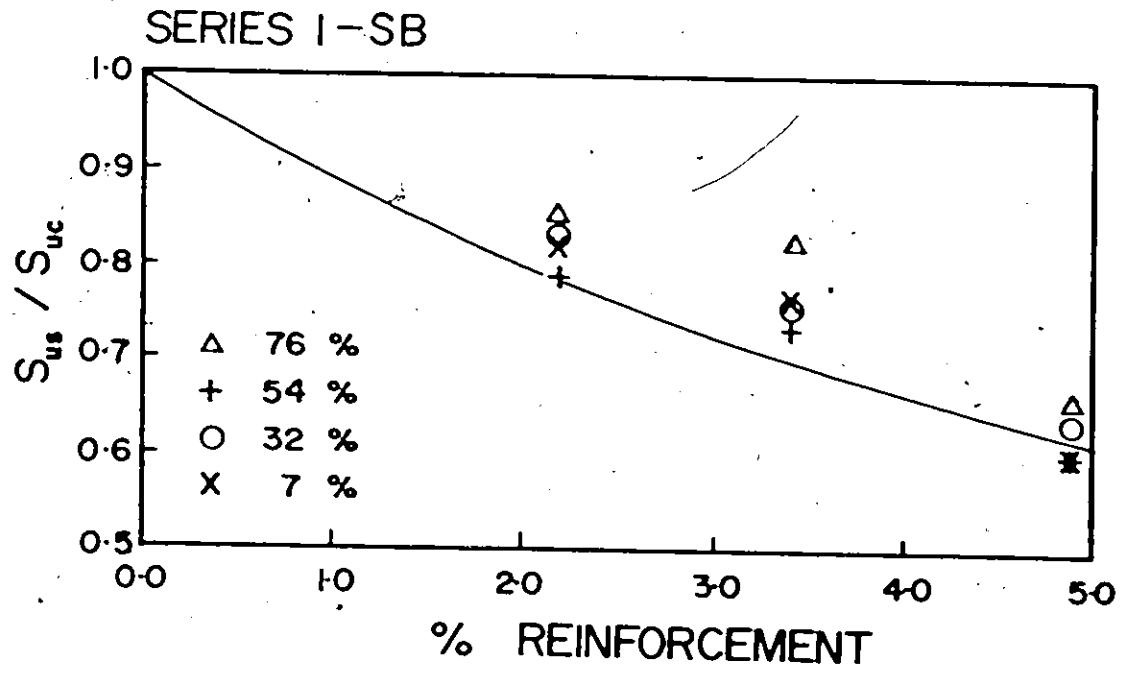


Figure 90

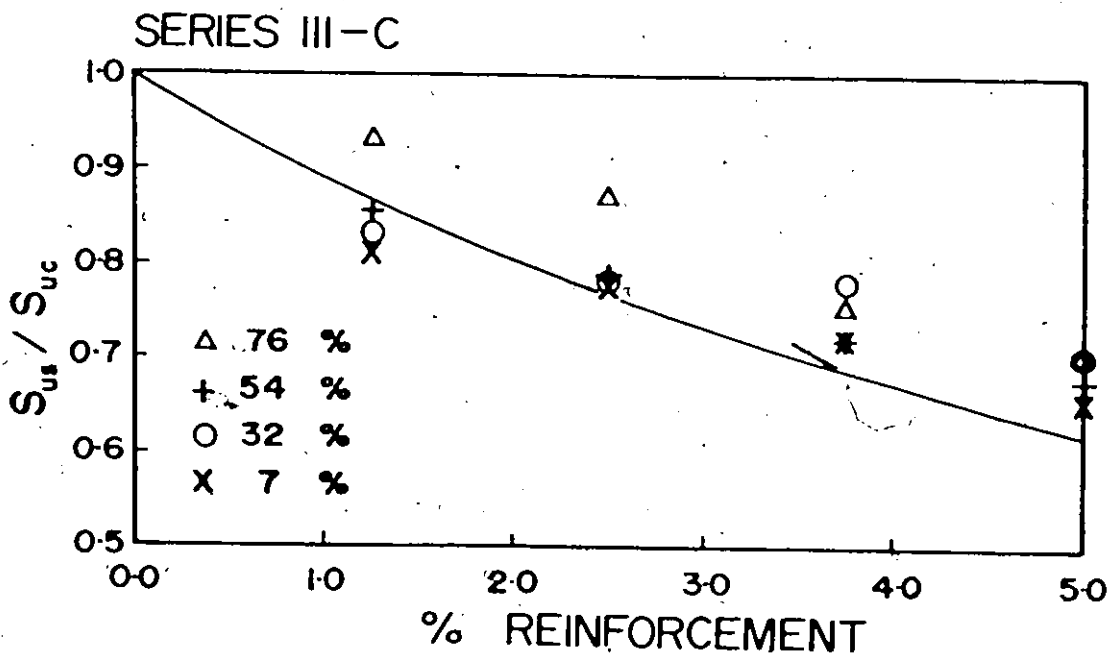
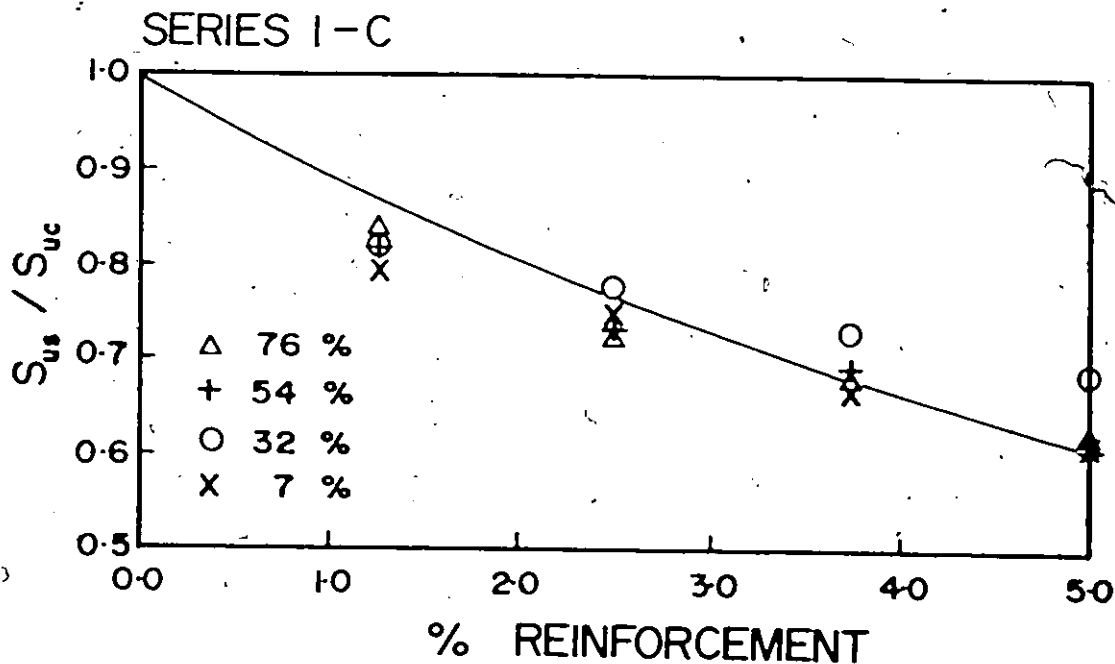


Figure 91

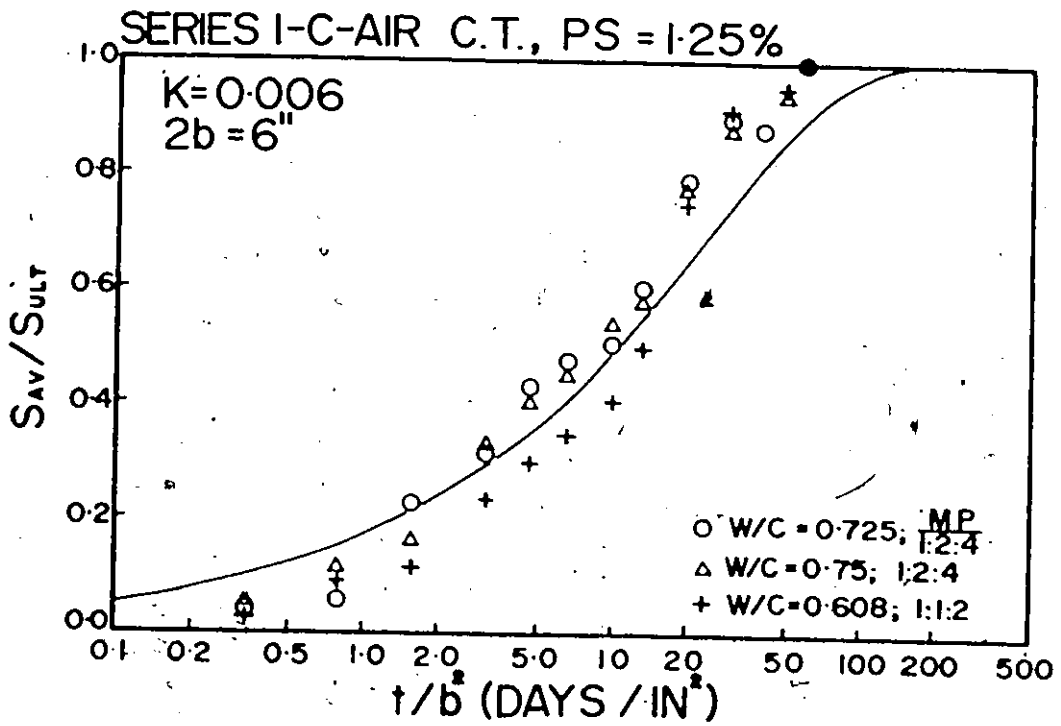
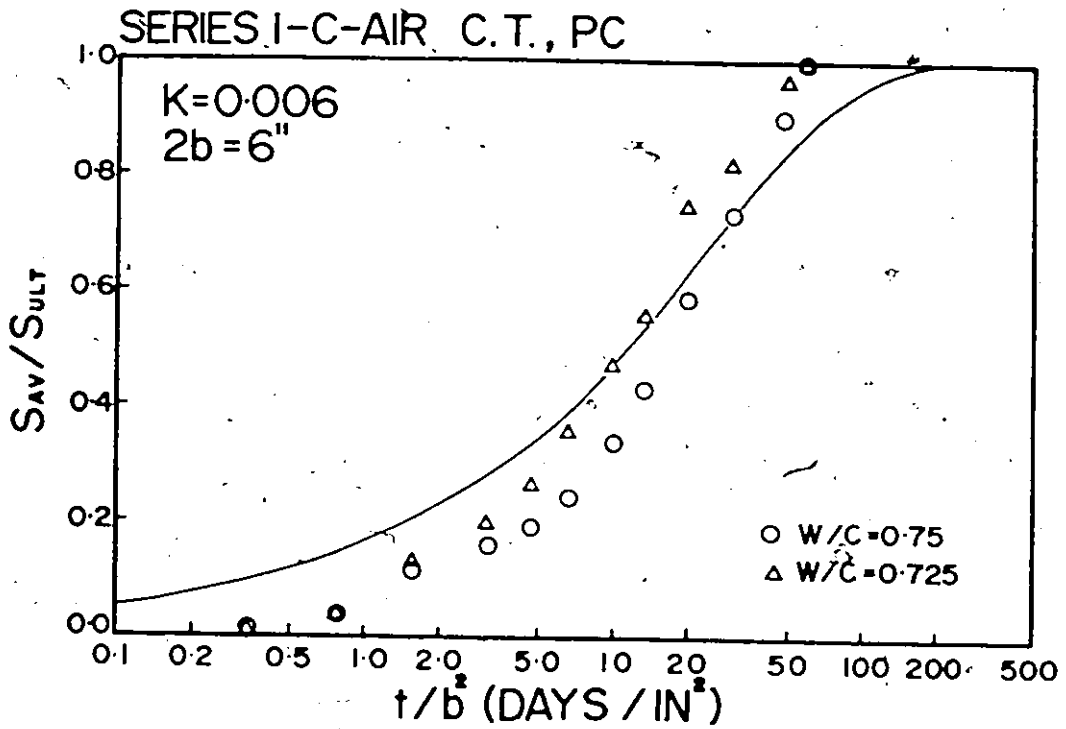


Figure 92 (Glanville)

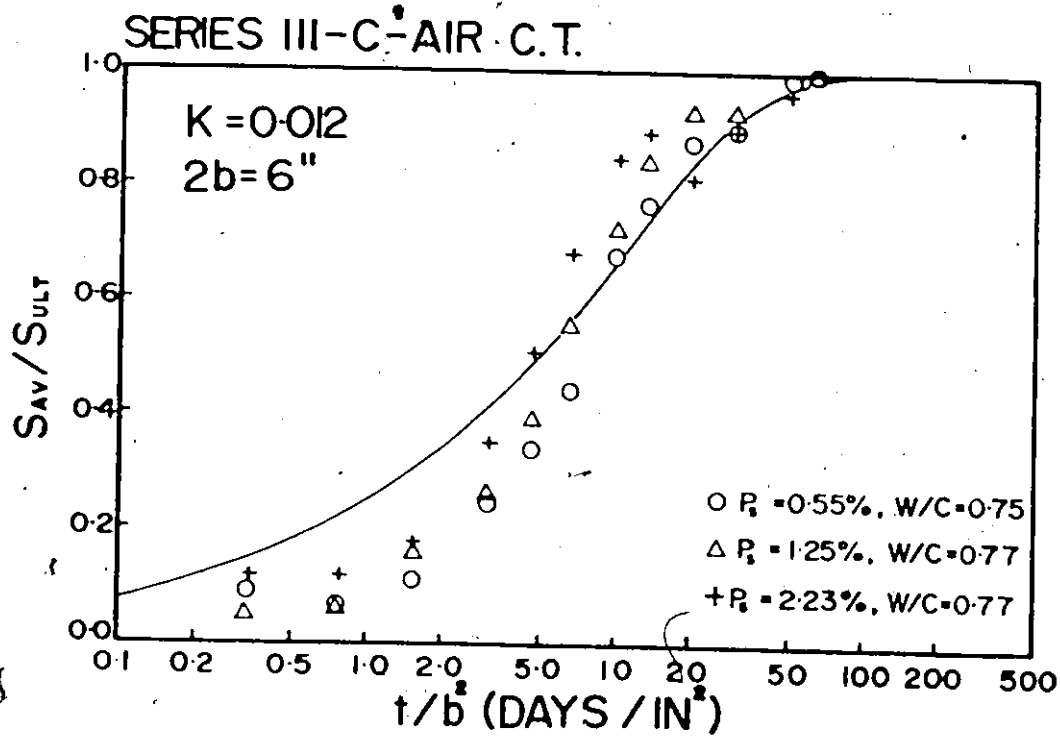
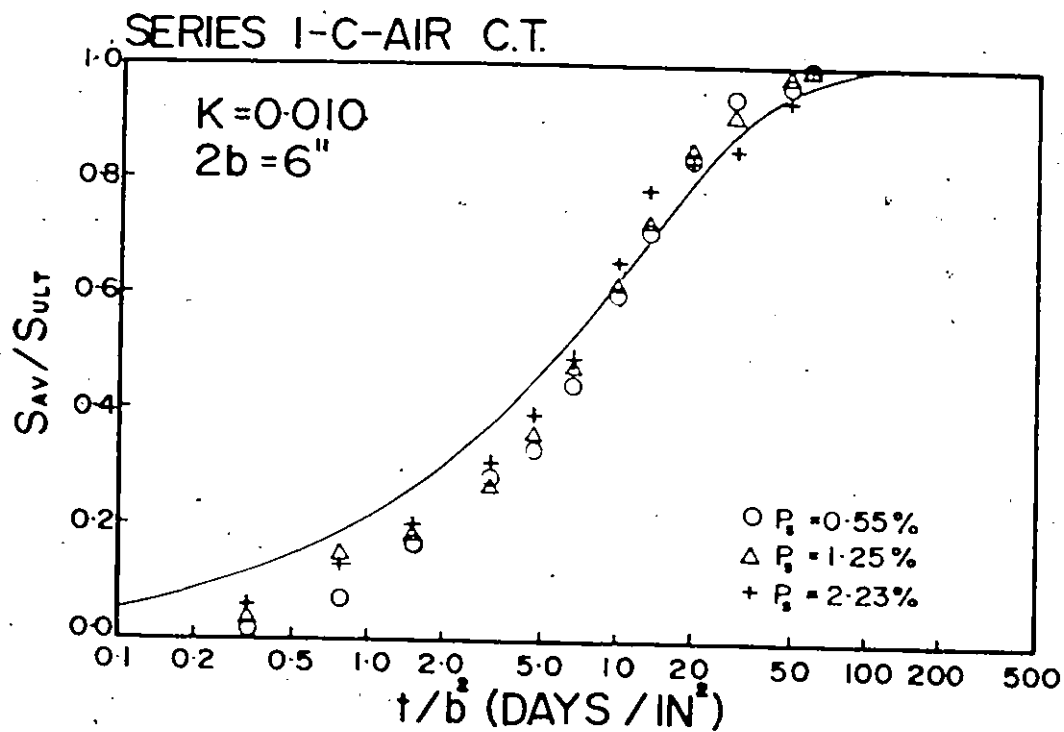


Figure 93 (Glanville)

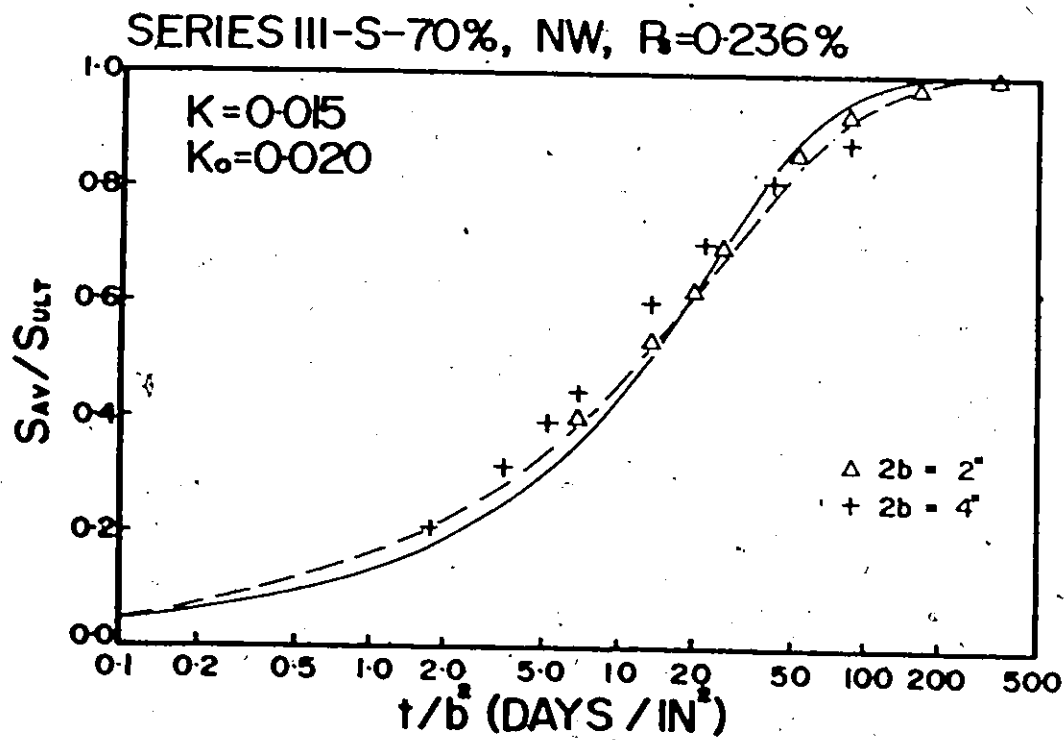
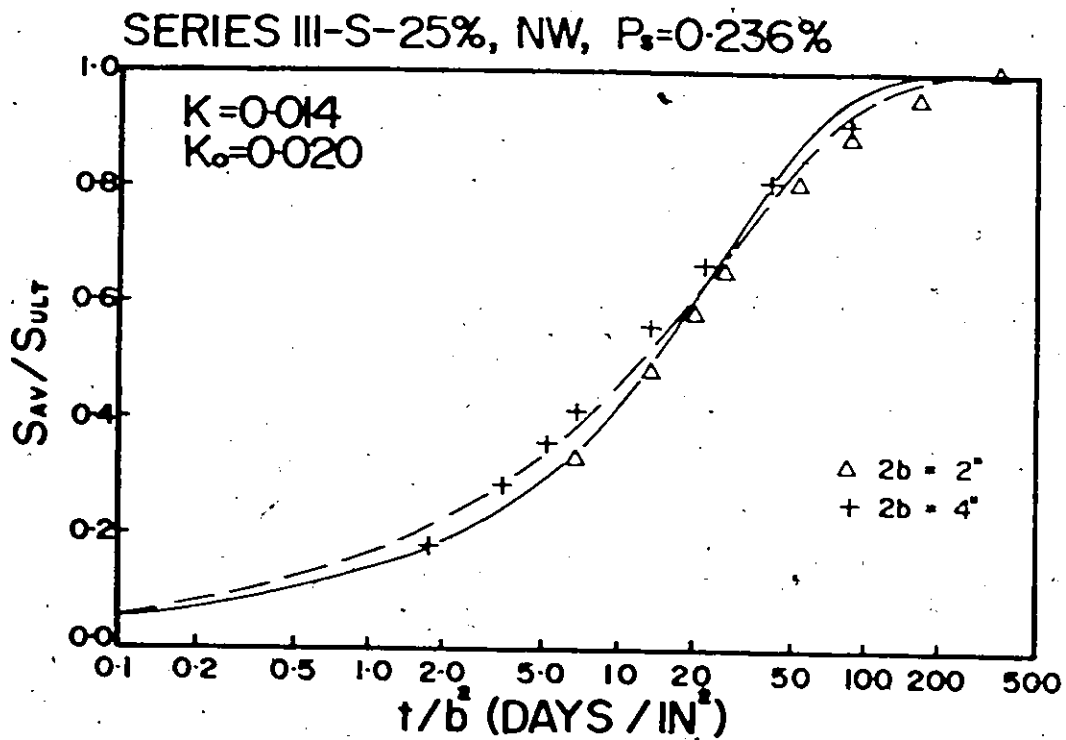


Figure 94 (Keeton)

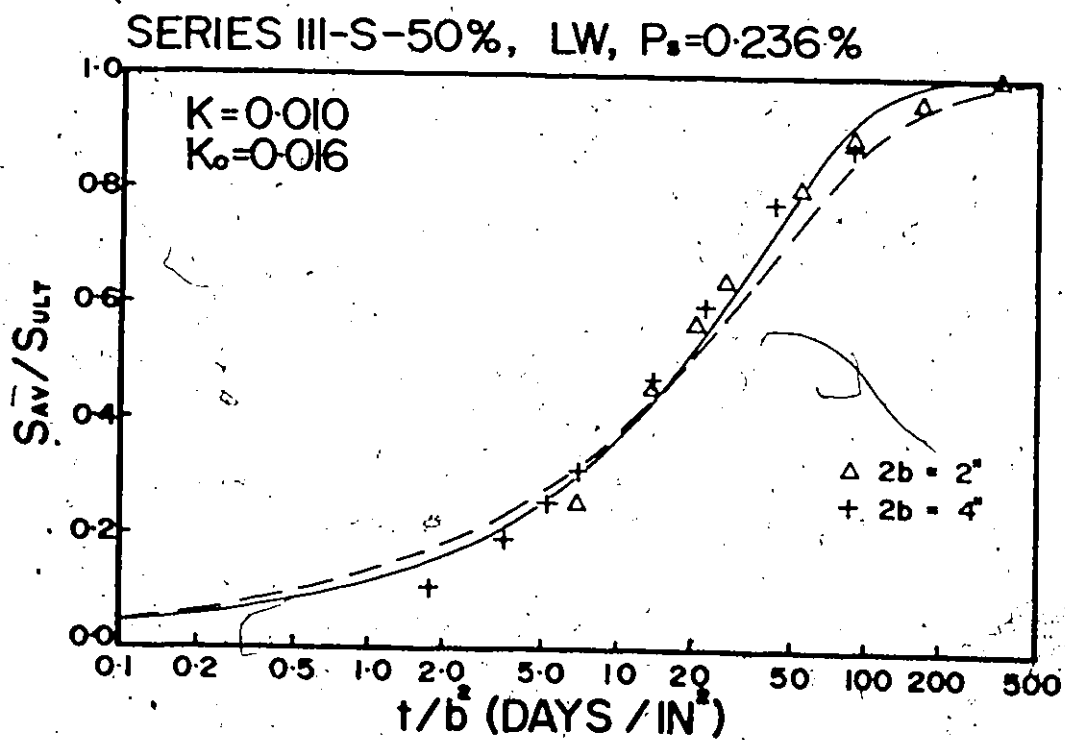
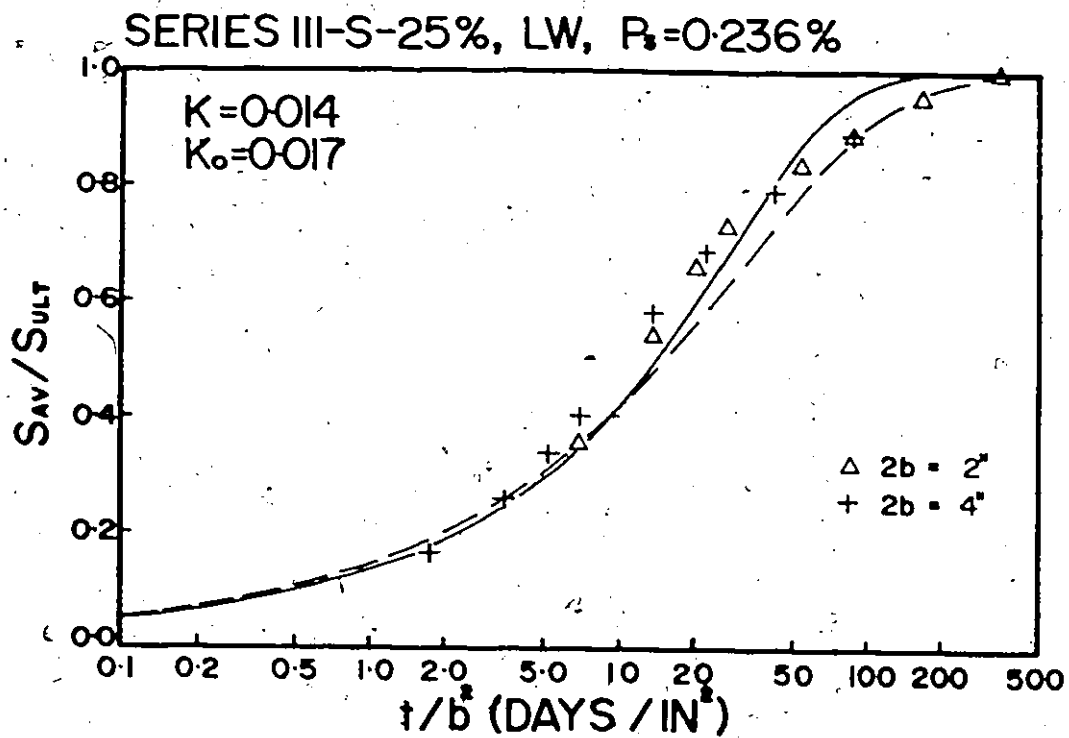


Figure 95 (Keeton)



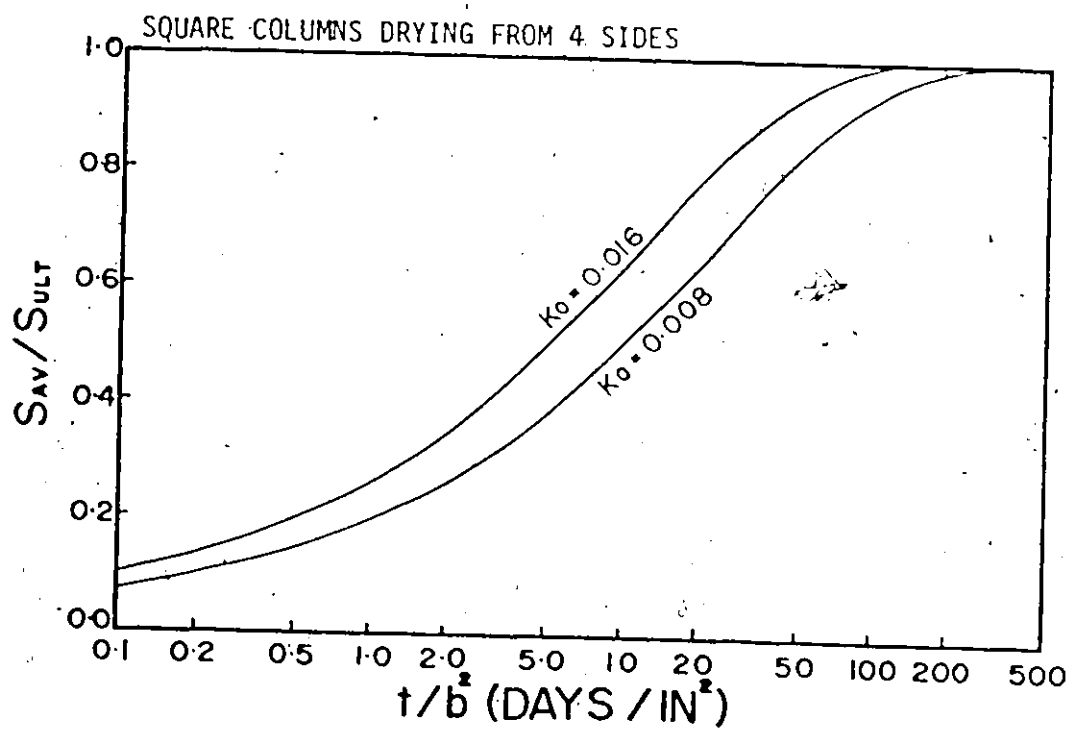
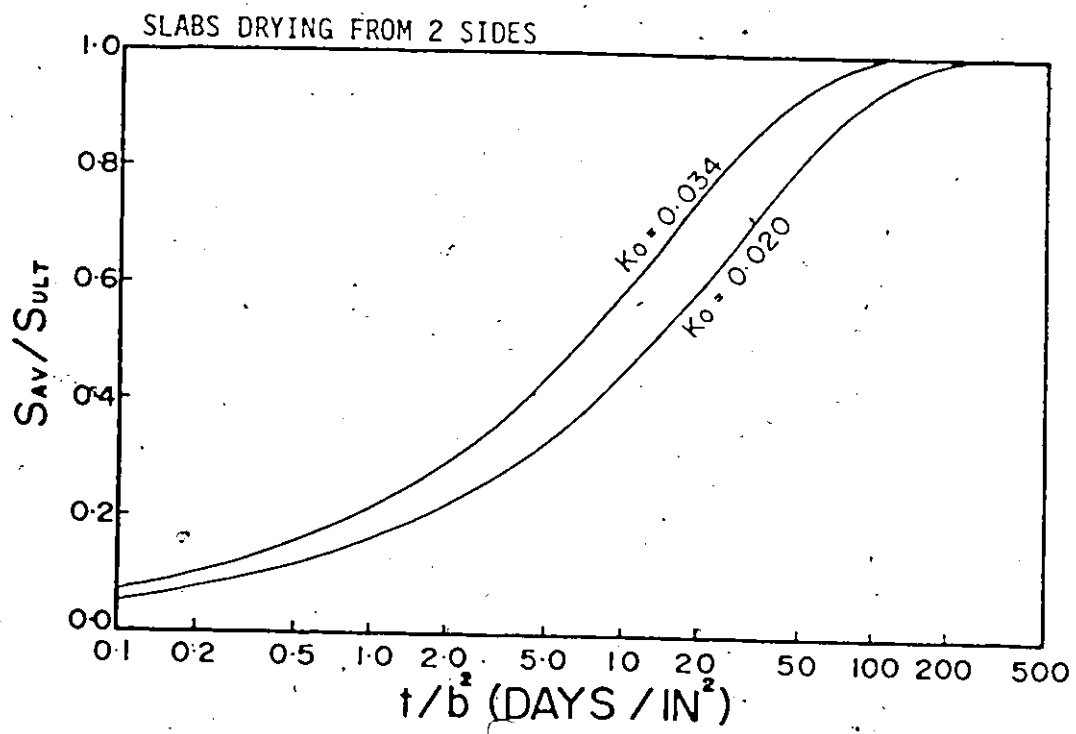


Figure 96

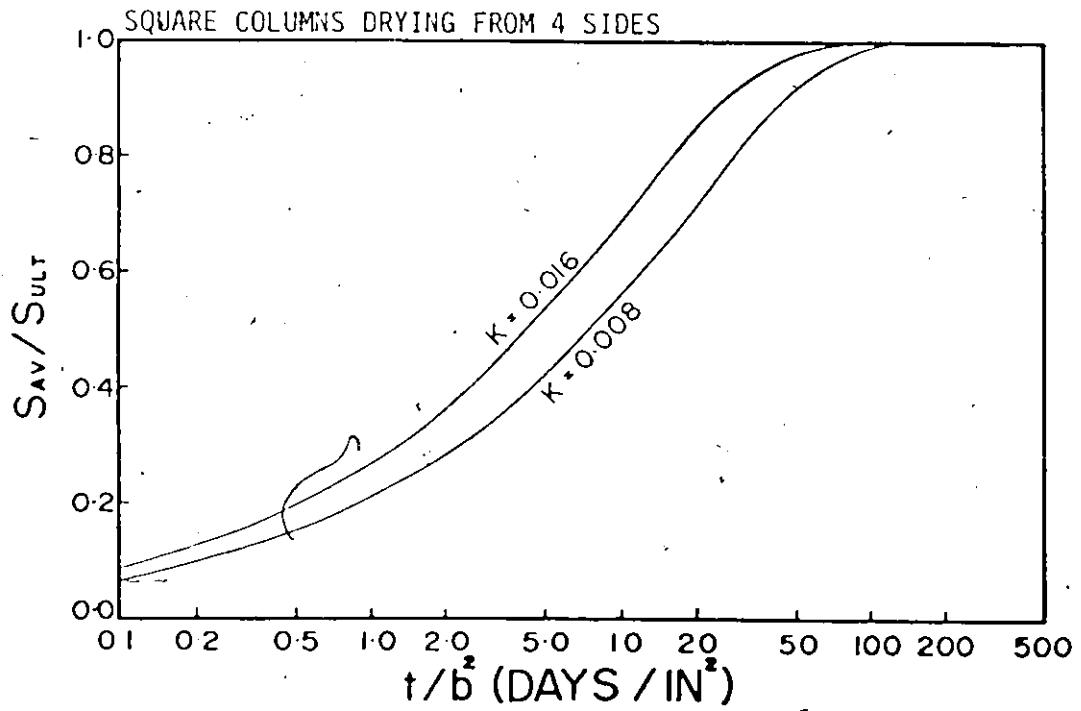
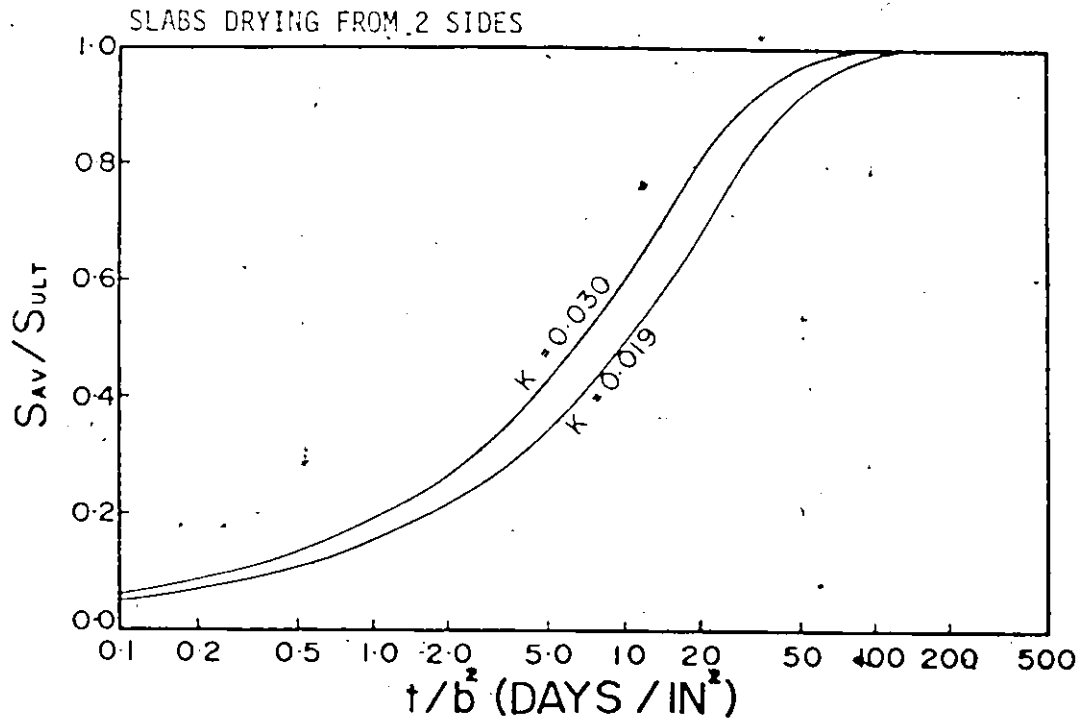


Figure 97

APPENDIX C  
EXPERIMENTAL MATERIALS

## APPENDIX C

## TABLE I

TYPICAL  
CHEMICAL AND PHYSICAL TEST RESULTS FOR  
LAKE ONTARIO NORMAL PORTLAND CEMENT

<u>Chemical Analysis:</u>	C <sub>3</sub> S	54%
	C <sub>2</sub> S	22%
	C <sub>3</sub> A	10.2%
	C <sub>4</sub> AF	6%

Physical Tests:

Blaine Fineness---fineness, cm<sup>2</sup>/g. 3816

Soundness:

Autoclave Expansion, per cent 0.12%

Time of Set, Gillmore Needle:

Initial, hr.: min. 2:25

Final, hr.: min. 4:00

Compressive Strength, psi.:

1 day	1491
7 day	2257
14 day	3794
28 day	4375

Normal consistency 24.0%

\*prepared by the Research Division of the Ontario Hydro.

## APPENDIX C

## TABLE I

PHYSICAL TEST RESULTS FOR CANADA  
HIGH EARLY PORTLAND CEMENTPhysical Tests

## Blaine Fineness

Fineness, sq cm/g	4025
-------------------	------

## Time of Set, Gillmore Needle

Initial, hr., :min.	1:35
Final, hr., :min.	3:15

## Compressive Strength, psi

1 day	3022
7 day	4631
14 day	4963
28 day	6725

APPENDIX C  
TABLE II  
COMPOSITION OF PARIS SAND

Sieve Sizes Percent Retained	Amount of Particles in Percent by Count in Various Sieve Sizes							Pass No. 100 1.9	Total No. 8 to - No. 100 Phys. Chem	Quality
	No. 4 12.5	No. 8 12.5	No. 14 15.4	No. 28 26.1	No. 48 30.6	No. 100 10.5	No. 100 25.4			
Dolomite	36.5	54.7	55.0	28.0	18.3	16.3	25.4	31.1		
Dolomite, pitted	3.6	3.7						.5		
Dolomite, calcitic	25.0	7.1	5.7	10.0	4.9			5.8		
Limestone	3.6	.3	1.7	2.7	2.7	12.7		3.2		
Limestone, dolomitic	3.6	2.0	7.0	12.7	6.7			6.7		
Marl, apthenitic	12.4	5.4	4.3	5.7	6.3	.3		4.8		
" , brittle		.7	1.0	.3	1.0			.7		Fair Delet.
" , friable	.9	.3	.7	1.0				.6		Poor Delet.
Shaly, calcareous		13.0	6.7	5.0	5.7	1.5		5.9		
Sandstone, brownish										
Shaly sandstone										
distinctly limonitic	2.7	1.7	2.3	1.0	1.0	1.2		1.3		Delet.
Ironstone	2.7	1.0	1.0	2.3	1.0	.3		1.3		Delet.
Sandstone		1.3	1.7	.3	.7	.3		1.7		
" , brittle		.3						X		Fair
Recent Sandstone		.7	1.0	.7	.7			.6		
Chert T. S. 1247	.9	1.0	.3	1.0	.3	.3		.5		
Aplite T. S. 1247		2.0	2.7	5.0	6.0	4.1		4.2		"
Granite	4.5	2.0	2.3	4.0	2.0	3.3		2.6		
" , brittle		.3	.3					.1		Fair
Gneiss		.7	1.3	.3				.4		
Diabase	.9	.7		.3	.3			.3		
Hornfels T. S. 1247		.3	1.3	1.3				.6		

## APPENDIX C

## TABLE II

QUALITY OF PANTS SAND.

<u>Fractions</u>	<u>No. 8 to No. 100 Per cent</u>	<u>No. 4 Per Cent</u>
<u>Physical Quality</u>		
Good particles	97.7	99.1
Fair particles	.8	
Poor particles	<u>1.5</u>	<u>1.9</u>
	100.0	100.0
<u>Chemical Quality</u>		
Innocuous particles	95.1	93.7
Deleterious (?) particles	2.0	2.7
Deleterious particles	1.9	3.6
	<u>100.0</u>	<u>100.0</u>
Harmful particles	4.8	6.3
Poor particles: Soft marl and micaceous minerals (mica, chlorite)		
Deleterious particles: Soft marl and ironstones		
Particles suspected of being deleterious: Brittle marl and limonitic calcareous sandstone, rich in limonite.		

APPENDIX C  
TABLE III  
PARTICLE SHAPE AND SURFACE OF PARIS SAND ( In Percent )

Shape of Particles	Retained on Sieve Sizes						Pass No. 100	T O T A L No. 8 59 No. 100
	No. 4	No. 8	No. 14	No. 28	No. 48	No. 100		
Angular, subangular								87
Cubic particles	67	83	89	88	78	90		
Flat particles	8	x	2	2	6	5		3
Oblong particles		x	x		1	x		x
Rounded, subrounded								
Cubic particles	25	9	9	10	15	5		10
	100	100	100	100	100	100		100

x = Amounts less than one percent

The surface of the particles was mainly crystalline, on limestones and on feldspar it was smooth, on the few sandstones, clastic.

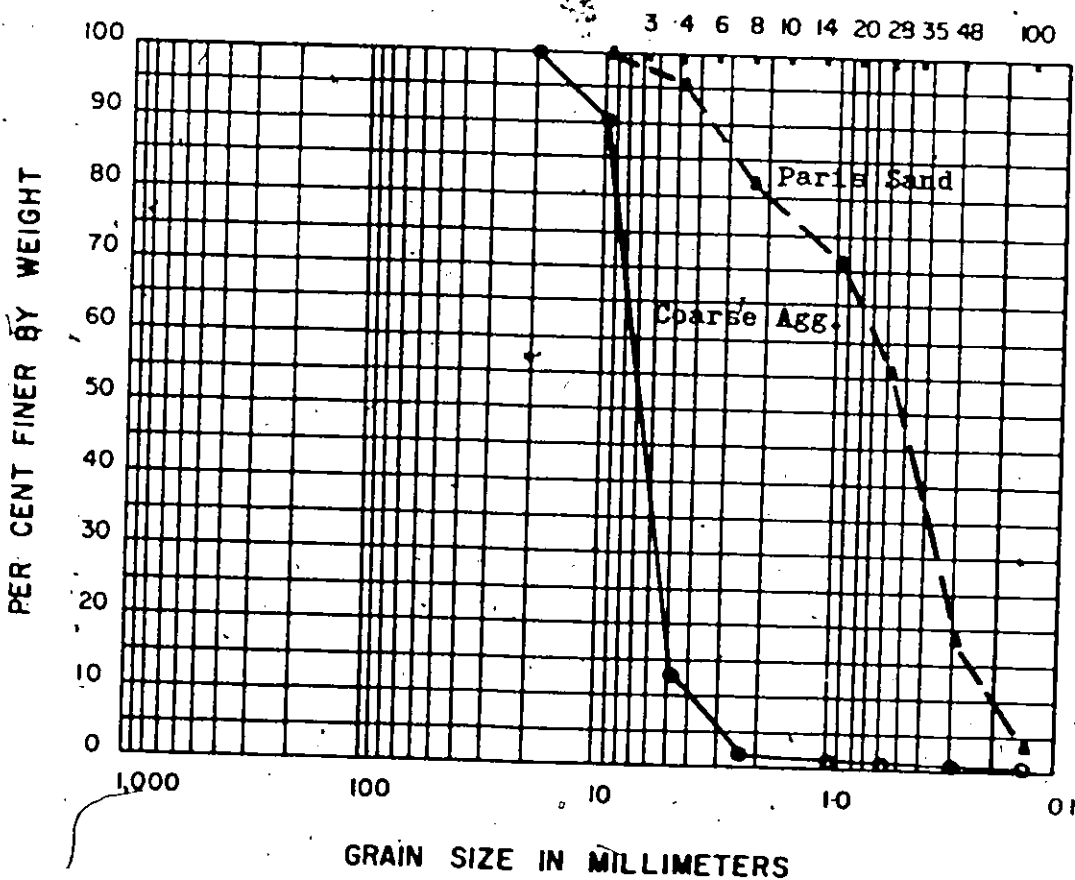


APPENDIX C

FIGURE I

SIEVE ANALYSIS OF AGGREGATE

TYLER STANDARD SIEVE NOS.



APPENDIX C

TABLE III

Mix Design Data

WATER (lbs)	CEMENT (lbs)	W/C Ratio	Sand (lbs)	Coarse Agg. (lbs)	Nominal Strength (PSI)	Slump (in.)
12.0	25.8	0.48	51.4	60.4	5000	2 to 4

Average Compressive Strength (after 28 days) = 5750 psi (Type I Cement)

= 6120 psi (Type III Cement)

APPENDIX D

MOISTURE LOSS AND SHRINKAGE DATA

Series I-S-7D-VAC., P.C.

Specimen	3 X 3"			3 X 6"			3 X 9"		
	t/b <sup>2</sup>	Sa/Su	I- $\bar{U}$	t/b <sup>2</sup>	Sa/Su	I- $\bar{U}$	t/b <sup>2</sup>	Sa/Su	I- $\bar{U}$
2	0.90	0.15	0.14	0.23	0.09	0.07	0.10	0.07	0.08
4	1.78	0.26	0.20	0.44	0.13	0.13	0.20	0.09	0.11
8	3.56	0.31	0.26	0.89	0.15	0.18	0.39	0.11	0.14
16	7.11	0.36	0.40	1.78	0.21	0.22	0.79	0.14	0.17
32	14.22	0.49	0.55	3.56	0.29	0.29	1.58	0.19	0.22
64	28.44	0.74	0.78	7.11	0.45	0.47	3.16	0.35	0.34
128	56.89	1.00	1.00	14.22	0.65	0.61	6.32	0.56	0.46

Series I-S-7D-VAC., P<sub>s</sub>=3.45%

Specimen	3 X 3"			3 X 6"			3 X 9"		
	t/b <sup>2</sup>	Sa/Su	I- $\bar{U}$	t/b <sup>2</sup>	Sa/Su	I- $\bar{U}$	t/b <sup>2</sup>	Sa/Su	I- $\bar{U}$
2	0.90	0.23	0.20	0.23	0.11	0.15	0.10	0.06	0.11
4	1.78	0.26	0.30	0.44	0.16	0.19	0.20	0.08	0.15
8	3.56	0.34	0.41	0.89	0.16	0.27	0.40	0.08	0.18
16	7.11	0.39	0.50	1.78	0.25	0.33	0.79	0.19	0.23
32	14.22	0.59	0.59	3.56	0.35	0.38	1.58	0.25	0.26
64	28.44	0.80	0.77	7.11	0.50	0.56	3.16	0.38	0.39
128	56.89	1.00	1.00	14.22	0.74	0.70	6.32	0.64	0.51

Series I-S-3D-VAC., P.C.

Specimen	3 X 3"			3 X 6"			3 X 9"		
	$t/b^2$	Sa/Su	$1-\bar{U}$	$t/b^2$	Sa/Su	$1-\bar{U}$	$t/b^2$	Sa/Su	$1-\bar{U}$
2	0.90	0.06	0.18	0.23	0.02	0.07	0.10	0.02	0.05
4	1.78	0.10	0.29	0.44	0.05	0.11	0.20	0.03	0.09
8	3.56	0.13	0.35	0.89	0.06	0.15	0.40	0.05	0.13
16	7.11	0.23	0.45	1.78	0.12	0.20	0.79	0.08	0.16
32	14.22	0.42	0.58	3.56	0.24	0.26	1.58	0.18	0.20
64	28.44	0.71	0.78	7.11	0.52	0.37	3.16	0.36	0.29
128	56.89	1.00	1.00	14.22	0.79	0.51	6.32	0.67	0.43

Series I-S-3D-VAC.,  $P_8=3.45\%$ 

Specimen	3 X 3"			3 X 6"			3 X 9"		
	$t/b^2$	Sa/Su	$1-\bar{U}$	$t/b^2$	Sa/Su	$1-\bar{U}$	$t/b^2$	Sa/Su	$1-\bar{U}$
2	0.90	0.07	0.14	0.23	0.02	0.06	0.10	0.02	0.06
4	1.78	0.13	0.25	0.44	0.08	0.10	0.20	0.04	0.11
8	3.56	0.15	0.37	0.89	0.08	0.17	0.40	0.04	0.16
16	7.11	0.22	0.45	1.78	0.12	0.24	0.79	0.09	0.20
32	14.22	0.44	0.60	3.56	0.26	0.30	1.58	0.17	0.24
64	28.44	0.65	0.78	7.11	0.47	0.45	3.16	0.33	0.35
128	56.89	1.00	1.00	14.22	0.75	0.61	6.32	0.62	0.43

Series I-S-1D-VAC., P.C.

Specimen	3 X 3"			3 X 6"			3 X 9"		
	Time(days)	$t/b^2$	Sa/Su	I- $\bar{U}$	$t/b^2$	Sa/Su	I- $\bar{U}$	$t/b^2$	Sa/Su
2	0.90	0.08	0.16	0.23	0.04	0.09	0.10	0.02	0.07
4	1.78	0.13	0.25	0.44	0.08	0.13	0.20	0.04	0.09
8	3.56	0.22	0.33	0.89	0.15	0.19	0.40	0.10	0.13
16	7.11	0.27	0.41	1.78	0.19	0.23	0.79	0.11	0.16
32	14.22	0.39	0.53	3.56	0.27	0.32	1.58	0.20	0.21
64	28.44	0.71	0.72	7.11	0.51	0.44	3.16	0.41	0.29
128	56.89	1.00	1.00	14.22	0.69	0.66	6.32	0.59	0.44

Series I-S-1D-VAC., P<sub>B</sub>=3.45%

Specimen	3 X 3"			3 X 6"			3 X 9"		
	Time(days)	$t/b^2$	Sa/Su	I- $\bar{U}$	$t/b^2$	Sa/Su	I- $\bar{U}$	$t/b^2$	Sa/Su
2	0.90	0.08	0.18	0.23	0.06	0.14	0.10	0.02	0.09
4	1.78	0.15	0.27	0.44	0.11	0.17	0.20	0.04	0.13
8	3.56	0.26	0.35	0.89	0.19	0.21	0.40	0.08	0.16
16	7.11	0.34	0.48	1.78	0.25	0.28	0.79	0.11	0.19
32	14.22	0.42	0.61	3.56	0.30	0.35	1.58	0.15	0.24
64	28.44	0.72	0.71	7.11	0.53	0.47	3.16	0.25	0.33
128	56.89	1.00	1.00	14.22	0.74	0.67	6.32	0.51	0.45

Series I-C-76Z, PC

Specimen	4 X 4"		6 X 6"		8 X 8"	
	t/b <sup>2</sup>	S <sub>e</sub> /S <sub>u</sub>	t/b <sup>2</sup>	S <sub>e</sub> /S <sub>u</sub>	t/b <sup>2</sup>	S <sub>e</sub> /S <sub>u</sub>
3	0.75	0.14	0.33	0.11	0.19	0.06
7	1.75	0.29	0.78	0.20	0.44	0.12
16	4.00	0.42	1.78	0.28	1.00	0.20
31	7.75	0.61	3.44	0.42	1.94	0.31
70	17.50	0.75	7.78	0.50	4.38	0.38
167	41.75	0.88	18.56	0.56	10.44	0.46
328	82.00	1.00	36.44	0.64	20.50	0.50

Series I-C-76Z, Ps=1.25Z

Specimen	4 X 4"		6 X 6"		8 X 8"	
	t/b <sup>2</sup>	S <sub>e</sub> /S <sub>u</sub>	t/b <sup>2</sup>	S <sub>e</sub> /S <sub>u</sub>	t/b <sup>2</sup>	S <sub>e</sub> /S <sub>u</sub>
3	0.75	0.97	0.33	0.06	0.19	0.05
7	1.75	0.26	0.78	0.16	0.44	0.11
16	4.00	0.37	1.78	0.29	1.00	0.20
31	7.75	0.58	3.44	0.47	1.94	0.35
70	17.50	0.71	7.78	0.55	4.38	0.40
167	41.75	0.81	18.56	0.61	10.44	0.45
328	82.00	1.00	36.44	0.74	20.50	0.52

Series I-C-76%, Ps=2.50%

Specimen	4 X 4"		6X6"		8 X 8"	
	$t/b^2$	$S_e/S_u$	$t/b^2$	$S_e/S_u$	$t/b^2$	$S_e/S_u$
3	0.75	0.08	0.33	0.08	0.19	0.07
7	1.75	0.22	0.78	0.21	0.44	0.19
16	4.00	0.34	1.78	0.35	1.00	0.27
31	7.75	0.60	3.44	0.57	1.94	0.44
70	17.50	0.72	7.78	0.68	4.38	0.52
167	41.75	0.84	18.56	0.80	10.44	0.60
328	82.00	1.00	36.44	0.91	20.50	0.68

Series I-C-76%, Ps=3.75%

Specimen	4 X 4"		6X6"		8 X 8"	
	$t/b^2$	$S_e/S_u$	$t/b^2$	$S_e/S_u$	$t/b^2$	$S_e/S_u$
3	0.75	0.15	0.33	0.08	0.19	0.06
7	1.75	0.29	0.78	0.16	0.44	0.16
16	4.00	0.42	1.78	0.28	1.00	0.24
31	7.75	0.64	3.44	0.52	1.94	0.42
70	17.50	0.79	7.78	0.62	4.38	0.49
167	41.75	0.91	18.56	0.72	10.44	0.56
328	82.00	1.00	36.44	0.82	20.50	0.69



Series I-C-76Z, Ps=5.00Z

Specimen	4 X 4"		6X6"		8 X 8"	
	$t/b^2$	$S_e/S_u$	$t/b^2$	$S_e/S_u$	$t/b^2$	$S_e/S_u$
3	0.75	0.09	0.33	0.09	0.19	0.05
7	1.75	0.18	0.78	0.19	0.44	0.12
16	4.00	0.30	1.78	0.30	1.00	0.21
31	7.75	0.53	3.44	0.47	1.94	0.36
70	17.50	0.69	7.78	0.56	4.38	0.44
167	41.75	0.85	18.56	0.68	10.44	0.53
328	82.00	1.00	36.44	0.78	20.50	0.64

Series I-C-54Z, Ps=5.00Z

Specimen	4 X 4"		6X6"		8 X 8"	
	$t/b^2$	$S_e/S_u$	$t/b^2$	$S_e/S_u$	$t/b^2$	$S_e/S_u$
4	1.00	0.15	0.44	0.13	0.25	0.11
7	1.75	0.25	0.78	0.18	0.44	0.16
14	3.50	0.35	1.56	0.27	0.88	0.22
34	8.50	0.51	3.78	0.42	2.13	0.36
72	18.00	0.70	8.00	0.59	4.50	0.48
172	43.00	0.88	19.11	0.75	10.75	0.58
323	80.75	1.00	35.89	0.85	20.19	0.67

Series I-C-54%,PC

Specimen	4 X 4"		6X6"		8 X 8"	
	$t/b^2$	$S_e/S_u$	$t/b^2$	$S_e/S_u$	$t/b^2$	$S_e/S_u$
4	1.00	0.19	0.44	0.16	0.25	0.12
7	1.75	0.31	0.78	0.27	0.44	0.19
14	3.50	0.51	1.56	0.42	0.88	0.33
34	8.50	0.68	3.78	0.56	2.13	0.44
72	18.00	0.78	8.00	0.62	4.50	0.52
172	43.00	0.90	19.11	0.69	10.75	0.59
323	80.75	1.00	35.89	0.76	20.19	0.65

Series I-C-54%,Ps=1.25%

Specimen	4 X 4"		6X6"		8 X 8"	
	$t/b^2$	$S_e/S_u$	$t/b^2$	$S_e/S_u$	$t/b^2$	$S_e/S_u$
4	1.00	0.19	0.44	0.15	0.25	0.11
7	1.75	0.30	0.78	0.22	0.44	0.19
14	3.50	0.48	1.56	0.30	0.88	0.26
34	8.50	0.63	3.78	0.41	2.13	0.35
72	18.00	0.74	8.00	0.52	4.50	0.44
172	43.00	0.89	19.11	0.63	10.75	0.52
323	80.75	1.00	35.89	0.74	20.19	0.63

Series I-C-54Z, Ps=2.50Z

Specimen	4 X 4"		6X6"		8 X 8"	
	$t/b^2$	$S_e/S_u$	$t/b^2$	$S_e/S_u$	$t/b^2$	$S_e/S_u$
4	1.00	0.19	0.44	0.15	0.25	0.12
7	1.75	0.29	0.78	0.22	0.44	0.17
14	3.50	0.46	1.56	0.33	0.88	0.27
34	8.50	0.65	3.78	0.43	2.13	0.37
72	18.00	0.77	8.00	0.54	4.50	0.48
172	43.00	0.88	19.11	0.65	10.75	0.56
323	80.75	1.00	35.89	0.73	20.19	0.63

Series I-C-54Z, Ps=3.75Z

Specimen	4 X 4"		6X6"		8 X 8"	
	$t/b^2$	$S_e/S_u$	$t/b^2$	$S_e/S_u$	$t/b^2$	$S_e/S_u$
4	1.00	0.18	0.44	0.16	0.25	0.14
7	1.75	0.26	0.78	0.22	0.44	0.20
14	3.50	0.41	1.56	0.32	0.88	0.28
34	8.50	0.57	3.78	0.46	2.13	0.40
72	18.00	0.72	8.00	0.53	4.50	0.45
172	43.00	0.88	19.11	0.64	10.75	0.57
323	80.75	1.00	35.89	0.72	20.19	0.67

Series I-C-32X, PC

Specimen	4 X 4"		6 X 6"		8 X 8"	
	$t/b^2$	$S_e/S_u$	$t/b^2$	$S_e/S_u$	$t/b^2$	$S_e/S_u$
3	0.75	0.19	0.33	0.16	0.19	0.13
7	1.75	0.30	0.78	0.26	0.44	0.16
14	3.50	0.47	1.56	0.38	0.88	0.28
29	7.25	0.65	3.22	0.55	1.81	0.39
70	17.50	0.78	7.78	0.64	4.38	0.46
168	42.00	0.93	18.67	0.74	10.50	0.53
324	81.00	1.00	36.00	0.80	20.25	0.60

Series I-C-32X, Ps=1.25X

Specimen	4 X 4"		6 X 6"		8 X 8"	
	$t/b^2$	$S_e/S_u$	$t/b^2$	$S_e/S_u$	$t/b^2$	$S_e/S_u$
3	0.75	0.20	0.33	0.11	0.19	0.10
7	1.75	0.37	0.78	0.20	0.44	0.16
14	3.50	0.53	1.56	0.30	0.88	0.24
29	7.25	0.71	3.22	0.43	1.81	0.34
70	17.50	0.80	7.78	0.51	4.38	0.40
168	42.00	0.91	18.67	0.57	10.50	0.49
324	81.00	1.00	36.00	0.66	20.25	0.54

Series I-C-32Z,  $P_S=2.50\%$ 

Specimen	4 X 4"		6 X 6"		8 X 8"	
	$t/b^2$	$S_e/S_u$	$t/b^2$	$S_e/S_u$	$t/b^2$	$S_e/S_u$
3	0.75	0.14	0.33	0.10	0.19	0.09
7	1.75	0.29	0.78	0.18	0.44	0.13
14	3.50	0.45	1.56	0.28	0.88	0.20
29	7.25	0.62	3.22	0.40	1.81	0.31
70	17.50	0.76	7.78	0.50	4.38	0.36
168	42.00	0.91	18.67	0.60	10.50	0.43
324	81.00	1.00	36.00	0.67	20.25	0.47

Series I-C-32Z,  $P_S=3.75\%$ 

Specimen	4 X 4"		6 X 6"		8 X 8"	
	$t/b^2$	$S_e/S_u$	$t/b^2$	$S_e/S_u$	$t/b^2$	$S_e/S_u$
3	0.75	0.15	0.33	0.11	0.19	0.13
7	1.75	0.26	0.78	0.17	0.44	0.18
14	3.50	0.42	1.56	0.26	0.88	0.25
29	7.25	0.60	3.22	0.39	1.81	0.35
70	17.50	0.74	7.78	0.49	4.38	0.45
168	42.00	0.90	18.67	0.59	10.50	0.53
324	81.00	1.00	36.00	0.65	20.25	0.58

Series I-C-32Z, Ps=5.00Z

Specimen	4 X 4"		6X6"		8 X 8"	
	$t/b^2$	$S_e/S_u$	$t/b^2$	$S_e/S_u$	$t/b^2$	$S_e/S_u$
3	0.75	0.19	0.33	0.11	0.19	0.08
7	1.75	0.32	0.78	0.18	0.44	0.12
14	3.50	0.42	1.56	0.29	0.88	0.20
29	7.25	0.60	3.22	0.42	1.81	0.30
70	17.50	0.75	7.78	0.53	4.38	0.40
168	42.00	0.91	18.67	0.66	10.50	0.49
324	81.00	1.00	36.00	0.75	20.25	0.56

Series I-C-7Z, Ps=5.00Z

Specimen	4 X 4"		6X6"		8 X 8"	
	$t/b^2$	$S_e/S_u$	$t/b^2$	$S_e/S_u$	$t/b^2$	$S_e/S_u$
3	0.75	0.12	0.33	0.10	0.19	0.09
7	1.75	0.21	0.78	0.18	0.44	0.15
15	3.75	0.34	1.67	0.27	0.94	0.24
33	8.25	0.52	3.67	0.39	2.06	0.34
72	18.00	0.68	8.00	0.51	4.50	0.44
172	43.00	0.88	19.11	0.65	10.75	0.55
323	80.75	1.00	35.89	0.78	20.19	0.65

Series I-C-7Z, PC

Specimen	4 X 4"		6X6"		8 X 8"	
	$t/b^2$	$S_e/S_u$	$t/b^2$	$S_e/S_u$	$t/b^2$	$S_e/S_u$
3	0.75	0.19	0.33	0.16	0.19	0.10
7	1.75	0.27	0.78	0.24	0.44	0.16
15	3.75	0.42	1.67	0.34	0.94	0.26
33	8.25	0.58	3.67	0.48	2.06	0.37
72	18.00	0.72	8.00	0.62	4.50	0.48
172	43.00	0.86	19.11	0.75	10.75	0.57
323	80.75	1.00	35.89	0.87	20.19	0.69

Series I-C-7Z, Ps=1.25Z

Specimen	4 X 4"		6X6"		8 X 8"	
	$t/b^2$	$S_e/S_u$	$t/b^2$	$S_e/S_u$	$t/b^2$	$S_e/S_u$
3	0.75	0.16	0.33	0.13	0.19	0.09
7	1.75	0.25	0.78	0.20	0.44	0.13
15	3.75	0.41	1.67	0.33	0.94	0.16
33	8.25	0.56	3.67	0.50	2.06	0.25
72	18.00	0.72	8.00	0.63	4.50	0.34
172	43.00	0.88	19.11	0.75	10.75	0.44
323	80.75	1.00	35.89	0.88	20.19	0.53

Series I-C-7%, Ps=2.50%

Specimen	4 X 4"		6X6"		8 X 8"	
	$t/b^2$	$S_e/S_u$	$t/b^2$	$S_e/S_u$	$t/b^2$	$S_e/S_u$
3	0.75	0.20	0.33	0.15	0.19	0.10
7	1.75	0.28	0.78	0.21	0.44	0.15
15	3.75	0.39	1.67	0.31	0.94	0.24
33	8.25	0.54	3.67	0.44	2.06	0.33
72	18.00	0.70	8.00	0.57	4.50	0.41
172	43.00	0.87	19.11	0.69	10.75	0.48
323	80.75	1.00	35.89	0.80	20.19	0.58

Series I-C-7%, Ps=3.75%

Specimen	4 X 4"		6X6"		8 X 8"	
	$t/b^2$	$S_e/S_u$	$t/b^2$	$S_e/S_u$	$t/b^2$	$S_e/S_u$
3	0.75	0.13	0.33	0.12	0.19	0.10
7	1.75	0.25	0.78	0.21	0.44	0.18
15	3.75	0.40	1.67	0.32	0.94	0.27
33	8.25	0.55	3.67	0.42	2.06	0.38
72	18.00	0.71	8.00	0.55	4.50	0.48
172	43.00	0.85	19.11	0.66	10.75	0.60
323	80.75	1.00	35.89	0.78	20.19	0.66



Series III-C-76%,PC

Specimen	4 X 4"		6 X 6"		8 X 8"	
	t / b <sup>2</sup>	S <sub>e</sub> / S <sub>u</sub>	t / b <sup>2</sup>	S <sub>e</sub> / S <sub>u</sub>	t / b <sup>2</sup>	S <sub>e</sub> / S <sub>u</sub>
3	0.75	0.18	0.33	0.16	0.19	0.08
7	1.75	0.32	0.78	0.27	0.44	0.15
16	4.00	0.50	1.78	0.40	1.00	0.24
34	8.50	0.64	3.78	0.54	2.13	0.40
74	18.50	0.76	8.22	0.64	4.63	0.49
163	40.75	0.88	18.11	0.75	10.19	-0.58
346	86.50	1.00	38.44	0.88	21.63	0.72

Series III-C-76%,Ps=1.25%

Specimen	4 X 4"		6 X 6"		8 X 8"	
	t / b <sup>2</sup>	S <sub>e</sub> / S <sub>u</sub>	t / b <sup>2</sup>	S <sub>e</sub> / S <sub>u</sub>	t / b <sup>2</sup>	S <sub>e</sub> / S <sub>u</sub>
3	0.75	0.22	0.33	0.09	0.19	0.08
7	1.75	0.32	0.78	0.19	0.44	0.12
16	4.00	0.47	1.78	0.32	1.00	0.20
34	8.50	0.61	3.78	0.43	2.13	0.31
74	18.50	0.72	8.22	0.24	4.63	0.36
163	40.75	0.84	18.11	0.59	10.19	0.43
346	86.50	1.00	38.44	0.76	21.63	0.57

Series III-C-76Z, Ps=2.50Z

Specimen	4 X 4"		6 X 6"		8 X 8"	
	$t/b^2$	$S_e/S_u$	$t/b^2$	$S_e/S_u$	$t/b^2$	$S_e/S_u$
3	0.75	0.18	0.33	0.13	0.19	0.10
7	1.75	0.27	0.78	0.23	0.44	0.16
16	4.00	0.45	1.78	0.39	1.00	0.27
34	8.50	0.60	3.78	0.52	2.13	0.39
74	18.50	0.71	8.22	0.61	4.63	0.45
163	40.75	0.82	18.11	0.71	10.19	0.55
346	86.50	1.00	38.44	0.85	21.63	0.68

Series III-C-76Z, Ps=3.75Z

Specimen	4 X 4"		6 X 6"		8 X 8"	
	$t/b^2$	$S_e/S_u$	$t/b^2$	$S_e/S_u$	$t/b^2$	$S_e/S_u$
3	0.75	0.15	0.33	0.14	0.19	0.08
7	1.75	0.27	0.78	0.25	0.44	0.15
16	4.00	0.44	1.78	0.42	1.00	0.27
34	8.50	0.58	3.78	0.57	2.13	0.37
74	18.50	0.71	8.22	0.67	4.63	0.45
163	40.75	0.82	18.11	0.78	10.19	0.55
346	86.50	1.00	38.44	0.94	21.63	0.69

Series III-C-76Z, Ps=5.00Z

Specimen	4 X 4"		6 X 6"		8 X 8"	
	$t/b^2$	$S_e/S_u$	$t/b^2$	$S_e/S_u$	$t/b^2$	$S_e/S_u$
3	0.75	0.13	0.33	0.12	0.19	0.07
7	1.75	0.27	0.78	0.23	0.44	0.13
16	4.00	0.44	1.78	0.38	1.00	0.24
34	8.50	0.60	3.78	0.55	2.13	0.34
74	18.50	0.73	8.22	0.66	4.63	0.42
163	40.75	0.84	18.11	0.75	10.19	0.52
346	86.50	1.00	38.44	0.89	21.63	0.68

Series III-C-54Z, Ps=5.00Z

Specimen	4 X 4"		6 X 6"		8 X 8"	
	$t/b^2$	$S_e/S_u$	$t/b^2$	$S_e/S_u$	$t/b^2$	$S_e/S_u$
4	1.00	0.14	0.44	0.11	0.25	0.10
8	2.00	0.26	0.89	0.20	0.50	0.17
18	4.50	0.42	2.00	0.32	1.13	0.26
34	8.50	0.56	3.78	0.44	2.13	0.34
74	18.50	0.69	8.22	0.57	4.63	0.45
163	40.75	0.83	18.11	0.70	10.19	0.56
343	85.75	1.00	38.11	0.87	21.44	0.73

Series III-C-54Z, PC

Specimen	4 X 4"		6X6"		8 X 8"	
	$t/b^2$	$S_e/S_u$	$t/b^2$	$S_e/S_u$	$t/b^2$	$S_e/S_u$
4	1.00	0.23	0.44	0.18	0.25	0.12
8	2.00	0.38	0.89	0.28	0.50	0.23
18	4.50	0.56	2.00	0.46	1.13	0.36
34	8.50	0.70	3.78	0.60	2.13	0.47
74	18.50	0.78	8.22	0.69	4.63	0.56
163	40.75	0.88	18.11	0.79	10.19	0.65
343	85.75	1.00	38.11	0.91	21.44	0.79

Series III-C-54Z, Ps=1.25Z

Specimen	4 X 4"		6X6"		8 X 8"	
	$t/b^2$	$S_e/S_u$	$t/b^2$	$S_e/S_u$	$t/b^2$	$S_e/S_u$
4	1.00	0.18	0.44	0.12	0.25	0.09
8	2.00	0.27	0.89	0.21	0.50	0.17
18	4.50	0.45	2.00	0.33	1.13	0.29
34	8.50	0.58	3.78	0.42	2.13	0.38
74	18.50	0.70	8.22	0.52	4.63	0.44
163	40.75	0.82	18.11	0.61	10.19	0.52
343	85.75	1.00	38.11	0.76	21.44	0.61

Series III-C-54Z, Ps=2.50Z

Specimen	4 X 4"		6 X 6"		8 X 8"	
	$t/b^2$	$S_e/S_u$	$t/b^2$	$S_e/S_u$	$t/b^2$	$S_e/S_u$
4	1.00	0.20	0.44	0.13	0.25	0.10
8	2.00	0.31	0.89	0.23	0.50	0.17
18	4.50	0.48	2.00	0.35	1.13	0.25
34	8.50	0.59	3.78	0.42	2.13	0.32
74	18.50	0.70	8.22	0.52	4.63	0.41
163	40.75	0.83	18.11	0.62	10.19	0.48
343	85.75	1.00	38.11	0.77	21.44	0.61

Series III-C-54Z, Ps=3.75Z

Specimen	4 X 4"		6 X 6"		8 X 8"	
	$t/b^2$	$S_e/S_u$	$t/b^2$	$S_e/S_u$	$t/b^2$	$S_e/S_u$
4	1.00	0.19	0.44	0.13	0.25	0.10
8	2.00	0.31	0.89	0.23	0.50	0.18
18	4.50	0.45	2.00	0.33	1.13	0.27
34	8.50	0.53	3.78	0.43	2.13	0.33
74	18.50	0.67	8.22	0.54	4.63	0.43
163	40.75	0.81	18.11	0.66	10.19	0.53
343	85.75	1.00	38.11	0.83	21.44	0.68

Series III-C-32%, PC

Specimen	4 X 4"		6 X 6"		8 X 8"	
	$t/b^2$	$S_e/S_u$	$t/b^2$	$S_e/S_u$	$t/b^2$	$S_e/S_u$
4	1.00	0.21	0.44	0.17	0.25	0.14
7	1.75	0.42	0.78	0.33	0.44	0.28
16	4.00	0.57	1.78	0.45	1.00	0.37
31	7.75	0.69	3.44	0.55	1.94	0.47
72	18.00	0.80	8.00	0.67	4.50	0.57
163	40.75	0.93	18.11	0.79	10.19	0.66
344	86.00	1.00	38.22	0.90	21.50	0.76

Series III-C-32%, Ps=1.25%

Specimen	4 X 4"		6 X 6"		8 X 8"	
	$t/b^2$	$S_e/S_u$	$t/b^2$	$S_e/S_u$	$t/b^2$	$S_e/S_u$
4	1.00	0.16	0.44	0.15	0.25	0.08
7	1.75	0.32	0.78	0.30	0.44	0.19
16	4.00	0.43	1.78	0.39	1.00	0.27
31	7.75	0.57	3.44	0.49	1.94	0.32
72	18.00	0.73	8.00	0.62	4.50	0.43
163	40.75	0.89	18.11	0.76	10.19	0.54
344	86.00	1.00	38.22	0.92	21.50	0.65

Series III-C-32%, Ps=2.50%

Specimen	4 X 4"		6 X 6"		8 X 8"	
	†/b <sup>2</sup>	S <sub>e</sub> /S <sub>u</sub>	†/b <sup>2</sup>	S <sub>e</sub> /S <sub>u</sub>	†/b <sup>2</sup>	S <sub>e</sub> /S <sub>u</sub>
4	1.00	0.20	0.44	0.17	0.25	0.09
7	1.75	0.34	0.78	0.34	0.44	0.21
16	4.00	0.46	1.78	0.42	1.00	0.28
31	7.75	0.56	3.44	0.51	1.94	0.36
72	18.00	0.71	8.00	0.61	4.50	0.47
163	40.75	0.86	18.11	0.74	10.19	0.57
344	86.00	1.00	38.22	0.89	21.50	0.70

Series III-C-32%, Ps=3.75%

Specimen	4 X 4"		6 X 6"		8 X 8"	
	†/b <sup>2</sup>	S <sub>e</sub> /S <sub>u</sub>	†/b <sup>2</sup>	S <sub>e</sub> /S <sub>u</sub>	†/b <sup>2</sup>	S <sub>e</sub> /S <sub>u</sub>
4	1.00	0.17	0.44	0.12	0.25	0.07
7	1.75	0.34	0.78	0.24	0.44	0.18
16	4.00	0.49	1.78	0.36	1.00	0.26
31	7.75	0.61	3.44	0.44	1.94	0.33
72	18.00	0.74	8.00	0.54	4.50	0.42
163	40.75	0.86	18.11	0.65	10.19	0.50
344	86.00	1.00	38.22	0.80	21.50	0.60

Series III-C-32%, Ps=5.00%

Specimen	4 X 4"		6X6"		8 X 8"	
	$t/b^2$	$S_e/S_u$	$t/b^2$	$S_e/S_u$	$t/b^2$	$S_e/S_u$
4	1.00	0.16	0.44	0.13	0.25	0.10
7	1.75	0.32	0.78	0.25	0.44	0.20
16	4.00	0.46	1.78	0.36	1.00	0.29
31	7.75	0.56	3.44	0.48	1.94	0.37
72	18.00	0.71	8.00	0.61	4.50	0.47
163	40.75	0.85	18.11	0.73	10.19	0.58
344	86.00	1.00	38.22	0.89	21.50	0.70

Series III-C-7%, Ps=5.00%

Specimen	4 X 4"		6X6"		8 X 8"	
	$t/b^2$	$S_e/S_u$	$t/b^2$	$S_e/S_u$	$t/b^2$	$S_e/S_u$
4	1.00	0.20	0.44	0.14	0.25	0.11
11	2.75	0.39	1.22	0.29	0.69	0.20
19	4.75	0.53	2.11	0.38	1.19	0.27
47	11.75	0.67	5.22	0.49	2.94	0.35
80	20.00	0.79	8.89	0.57	5.00	0.45
164	41.00	0.89	18.22	0.65	10.25	0.54
343	85.75	1.00	38.11	0.75	21.44	0.64



Series III-C-7%, PC

Specimen	4 X 4"		6 X 6"		8 X 8"	
	$t/b^2$	$S_e/S_u$	$t/b^2$	$S_e/S_u$	$t/b^2$	$S_e/S_u$
4	1.00	0.26	0.44	0.22	0.25	0.18
11	2.75	0.46	1.22	0.37	0.69	0.31
19	4.75	0.58	2.11	0.46	1.19	0.39
47	11.75	0.77	5.22	0.58	2.94	0.45
80	20.00	0.84	8.89	0.66	5.00	0.54
164	41.00	0.92	18.22	0.75	10.25	0.63
343	85.75	1.00	38.11	0.84	21.44	0.72

Series III-C-7%, Ps=1.25%

Specimen	4 X 4"		6 X 6"		8 X 8"	
	$t/b^2$	$S_e/S_u$	$t/b^2$	$S_e/S_u$	$t/b^2$	$S_e/S_u$
4	1.00	0.20	0.44	0.17	0.25	0.17
11	2.75	0.37	1.22	0.29	0.69	0.26
19	4.75	0.49	2.11	0.37	1.19	0.31
47	11.75	0.63	5.22	0.46	2.94	0.40
80	20.00	0.77	8.89	0.57	5.00	0.46
164	41.00	0.89	18.22	0.69	10.25	0.54
343	85.75	1.00	38.11	0.80	21.44	0.63

Series III-C-7%, Ps=2.50%

Specimen	4 X 4"		6 X 6"		8 X 8"	
	t/b <sup>2</sup>	S <sub>t</sub> /S <sub>u</sub>	t/b <sup>2</sup>	S <sub>t</sub> /S <sub>u</sub>	t/b <sup>2</sup>	S <sub>t</sub> /S <sub>u</sub>
4	1.00	0.23	0.44	0.18	0.25	0.14
11	2.75	0.38	1.22	0.33	0.69	0.25
19	4.75	0.51	2.11	0.43	1.19	0.32
47	11.75	0.66	5.22	0.52	2.94	0.39
80	20.00	0.77	8.89	0.62	5.00	0.48
164	41.00	0.89	18.22	0.72	10.25	0.57
343	85.75	1.00	38.11	0.82	21.44	0.67

Series III-C-7%, Ps=3.75%

Specimen	4 X 4"		6 X 6"		8 X 8"	
	t/b <sup>2</sup>	S <sub>t</sub> /S <sub>u</sub>	t/b <sup>2</sup>	S <sub>t</sub> /S <sub>u</sub>	t/b <sup>2</sup>	S <sub>t</sub> /S <sub>u</sub>
4	1.00	0.21	0.44	0.16	0.25	0.11
11	2.75	0.39	1.22	0.30	0.69	0.21
19	4.75	0.52	2.11	0.40	1.19	0.28
47	11.75	0.67	5.22	0.50	2.94	0.35
80	20.00	0.78	8.89	0.60	5.00	0.43
164	41.00	0.89	18.22	0.69	10.25	0.51
343	85.75	1.00	38.11	0.77	21.44	0.60

Series I-S-76Z, PC

Specimen	3X3"		3X6"		3X9"		3X12"	
	$t/b^2$	$S_e/S_u$	$t/b^2$	$S_e/S_u$	$t/b^2$	$S_e/S_u$	$t/b^2$	$S_e/S_u$
3	1.33	0.15	0.33	0.05	0.15	0.08	0.10	0.11
7	3.11	0.33	0.78	0.16	0.35	0.12	0.19	0.18
14	6.22	0.43	1.56	0.26	0.69	0.21	0.39	0.26
28	12.44	0.60	3.11	0.43	1.38	0.31	0.78	0.33
70	31.11	0.80	7.78	0.69	3.46	0.44	1.94	0.48
209	92.89	0.98	23.22	0.81	10.32	0.59	5.81	0.61
274	121.78	1.00	30.44	0.80	13.53	0.59	7.61	0.62

Series I-S-76Z, Ps=2.22Z

Specimen	3X3"		3X6"		3X9"		3X12"	
	$t/b^2$	$S_e/S_u$	$t/b^2$	$S_e/S_u$	$t/b^2$	$S_e/S_u$	$t/b^2$	$S_e/S_u$
3	1.33	0.14	0.33	0.07	0.15	0.14	0.10	0.08
7	3.11	0.35	0.78	0.16	0.35	0.20	0.19	0.11
14	6.22	0.49	1.56	0.27	0.69	0.27	0.39	0.18
28	12.44	0.67	3.11	0.35	1.38	0.34	0.78	0.22
70	31.11	0.88	7.78	0.58	3.46	0.49	1.94	0.35
209	92.89	0.98	23.22	0.89	10.32	0.68	5.81	0.53
274	121.78	1.00	30.44	0.95	13.53	0.71	7.61	0.55

Series I-S-76Z, Ps=3.45Z

Specimen	3X3"		3X6"		3X9"		3X12"	
	t/b <sup>2</sup>	S <sub>e</sub> /S <sub>u</sub>	t/b <sup>2</sup>	S <sub>e</sub> /S <sub>u</sub>	t/b <sup>2</sup>	S <sub>e</sub> /S <sub>u</sub>	t/b <sup>2</sup>	S <sub>e</sub> /S <sub>u</sub>
3	1.33	0.11	0.33	0.09	0.15	0.11	0.10	0.15
7	3.11	0.40	0.78	0.22	0.35	0.16	0.19	0.22
14	6.22	0.51	1.56	0.32	0.69	0.22	0.39	0.27
28	12.44	0.65	3.11	0.45	1.38	0.32	0.78	0.35
70	31.11	0.84	7.78	0.64	3.46	0.49	1.94	0.46
209	92.89	0.98	23.22	0.82	10.32	0.69	5.81	0.58
274	121.78	1.00	30.44	0.85	13.53	0.76	7.61	0.62

Series I-S-76Z, Ps=4.90Z

Specimen	3X3"		3X6"		3X9"		3X12"	
	t/b <sup>2</sup>	S <sub>e</sub> /S <sub>u</sub>	t/b <sup>2</sup>	S <sub>e</sub> /S <sub>u</sub>	t/b <sup>2</sup>	S <sub>e</sub> /S <sub>u</sub>	t/b <sup>2</sup>	S <sub>e</sub> /S <sub>u</sub>
3	1.33	0.14	0.33	0.07	0.15	0.05	0.10	0.05
7	1.33	0.23	0.78	0.16	0.35	0.11	3.46	0.45
14	6.22	0.36	1.56	0.27	0.69	0.18	0.39	0.14
28	12.44	0.50	3.11	0.41	1.38	0.27	0.78	0.20
70	31.11	0.73	7.78	0.64	3.46	0.45	1.94	0.36
209	92.89	0.10	23.22	0.82	10.32	0.71	5.81	0.61
274	121.78	1.00	30.44	0.86	13.53	0.77	7.61	0.66

Series I-S-54Z, PC

Specimen	3X3"		3X6"		3X9"		3X12"	
	t/b <sup>2</sup>	S <sub>e</sub> /S <sub>u</sub>	t/b <sup>2</sup>	S <sub>e</sub> /S <sub>u</sub>	t/b <sup>2</sup>	S <sub>e</sub> /S <sub>u</sub>	t/b <sup>2</sup>	S <sub>e</sub> /S <sub>u</sub>
3	1.33	0.09	0.33	0.08	0.15	0.07	0.10	0.08
7	3.11	0.21	0.78	0.15	0.35	0.15	0.19	0.15
14	6.22	0.34	1.56	0.24	0.69	0.22	0.39	0.22
28	12.44	0.50	3.11	0.37	1.38	0.32	0.78	0.32
74	32.89	0.78	8.22	0.50	3.65	0.43	2.06	0.42
202	89.78	0.93	22.44	0.59	9.98	0.51	5.61	0.49
288	128.00	0.96	32.00	0.61	14.22	0.50	8.00	0.47

Series I-S-54Z, Ps=2.22Z

Specimen	3X3"		3X6"		3X9"		3X12"	
	t/b <sup>2</sup>	S <sub>e</sub> /S <sub>u</sub>	t/b <sup>2</sup>	S <sub>e</sub> /S <sub>u</sub>	t/b <sup>2</sup>	S <sub>e</sub> /S <sub>u</sub>	t/b <sup>2</sup>	S <sub>e</sub> /S <sub>u</sub>
3	1.33	0.07	0.33	0.07	0.15	0.03	0.10	0.06
7	3.11	0.17	0.78	0.15	0.35	0.11	0.19	0.11
14	6.22	0.30	1.56	0.22	0.69	0.17	0.39	0.22
28	12.44	0.43	3.11	0.35	1.38	0.25	0.78	0.28
74	32.89	0.73	8.22	0.47	3.65	0.42	2.06	0.42
202	89.78	0.90	22.44	0.57	9.98	0.50	5.61	0.51
288	128.00	0.93	32.00	0.60	14.22	0.53	8.00	0.53

Series I-S-54Z, Ps=3.45Z

Specimen	3X3"		3X6"		3X9"		3X12"	
	t/b <sup>2</sup>	S <sub>e</sub> /S <sub>u</sub>	t/b <sup>2</sup>	S <sub>e</sub> /S <sub>u</sub>	t/b <sup>2</sup>	S <sub>e</sub> /S <sub>u</sub>	t/b <sup>2</sup>	S <sub>e</sub> /S <sub>u</sub>
3	1.33	0.04	0.33	0.04	0.15	0.04	0.10	0.05
7	3.11	0.15	0.78	0.15	0.35	0.10	0.19	0.12
14	6.22	0.30	1.56	0.22	0.69	0.17	0.39	0.18
28	12.44	0.43	3.11	0.33	1.38	0.25	0.78	0.27
74	32.89	0.78	8.22	0.50	3.65	0.36	2.06	0.44
202	89.78	0.96	22.44	0.69	9.98	0.48	5.61	0.54
288	128.00	1.00	32.00	0.74	14.22	0.50	8.00	0.57

Series I-S-54Z, Ps=4.90Z

Specimen	3X3"		3X6"		3X9"		3X12"	
	t/b <sup>2</sup>	S <sub>e</sub> /S <sub>u</sub>	t/b <sup>2</sup>	S <sub>e</sub> /S <sub>u</sub>	t/b <sup>2</sup>	S <sub>e</sub> /S <sub>u</sub>	t/b <sup>2</sup>	S <sub>e</sub> /S <sub>u</sub>
3	1.33	0.23	0.33	0.05	0.15	0.06	0.10	0.05
7	3.11	0.36	0.78	0.09	0.35	0.13	0.19	0.09
14	6.22	0.50	1.56	0.18	0.69	0.20	0.39	0.16
28	12.44	0.64	3.11	0.31	1.38	0.35	0.78	0.27
74	32.88	0.77	8.22	0.51	3.65	0.55	2.06	0.45
202	89.78	0.86	22.44	0.68	9.98	0.66	5.61	0.56
288	128.00	0.91	32.00	0.77	14.22	0.70	8.00	0.57

Series I-S-32Z, PC

Specimen	3 X 3"		3X6"		3X9"		3X12"	
	t/b <sup>2</sup>	S <sub>e</sub> /S <sub>u</sub>	t/b <sup>2</sup>	S <sub>e</sub> /S <sub>u</sub>	t/b <sup>2</sup>	S <sub>e</sub> /S <sub>u</sub>	t/b <sup>2</sup>	S <sub>e</sub> /S <sub>u</sub>
3	1.33	0.08	0.33	0.09	0.15	0.09	0.10	0.06
7	3.11	0.13	0.78	0.14	0.35	0.14	0.19	0.12
14	6.22	0.27	1.56	0.22	0.69	0.21	0.39	0.19
28	12.44	0.42	3.11	0.31	1.38	0.29	0.78	0.24
72	32.00	0.69	8.00	0.51	3.56	0.46	2.00	0.40
207	92.00	0.94	23.00	0.63	10.22	0.58	5.75	0.46
278	123.56	0.96	30.89	0.61	13.73	0.55	7.72	0.47

Series I-S-32Z, Ps=2.22Z

Specimen	3X3"		3X6"		3X9"		3X12"	
	t/b <sup>2</sup>	S <sub>e</sub> /S <sub>u</sub>	t/b <sup>2</sup>	S <sub>e</sub> /S <sub>u</sub>	t/b <sup>2</sup>	S <sub>e</sub> /S <sub>u</sub>	t/b <sup>2</sup>	S <sub>e</sub> /S <sub>u</sub>
<del>3</del>	1.33	0.09	0.33	0.09	0.15	0.09	0.10	0.09
<del>7</del>	3.11	0.16	0.78	0.13	0.35	0.13	0.19	0.13
14	6.22	0.25	1.56	0.19	0.69	0.20	0.39	0.20
28	12.44	0.44	3.11	0.25	1.38	0.26	0.78	0.25
72	32.00	0.78	8.00	0.49	3.56	0.41	2.00	0.45
207	92.00	0.97	23.00	0.70	10.22	0.53	5.75	0.54
278	123.56	1.00	30.89	0.72	13.73	0.55	7.72	0.55

Series I-S-32%, Ps=3.45%

Specimen	3X3"		3X6"		3X9"		3X12"	
	t/b <sup>2</sup>	S <sub>e</sub> /S <sub>u</sub>	t/b <sup>2</sup>	S <sub>e</sub> /S <sub>u</sub>	t/b <sup>2</sup>	S <sub>e</sub> /S <sub>u</sub>	t/b <sup>2</sup>	S <sub>e</sub> /S <sub>u</sub>
3	1.33	0.14	0.33	0.10	0.15	0.10	0.10	0.09
7	3.11	0.21	0.78	0.21	0.35	0.17	0.19	0.12
14	6.22	0.34	1.56	0.25	0.69	0.22	0.39	0.16
28	12.44	0.52	3.11	0.33	1.38	0.29	0.78	0.21
72	32.00	0.69	8.00	0.49	3.56	0.45	2.00	0.37
207	92.00	0.93	23.00	0.66	10.22	0.59	5.75	0.45
278	123.56	1.00	30.89	0.69	13.73	0.63	7.72	0.47

Series I-S-32%, Ps=4.90%

Specimen	3X3"		3X6"		3X9"		3X12"	
	t/b <sup>2</sup>	S <sub>e</sub> /S <sub>u</sub>	t/b <sup>2</sup>	S <sub>e</sub> /S <sub>u</sub>	t/b <sup>2</sup>	S <sub>e</sub> /S <sub>u</sub>	t/b <sup>2</sup>	S <sub>e</sub> /S <sub>u</sub>
3	1.33	0.12	0.33	0.12	0.15	0.08	0.10	0.07
7	3.11	0.20	0.78	0.16	0.35	0.16	0.19	0.13
14	6.22	0.31	1.56	0.24	0.69	0.20	0.39	0.16
28	12.44	0.41	3.11	0.33	1.38	0.29	0.78	0.24
72	32.00	0.71	8.00	0.53	3.56	0.45	2.00	0.37
207	92.00	0.94	23.00	0.69	10.22	0.59	5.75	0.53
278	123.56	1.00	30.89	0.76	13.73	0.67	7.72	0.57



Series I-S-7Z, PC

Specimen	3X3"		3X6"		3X9"		3X12"	
	t/b <sup>2</sup>	S <sub>e</sub> /S <sub>u</sub>	t/b <sup>2</sup>	S <sub>e</sub> /S <sub>u</sub>	t/b <sup>2</sup>	S <sub>e</sub> /S <sub>u</sub>	t/b <sup>2</sup>	S <sub>e</sub> /S <sub>u</sub>
3	1.33	0.11	0.33	0.09	0.15	0.09	0.10	0.10
7	3.11	0.22	0.78	0.17	0.35	0.18	0.19	0.16
14	6.22	0.32	1.56	0.26	0.69	0.24	0.39	0.23
28	12.44	0.49	3.11	0.40	1.38	0.34	0.78	0.32
70	31.11	0.75	7.78	0.58	3.46	0.44	1.94	0.41
203	90.22	0.92	22.56	0.67	10.02	0.52	5.64	0.51
275	122.22	0.97	30.56	0.67	13.58	0.53	7.64	0.51

Series I-S-7Z, Ps=2.22Z

Specimen	3X3"		3X6"		3X9"		3X12"	
	t/b <sup>2</sup>	S <sub>e</sub> /S <sub>u</sub>	t/b <sup>2</sup>	S <sub>e</sub> /S <sub>u</sub>	t/b <sup>2</sup>	S <sub>e</sub> /S <sub>u</sub>	t/b <sup>2</sup>	S <sub>e</sub> /S <sub>u</sub>
3	1.33	0.09	0.33	0.06	0.15	0.04	0.10	0.05
7	3.11	0.18	0.78	0.14	0.35	0.14	0.19	0.10
14	6.22	0.28	1.56	0.20	0.69	0.18	0.39	0.15
28	12.44	0.43	3.11	0.32	1.38	0.25	0.78	0.22
70	31.11	0.65	7.78	0.54	3.46	0.33	1.94	0.30
203	90.22	0.89	22.56	0.69	10.02	0.51	5.64	0.42
275	122.22	0.92	30.56	0.72	13.58	0.54	7.64	0.43

Series I-S-7Z, Ps=3.45Z

Specimen	3X3"		3X6"		3X9"		3X12"	
	t/b <sup>2</sup>	S <sub>e</sub> /S <sub>u</sub>	t/b <sup>2</sup>	S <sub>e</sub> /S <sub>u</sub>	t/b <sup>2</sup>	S <sub>e</sub> /S <sub>u</sub>	t/b <sup>2</sup>	S <sub>e</sub> /S <sub>u</sub>
3	1.33	0.10	0.33	0.07	0.15	0.05	0.10	0.04
7	3.11	0.20	0.78	0.13	0.35	0.10	0.19	0.08
14	6.22	0.27	1.56	0.20	0.69	0.17	0.39	0.13
28	12.44	0.47	3.11	0.33	1.38	0.27	0.78	0.20
70	31.11	0.67	7.78	0.52	3.46	0.43	1.94	0.37
203	90.22	0.93	22.56	0.67	10.02	0.53	5.64	0.47
275	122.22	1.00	30.56	0.73	13.58	0.58	7.64	0.53

Series I-S-7Z, Ps=4.90Z

Specimen	3X3"		3X6"		3X9"		3X12"	
	t/b <sup>2</sup>	S <sub>e</sub> /S <sub>u</sub>	t/b <sup>2</sup>	S <sub>e</sub> /S <sub>u</sub>	t/b <sup>2</sup>	S <sub>e</sub> /S <sub>u</sub>	t/b <sup>2</sup>	S <sub>e</sub> /S <sub>u</sub>
3	1.33	0.13	0.33	0.04	0.15	0.05	0.10	0.05
7	3.11	0.17	0.78	0.08	0.35	0.10	0.19	0.08
14	6.22	0.25	1.56	0.13	0.69	0.15	0.39	0.13
28	12.44	0.38	3.11	0.23	1.38	0.23	0.78	0.23
70	31.11	0.67	7.78	0.40	3.46	0.38	1.94	0.30
203	90.22	0.96	22.56	0.65	10.02	0.61	5.64	0.50
275	122.22	1.00	30.56	0.71	13.58	0.61	7.64	0.54

Series III-S-32%, PC

Specimen	3X3"		3X6"		3X9"		3X12"	
	t/b <sup>2</sup>	S <sub>e</sub> /S <sub>u</sub>	t/b <sup>2</sup>	S <sub>e</sub> /S <sub>u</sub>	t/b <sup>2</sup>	S <sub>e</sub> /S <sub>u</sub>	t/b <sup>2</sup>	S <sub>e</sub> /S <sub>u</sub>
3	1.33	0.11	0.33	0.10	0.15	0.09	0.10	0.07
7	3.11	0.22	0.78	0.17	0.35	0.13	0.19	0.12
14	6.22	0.34	1.56	0.25	0.69	0.20	0.39	0.17
29	12.89	0.45	3.22	0.34	1.43	0.26	0.81	0.22
74	32.89	0.67	8.22	0.52	3.65	0.40	2.06	0.35
183	81.33	0.90	20.33	0.64	9.04	0.53	5.08	0.45
290	128.89	0.90	32.22	0.66	14.32	0.55	8.06	0.46

Series III-S-32%, P<sub>a</sub>=2.22%

Specimen	3X3"		3X6"		3X9"		3X12"	
	t/b <sup>2</sup>	S <sub>e</sub> /S <sub>u</sub>	t/b <sup>2</sup>	S <sub>e</sub> /S <sub>u</sub>	t/b <sup>2</sup>	S <sub>e</sub> /S <sub>u</sub>	t/b <sup>2</sup>	S <sub>e</sub> /S <sub>u</sub>
3	1.33	0.11	0.33	0.09	0.15	0.06	0.10	0.05
7	3.11	0.18	0.78	0.18	0.35	0.11	0.19	0.10
14	6.22	0.32	1.56	0.30	0.69	0.17	0.39	0.15
29	12.89	0.42	3.22	0.36	1.43	0.23	0.81	0.18
74	32.89	0.63	8.22	0.58	3.65	0.37	2.06	0.35
183	81.33	0.88	20.33	0.75	9.04	0.50	5.08	0.47
290	128.89	0.91	32.22	0.78	14.32	0.53	8.56	0.50

Series III-S-32%, Ps=3.45%

Specimen	3 X 3"		3X6"		3X9"		3X12"	
	t/b <sup>2</sup>	S <sub>e</sub> /S <sub>u</sub>	t/b <sup>2</sup>	S <sub>e</sub> /S <sub>u</sub>	t/b <sup>2</sup>	S <sub>e</sub> /S <sub>u</sub>	t/b <sup>2</sup>	S <sub>e</sub> /S <sub>u</sub>
3	1.33	0.11	0.33	0.07	0.15	0.04	0.10	0.05
7	3.11	0.22	0.78	0.23	0.35	0.08	0.20	0.11
14	6.22	0.40	1.56	0.22	0.69	0.16	0.39	0.17
29	12.89	0.55	3.22	0.31	1.43	0.27	0.81	0.25
74	32.89	0.77	8.22	0.49	3.65	0.41	2.06	0.40
183	81.33	0.92	20.33	0.66	9.04	0.57	5.08	0.50
290	28.89	0.94	32.22	0.70	14.32	0.59	8.06	0.55

Series III-S-32%, Ps=4.90%

Specimen	3X3"		3X6"		3X9"		3X12"	
	t/b <sup>2</sup>	S <sub>e</sub> /S <sub>u</sub>	t/b <sup>2</sup>	S <sub>e</sub> /S <sub>u</sub>	t/b <sup>2</sup>	S <sub>e</sub> /S <sub>u</sub>	t/b <sup>2</sup>	S <sub>e</sub> /S <sub>u</sub>
3	1.33	0.08	0.33	0.06	0.15	0.05	0.10	0.05
7	3.11	0.16	0.78	0.14	0.35	0.12	0.19	0.10
14	6.22	0.33	1.56	0.33	0.69	0.21	0.39	0.17
29	12.89	0.45	3.22	0.43	1.43	0.26	0.81	0.25
74	32.89	0.68	8.22	0.62	3.65	0.42	2.06	0.38
183	81.33	0.91	20.33	0.78	9.04	0.62	5.08	0.48
290	28.89	0.97	32.22	0.82	14.32	0.63	8.06	0.49

Series III-S-54%, PC

Specimen	3X3"		3X6"		3X9"		3X12"	
	$t/b^2$	$S_e/S_u$	$t/b^2$	$S_e/S_u$	$t/b^2$	$S_e/S_u$	$t/b^2$	$S_e/S_u$
3	1.33	0.12	0.33	0.10	0.15	0.08	0.10	0.07
7	3.11	0.29	0.78	0.21	0.35	0.16	0.19	0.15
14	6.22	0.49	1.56	0.37	0.69	0.25	0.39	0.23
31	13.78	0.69	3.44	0.49	1.53	0.36	0.86	0.33
73	32.44	0.83	8.11	0.64	3.60	0.47	2.03	0.46
183	81.33	0.56	20.33	0.77	9.04	0.56	5.08	0.56
287	127.56	0.67	31.89	0.78	14.17	0.56	7.97	0.56

Series III-S-54%, Pb=2.22%

Specimen	3X3"		3X6"		3X9"		3X12"	
	$t/b^2$	$S_e/S_u$	$t/b^2$	$S_e/S_u$	$t/b^2$	$S_e/S_u$	$t/b^2$	$S_e/S_u$
3	1.33	0.14	0.33	0.08	0.15	0.06	0.10	0.05
7	3.11	0.28	0.78	0.18	0.35	0.23	0.19	0.13
14	6.22	0.49	1.56	0.33	0.69	0.19	0.39	0.19
31	13.78	0.70	3.44	0.46	1.53	0.30	0.86	0.30
73	32.44	0.84	8.11	0.58	3.60	0.42	2.03	0.39
183	81.33	0.96	20.33	0.75	9.04	0.54	5.08	0.46
287	127.56	1.00	31.89	0.82	14.17	0.57	7.97	0.48

Series III-S-54%,  $P_8=3.45\%$ 

Specimen	3X3"		3X6"		3X9"		3X12"	
	$t/b^2$	$S_e/S_u$	$t/b^2$	$S_e/S_u$	$t/b^2$	$S_e/S_u$	$t/b^2$	$S_e/S_u$
3	1.33	0.12	0.33	0.08	0.15	0.05	0.10	0.05
7	3.11	0.24	0.78	0.18	0.35	0.12	0.19	0.12
14	6.22	0.44	1.56	0.34	0.69	0.21	0.39	0.22
31	13.78	0.68	3.44	0.47	1.53	0.32	0.86	0.34
73	32.44	0.92	8.11	0.64	3.60	0.44	2.03	0.45
183	81.33	0.96	20.33	0.78	9.04	0.56	5.08	0.59
287	127.56	1.00	31.89	0.83	14.17	0.58	7.97	0.62

Series III-S-54%,  $P_8=4.90\%$ 

Specimen	3X3"		3X6"		3X9"		3X12"	
	$t/b^2$	$S_e/S_u$	$t/b^2$	$S_e/S_u$	$t/b^2$	$S_e/S_u$	$t/b^2$	$S_e/S_u$
3	1.33	0.13	0.33	0.08	0.15	0.06	0.10	0.06
7	3.11	0.30	0.78	0.16	0.35	0.12	0.19	0.11
14	6.22	0.43	1.56	0.29	0.69	0.20	0.39	0.19
31	13.78	0.60	3.44	0.42	1.53	0.29	0.86	0.30
73	32.44	0.82	8.11	0.54	3.60	0.41	2.03	0.43
183	81.33	0.95	20.33	0.69	9.04	0.54	5.08	0.57
287	127.56	1.00	31.89	0.72	14.17	0.58	7.97	0.59

Series III-S-7%, PC

Specimen	3X3"		3X6"		3X9"		3X12"	
	t/b <sup>2</sup>	S <sub>0</sub> /S <sub>u</sub>	t/b <sup>2</sup>	S <sub>0</sub> /S <sub>u</sub>	t/b <sup>2</sup>	S <sub>0</sub> /S <sub>u</sub>	t/b <sup>2</sup>	S <sub>0</sub> /S <sub>u</sub>
3	1.33	0.10	0.33	0.09	0.15	0.07	0.10	0.05
7	3.11	0.23	0.78	0.20	0.35	0.15	0.19	0.14
14	6.22	0.31	1.56	0.26	0.69	0.21	0.39	0.19
30	13.33	0.52	3.33	0.41	1.48	0.32	0.83	0.30
73	32.44	0.70	8.11	0.57	3.60	0.42	2.03	0.39
181	80.44	0.91	20.11	0.73	8.94	0.52	5.03	0.49
284	126.22	0.97	31.56	0.74	14.02	0.52	7.89	0.51

Series III-S-7%, P<sub>8</sub>=2.22%

Specimen	3X3"		3X6"		3X9"		3X12"	
	t/b <sup>2</sup>	S <sub>0</sub> /S <sub>u</sub>	t/b <sup>2</sup>	S <sub>0</sub> /S <sub>u</sub>	t/b <sup>2</sup>	S <sub>0</sub> /S <sub>u</sub>	t/b <sup>2</sup>	S <sub>0</sub> /S <sub>u</sub>
3	1.33	0.13	0.33	0.07	0.15	0.06	0.10	0.07
7	3.11	0.28	0.78	0.20	0.35	0.13	0.19	0.14
14	6.22	0.41	1.56	0.25	0.69	0.18	0.39	0.19
30	13.33	0.63	3.33	0.40	1.48	0.31	0.83	0.30
73	32.44	0.78	8.11	0.58	3.60	0.46	2.03	0.41
181	80.44	0.94	20.11	0.73	8.94	0.58	5.03	0.52
284	126.22	1.00	31.56	0.77	14.02	0.61	7.89	0.55

Series III-S-7%, P<sub>B</sub>=3.45%

Specimen	3 X 3"		3X6"		3X9"		3X12"	
	t/b <sup>2</sup>	S <sub>e</sub> /S <sub>u</sub>	t/b <sup>2</sup>	S <sub>e</sub> /S <sub>u</sub>	t/b <sup>2</sup>	S <sub>e</sub> /S <sub>u</sub>	t/b <sup>2</sup>	S <sub>e</sub> /S <sub>u</sub>
3	1.33	0.10	0.33	0.07	0.15	0.05	0.10	0.04
7	3.11	0.20	0.78	0.13	0.35	0.12	0.19	0.11
14	6.22	0.40	1.56	0.18	0.69	0.17	0.39	0.15
30	13.33	0.68	3.33	0.31	1.48	0.27	0.83	0.26
73	32.44	0.87	8.11	0.48	3.60	0.40	2.03	0.38
181	80.44	0.97	20.11	0.63	8.94	0.52	5.03	0.48
284	126.22	1.00	31.56	0.67	14.02	0.55	7.89	0.51

Series III-S-7%, P<sub>B</sub>=4.90%

Specimen	3X3"		3X6"		3X9"		3X12"	
	t/b <sup>2</sup>	S <sub>e</sub> /S <sub>u</sub>	t/b <sup>2</sup>	S <sub>e</sub> /S <sub>u</sub>	t/b <sup>2</sup>	S <sub>e</sub> /S <sub>u</sub>	t/b <sup>2</sup>	S <sub>e</sub> /S <sub>u</sub>
3	1.33	0.11	0.33	0.07	0.15	0.07	0.10	0.07
7	3.11	0.22	0.78	0.15	0.35	0.15	0.19	0.14
14	6.22	0.27	1.56	0.22	0.69	0.19	0.39	0.19
30	13.33	0.51	3.33	0.35	1.48	0.31	0.83	0.31
73	32.44	0.73	8.11	0.53	3.60	0.48	2.03	0.46
181	80.44	0.87	20.11	0.71	8.94	0.65	5.03	0.60
284	126.22	0.95	31.56	0.75	14.02	0.70	7.89	0.64



REFERENCES


1. ACI Committee 209, "The Effects of Concrete Constituents, Environment, and Stress on the Creep and Shrinkage of Concrete", Annual ACI Convention, 1970.
2. Feldman, F.F. and Sereda, P.J., "A Model for Hydrated Portland Cement Paste as Deduced from Sorption-Length Change and Mechanical Properties", N.R.C., DBR Research Paper No. 400, Ottawa, 1969.
3. Powers, T.C., "Mechanisms of Shrinkage and Reversible Creep of Hardened Cement Paste", International Conferance on the Structure of Concrete, London, 1965.
4. Powers, T.C., "Physical Properties of Cement Paste", Proc., Fourth Int., Symposium on Chemistry of Cement, Washington, 1960.
5. Davis, H.I., "Autogenous Volume Changes in Concrete", Proc., A.S.T.M., Vol. 40, 1940.
6. Ross A.D., "Shape, Size and Shrinkage", Concrete and Constructional Engineering. Vol. 39, Aug., 1944.
7. L'Hermite, R., "Volume Changes of Concrete", Proc., 4th Int., Symp., On the Chemistry of Cement, Washington D.C., 1960.
8. Neville, A.M., "Properties of Concrete", John Wiley and Sons Inc., New York, 1963.
9. Hansen, I.C., "Notes from a Seminar on Structure and Properties of Concrete", Dept., of Civil Engineering,

- Stanford University, Tech. Report No. 71, California, 1966.
10. Swenson, E.G., and Sereda, P.J., "Mechanisms of the Carbonation Shrinkage of Lime and Hydrated Cement", Jour. of Applied Chemistry, Vol. 18, No 4, 1968.
  11. Shacklock, B.W., "The Early Shrinkage Characteristics of Hand Placed Concrete", Mag. Concr. Res., Vol. 10, No 28, 1958.
  12. Lerch, W., "Plastic Shrinkage", Journ. ACI, Vol. 53, 1957.
  13. CeLani, et al., "Recherches Sur Le Retrait Plastique Du Beton Frais", Proc., The Shrinkage of Hydraulic Concretes, Rilem/Cembureau, 1968.
  14. Jaegermann, C.H. and Glucklich, E.J., "Effect of Plastic Shrinkage on Subsequent Shrinkage and Swelling of Hardened Concrete", Proc., The Shrinkage of Hydraulic Concretes, Rilem/Cembureau, 1968.
  15. Becker, N.K., "The Prediction of Concrete Drying Shrinkage by Mathematical Diffusion Analogies, "Ph. D. Thesis, University of Windsor, Faculty of Graduate Studies, 1970.
  16. Pihlajavaara, S.E. "On the Main Features and Methods of Investigation of Drying and Related Phenomenon in Concrete", Ph. D. Thesis, University of Helsinki, 1965.
  17. Mills, R.H., "Dependence of Drying Shrinkage on Dimensions of Specimens", Trans. S.Afr., Institution of Civil Engrs., Nov., 1969.

18. Powers, T.C., "Causes and Control of Volume Changes", Jour., of the PCA Research and Development Laboratories Jan., 1956.
19. Kreijger, M., "Influence of the Concrete Composition on the Shrinkage of Hydraulic Concretes", Int., Colloquium on the Shrinkage of Hydraulic Concretes, RILEM, Madrid, March, 1968.
20. Blaine, R.L., et al., "Shrinkage of Hardened Portland Cement Pastes", Section 9, Interrelations Between Cement and Concrete Properties, Part 4, Building Science Series 15, National Bureau of Standards, Washington, March., 1969.
21. Rostasy, F.S., "Theoretical and Experimental Contributions to research Concerning Shrinkage Stresses of Concrete", Ph. D. Thesis, Technical University Stuttgart, 1958.
22. Pickett, G., "Effect of Aggregate on Shrinkage of Concrete and a Hypothesis Concerning Shrinkage", Proceedings, American Concrete Institute, 1956.
23. Nepper-Christensen, P., et al., "Drying Shrinkage of Low Pressure Steam-Cured Concrete Units", Int., Conference on the Problems of Accelerated Hardening of Concrete, RILEM, Moscow, July, 1964.
24. L'Hermite, R.G., and Mamillan, M., "Further Results of Shrinkage and Creep Tests", Proc., Int., Conference on the Structure of Concrete, London, Sept., 1965.
25. Dutron, R. "Creep in Concrete", Bulletin No. 34, RILEM, 1957.

26. Ross, A.D., and England, G.L., "Reinforced Concrete Under Thermal Gradients", Magazine of Concrete Research, March, 1962.
27. Pickett, G., "Shrinkage Stresses in Concrete", Proceedings, ACI, 1946.
28. Ross, A. D., "Creep and Shrinkage in Plain, Reinforced and Prestressed Concrete-- A General Method of Calculation", Institution of Civil Engineering, 1943.
29. Hansen, T. C. and Matock, A. H., "Influence of Size and Shape of Member on the Shrinkage and Creep of Concrete", Proceedings, American Concrete Institute, 1966.
30. Troxell, et al., "Long Time Creep and Shrinkage Tests of Plain and Reinforced Concrete", Proc., ASTM Vol. 58, 1958.
31. Glanville, W. H., "Studies in Reinforced Concrete: Shrinkage Stresses"; Building Research Technical Paper No. 11, H.M.S.O. 1930.
32. Beyer, F. R., "Stresses in Reinforced Concrete Due to Volume Changes", ACI Jour., Proc., V.45, June, 1949.
33. Lyse, I., "Shrinkage and Creep of Concrete", Proceedings, ACI, 1960.
34. Wallo, et al., "Prediction of Creep in Structural Concrete", Bulletin No. 498, College of Engineering, Univ., of Illinois, 1968.
35. Fintel, M., and Khan, F., "Effects of Column Creep and Shrinkage in Tall Structures: Analysis for Differential

- "Shortening of Columns and Field Observation of Structures",  
Proceedings, ACI, 1969.
36. American Concrete Institute, Committee 209, "Prediction of  
Creep, Shrinkage, and Temperature Effects in Concrete  
Structures", Presented at the 1970 Annual Meeting of ACI.
37. Carlson, R. W., "Drying Shrinkage of Large Concrete  
Members", Proceedings, ACI, 1937.
38. Shank, T. R., "The Mechanics of Plastic Flow of Concrete",  
Proceedings, ACI, 1935.
39. Odman, S., "Formulae for Stresses, Strains and Deflection  
of Reinforced Concrete Beams Due to Shrinkage of Concrete",  
The Swedish Cement and Concrete Research Institute, Royal  
Institute of Technology.
40. Elvery, R. H., and Shaffi, M., "Analysis of Shrinkage  
Effects on Reinforced Concrete Structural Members",  
Proceedings, ACI, 1970.
41. Keeton, J. R., "Creep and Shrinkage of Reinforced Thin-  
Shell Concrete", Technical Report No. R 704, U.S. Naval  
Civil Engineering Laboratory, California, 1970.
42. Miller, A. L., "Warping of Reinforced Concrete Due to  
Shrinkage", Proceedings, ACI, 1958.
43. Corley, W. G., and Sozen, M. A., "Time-Dependent Deflections  
of Reinforced Concrete Beams", Proceedings, ACI, 1966.
44. Crank, J., "The Mathematics of Diffusion", Oxford at the  
Clarendon Press, London, 1967.

45. Kennedy, U., Neville, A., "Basic Statistical Methods for Engineers and Scientists", Int., Testbook 8., Scranton, 1964.
  46. Washa, G. W., "Plastic Flow of Thin Reinforced Concrete Slabs", ACI Journal, Proceedings V. 44, No. 3, Nov. 1947.
  47. Washa, G. W., and Fluck, P. G., "Effect of Compressive Reinforcement on the Plastic Flow of Reinforced Concrete Beams", ACI Journal, Proceedings V. 49, No. 2, Oct. 1952.
  48. Elstner, R.C., and Hognestad, E., "Laboratory Investigation of Rigid Frame Failure", ACI Journal, Proceedings V. 53, No. 7, Jan. 1957.
- 

## VITA AUCTORIS

- 1943 Omar Ahmed El-Zein was born in Gaza, Palestine, On May 4, 1943.
- 1949 In September, 1949, he entered Gaza College, where he obtained his elementary education.
- 1953 In September, 1953, he enrolled at Yarmook Preparatory School, where he obtained his preparatory education.
- 1957 In September, 1957, he enrolled at Palestine Secondary School, where he obtained his secondary education.
- 1960 In September, 1960, he enrolled at the University of Cairo, Faculty of Engineering, in June, 1965, he was graduated from the University of Cairo with a Bachelor of Civil Engineering Degree.
- 1965 In November, 1965, he worked at the Ministry of Public Works, Kuwait, as Structural Engineer.
- 1967 In September, 1967, he enrolled at the University of Windsor in order to obtain the degree of Master of Applied Science in Civil Engineering.
- 1969 In May, 1969, he enrolled at the University of Windsor in order to obtain the degree of Doctor of Philosophy in Civil Engineering.

1973 In February, 1973, he started working at Wilson,  
Dario and Valdez Limited, Consulting Engineers,  
Windsor, Ontario, as Project Engineer.